TREM2 and Complement in Microglia; Implications for Neurodegeneration

Alexandra Elisabeth Margaret Phillips

UCL Institute of Neurology

A thesis submitted for the degree of Doctor of Philosophy (Ph.D)

Declaration

I, Alexandra Phillips confirm that the work presented in this thesis is my own. Where information has been derived from other sources, I confirm that this has been indicated in the thesis.

- The generation of the CRISPR/Cas9 gene edited BV2 cell lines was performed by Claudio Villegas Llerena, UCL Institute of Neurology
- The generation of iPSC lines from patient fibroblasts was performed by the NIHR Cambridge Biomedical Research Centre Human Induced Pluripotent Stem Cells core facility (Cambridge, United Kingdom) as well as characterisation to ensure efficient reprogramming
- The cell culture and protocol development for the differentiation of iPSC-derived microglial-like cells was performed by Dr Pablo Garcia Reitböck and Dr Thomas Piers, UCL Institute of Neurology
- Figure 3.1 'CRISPR/Cas9 nickase modification of the *Trem2* gene in BV2 cells' kindly provided by Claudio Villegas Llerena
- Microscope images in figure 4.1 'The generation and characterisation of iPSC-MGLC' kindly provided by Dr Pablo Garcia Reitböck
- Figure 4.6 'Expression of TREM2 protein in control and TREM2 mutant iPSC-MGLC' kindly provided by Dr Thomas Piers

Abstract

Microglial responses critically underpin pathological processes associated with progressive neurodegenerative diseases including Alzheimer's disease (AD) and Parkinson's disease. Regulated inflammation is essential in the healthy brain for the removal of debris and apoptotic cells. However, prolonged inflammation, often attributed to dysregulated microglial activation, is neurotoxic and implicated in the pathogenesis of multiple neurodegenerative diseases. GWAS have identified mutations in the genes for triggering receptor expressed on myeloid cells (TREM2) and Complement Receptor 1 (CR1) as putative risk factors for late-onset Alzheimer's disease (LOAD) (Guerreiro et al. 2013a; Jonsson et al. 2013; Lambert et al. 2013).TREM2 is a major microglia-specific gene and may act as a lock to repress microglial pro-inflammatory activity, whilst promoting protective responses such as chemotaxis and phagocytosis. CR1 is a member of the regulators of the complement activation family and is reported to be expressed on rodent microglia, although there is a lack of clear evidence of human microglial expression. CR1 acts to clear opsonised immune complexes from the blood as well as acting as a complement activation regulator.

CRISPR/Cas9-generated TREM2 knockdown and knockout mouse microglia cell lines have been characterised and utilised for functional experiments in order to further appreciate the role of TREM2 in microglia, alongside iPSC-derived microglia-like cells (iPSC-MGLC) generated from patients carrying TREM2 mutations linked to AD and Nasu Hakola Disease. TREM2 knockout lines have altered actin structures and demonstrate defective responses to stimuli compared with WT cells. Both TREM2 knockout cell lines and human iPSC-MGLC display altered cytokine responses and phagocytosis compared to control cells. Human tissues, including AD brain samples and blood derived cells, have been used to confirm a lack of CR1 in unstimulated human microglia and iPSC-MGLC were utilised to investigate the effect of TREM2 mutations on the expression of other AD-linked complement factors, including C1q and CR3.

Acknowledgements

Firstly I would like to thank my supervisors Dr Jennifer Pocock, Professor John Hardy and Professor Simon Lovestone for their guidance during my PhD. Particularly thank you to Jenny for giving me the opportunity to undertake my PhD in her lab and for supporting and encouraging me up the steep PhD learning curve. I would also like to acknowledge Complement UK and Alexion for funding my PhD.

I would like to thank all those who have been members of the Pocock lab during my PhD. In particular Claudio Villegas-Llerena for the BV2s and for being my partner in crime throughout the last 4 years, Dr Pablo Garcia Reitböck for introducing the iPSCs and inspiring me to eat an unhealthy amount of Franco Manca, Dr Katharina Cosker for all the advice, the girl power and for training me in the art of being a western blot ninja, and Dr Thomas Piers for his keen eye for formatting errors, willingness to discuss new results and experiments with me, and for always making the tea. Thank you also to Dimitra Schiza for her expert training on confocal microscopy, Professor Ken Smith for allowing me to use his group's confocal, and to Michael Clark for his supervision of my immunohistochemistry. I am also grateful to Charlotte Burt for all of her administrative help and, more importantly, for supplying the office with a constant supply of biscuits.

I could not have finished this thesis without my work wife, Dimitra. Thank you for always being there during the weekends in the lab, the long boring days of writing up, and the horrible early mornings in the gym. Thank you for helping me to overcome the many challenges faced both inside and outside of the lab, and for always keeping us going with feta, frappes and protein shakes.

Special love and thanks go to those who kept the benches outside The Harrison warm all through the winters I was forced to endure outside: Dimitra, Kim, Alina, Mario, Tom, Kat, Mikey and, of course, Jack. I have spent some of the best years of my life and the vast majority of my stipend on those benches, and I can't think of better people to have shared it with.

Away from the lab, I would like to thank my amazing Sutton High girls and the ladies of Number 46 for always being there to remind me that there is life beyond the bench and my desk. You have all been terrible, but extremely welcome, distractions and I can't wait to have my freedom back to celebrate properly with you all.

Finally, and most importantly, I want to thank Mum, Dad, Laura and Grandma for all of their love, encouragement and advice. Your support for me has been unfaltering through all of the highs and lows, but your understanding and reassurance during the final stressful few months of experiments and writing up gave me the strength to complete this thesis.

Table of Contents

List of Figures

List of Tables

Abbreviations

A: Aβ (amyloid-β), AD (Alzheimer's disease), ALS (amyotrophic lateral sclerosis), ApoE (apolipoprotein E), ANOVA (analysis of variance), APP (amyloid precursor protein), ATP (adenosine triphosphate)

B: BBB (blood brain barrier), BMP-4 (bone morphogenetic factor 4), BDNF (brain-derived neurotrophic factor), bp (base pair), BSA (bovine serum albumin)

C: C5a (complement component 5a), Cas9 (CRISPR-associated protein 9), CNV (copy number variation), CNS (central nervous system), CR1 (complement receptor 1), CR3 (complement receptor 3), CREG (regulators of complement), CRISPR (clustered regularly interspaced short palindromic repeats), Crry (complement receptor 1-related gene/protein Y), CSF (cerebrospinal fluid), Ct (cycle threshold), CTF (C-terminal fragment), CytoD (cytochalasinD)

D: DAB (3,3'-diaminobenzidine), DAMP (damage-associated molecular pattern), DAP12 (DNAX-activating protein of 12kDa), DAPI (4',6-diamidino-2-phenylindole), ddH_2O (double-distilled water), DNA (deoxyribose nucleic acid)

E: EAE (experimental autoimmune encephalitis), EB (embryoid body), EDTA (ethylenediaminetetraacetic acid), ELISA (enzyme-linked immunosorbent assay), EOAD (early onset Alzheimer's disease), ER (endoplasmic reticulum), ESC (embryonic stem cell)

F: FBS (foetal bovine serum), FGF (fibroblast growth factor), FTD (fronto-temporal dementia)

G: GFP (green fluorescent protein), GWAS (genome-wide association study)

H: HBSS (Hanks' balanced saline solution), HRP (horseradish peroxidase)

I: Iba1 (ionized calcium binding adaptor molecule 1), IGF-1 (insulin-like growth factor 1), IFNγ (interferon-γ), IL-1β (interleukin-1β), IL-3 (interleukin-3), IL-6 (interleukin-6), IL-10 (interleukin-10), IL-12 (interleukin-12), IL-34 (interleukin-34), iPSC (induced pluripotent stem cell), iPSC-MGLC (induced pluripotent stem cell-derived microglia-like cell), iNOS (inducible nitric oxide synthase), ITAM (immunoreceptor tyrosine-based activation motif)

K: KD (knockdown), KO (knockout)

L: LHR (long homologous repeat), LOAD (late onset Alzheimer's disease), LPS (lipopolysaccharide), LTP (long term potentiation)

M: MAC (membrane attack complex), MCSF (macrophage colony-stimulating factor), MGCM (microglia conditioned medium), MHC (major histocompatibility complex), MS (multiple sclerosis)

N: NGF (nerve growth factor), NHD (Nasu Hakola Disease), NO (nitric oxide)

O: OR (odds ratio)

P: PAMP (pathogen-associated molecular pattern), PBMC (peripheral blood mononuclear cell), PBS (phosphate-buffered saline), PBS-T (1x PBS/0.1% Tween-20), (PCR (polymerase chain reaction), PD (Parkinson's disease), PFA (paraformaldehyde), PLOSL (polycystic lipomembranous osteodysplasia with sclerosing leukoencephalopathy), PNGase (peptide:N-gycosidase), PRR (pattern recognition receptor), PS (phosphatidylserine), PSEN1 & 2 (presenilin 1 & 2)

Q: qPCR (quantitative polymerase chain reaction)

R: RNA (ribonucleic acid), ROS (reactive oxygen species), RPKM (reads per kilobase per million mapped reads), RPMI (Roswell Park Memorial Institute medium 1640), RT-PCR (reverse transcription polymerase chain reaction)

S: SCF (stem cell factor), SCR (short consensus repeats), SDS-PAGE (sodium dodecyl polyacrylamide gel electrophoresis), SEM (standard error of the mean), SNP (small nuclear polymorphism), sTREM2 (soluble TREM2)

T: T66Mhet (iPSC-derived microglia-like cell line carrying heterozygous T66M mutation in TREM2 gene), T66Mhom (iPSC-derived microglia-like cell line carrying homozygous T66M mutation in TREM2 gene), TALENs (transcription activator-like effector nucleases), TLR (toll-like receptor), TMB (3,3',5,5'-tetramethylbenzidine), TNFα (tumour necrosis factor α), TPM (transcripts per million), TREM2 (triggering receptor expressed in myeloid cells-2), TYROBP (tyrosine kinase binding protein)

U: UCL (University College London)

V: VEGF (vascular endothelial growth factor)

W: W50Chom (iPSC-derived microglia-like cell line carrying homozygous W50C mutation in TREM2 gene), WT (wildtype)

Z: ZFN (zinc finger nucleases)

1. Introduction

1.1 Microglia

The mammalian central nervous system (CNS) is comprised of the brain and the spinal cord, and, in humans, is populated by an estimated 86 billion neurons and a further 84 billion non-neuronal glial cells (Azevedo *et al.*, 2009). Despite the overall 1:1 ratio in the brain of glia to neurons, the ratio varies across brain regions, with glia outnumbering neurons by as much as 17:1 in the thalamus (Pakkenberg and Gundersen, 1997). There are three main cell types defined as glia: astrocytes, oligodendrocytes and microglia. Glia were traditionally viewed as merely neuronal support cells, hence the derivation of the name from the Greek word for 'glue'. However this opinion has gradually been found to be outdated, as key functions performed by glia during CNS development, homeostasis and disease continue to be identified (reviewed by Barres et al. 2008; Reemst et al. 2016; Colonna & Butovsky 2017). The importance of understanding the interactions between neurons and glia is becoming increasingly relevant for both the study of the human brain and also for understanding and treating neurodegenerative diseases.

Microglia are the resident phagocytes of the CNS and make up approximately 15% of the glial cells in the adult CNS, where their primary functions are to provide an innate immune response and to ensure clearance of debris resulting from cell death, infection or insult. They are found in all regions of the brain, at densities in the adult mouse brain ranging from 5% in the corpus callosum to 12% in the substantia nigra (Lawson *et al.*, 1990). The first description of microglia was made by Franz Nissl in 1899, who described 'Stabchenzellen', or rod cells, with migratory, phagocytic and proliferative potential. The term 'microglial cell' was introduced in 1939 by Del Rio-Hortega to distinguish microglia from oligodendrocytes within the non-neuronal, non-astrocytic group of cells found in the CNS.

1.1.1 Microglial Ontogeny

For decades microglia were believed to share a neuro-ectodermal origin with other glial cells, however it has now been established that they originate from yolk sac-derived primitive macrophages (reviewed by Ginhoux et al. 2013) that share the same myeloid-origins as blood monocytes and monocyte-derived macrophages but differ in their dependence on the transcription factor Myb. The myeloid origin of microglia was demonstrated in a mouse model with disrupted expression of the gene encoding for

PU.1, an essential transcription factor for myeloid cells including macrophages, in which microglia failed to develop in the CNS (McKercher *et al.*, 1996). Similarly, disruptions in the formation of other cells, including macrophages, neutrophils and monocytes were reported in this model confirming their common myeloid origin.

Yolk sac blood island derived-primitive macrophages, which eventually differentiate into microglia, populate the mouse neuroepithelium from embryonic day 9.5 (Ginhoux *et al.*, 2010). As the yolk sac is the only source of haematopoiesis at this stage of development (Alliot, Godin and Pessac, 1999), with fetal liver haematopoiesis not occurring until after the initiation of blood brain barrier closure from E13.5 (Daneman, 2012), the microglial progenitors present in the CNS must therefore be yolk sac-derived. A clear distinction between the yolk sac-derived primitive macrophages and the haematopoietic stem cell-derived monocytes and macrophages can be made based upon their dependence on Myb. Schulz et al demonstrated using *Myb*$^{-/-}$ mice that tissue resident macrophages with yolk sac origins, such as CNS microglia, liver Kupffer cells and epidermal Langerhans cells, do not require the Myb transcription factor for development, unlike monocytes and monocyte-derived cells (Schulz *et al.*, 2012).

The brain resident population of microglia that are present since embryonic development proliferate slowly but at a rate that is sufficient to maintain microglial numbers throughout adulthood, at least during homeostasis. However, monocytes have been shown to be recruited to the adult brain under certain conditions, including inflammation (Priller *et al.*, 2001), although whether these cells differentiate into fully functional microglia is not yet known. During CNS inflammation and neurodegeneration, reactive microgliosis occurs resulting in microglial population increases although definitive evidence of the origin of these microglia are lacking; are numbers increased by proliferation of existing brain resident microglia or are monocytes recruited from the periphery? In models deficient in embryonic microglia, bone marrow-derived myeloid cells are capable of populating the CNS and adopting the morphology and activity of microglia following bone marrow transplantation (Beers *et al.*, 2006). Furthermore, ablation of microglia by irradiation resulted in recruitment of bone marrow-derived monocytes to the CNS (Mildner *et al.*, 2007), likely due to inflammation induced by the irradiation procedure. Long term study of microglial population maintenance through the use of parabiosis studies in mice have shown that bone marrow derived cells from control mice were not identified in the CNS of irradiated mice (Ginhoux *et al.*, 2010), demonstrating that local self-renewal is sufficient for maintaining the microglial population, even following denervation and amytotrophic lateral sclerosis (ALS) models of neurodegeneration (Ajami *et al.*, 2007).

It is has been demonstrated that monocytes are recruited to the CNS during inflammatory disease and, although they do not persist and differentiate into microglia, can contribute to pathogenesis (Ajami *et al.*, 2011). Therefore, in the healthy brain, existing microglia self-renew in order to maintain the necessary cell population numbers but peripheral monocytes are occasionally found in the parenchyma, particularly following priming due to inflammation or injury where they can alter disease severity despite their transient presence.

1.1.2 Microglia in Surveillance

Microglia play a role in a wide range of biological functions in both the developing and the adult brain, responding to a multitude of stimuli in physiological and pathological conditions. They are responsible for mounting immunological responses in the immune privileged CNS and the ability of these cells to release a vast array of cytokines, chemokines and growth factors allows microglia to orchestrate the responses of both CNS resident cells and infiltrating immune cells. Microglia also regulate neuron number and synapse strength to ensure proper signalling in the neuronal network of the adult brain. This assortment of functions means that any dysregulation of microglial activity could have widespread effects throughout the CNS.

In vivo analysis of so called 'resting' microglia in the adult brain demonstrated that these cells display surprisingly high levels of motility, even in physiological conditions (Nimmerjahn, Kirchhoff and Helmchen, 2005). Microglia exist in non-overlapping domains which they constantly monitor through random outgrowth and retraction of their ramified processes (Davalos *et al.*, 2005; Nimmerjahn, Kirchhoff and Helmchen, 2005), ensuring continuous surveillance of their environment. The CNS has an immune privileged existence due to the lack of lymphatic system, absence of adaptive immune responses and protection from free diffusion of molecular and cellular components thanks to the blood brain barrier (Ousman and Kubes, 2012). Therefore microglia act as sentinels to monitor and protect the CNS from any potential mediators of infection or insult, ensuring that any pathogens or tissue damage are rapidly identified and resolved.

Microglia express a wide range of pattern-recognition receptors (PRRs) for the detection of pathogen- or damage-associated molecular patterns (PAMPs and DAMPs) including the toll like receptors 4 and 1/2 (TLR4 and TLR1/2) and their co-receptors CD14, CD36 and CD47 (Lehnardt, 2010). Detection of microbes and pathogen associated signals through TLRs results in a phagocytic response associated with

release of pro-inflammatory mediators, including TNFα and nitric oxide (NO), to encourage further pathogen removal. However, this response can have off target neurotoxic effects if inflammatory conditions are prolonged. In addition to this innate immune response, activated microglia are capable of upregulating the necessary machinery for inducing an adaptive immune responses through antigen presentation including MHC I and II (Mack *et al.*, 2003; Malone *et al.*, 2008).

1.1.3 Microglia in Homeostasis

Microglial phagocytosis is essential for maintaining homeostasis in the developing and adult brain as it is required for tackling infections, the removal of surplus neurons during development and the clearance of protein aggregates and apoptotic cells induced by neurodegeneration or aging (Tremblay *et al.*, 2011). Phagocytosis is the process by which phagocytes recognise, bind and engulf a range of solid particulates including cellular debris, pathogens and apoptotic cells, into membrane protrusions called phagosomes, which fuse with acidic lysomes for degradation. The word derives from the Greek words ‘phagein’ (to devour), ‘kytos’ (cell) and ‘-osis’ (process).

The uptake of dead and apoptotic cells prior to complete cellular disintegration is important to minimise inflammation, as they are a source of self-antigens and intracellular contents that may be toxic to surrounding cells (Neumann, Kotter and Franklin, 2009). Furthermore, clearance of apoptotic cells has been shown to downregulate microglial expression of pro-inflammatory cytokines (Magnus *et al.*, 2001), which are excitotoxic to neurons (Pickering, Cumiskey and O’Connor, 2005). It is hypothesised that microglia utilise ‘eat me’ signals found on the surface of apoptotic cells to direct their selection of cells for clearance. Similarly, ‘don’t eat me’ signals are recognised on healthy, ‘self’ cells to ensure that inappropriate phagocytosis does not occur.

Examples of ‘eat me’ signals include calreticulin, a lack of sialylation on cell surface and phosphatidylserine (PS). PS is usually expressed on the inner layer of the cell membrane, however, during apoptosis or cell stress this is flipped out and is either recognised directly by multiple microglial receptors or is tagged for clearance by opsonins (Tyurina *et al.*, 2007; Segawa *et al.*, 2014). These PS recognising receptors include milk fat globule epidermal growth factor 8 (MFG-E8) (Hanayama *et al.*, 2002), BAI1, TIM4 (Mazaheri *et al.*, 2014), scavenger receptors CD36 and SR1 (Areschoug and Gordon, 2009), and the TAM receptor tyrosine kinases (Tyro3, Axl and Mertk) which recognise PS via the opsonins growth arrest-specific 6 (GAS6) and protein-S

(Lemke, 2013). Similarly, cell stress induces the cell surface exposure of calreticulin (Panaretakis *et al.*, 2009), typically found within the endoplasmic reticulum (ER), which upon recognition by low density lipoprotein receptor related protein (LRP), induces phagocytosis of the cell by microglia (Gardai *et al.*, 2005). Thus, microglia are capable of efficiently identifying and clearing dying cells before significant degradation occurs that they might cause an inflammatory insult.

In addition to cell-cell communications initiating phagocytosis of apoptotic cells, microglia are also recruited to areas of injury and neuronal death by long distance soluble factors acting as 'find me' signals such as the nucleotides ATP and UDP, chemokines and fractalkine. Microglia express purinergic receptors allowing them to detect ATP released from intracellular stores of lysed, necrotic cells or from apoptotic cells, in which ATP is generated in a caspase-dependent manner (Elliott *et al.*, 2009). ATP has been shown to induce rapid migration of microglial processes towards sites of damage in a model of traumatic brain injury (Davalos *et al.*, 2005). Expression of the receptor for the chemokine CXCL10, another 'find me' signal, is essential for microglial migration to the site of injury and for microglial clearance of denervated dendrites in a model of brain lesions (Rappert *et al.*, 2004).

Fractalkine exists either tethered to neuronal membranes, where it is thought to play a role in adhesion, or as a soluble factor released by ADAM17 cleavage (Garton *et al.*, 2001), which acts as a microglial chemokine (Sokolowski *et al.*, 2014). In the CNS, fractalkine is primarily expressed by neurons and microglia are the only CNS cell type to express the fractalkine receptor, CX_3CR1. Knockout of CX_3CR1 results in reduced microglial process motility and impaired migration to sites of neuronal injury (Liang *et al.*, 2009). In addition to acting as a long distance chemokine for the recruitment of microglia, fractalkine has also been reported to downregulate microglial activation (Cardona *et al.*, 2015; Ślusarczyk *et al.*, 2016).

Phagocytic clearance by microglia following injury may be fundamental for reorganisation of neural circuits and triggering repair. Declines in this clearance, which are often associated with aging, or insufficient clearance during disease may prevent the formation of adequate repair responses (Neumann, Kotter and Franklin, 2009). The presence of uncleared myelin may actively block regrowth following injury as it prevents the differentiation of oligodendrocyte precursors (Kotter *et al.*, 2005). Furthermore myelin contains molecules such as Nogo A which inhibit axonal regeneration (Schwab, 2004). Therefore the phagocytic activity of microglia is essential for myelin regeneration and repair following periods of demyelination. In models of demyelination, IL-1β and TNFα have also been shown to be necessary for the initiation

of efficient remyelination responses (Arnett *et al.*, 2001; Mason *et al.*, 2001), indicating that these microglial-secreted factors that typically associated with pro-inflammatory, damaging responses are necessary in certain contexts for protective and regenerative effects.

Glutamate is the primary excitatory neurotransmitter and dysregulation of extracellular levels of glutamate can cause neuronal excitotoxicity, due to excessive cation influxes causing osmotic and mitochondrial stress (Barger *et al.*, 2007). Although astrocytes take up the majority of excess glutamate, this function is also performed by microglia (Nakajima *et al.*, 2001). Microglia both express glutamatergic receptors (Pocock and Kettenmann, 2007), allowing them to detect and respond to this neurotransmitter, as well as act as a source of glutamate generation, particularly following activation (Barger *et al.*, 2007). Neuronal NMDA receptor activation has been shown to result in ATP release, which is detected by microglial purinergic receptors, inducing microglial process outgrowth (Dissing-Olesen *et al.*, 2014) and TNFα release (Masuch *et al.*, 2016). Interestingly, microglial release of TNFα, a well-known pro-inflammatory cytokine, has been found to play both protective and detrimental roles in the response to disproportionate neurotransmitter release. TNFα can augment glutamate-induced excitotoxicity by activating microglia in an autocrine manner, which upregulates glutaminase activity (Takeuchi *et al.*, 2006). Conversely, TNFα release has also been shown to protect neurons against AMPA and NMDA-induced excitotoxicity (Bernardino *et al.*, 2005; Masuch *et al.*, 2016). The ability of microglia to detect both excessive neurotransmitter and ATP release, which is often associated with the presence of apoptotic neurons, allows them to generate neuroprotective responses to maintain homeostasis and ensure proper neuronal network signalling.

1.1.4 Microglia in Neurogenesis

In addition to their role immune surveillance and clearing any stimuli that could initiate inflammation, microglia play an important role in neurogenesis. Microglia exert both positive and negative regulatory effects on neurogenesis and neuronal cell numbers during CNS development. Microglia secrete growth and trophic factors that encourage neural precursor survival and differentiation, as well as concurrently contributing to the programmed cell death and pruning of supernumerary neurons and synapses. Migration to the brain by the primitive macrophages that become the resident microglial population occurs early on in CNS development, at approximately embryonic day 9.5 (Ginhoux et al. 2010, see 1.1.1 Microglial Ontogeny).

It is well documented that neurons are produced in excess in the developing brain and up to half of cells in certain regions are removed during the process of network remodelling during pre and postnatal development (Oppenheim, 1991; de la Rosa and de Pablo, 2000). This process of network refinement during development results in the generation of large amounts of apoptotic cells, which if not cleared appropriately, as discussed previously, can damage surrounding cells (Neumann, Kotter and Franklin, 2009). As the resident phagocytes of the brain, microglia play a key role in the clearance of these neurons that fail to become established in networks, but more recently have also been identified as active contributors to the elimination of neuronal numbers.

Several mechanisms have been hypothesised to be involved in microglial elimination of excessive neurons including initiation of apoptosis via superoxide ion generation and subsequent phagocytosis of viable cells, known as primary phagocytosis or phagoptosis (Brown and Neher, 2014) and the targeting of neural precursors to limit further neuron generation (Cunningham, Martínez-Cerdeño and Noctor, 2013). In the cerebral cortex of pre- and post-natal rats and monkeys, microglia have been shown to phagocytose neural precursor cells in order to control the formation of cortical neurons (Cunningham, Martínez-Cerdeño and Noctor, 2013). This regulation of neural precursor cell number was found to be dependent upon microglial activation state as maternal immune activation *in utero* resulted in augmented removal of these viable neural precursor cells.

Microglia selectively remove Purkinje cells in the cerebellum (Marín-Teva *et al.*, 2004) and neurons in the hippocampus (Wakselman *et al.*, 2008) through the generation of reactive oxygen species. Reactive oxygen species, such as superoxide anions, induce the exposure of PS on viable neurons, providing the ‘eat me’ signal for clearance by microglia (Neher *et al.*, 2011). Ablation of microglia or knockout of the CR3 receptor responsible for phagocytosis of the targeted neurons resulted in increases in surviving neurons (Marín-Teva *et al.*, 2004; Wakselman *et al.*, 2008), demonstrating that microglial phagocytosis contributes to removal of neurons during development through apoptosis and cell death.

Microglia continue to alter neurogenesis in the adult brain. The subgranular zone of the hippocampus continues to give rise to neuroblasts throughout adulthood, however very few of these cells are maintained and integrated into the neuronal circuitry. Excess newborn cells that are undergoing apoptosis have been shown to be cleared by rapid and highly efficient microglial phagocytosis, with 90% of apoptotic cells engulfed within 1.5 hours (Sierra *et al.*, 2010).

Conversely, fractalkine signalling has been shown to be important for microglial neurotrophic support during postnatal neuronal network refinement. In $CX_3CR1^{-/-}$ mice, increased levels of apoptosis were identified in the layer V cortical neurons (Ueno *et al.*, 2013) in addition to cognitive function deficits and LTP impairment (Rogers *et al.*, 2011). It was demonstrated that the increase in apoptosis identified in $CX_3CR1^{-/-}$ mice was due to an increase in the expression of inhibitors of the trophic factor insulin-like growth factor 1 (IGF-1). Furthermore, both inhibition of microglial activation and selective ablation of microglia, resulted in significant increases in layer V neuron cell death (Ueno *et al.*, 2013), demonstrating the importance of the trophic factors released by activated microglia for neuronal survival during early postnatal development.

1.1.5 Microglia in Synaptic Connectivity

In addition to their role in regulating neuronal cell number, microglia play a role in monitoring synapses and altering synaptic density and connectivity. In the adult brain, microglia have been observed to have frequent, brief interactions with synapses, occurring approximately once per hour and lasting 5 minutes (Wake *et al.*, 2009). Therefore, as the synaptic interactions were found to be activity dependent, this could be a mechanism through which microglia contribute to synaptic plasticity. In the $CX_3CR1^{-/-}$ model, which is associated with reduced microglial density, increased dendritic spines and immature synapses were found in the developing hippocampus (Paolicelli *et al.*, 2011), indicating that microglial synapse surveillance and phagocytosis contributes to regulation of synapse and dendritic spine numbers.

It has been observed that microglia are capable of sensing synaptic activity and detecting weaker synapses, which are then preferentially phagocytosed (Schafer *et al.*, 2012). Schafer et al. demonstrated, using transgenic models deficient in various complement cascade components, that early postnatal synaptic activity modulates complement-mediated phagocytosis of synapses by microglia. Deficiencies in any of these essential complement components, C1q, C3 or CR3, which will be described in more detail at a later point (1.5.1 Complement in the Brain), resulted in aberrant synaptic connectivity and a reduction in eye-specific segregation in the dorsal lateral geniculate nucleus (Schafer *et al.*, 2012). The importance of complement-mediated synaptic pruning by microglia has been further demonstrated by the development of epileptic symptoms in C1q deficient models, due to the maintenance of inappropriate connections in the sensorimotor cortical regions (Chu *et al.*, 2010). Manipulation of visual experience alters the strength of synapses in the visual cortex of juvenile mice, such as the reduction in synaptic strength induced by a light deprivation paradigm

(Maffei *et al.*, 2006). Following light deprivation, microglial processes were found to make more contacts with smaller, weak synapses and microglia contained more structures associated with phagocytosis (Tremblay, Lowery and Majewska, 2010), suggesting that synapse strength and experience may alter microglial remodelling of synaptic structures.

Microglial activity has been shown to alter synaptic plasticity through the release of pro-inflammatory cytokines, reactive oxygen species (ROS) and neurotrophic factors (Vezzani and Viviani, 2015). Synaptic plasticity is the process by which synaptic activity modifies the strength or efficacy of existing synapses, affecting both the pre and post synaptic regions, contributing to learning and memory formation (Citri and Malenka, 2008).

Microglial brain-derived neurotrophic factor (BDNF) has been shown to promote the expression of glutamatergic receptor subunits at synapses in a learning-dependent manner in the developing mouse hippocampus and cortex (Parkhurst *et al.*, 2013). Depletion of microglia in this model, thus removing the BDNF source, reduced the number of learning-dependent glutamatergic excitatory synapses and resulted in a lower score in learning tasks. Glutamate-induced generation of ROS by microglia modulates synaptic plasticity by altering the expression of serine/threonine protein phosphatase 2A (PP2A) in neurons, which promotes the internalisation of AMPA receptors, weakening AMPA receptor mediated signalling (Collingridge and Peineau, 2014). Therefore microglia can contribute to glutamate-induced LTD, which could precede microglial pruning of these weakened synapses.

1.1.6 Microglial Activation

The M1/M2 paradigm of macrophage activation states (Mills *et al.*, 2000) is often also applied to microglia, in which activation is classified as classical, pro-inflammatory, neurotoxic M1 activation or alternative, anti-inflammatory, reparative M2 activation (Colton, 2009). M1 activation can be achieved *in vitro* through LPS and interferon-γ stimulation and results in the secretion of pro-inflammatory cytokines, including TNFα, IL-6 and IL-12, in addition to NADPH oxidase-mediated superoxide and reactive oxygen species (ROS) generation. Anti-inflammatory M2 activation is promoted by IL-4 and IL-13 signalling and induces IL-10 and TGF-β release, resulting in arginase 1 expression and the release of multiple growth and neurotrophic factors that are neuroprotective and encourage tissue repair, including insulin growth factor I (IGF-I), fibroblast growth factor (FGF), nerve growth factor (NGF) and BDNF.

This nomenclature has primarily been used to define the activity and the nature of microglia *in vitro*, however it has since been argued that advances in our abilities to study and model microglia, as well as the macrophages which were first defined as being either M1/M2, *in vivo* have rendered this bipolar framework redundant as ever increasing activation states and associated functions are identified (Martinez and Gordon, 2014; Ransohoff, 2016). Transcriptomic evidence has shown that microglial activation states are highly varied and, particularly in the context of neurodegenerative disease, are capable of expressing both M1 and M2 associated factors (Wes *et al.*, 2016). Therefore, it is difficult to justify the use a paradigm that restricts the activity of cells as plastic and varied as microglia into just two states. It is likely that microglial activity is more accurately represented as a spectrum of activation states that are heavily influenced by environmental and context-dependent signalling.

1.1.7 Microglia and Neurodegenerative Disease

Inflammation is widely recognised as a pathological component of most neurodegenerative diseases and, as microglia are the primary contributors of pro-inflammatory cytokines in the CNS, they are likely to be playing an active role in pathogenesis (Wolf, Boddeke and Kettenmann, 2017). Furthermore, due to the extensive influence of microglial activity on the developing and adult brain, it is not surprising that microglial dysfunction has been identified in a range of CNS diseases including Alzheimer's disease, Parkinson's disease, multiple sclerosis and amyotrophic lateral sclerosis (ALS). Expression in microglia of several risk alleles associated with progressive neurodegenerative diseases further supports a link between the innate immune response and pathogenesis (Gosselin *et al.*, 2017).

Microglia express a range of pattern recognition receptors PRRs that are capable of detecting DAMPs associated with neurodegenerative diseases, including misfolded and aggregated proteins, nucleic acids and apoptotic cells. It is postulated that in the early stages of disease, microglial phagocytic activity is neuroprotective, ensuring the clearance of apoptotic cells and pathological protein aggregates such as amyloid-β (Aβ) (Lee and Landreth, 2010). Indeed, knockout of the microglia-expressed chemokine receptor CCR2, which is thought to be important for microglial recruitment to areas of high pathology, resulted in increased pathology and mortality (El Khoury *et al.*, 2007). Furthermore, $C3^{-/-}$ mice, which are deficient in one of the key components required for complement mediated phagocytosis, had greater plaque loads and neuronal loss compared to C3 expressing mice in a model of Alzheimer's disease (Maier *et al.*, 2008), suggesting that microglial activity is neuroprotective in this context.

Ligation of PRRs by DAMPs is associated with continual release of pro-inflammatory mediators by microglia (Wolf, Boddeke and Kettenmann, 2017) that can lead to an augmented generation of pathological proteins, pro-inflammatory cytokines and apoptosis, thereby contributing to disease progression. In agreement with this, in a model of ALS, minimising microglial activation via inhibition of NF-κB signalling protected motor neurons from microglia-mediated neurotoxicity and improved transgenic mouse survival (Frakes *et al.*, 2014). Microglial processes essential for the development of neural networks or for defence from pathogens can become dysregulated following inflammatory or degenerative disease-associated priming of microglia, resulting in neurotoxicity and aberrant removal of viable neurons and synapses. Following LPS-induced inflammation or Aβ exposure, microglia have been shown to target viable cells rather than clearing apoptotic neurons, resulting in inappropriate phagoptosis and neuronal loss (Neniskyte, Neher and Brown, 2011; Fricker *et al.*, 2012). C1q, which plays a role in refining synaptic connectivity during CNS development, has been shown to be necessary for the toxic effects of Aβ on synapses, and C1q or C3 inhibition are protective against Aβ-induced microglial dysfunction in an AD model (Hong *et al.*, 2016). Furthermore, C1q has been shown to be associated with Aβ plaques in patient samples (Afagh *et al.*, 1996).

The net effect of microglia, in particular microglial activation, in neurodegenerative disease is contentious. It appears to be context dependent, as exemplified by conflicting results regarding the neuroprotective nature of C3 and complement mediated phagocytosis (Maier *et al.*, 2008; Hong *et al.*, 2016). As microglial activity is implicated in so many neurodegenerative diseases, greater understanding of how to appropriately control the activity of these cells in disease-specific contexts could prove to be significant for the development of therapies.

1.2 Models of Microglia

Microglial function has been studied *in vitro* for decades however, increasing evidence associating microglia-expressed genes with neurodegenerative diseases, including Alzheimer's disease, has recently been identified (reviewed by Villegas-Llerena et al. 2016), igniting the microglia field. Here the classic models for studying microglial function and also the emergence of iSPC models that have allowed the investigation of microglia in neurodegenerative diseases will be reviewed.

1.2.1 Primary Microglia

Despite making up approximately 15% of the cells in the CNS, microglia contribute to less than 0.1% of the protein and RNA, therefore, in order to obtain information on the expression and function of these rare cells, it is usual to study them in isolation. Studying cells *in vitro* allows the modification of conditions in isolation to establish the effects of individual factors, providing information on aspects such as activation, secretion and motility, which are difficult to monitor *in vivo*. Various methods for the extraction and culture of microglia from brain tissue samples have been developed and rely upon density gradient separation of glia from the rest of the CNS cell types. Mixed glial cultures can be generated from which microglia 'bud off' into the cell supernatant or magnetic bead separation based on cell-specific antibodies can be used to generate pure microglia cultures. Primary cell cultures are frequently used as they are thought to bear many similarities in phenotype and function to cells found *in vivo*. However, particularly in the case of human microglia, a lack of tissue availability represents a significant obstacle to performing these experiments. Human microglia have been isolated from biopsy and autopsy samples, however due to the scarcity of samples for immediate isolation post mortem it is difficult to get sufficient numbers for statistical analysis and yields from small pieces of biopsy tissue are too low for high throughput assays.

Monocyte derived macrophages are often used as a model of microglia due to similarities in function with the benefit of providing higher cell yields for study. Methods for the isolation of monocytes from blood samples are well established and easily performed and the collection of blood is non-invasive relative to brain biopsies. Monocytes are cultured for 7 days with macrophage colony stimulating factor (MSCF) to induce differentiation into macrophages, providing a source of human cells of the same myeloid origin as microglia. However, recent developments in the understanding of the ontogeny of microglia in the developing CNS have shown that microglia are derived from the yolk sac and migrate to the CNS prior to the closure of the blood brain barrier (BBB) (Ginhoux *et al.*, 2010, 2013) whereas blood monocytes are renewed by hematopoietic stem cells that populate the bone marrow after the closure of the BBB (Ginhoux *et al.*, 2010; Hoeffel *et al.*, 2015). Therefore, monocyte derived macrophages do not recapitulate the ontogeny of microglia and may not act as a suitable model of the yolk sac-derived microglia.

The majority of primary microglia cultures are derived from neonatal and adult rat and mouse brain tissue. Mammalian genomes are highly evolutionarily conserved so the

use of mouse and rat models has been extremely valuable for not only modelling development and disease *in vivo* but also providing tissue for the extraction of primary cells for studying microglia in isolation. Furthermore the development of transgenic animals in which specific genes have been modified in order to mimic previously identified disease-associated mutations or to facilitate observations of specific cell types, such as GFP-tagged CX_3CR1 for microglia (Jung *et al.*, 2000), have provided vast amounts of data that would not be attainable through the study of post-mortem human tissue alone.

There are disadvantages associated with the use of primary cells for the study of microglia including the ethical implications of using embryonic human and animal tissue as well as the use of animal tissue of any kind. Despite most human and mouse genes being orthologous, approximately 20% do not have a clear orthologue and 1% are without a homologue (Chinwalla *et al.*, 2002), therefore posing the question of whether animals should be sacrificed in order to provide cells that may not accurately express the genes of interest. Furthermore, analysis of human and mouse microglia showed that human microglia highly expressed 400 genes that were not in mouse microglia (Gosselin *et al.*, 2017), indicating that differences exist in the transcriptional mechanisms between these species. Other disadvantages to primary culture is that once isolated, microglia do not replicate so, in addition to being scarce in difficult to acquire tissue, the numbers of cells available to use for experiments are finite.

1.2.2 Immortalised Microglial Cell Lines

The use of immortalised cell lines overcomes several of the difficulties associated with primary microglia. Primarily, due to the immortalised nature of the lines, they are proliferative and provide large numbers of cells for high throughput assays, whilst also being derived from a single donor which minimises the number of embryos and animals that need to be sacrificed to derive the cell line from. The increased yield of cells allows more complex experiments such as genome editing, which can have very low efficiency rates so requires large numbers of cells for successful clones to be generated.

Several microglial cell lines of mouse and human origin have been generated by genetically immortalising primary microglia through the use of retroviruses. Two of the most frequently used are the murine BV2 and N9 microglial cell lines, which were both generated through transfection of mouse primary microglia with a retrovirus expressing the *v-myc* oncogene to induce immortalisation (Righi *et al.*, 1989; Blasi *et al.*, 1990). In a comparable manner to primary microglia, these cells have been shown to express

microglial markers, respond similarly to pro-inflammatory activation and perform phagocytic functions (Righi *et al.*, 1989; Blasi *et al.*, 1990; Kopec and Carroll, 1998; Fleisher-Berkovich *et al.*, 2010; Fu *et al.*, 2012).

The HM06 human microglia cell line was generated by transfection of primary human embryonic microglia cultures with a *v-myc* oncogene-expressing retroviral vector. This cell line has been shown to have similar gene expression responses to Aβ and LPS as found in primary cells as well as behaving as predicted in regards to cytokine release (Nagai *et al.*, 2001).

Despite their usefulness, all immortalised cell lines carry similar disadvantages that, as the technology for the generation of iPSC-derived cells improves, may render these cells no longer suitable as models for the study of microglia. Due to the immortalisation process, genetic footprints in the form of retroviral insertions into the genome are left behind. This insertional mutagenesis can alter the karyotype, phenotype, proliferation and gene expression of the cells, significantly altering them from the primary cells from which they were derived. Indeed, increased proliferation, altered adhesion and variable morphologies have been reported in mouse microglial cell lines (Horvath *et al.*, 2008) compared with primary microglia. Microglia in physiological conditions typically proliferate very slowly so these highly proliferative, immortalised cell lines do not accurately mimic the behaviour of the microglia *in vivo.*

1.2.3 Induced pluripotent stem cell (iPSC) models

In 2006, the method for the generation of induced pluripotent stem cells (iPSC) was first published (Takahashi and Yamanaka, 2006). These cells resembled embryonic stem cells (ESCs) and were generated from mouse embryonic and adult fibroblasts (Takahashi and Yamanaka, 2006). Protocols for the differentiation of iPSCs into virtually all somatic cell types, including microglia, are being developed, providing an extremely useful tool for modelling human cells and disease. In their ground-breaking paper, Takahashi and Yamanaka demonstrated that the ectopic expression of a few key transcription factors in somatic cells was sufficient to reprogram the cells to a pluripotent state. In order to develop their protocol, information was pooled from the past four decades of research into somatic cell nuclear transfer and ESC culture techniques (Yamanaka *et al.*, 2012).

ESCs had previously been the only source of pluripotent cells but are associated with a range of ethical issues and have extremely limited availability. Once methods had been developed for the isolation of both human and mouse ESCs (Evans and Kaufman,

1981; Martin, 1981; Thomson *et al.*, 1998), optimisation of culture methods was performed to identify the factors required for the maintenance of pluripotency. It has been established that in the case of mouse ESCs, LIF/Stat3 is required to maintain pluripotency (Smith *et al.*, 1988) and BMP4 can be used to block the MAPK/ERK differentiation signalling pathway and therefore maintain cell renewal (Qi *et al.*, 2004). Interestingly, the factors required to maintain pluripotency differ between mouse and human cells; human ESC require basic fibroblast growth factor to alter MAPK/ERK signalling (Xu *et al.*, 2005). Thus it was possible to isolate cells from the inner cell mass of explanted blastocysts that could either be differentiated into cells of the three germ layers or be cultured with the appropriate growth factors to maintain renewal and pluripotency. Following experiments performed initially in tadpoles (Gurdon, 1962) and later in mammals such as Dolly the sheep (Wilmut *et al.*, 1997), the observation that oocytes contain the necessary factors required to reprogram the genetic information found in the nuclei of differentiated somatic cells was incorporated with knowledge garnered from the discovery of the existence of master transcription factors (Davis, Weintraub and Lassar, 1987) to design experiments to identify the factors capable of inducing pluripotency in somatic cells.

Takahashi and Yamanaka generated a panel of 24 candidate genes that are found at high levels in pluripotent cells and, through the use of integrating retroviruses to express them in differentiated adult cells, were able to systematically narrow down the cocktail of genes required for expression of Fbx15, a gene essential for the maintenance of pluripotency not found in adult somatic cells. Thus, the essential combination of Klf4, Sox2, Oct4 and c-Myc, now known as the Yamanaka factors, was identified. The efficacy of this combination in reprogramming cells was confirmed by comparing the iPSCs to ESCs in a variety of assays: the gene expression profiles were assessed using DNA microarrays, the ability to form differentiated cells derived from all three germ layers was assessed by teratoma formation assays and the contribution to chimeric mice following injection into blastocysts was assessed by immunohistochemistry. These experiments together showed that only four factors were required to induce pluripotency in adult cells.

Only a year later, the Yamanaka group reported modifications of the mouse protocol for the generation of human iPSCs. Retroviral transduction and cell culture methods were optimised but the four key factors required for reprogramming were found to be the same (Takahashi et al. 2007a). Following this initial publication, various other combinations of transcription factors that are also able to induce pluripotency with similar efficacies have been discovered (Yu *et al.*, 2007; Buganim *et al.*, 2012;

Apostolou and Hochedlinger, 2013). This wide range of factors capable of reprogramming cells indicates that a lot more is to be learnt about the networks that allow cells to regain pluripotency through different signalling pathways.

Initially lentivirus or retroviruses were used to transfect cells with reprogramming factors but these viruses carry risks of insertional mutagenesis and integration of vectors into the genome. Modifications have therefore been made to transfection protocols in order to minimise the likelihood of integration whilst simultaneously increasing the efficacy of transfection. The adenovirus and the sendai virus have been used as alternatives because they are both non-integrating viruses, although reprogramming efficacies of adenovirus methods are only 0.0002% in human cells (Zhou and Freed, 2009) compared with the 0.02% found using retroviruses in the original protocols (Takahashi et al. 2007a). The sendai virus is one of the most commonly used methods (Hockemeyer and Jaenisch, 2016) as it is an RNA virus that does not enter the nucleus so can be diluted from cells through passaging, it generates large amounts of protein and has been shown to have an efficacy of approximately 1% in reprogramming fibroblasts (Fusaki *et al.*, 2009). The delivery of exogenous proteins to reprogram fibroblasts has also been trialled (Kim et al. 2009a) as well as synthesised mRNAs (Warren *et al.*, 2010) and episomal vectors (Yu *et al.*, 2009).

iPSCs offer a wide range of benefits over the use of primary cells and immortalised cell lines. By definition, these pluripotent cells are capable of being differentiated into virtually all cell types as well as being easily accessible and expandable, unlike most terminally differentiated primary cells. The use of somatic cells as a starting point means that ESCs are no longer required, avoiding any ethical issues and difficulties arising from a limited supply of embryos. Similar ethical advantages are found through the use of human iPSCs rather than animal model-derived primary cells, in addition to being more applicable for the study of human disease. This is particularly relevant in the case of neurodegenerative diseases such as AD where the accurate recapitulation of pathology in animal models has been challenging. Furthermore, if the differentiated cells are to be used for cell replacement therapies, the use of ESCs could result in immune rejection, which can be avoided through the use of self-derived cells for each individual patient. iPSCs generated from patients carrying disease-causing mutations are extremely useful for modelling and studying the mechanisms underlying disease, as well as screening potential drug therapies in the most relevant patient population. iPSC-derived neurons for cell replacement therapy have been trialled successfully recently in non-human primate models of Parkinson's disease (Kikuchi *et al.*, 2017) and could pave the way for the use of this technology in humans.

Through the modification of cell culture conditions, iPSCs can be differentiated in a multitude of different cell types, including microglia. The increasingly recognised role of microglia in neurodegenerative diseases has led to the publication in quick succession of multiple methods for iPSC-derived microglia-like cells in order to produce cells of human origin that avoid the karyoptic abnormalities of cell lines and the low yields of primary cells.

Initial efforts to generate iPSC-derived microglia involved driving embryoid bodies through neuronal differentiation (Almeida *et al.*, 2012), which does not represent the yolk sac ontogeny of microglia. The recapitulation of microglial yolk sac ontogeny is a key element in more recent microglia differentiation protocols; it is important that cells are Myb-independent and are not derived from monocytes in order to truly model microglial development. Human iPSC-macrophage differentiation protocols have been generated (Van Wilgenburg *et al.*, 2013), which, despite initially being described as a method to produce monocyte-derived macrophages, have been shown to produce cells that are Myb-independent (Hoeffel *et al.*, 2015; Buchrieser *et al.*, 2017) and thus model the primitive tissue macrophages that populate the brain during development. Other publications have since utilised this theory of generating Myb-independent macrophage precursors (Muffat *et al.*, 2016; Abud *et al.*, 2017; Haenseler *et al.*, 2017) and then utilising factors in the culture conditions to skew differentiation towards microglia of the CNS, rather than the Kuppfer cells of the liver or the Langerhans cells of the skin.

A differentiation protocol generated by Abud et al. incorporates factors that are secreted by other CNS cell types, including neurons, astrocytes and endothelial cells, to mimic the cues present during microglial development with the hypothesis that the inclusion of CX3CL1, CD200 and TGFβ will recapitulate the cellular interactions that influence microglial gene expression and function (Abud *et al.*, 2017). A more complex differentiation medium has been developed by Muffat et al. in which the concentrations of the various components are matched to those found in human CSF, which can be used for the differentiation of both neuronal and glial cultures (Muffat *et al.*, 2016). This multifaceted medium has also been shown to maintain primary microglial cultures for up to a month without passaging (Muffat *et al.*, 2016) demonstrating its successful recreation of the endogenous CNS environment. Co-culture with neurons has been shown to alter microglial gene expression, including the downregulation of early microglial genes which are typically expressed in iPSC-derived microglia generated in monoculture (Abud *et al.*, 2017). Muffat et al demonstrated that culturing iPSC-derived microglia with conditioned medium from differentiating neural cultures resulted in a shift in gene expression patterns away from foetal primary microglia and towards adult

primary microglia. The development of co-culture systems may therefore result in the generation of more mature genotypes and phenotypes in iPSC-derived microglia.

Published protocols differ in their medium definition with some containing serum, which can have batch variation, whilst others use defined factors to model the signals found in the extracellular milieu of the brain. Despite the use of different growth factors and variations in time frames, all protocols have the same aim; to define and recreate the endogenous environment of microglia in order to stimulate the differentiating cells with developmentally relevant cues in the hopes of producing the most microglia-like cells. The precise definition of microglia is not yet known so it is difficult to determine when successful recapitulation of this cell type has been performed. A unique gene expression signature capable of distinguishing microglia from peripheral monocytes and monocyte-derived macrophages (Butovsky *et al.*, 2014) is the current gold standard for determining the efficacy of iPSC differentiation protocols for the generation of microglia. The highly plastic nature of these cells means that challenges remain in defining the expression signature of physiological microglia though as the process of isolating the cells can have dramatic effects on their gene expression (Gosselin *et al.*, 2017).

1.2.4 CRISPR-Cas9 Genome Editing of Microglia

A benefit of iPSC-derived microglia-like cells over primary microglia is the ability to perform genome modification at the iPSC level, when the cells are more amenable to transfection. Genome editing can also be performed on differentiated iPSC-derived microglia, primary cells and microglial cell lines although large numbers of cells are needed because the transfection efficiencies are low, likely due to the recognition and clearance of foreign DNA and RNA via microglial pathogen-associated molecular pattern responses. Genome editing can provide cell models in which a specific gene of interest is knocked down or knocked out through disruption or removal of regions of the DNA sequence. These knockout models are useful for understanding the function of the gene products and also can be used to model disease in which loss of function mutations are found. Various methods of genome editing for the knockdown of gene expression exist including RNA interference, transcription activator-like effector nucleases (TALENs), zinc finger nucleases (ZFNs) and finally CRISPR (clustered regularly interspaced short palindromic repeats)/Cas9 technology, which has greater cleavage efficiency and is easier to design and generate.

CRISPR is a component of the bacterial adaptive immune system (Barrangou *et al.*, 2007) which acts to protect against viruses and plasmids through the acquisition of

DNA fragments from invading pathogens into CRISPR arrays in the host genome (Bhaya, Davison and Barrangou, 2011; Wiedenheft, Sternberg and Doudna, 2012). These protospacers are then transcribed to generate CRISPR RNAs (crRNAS) that allow direct cleavage by Cas (CRISPR-associated) proteins of the invading RNA or DNA through complementary base pairing to the invading targets. The Cas9 protein is an RNA-guided DNA endonuclease that can be reprogrammed to make site-specific DNA breaks by interacting with single guide RNA (sgRNA) designed to be complementary by Watson-Crick base pairing to a region of the gene of interest (Jinek *et al.*, 2012). This sgRNA replaces the invading RNAs that are endogenously incorporated in to the CRISPR machinery in order to recognise and attack pathogen DNA. Thus Cas9 introduces a blunt double stranded break in DNA that complements the 20nt sequence in the sgRNA, triggering enzymes to repair the break at the cleavage site by non-homologous end joining, disrupting the sequence of the target DNA and therefore expression of the gene of interest. The discovery of the ability to easily modify this prokaryotic immune response mechanism in order to perform precise, sequence-specific targeting of DNA regions of choice has opened up a wealth of opportunities for basic biology and translational research.

Modifications have been made to the Cas9 protein to function as a nickase (nCas9) by incorporating an inactivating mutation allowing the generation of staggered rather than blunt breaks in both strands of the target DNA. The use of paired guide RNAs and engineered nCas9 results in enhanced specificity and fewer off target effects (Cho *et al.*, 2014; Shen *et al.*, 2014). The staggered DNA breaks facilitate the insertion of repair DNA in the correct orientation during homology-directed repair, allowing the insertion of specific point mutations which is frequently used in order to study or repair disease-associated mutations. This genetic editing can be performed on individual cells to generate lines carrying the genetic modifications or can be used to generate new animal models carrying specific mutations.

Increasing numbers of groups are now utilising CRISPR/Cas9 to generate new models of microglia. Kleinberger et al used CRISPR/Cas9 to insert a frontotemporal dementia and Nasu-Hakola disease-associated mutation into the *Trem2* gene to generate transgenic mice, from which primary microglia were isolated for experiments investigating the functional effects of the T66M mutation (Kleinberger *et al.*, 2017). RANK knockout BV2 microglia cell lines have also been generated to determine the role of RANK signalling in modifying microglia responses to TLR3/4 signalling (Kichev *et al.*, 2017). CRISPR/Cas9 has also been used in iPSC-derived tissue macrophages to demonstrate that they mimic the ontogeny of microglia (Buchrieser *et al.*, 2017). The

list of publications demonstrating the usefulness of this technology for generating new models of iPSC-derived, primary and immortalised microglia will no doubt continue to grow as CRISPR/Cas9 technology becomes increasingly accessible and widespread.

1.3 Alzheimer's Disease

First described by German psychiatrist Alois Alzheimer in a 50 year old female patient in 1901, Alzheimer's disease is the most common form of dementia, with over 46.5 million people diagnosed with the disease worldwide and 13% of people aged 60 or over requiring long-term care. The prevalence of AD is expected to triple by 2050 to 130 million, according to the World Alzheimer's Report in 2016. AD is a progressive neurodegenerative disorder characterised by cognitive impairment and histopathological hallmarks of extracellular Aβ plaques and hyperphosphorylated tau-associated neurofibrillary tangles, in addition to brain shrinkage and loss of synapses and neurons, particularly in the hippocampus and cerebral cortex (Huang and Mucke, 2012). Patients present with symptoms of memory loss and other cognitive declines, however it is thought that the causal neuronal loss and brain atrophy commences up to 20 years prior to the deterioration of memory function. Despite extensive research into the field, at the moment there is no cure to halt disease progression with currently approved therapies only providing transient symptomatic relief.

AD cases can be categorised in to two main groups depending on the age of symptom onset: late onset Alzheimer's disease (LOAD) and early onset Alzheimer's disease (EOAD). Only 1-2% of all AD cases are classed as EOAD, characterised by an age of onset of less than 65 (Rogaeva, 2002). LOAD is far more common, with 50% of people over the age of 85 suffering from the disease.

Genetic linkage analysis of families affected by EOAD allowed the identification of pathogenic variations in three key genes: *Amyloid precursor protein (APP)* (Goate *et al.*, 1991), *Presenilin 1 (PSEN1)* (Sherrington *et al.*, 1995) and *Presenilin 2 (PSEN2)* (Sherrington *et al.*, 1996). These rare autosomal dominant mutations alter the production of Aβ, providing evidence for the importance of Aβ in AD pathogenesis. APP is proteolytically cleaved by α-, β- and γ-secretases to form both non-pathogenic fragments (sAPPα and C-terminal fragments) and Aβ peptides of varying length with varying propensity to aggregate. $A\beta_{1-42}$ constitutes 10% of the Aβ species, is the most aggregation prone form and is found in the AD-associated Aβ plaques. Both presenilin proteins are found in the γ-secretase complex, responsible for catalysing the generation of Aβ through APP cleavage. Mutations in *PSEN1* or *PSEN2* affect APP cleavage and result in increased $A\beta_{1-42}$ generation.

Mechanisms of AD pathogenesis are not fully known but an imbalance of Aβ processing and clearance is thought to result in the formation of the hallmark senile plaques. Aβ oligomers, which are the building blocks of the fibrillar plaques, impair the proper functioning of synapses, altering neuronal signalling as well as triggering the activation of microglia, resulting in the release of neurotoxic inflammatory mediators (Reviewed by Selkoe 2002). The dysfunction and loss of synapses and dendritic spines are thought to be some of the earliest stages of AD pathology and ultimately lead to cognitive impairment. The pathogenesis of AD does not only silence neurons and their networks, but also causes atypical network activity thought to disrupt complex processes essential for learning and memory, which may result in excitotoxic cell death (Huang and Mucke, 2012).

LOAD is a genetically complex, heterogeneous disease and multifaceted interactions between multiple risk factors, including genetic, epigenetic and environmental aspects, are likely to exist. Twin studies have indicated that 60-80% of LOAD risk is inherited (Gatz *et al.*, 2006), leaving a considerable proportion of AD susceptibility resulting from non-genetic risk factors. Age is the greatest non-genetic risk factor for the development of AD with other environmental risk factors including head injury, low education levels, vascular risk factors, lifestyle choices and depression (Jiang *et al.*, 2013).

The *Apolipoprotein E*4 (*APOE ε4*) allele has been identified as a strong genetic risk factor for the development of both familial and sporadic EOAD and LOAD (Saunders *et al.*, 1993). Indeed, it is the greatest genetic risk factor for the development of LOAD and has a gene-dose effect on increasing risk and lowering the age of disease onset (Corder *et al.*, 1993). Heterozygous carriers of the *APOE ε4* allele have a 3-fold increased risk for AD, which increases to 15-fold for those who are homozygous, whilst the *ε2* allele has protective effects (Corder *et al.*, 1993; Saunders *et al.*, 1993). ApoE is a glycoprotein that plays a role in cholesterol transport and metabolism, and supports neuronal growth, tissue repair responses, immunoregulation and contributes to the clearance of soluble and aggregated Aβ. The ApoE4 isoform is less effective at this Aβ clearance (Deane *et al.*, 2008), whilst simultaneously promoting Aβ deposition through modifying γ-secretase activity via lipid environment dysregulation (Osenkowski *et al.*, 2008). Furthermore, under stress, neurons upregulate expression of ApoE to facilitate neuronal repair, however, ApoE4 is more susceptible to proteolytic cleavage than other isoforms resulting in the generation of neurotoxic fragments that cause tau pathology and mitochondrial damage (Huang, 2006). The *APOE ε4* allele is not an invariant cause of AD and is thought to act concurrently alongside other environmental or genetic risk factors to cause disease.

These four aforementioned AD genes account for less than 30% of the genetic variance found in EOAD and LOAD (Guerreiro, Gustafson and Hardy, 2012). Thanks to genome wide association studies (GWAS) and whole genome/exome sequencing, at least 20 additional genetic risk factor variants for LOAD have now been identified (Van Cauwenberghe, Van Broeckhoven and Sleegers, 2016). Many of these risk variants have been found to cluster in several common physiological pathways, highlighting and confirming three pathobiological processes that have previously been thought to contribute to the development of AD (Guerreiro and Hardy, 2014): the immune system and the inflammatory response; cholesterol and lipid metabolism; and endosomal vesicle recycling.

Recently, common variances in the receptors CR1 (Lambert *et al.*, 2009) and TREM2 (Jonsson et al. 2013; Guerreiro et al. 2013a) have been identified as risk factors for LOAD. A copy-number variation in the intronic region of the gene encoding CR1 was identified by GWAS and is thought to alter protein isoform expression (Brouwers *et al.*, 2012). A low frequency, rare TREM2 AD risk variant was identified through exome sequencing following the discovery of homozygous TREM2 mutations in dementia families presenting with other disease phenotypes (Guerreiro et al. 2013a). The heterozygous R47H TREM2 mutation was the first gene with a moderate risk effect on AD (OR>3) to be identified since *APOE ε4.*

Both CR1 and TREM2 are thought to be expressed on microglia and play important roles in directing microglial and immune activation cascades. Inflammation is essential in the healthy brain for the removal of debris, apoptotic cells and, in the case of AD, Aβ. The failure of a clinical trial of anti-inflammatory medication in AD patients demonstrated that low-levels of immunological and inflammatory activity are essential for tackling the disease (Imbimbo, 2009). However, prolonged inflammation, often attributed to chronic microglial activation, is neurotoxic and implicated in the pathogenesis of multiple neurodegenerative diseases, including AD (Eikelenboom *et al.*, 2006).

1.3.1 The Role of Microglia in Alzheimer's disease

The amyloid cascade hypothesis, which has been the major AD pathogenesis theory since first being described by Hardy and Higgins in 1992, posits that Aβ deposition and accumulation precedes the formation of neurofibrillary tangles, the loss of synapses and neurons, and cognitive decline found in AD (Hardy and Higgins, 1992). However, increasing genetic, clinical trial and experimental evidence suggest that

neuroinflammation, rather than simply being an epiphenomenon, plays a crucial role in driving and maintaining AD pathogenesis. It has even been suggested that immune processes are capable of inducing AD pathology independently of Aβ by inducing neurodegeneration and neuronal cell loss (Heppner, Ransohoff and Becher, 2015). Inflammation in the brain is typically attributed to microglial activity and recent GWAS have highlighted several mutations linked to increased LOAD risk in genes which encode microglial expressed proteins including *CR1, CD33, MSA4, CLU, ABCA7, HLA-DRB5-HLA-DRB1* and *APOE* (Reviewed by Villegas-Llerena et al. 2016).

AD pathology-associated microglia were first described nearly 100 years ago during the initial observations of microglia by del Rio Hortega and Penfield. The presence of microglia surrounding Aβ plaques and neurofibrillary tangle-bearing neurons in the AD patient brains is near universal (Mrak, 2012). The lesion-associated microglia are typically found in an activated state, which is associated with the release of pro-inflammatory cytokines. Multiple cytokines are known to be upregulated in both the human AD brain and cerebrospinal fluid (CSF), and in AD mouse models, including IL-1, IL-6, IL-8, IL-12, TNFα, MIP1α, IL-23 and MCSF (Griffin *et al.*, 1989; Walker, Kim and McGeer, 1995; Meda *et al.*, 1999; Lue *et al.*, 2001; Patel *et al.*, 2005). Microglial activation has been shown to correlate with AD pathology load and clinical scoring of dementia (Xiang *et al.*, 2006). Furthermore, conditions that increase the risk of the development of AD, including head injury, diabetes, vascular disease and normal aging are also associated with microglial activation (Griffin *et al.*, 1994; Sheng, Mrak and Griffin, 1998; Valente *et al.*, 2010).

There are two primary routes through which Aβ is removed: proteolytic degradation by enzymes such as neprilysin and insulin degrading enzyme, or uptake by astrocytes and microglia for intracellular degradation. As microglia are capable of producing these extracellular proteases and express receptors that recognise Aβ for phagocytosis and macropinocytosis, they are capable of exerting protective effects through both of these Aβ clearance pathways (Lee and Landreth, 2010). There are numerous receptors expressed on the surface of microglia that bind to both soluble and fibrillar Aβ including CD14, CD36, CD47, α6β1 integrin, class A scavenger protein, RAGE and TLRs (Heppner, Ransohoff and Becher, 2015) resulting in a range of microglial responses including the production of inflammatory cytokines.

Aβ deposition induces reactive microgliosis; the expansion and activation of brain-resident microglia. Knockout of chemokine receptors, such as CCR2, has been shown to increase Aβ deposition and accelerate mortality in mouse AD models (El Khoury *et al.*, 2007), suggesting that recruitment of microglia is protective through Aβ clearance.

Paradoxically, during the late stages of disease, the build-up of Aβ continues despite increasing numbers of microglia, likely due to prolonged microglial exposure to Aβ and plaque-associated cytokines causing microglial functional impairment (Heneka *et al.*, 2015). Aβ-induced phenotypic changes result in microglia becoming overwhelmed and contributing to disease progression by inducing the adoption of a pro-inflammatory phenotype and the release of further cytokines. In turn, these cytokines downregulate both the microglial receptors responsible for Aβ phagocytosis and also Aβ-degrading enzymes (Hickman, Allison and El Khoury, 2008).

Moreover, the pro-inflammatory molecules secreted by Aβ-activated microglia further increase the activity and expression of the γ- and β-secretases that generate Aβ (Hong *et al.*, 2003; Liao *et al.*, 2004), exacerbating the accumulation of toxic Aβ. Consequently, the toxic effects of microglial inflammatory responses are twofold: firstly by promoting neurotoxic, pro-inflammatory cytokine and reactive oxygen species generation and secondly by inducing the further generation of Aβ, generating a feedback loop that accelerates pathology. Furthermore, the microglial dysfunction may further damage cells via a loss of physiological functions such as tissue homeostasis and provision of supportive trophic factors, resulting in additional loss of neuronal integrity throughout the course of disease (Heppner, Ransohoff and Becher, 2015).

Therefore, microglia play a dichotomous role in the pathogenesis of AD. In the early stages of disease, microglia help to clear Aβ however, this ability declines with time. Chronic Aβ accumulation drives microglial activation resulting in the generation of a proinflammatory environment that is capable of propagating further inflammation, Aβ-accumulation, microglial dysregulation and ultimately augmented disease progression.

1.4 TREM2

TREM2 has been known to play a role in neurodegeneration since the discovery that homozygous mutations cause a form of early onset dementia known as polycystic lipomembranous osteodysplasia with sclerosing leukoencephalopathy (PLOSL), or Nasu Hakola Disease (Paloneva *et al.*, 2002). However, huge interest in the gene expression and function was only sparked upon identification of TREM2 variants as risk factors for Alzheimer's disease (Guerreiro et al. 2013a; Jonsson et al. 2013). Mutations in the TREM2 gene have also been identified in other neurodegenerative diseases suggesting that immune dysregulation through alterations to TREM2 function could be a primary contributor to the pathogenesis of multiple neurodegenerative diseases.

As the name suggests, Triggering Receptor Expressed in Myeloid Cells 2 (TREM2) is expressed on the surface of many myeloid cells including dendritic cells, granulocytes, monocyte-derived macrophages, tissue resident macrophages, osteoclasts and microglia. TREM2 is also reported to be expressed on circulating monocytes (Hu *et al.*, 2014; Chan *et al.*, 2015) but evidence is conflicting (Forabosco *et al.*, 2013; Song *et al.*, 2017). RNA sequencing data indicates that in the CNS, under steady-state conditions, TREM2 RNA is specifically expressed only in microglia (Butovsky *et al.*, 2014). Indeed, when microglia are depleted from the brain, TREM2 expression in the brain is eliminated (Hsieh *et al.*, 2009; Thrash, Torbett and Carson, 2009; Elmore *et al.*, 2014). TREM2 is one of the highest expressed receptors in microglia (ranked at 31) and is expressed 300 times higher in microglia compared with astrocytes (Hickman and El Khoury, 2014).

The TREM gene family encodes for three receptors each with an immunoglobulin superfamily domain in their extracellular domain. The *TREM2* gene is found on chromosome 6p21.1 and encodes for 5 exons that are translated into a 230 amino acid long transmembrane glycoprotein consisting of an extracellular Ig-like domain, a transmembrane domain and a cytosolic tail. The intracellular region lacks a cytoplasmic signalling element so is reliant on the signalling capacity of its transmembrane adaptor protein, DNAX-activating protein of 12kDa (DAP12; also known as tyrosine kinase binding protein, TYROBP) (Daws *et al.*, 2001). DAP12 signalling results in Src-family mediated phosphorylation of ITAM (immunoreceptor tyrosine-based activation motif) domains, subsequent Syk recruitment and the activation of downstream signalling mediators (Figure 1.1). DAP12 is the only adaptor protein associated with TREM2, however DAP12 couples to other receptors, including CSF1R, members of the lectin family and the Ig superfamily, including TREM1 (Hamerman *et al.*, 2009).

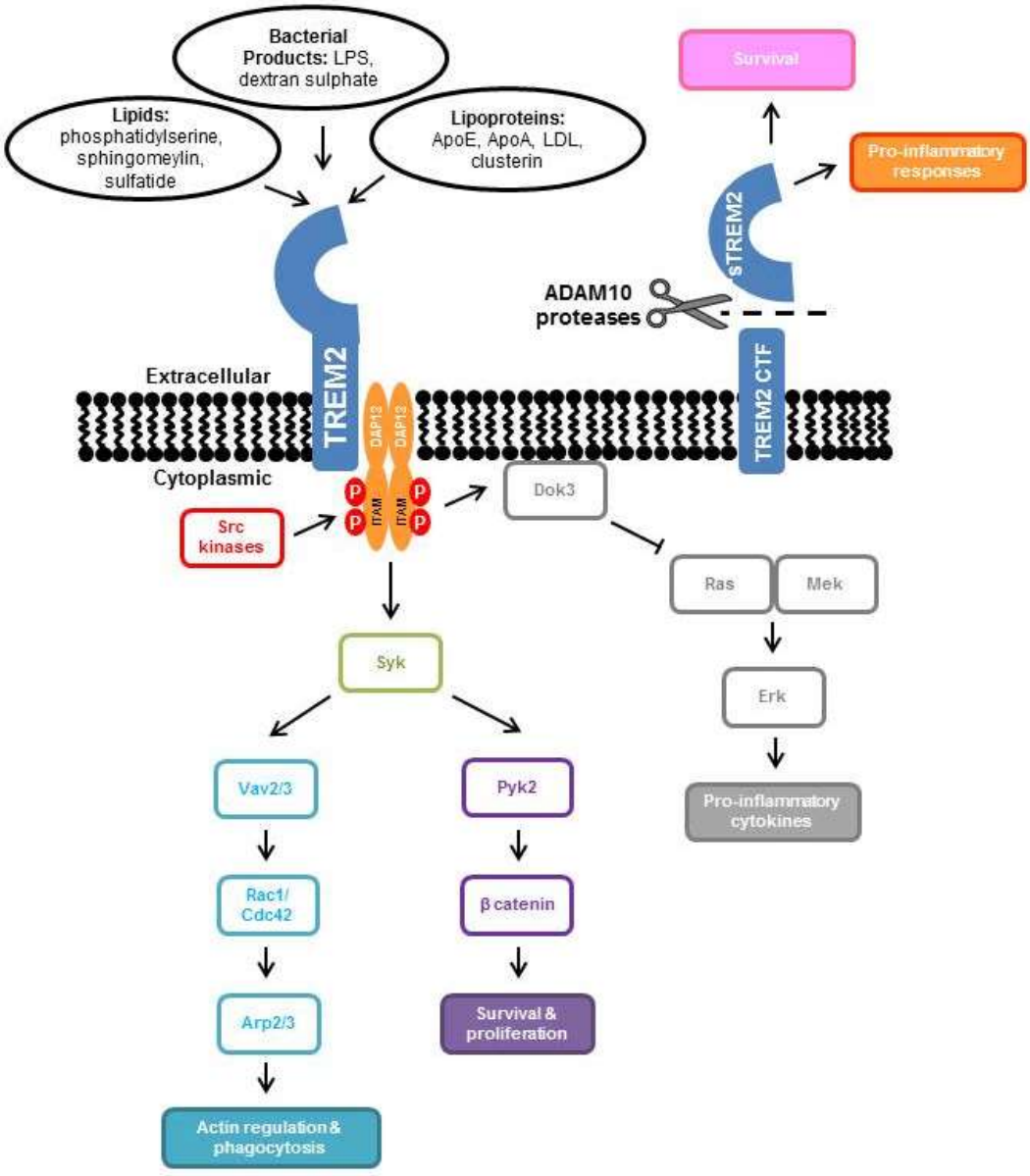

Figure 1.1 Summary of proposed TREM2 ligands, signalling and function

TREM2 expression is widely distributed with high levels in the white matter, hippocampus and neocortex (Guerreiro et al. 2013a). Expression levels increase with age in the human brain (Forabosco *et al.*, 2013) and correlate with aging in mouse models (Jiang et al. 2014a; Raha et al. 2017). TREM2 expression is highly responsive to inflammation, injury and disease-associated stimuli although marked differences are found between responses *in vitro* and *in vivo*. *In vitro* stimulation with pro-inflammatory factors such as TNFα, IL-1β, LPS and IFNγ cause a decrease in TREM2 expression

levels (Bouchon *et al.*, 2001; Turnbull *et al.*, 2006; Zheng *et al.*, 2016), whereas conditions of inflammation *in vivo* including sepsis, macular degeneration, traumatic brain injury, stroke and models of demyelination lead to augmented TREM2 levels (Kawabori et al. 2015; Chen et al. 2013; Bhattacharjee et al. 2016; Saber et al. 2017; Takahashi et al. 2007b). These contrasting effects could be due to recruitment of other cell types to sites of inflammation in vivo, which provide additional sources of TREM2 expression, or due to alterations to cell expression signatures following isolation for *in vitro* analysis (Bohlen *et al.*, 2017; Gosselin *et al.*, 2017).

Endogenous ligands of TREM2 have not been categorically identified but are thought to include anionic and zwitterionic lipids (Wang *et al.*, 2015), highly anionic bacterial products such as dextran sulphate (Daws *et al.*, 2003) and lipoproteins including ApoA-1, clusterin, low-density lipoprotein and ApoE (Atagi *et al.*, 2015; Bailey, DeVaux and Farzan, 2015; Yeh *et al.*, 2016; Jendresen *et al.*, 2017). Putative TREM2 ligands have been found on primary neurons and neuronal cell lines, which increase significantly following induction of apoptosis (Hsieh *et al.*, 2009). The TREM2/DAP12 complex was later shown to be activated by cell membrane components that become exposed during neuronal death and degeneration including sulfatide, sphingomyelin, phosphatidylserine and myelin lipids (Poliani *et al.*, 2015). The binding of TREM2 to lipids that are exposed during neuronal cell death, which also associate with fibrillar Aβ, suggests TREM2 may detect local cell damage, promoting microglial responses to Aβ accumulation and cellular toxicity (Wang *et al.*, 2015). TREM2 reporter assays suggest that Aβ alone does not result in TREM2 activation however, interestingly, ApoE is capable of binding to both Aβ (Atagi et al. 2015; Kim et al. 2009b) and apoptotic cells (Atagi *et al.*, 2015). Thus, if ApoE is a ligand of TREM2 it may act as an intermediary enabling TREM2 recognition and uptake of these factors.

A key function of TREM2 is phagocytosis signalling. Overexpression of FLAG-tagged TREM2 and subsequent FLAG antibody-mediated crosslinking induces actin cytoskeletal reorganisation and phagocytosis of microsphere beads in a DAP12 dependent manner (Takahashi, Rochford and Neumann, 2005). TREM2-mediated phagocytosis requires Src kinase phosphorylation of DAP12, Syk recruitment and downstream GTPases Rac1 and Cdc42 (N'Diaye *et al.*, 2009), which are activated by Vav (Turner and Billadeau, 2002). Subsequently, Arp2 has been identified, along with the genes encoding the other components of phagocytic signalling, as being highly connected to *TREM2* expression (Forabosco *et al.*, 2013). Phagocytic deficits in TREM2-lacking cells have been reported in studies utilising a range of substrates including apoptotic neurons (Takahashi, Rochford and Neumann, 2005; Atagi *et al.*,

2015), bacterial products (Kleinberger *et al.*, 2014; Gawish *et al.*, 2015), Aβ (Jiang et al. 2014a; Kleinberger et al. 2014) and lipids (Yeh et al. 2016; Park et al. 2015b). The role of TREM2 in phagocytosis is further demonstrated by overexpression or activation of the receptor resulting in augmented uptake of Aβ, apoptotic neurons and other cellular debris (Melchior et al. 2010; Takahashi et al. 2005; Takahashi et al. 2007b). Furthermore, transfection of CHO cells with a TREM2/DAP12 chimera expression construct was sufficient for enabling phagocytosis of bacteria by these endogenously non-phagocytic cells (N'Diaye *et al.*, 2009).

Typically TREM2 has been viewed as playing a critical role in the regulation of pro-inflammatory genes. However, there appears to be a complex interplay of stimulation, cell type and disease condition which results in TREM2 induction of pro-inflammatory effects in certain conditions (Jay et al. 2017b). *In vitro*, TREM2 signalling has anti-inflammatory effects as demonstrated by TREM2 knockdown resulting in increased expression of iNOS, TNFα, IL-6 and IL-1β following stimulation with apoptotic cells (Takahashi, Rochford and Neumann, 2005), TLR2/6, 9 and 4 ligands (Hamerman et al. 2006; Takahashi et al. 2007b) and Aβ (Jiang, et al. 2014b). Downstream of TREM2, anti-inflammatory signalling is reported to be mediated via DAP12 ITAM association with Src-phosphorylated Dok3, which becomes trapped at the cell membrane and thus is unavailable for interactions with Ras-Mek, reducing the activation of Erk and downstream transcription of pro-inflammatory cytokines (Peng *et al.*, 2013). Furthermore, in models of aging, siRNA mediated knockdown of TREM2 resulted in significant increases in brain TNFα and IL-6 expression (Jiang et al. 2014a; Jiang et al. 2015). TREM2 overexpression in AD models of Aβ and tau was shown to result in reduced expression of mRNA encoding inflammatory factors and had neuroprotective effects on synaptophysin expression and pathology-related neuronal loss (Jiang et al. 2014b; Jiang et al. 2016b).

However, other data conflicts with this suggestion of anti-inflammatory TREM2 activity, including decreased transcription of inflammation associated genes in TREM2 knockout AD models (Wang et al. 2015; Jay et al. 2015; Jay et al. 2017a) and diminished pro-inflammatory cytokine release in TREM2-deficient models of TBI, ischemia and demyelination (Sieber *et al.*, 2013; Poliani *et al.*, 2015; Saber *et al.*, 2017). Conflicting results may result from analysis being conducted on whole tissue versus individual cell types in isolation. As mentioned previously, significant alterations to gene expression are found in cells that have been isolated (Bohlen *et al.*, 2017; Gosselin *et al.*, 2017), which may also explain these discrepancies.

TREM2 has also been reported to affect myeloid cell proliferation and survival. Modulation of TREM2 expression has shown varying effects on cell number in physiological conditions (Paloneva *et al.*, 2003; Humphrey *et al.*, 2006; Zheng *et al.*, 2016) however, it has a marked impact on myeloid cell expansion in response to inflammation and disease. A lack of TREM2 resulted in blockade of proliferation in models of traumatic brain injury, ischaemia and aging (Kawabori *et al.*, 2015; Poliani *et al.*, 2015; Saber *et al.*, 2017). In models of AD, decreased numbers of microglia were found associated with Aβ plaques in TREM2 knockdown and knockout brains (Wang et al. 2015; Yuan et al. 2016; Ulrich et al. 2014; Jay et al. 2017a). Whether this is due to the decreased overall number of microglia that has been reported in some TREM2$^{-/-}$ AD mice (Wang *et al.*, 2015, 2016) or due to a loss of cells in the plaque specific regions is not yet known (Yuan et al. 2016; Jay et al. 2017a).

Evidence for a role of TREM2 in cell survival has also been identified which could explain why TREM2 deficient models have decreased accumulation of myeloid cells in the toxic, inflammatory environment surrounding Aβ plaques. TREM2 knockout cells were found to have augmented levels of apoptosis markers including caspase 3, annexin V and TUNEL positivity (Otero *et al.*, 2012; Wu *et al.*, 2015), as well as decreased expression of survival pathway factors (Zheng *et al.*, 2017). Equally, TREM2 activation promoted survival of dendritic cells and osteoclasts (Bouchon *et al.*, 2001). The anti-apoptotic signalling of TREM2 was marked in cells undergoing MCSF-starvation induced cell stress, in which microglia and bone marrow derived macrophages were more likely to undergo apoptosis if TREM2 was abrogated, when compared with wildtype cells (Wang *et al.*, 2015; Wu *et al.*, 2015). MSCF and its receptor CSF1R are thought to be important for TREM2/DAP12 survival signals as DAP12 phosphorylation is required for the subsequent Pyk2-dependent β-catenin activation (see Figure 1.1) (McVicar and Trinchieri, 2009; Otero *et al.*, 2009, 2012). TREM2 has recently been further linked to β-catenin signalling through the stabilisation of the protein and therefore the promotion of the survival-associated Wnt signalling pathway (Zheng *et al.*, 2017).

Full length, surface-expressed TREM2 undergoes sequential regulated intramembrane proteolysis (RIP) by ADAM10 and γ-secretase (Wunderlich *et al.*, 2013; Kleinberger *et al.*, 2014) to generate soluble TREM2 (sTREM2). The catalytically active components of the γ-secretase complex are presenilins-1 & -2, both of which have been linked to AD via altered Aβ generation pathways. Inhibition of γ-secretase leads to accumulation of TREM2 c-terminal fragments (CTFs) tethered at the cell surface, which trap and impair DAP12 signalling with full-length TREM2 (Wunderlich *et al.*, 2013). The role of γ-

secretase in TREM2 processing provides evidence of a functional connection between two identified pathways in AD pathogenesis. Disease-associated TREM2 variants R47H, T66M and Y38C alter the generation of sTREM2 in *in vitro* models (Kleinberger *et al.*, 2014; Piccio *et al.*, 2016). Decreased levels of sTREM2 are also found in the CSF of T66M heterozygous and homozygous carriers compared to age and gender matched control individuals (Kleinberger *et al.*, 2014; Piccio *et al.*, 2016).

The function of sTREM2 is not yet known but the fact that it is generated physiologically and upregulated during inflammatory disease (Heslegrave *et al.*, 2016; Piccio *et al.*, 2016) suggests that it may play a role in TREM2 signalling. Treatment with sTREM2 resulted in increased survival in microglial cell lines (Zhong *et al.*, 2017) and bone-marrow derived macrophages (Wu *et al.*, 2015), including those that were deficient in TREM2, suggesting that sTREM2 signalling does not require full length TREM2 to function. In addition to improving microglial survival, sTREM2 treatment caused a proinflammatory response in primary cultured microglia and in the hippocampus of mice injected with sTREM2 (Zhong *et al.*, 2017). Interestingly, CSF levels of sTREM2 have been found to peak specifically at the early symptomatic stages of AD (Suárez-Calvet et al. 2016a; Suárez-Calvet et al. 2016b), suggesting that increased sTREM2 generation may be a responses to early stage AD pathology.

Variants in TREM2 have been identified as genetic risk factors for a range of neurodegenerative diseases including Alzheimer's disease, Parkinson's disease, amyotrophic lateral sclerosis (ALS), frontotemporal dementia (FTD) and Nasu Hakola disease (Guerreiro et al. 2013a; Guerreiro et al. 2013b; Cady et al. 2014; Thelen et al. 2014; Rayaprolu et al. 2013; Jonsson et al. 2013). All TREM2 variants associated with these neurodegenerative diseases are thought to cause loss of receptor function (Jay et al. 2017b). The association of TREM2 with multiple neurodegenerative diseases indicates that it may play an important role in the common biological pathways that underlie multiple pathologies.

Links have also been identified between TREM2 and other genes associated with AD and neurodegeneration. CD33, variants in which have also been associated with AD, has been reported to modulate TREM2 expression, such that variants increasing monocyte expression of CD33 exhibit decreased levels of TREM2 (Chan *et al.*, 2015). MSA4, SNPs in which have recently been identified as conferring risk for AD (Lambert *et al.*, 2013), may play a role in regulating TREM2 expression as carriers of AD-associated SNPs have altered CSF levels of sTREM2 (Piccio *et al.*, 2016). Furthermore MSA4 expression is augmented on monocytes isolated from carriers of TREM2 variants (Piccio *et al.*, 2016). Furthermore ApoE, the greatest risk factor for

LOAD, is also a putative TREM2 ligand (Atagi *et al.*, 2015; Bailey, DeVaux and Farzan, 2015).

A link between TREM2 and neurodegenerative diseases was first identified in Nasu-Hakola patients carrying homozygous TREM2 and DAP12 mutations (Paloneva *et al.*, 2002). Nasu-Hakola patients present typically with bone-cysts and fractures, and early onset dementia around the age of 30 and a life expectance of 40-50 years. Despite the characteristic bone features, Nasu-Hakola can also occur in the absence of osteopathic symptoms (Bock *et al.*, 2013; Yamazaki *et al.*, 2015). To date multiple variants have been identified as causing Nasu-Hakola disease including E14X, W44X, T66M, W50C, W78X, D134G and K186N (Guerreiro et al. 2013b; Paloneva et al. 2002; Dardiotis et al. 2017).These predicted autosomal recessive loss of function mutations are thought to cause the disease manifestations by affecting osteoclasts and microglia, both myeloid lineage cell types. Pronounced inflammatory responses are found including microgliosis and astrocytosis (Satoh *et al.*, 2011) and neuropathological hallmarks comprise of axonal degeneration, white matter loss in the corpus callosum and basal ganglia, and cortical atrophy (Paloneva *et al.*, 2001; Bianchin *et al.*, 2004; Sasaki *et al.*, 2015). The manifestation of Nasu-Hakola disease in the CNS has provided insight into TREM2 function and has indicated that TREM2 activity is important for normal brain function and cognition.

Analysis of dementia families has also identified TREM2 variants previously linked to NHD as risk factors for FTD/FTLD, both in homozygosity or heterozygosity. These variants include T66M, W198X, Q33X and Y38C (Guerreiro et al. 2013b; Giraldo et al. 2013). However, it is not yet clear whether TREM2 mutations increase the risk of FTD in the general population.

1.4.1 TREM2 in Alzheimer's Disease

A rare missense mutation (rs75932628-T) in the TREM2 gene, conferring an arginine-47-histidine (R47H) substitution, was identified as causing a substantial increase in risk of developing AD (Guerreiro et al. 2013a; Jonsson et al. 2013). In simultaneously published reports, the R47H TREM2 variant was identified by GWAS (Jonsson *et al.*, 2013) and by exome and Sanger sequencing (Guerreiro et al. 2013a). From pooling further studies, it is thought that variants are rare (population frequency of 0.3%) but the effect size is high (odds ratio >3) which is similar to that of a single copy of the ApoE ε4 allele. So far, five further variants have been associated with risk for AD when found in heterozygosity (Lu et al. 2015; Jin et al. 2015; Guerreiro et al. 2013b; Jonsson

et al. 2013; Jiang et al. 2016a), although none have surpassed the odds ratio found in the case of R47H.

In AD patients, R47H mutations in TREM2 are associated with an earlier age of symptom onset (Jin *et al.*, 2014; Slattery *et al.*, 2014) and a more rapid rate of disease progression (Rajagopalan, Hibar and Thompson, 2013; Korvatska *et al.*, 2015). Compared with healthy controls, increased TREM2 expression is found in AD patient brains (Lue *et al.*, 2015; Strobel *et al.*, 2015; Perez *et al.*, 2017) and, in mouse models, increased TREM2 expression coincides with the onset of Aβ pathology (Jiang, et al. 2014b; Chan et al. 2015). In tau models, upregulation occurs with a delay, and is only identified following formation of neurofibrillary tangles (Matarin *et al.*, 2015).

Despite TREM2 upregulation being found to be concomitant with Aβ deposition, it is not yet known how, or if, Aβ alters TREM2 expression. Myeloid cells associated with plaques have increased TREM2 expression (Frank *et al.*, 2008; Jay *et al.*, 2015; Savage *et al.*, 2015; Yin *et al.*, 2017) and injection of Aβ1-42 into the cortex and hippocampus of mice induced upregulation of TREM2 mRNA within 24 hours (Jiang et al. 2014b). There is currently controversy over the origin of the TREM2 expressing cells that are found surrounding Aβ plaques in AD brains. Jay et al found that these myeloid cells lacked expression of the key microglial-specific marker P2YR12, suggesting that these TREM2+ cells were monocyte-derived macrophages that had infiltrated the brain. On the other hand, Wang et al used parabiosis experiments to demonstrate that peripheral macrophages from WT mice did not contribute to the pool of cells in the AD mice. *In vitro,* Aβ1-42 stimulation failed to elicit a TREM2 expression response in microglia cultured in isolation, however microglia in mixed glial cultures upregulated TREM2 expression in response to Aβ1-42 (Melchior *et al.*, 2010). This suggests that Aβ may not act directly upon the TREM2 expressing microglia and upregulation may be induced through signals from another cell type.

AD-associated TREM2 variants have been shown to attenuate ligand binding affinities (Bailey, DeVaux and Farzan, 2015; Kober *et al.*, 2016) and therefore are likely to affect the downstream signalling for key functions such as phagocytosis. These mutations may alter the ability of microglia to clear Aβ since TREM2$^{-/-}$ AD models have increased accumulation of Aβ and neuronal loss (Wang *et al.*, 2015), whilst expression of R47H mutations also decreased microglial phagocytosis of Aβ1-42 (Kleinberger *et al.*, 2014). Indeed, in AD patients carrying R47H mutations, increased Aβ plaque loads have been identified compared with non-carriers (Roussos *et al.*, 2015). The exact mechanisms through which AD-associated variants contribute to AD pathogenesis are not yet certain but the fact that they are found in the coding regions of the TREM2 gene makes

them relatively more amenable for the necessary ongoing *in vitro* studies and modelling required to further understand these disease-altering mutations.

1.5 The Complement System

The complement system, consisting of over 30 plasma and membrane bound proteins, was discovered in the 1890s as a heat-labile component of serum that was found to 'complement' the antibacterial activity of antibodies (Walport, 2001). It is a phylogenetically ancient part of the innate immune system which acts swiftly to protect the host from a wide range of stimuli through surveillance and rapid activation, incorporating essential, strict regulation to prevent complement-mediated damage to host cells. Despite primarily functioning to opsonise pathogens, recruit innate and adaptive immune cells and amplify signals to stimulate the immune response, complement has an increasingly appreciated role in orchestrating a range of immunological and homeostatic responses. Complement has been found to be more than just an innate first line of defence; it is involved in angiogenesis, lipid metabolism, synapse maturation and tissue regeneration as well as playing a key role in the adaptive immune system (Walport, 2001; Dunkelberger and Song, 2010).

Complement activation can occur through either the classical, alternative or lectin pathways depending on the source of stimulation. Activation can occur on the surface of recognised pathogens or on host tissues and results in a series of specific proteolytic cleavages, finally resulting in the formation of the membrane attack complex (MAC). All three pathways converge on the assembly of C3 convertases which cleave C3, resulting in the formation of activation products and the MAC (Sarma and Ward, 2011) (See Figure 1.2). The MAC assembles in the membrane of the target cell, causing membrane disruption and cell lysis. The complement system is capable of identifying pathogens or perturbations to tissue homeostasis via defence collagens such as C1q and then marks these risks by opsonisation for clearance via phagocytosis. Complement recruits immune cells using fluid-phase inflammatory mediators known as anaphylatoxins which act as chemoattractants for phagocytic cells, vasodilators and smooth muscle contractors (Miwa and Song, 2001).

The classical pathway is activated in response to C1q binding antigen-antibody complexes as well as direct binding to pathogen surfaces and some host surfaces such as Aβ and phosphorylated tau (Afagh *et al.*, 1996). The lectin pathway is activated by the binding of the mannan-binding lectin protein to residues and sugars on the outer surface of pathogens. In the alternative pathway of complement activation, there is a

low level of constant C3 hydrolysis, known as 'tick over', to form C3b which is capable of binding carbohydrates, lipids and proteins found on microbial and eukaryotic surfaces with low sialic acid content (Veerhuis, Nielsen and Tenner, 2011). This spontaneous hydrolysis allows priming of the complement system and continually probes for challenged host cells or foreign cells. C3b inactivation by factor H and factor I is much more efficient on sialic acid rich surfaces, such as host cells, which prevents damage to the host. These different routes for the activation of complement are no longer viewed as three separate, linear pathways but as a network of tightly regulated proteins that continually survey the environment and cooperate to clear infection.

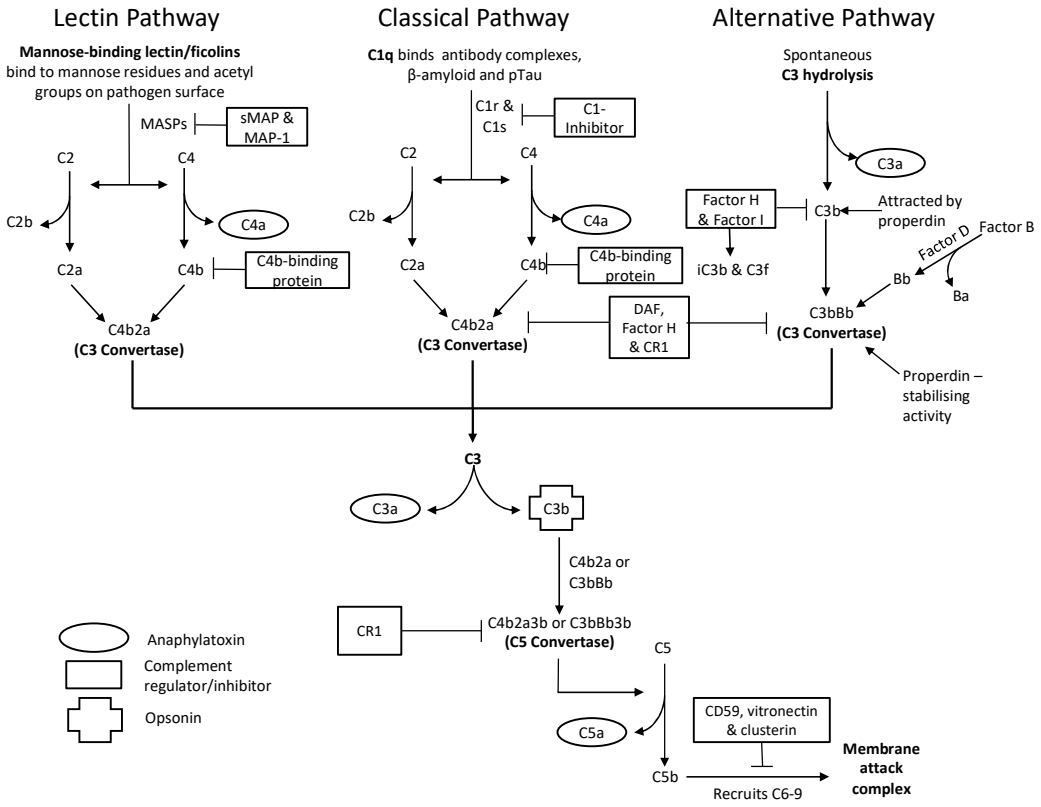

Figure 1.2: Diagram showing the convergence of the three pathways of complement activation

A critical component of the complement system is the network of regulators of complement (CREGs) that is in place, including CR1, Factor H, DAF, CD59 and C4b-binding protein which act not only to prevent inappropriate activation but to also determine what level of response is appropriate. For example, in the case of apoptotic cells, debris that would otherwise cause inflammation is tactfully removed avoiding further complement activation and the particularly inflammatory components downstream of C3 (Ricklin *et al.*, 2010), which are not necessary for the clearance of

this low risk debris. This fine balance between activation and regulation within the system is carefully maintained, but if allowed to go awry, can contribute to the underlying pathology of several inflammatory, neurodegenerative, ischaemic and age-related diseases (Ricklin *et al.*, 2010).

1.5.1 Complement in the Brain

Due to the integrity of a healthy BBB, neither the immune cells circulating in the periphery nor the primarily liver-derived complement proteins are able to penetrate the brain parenchyma (Veerhuis, Nielsen and Tenner, 2011). Therefore, any complement found in the brain must be synthesised locally in order to ensure essential local surveillance and defence in this immuno-privileged site. Although levels of production are typically low under non-pathological conditions, it has been confirmed that complement activators and regulators are synthesised in the human brain by neurons (Walker and McGeer, 1993; Thomas *et al.*, 2000), microglia (Walker, Kim and McGeer, 1995; Veerhuis *et al.*, 1998), astrocytes (Barnum, Jones and Benveniste, 1992) and oligodendrocytes (Gasque and Morgan, 1996; Hosokawa *et al.*, 2003). The expression of these complement factors and receptors have been found to increase following infection (Stahel and Barnum, 1997), inflammatory stimulation (Stahel *et al.*, 1997) and in neurodegenerative disease (Yasojima *et al.*, 1999).

Complement proteins and receptors have been found to have functions beyond innate immune responses including mediating neurogenesis, synaptogenesis, cell migration, neuroprotection, proliferation and regeneration. In the brain, complement receptors and proteins are expressed in a temporally- and spatially-regulated manner, suggesting that the complement system has more than just an immunological role. During CNS development, various complement components are upregulated resulting in contrasting promotion of cell survival and induction of synapse removal.

Complement anaphylatoxins are primarily known for their role in recruitment of phagocytes and activation of immune cells to clear infections. However, C3aR and C5aR, the receptors for the anaphylatoxins C3a and C5a, have been shown to be transiently expressed on cerebellar granule cells during rat CNS development (Bénard *et al.*, 2004). Furthermore, activation of C5aR with C5a resulted in inhibition of Caspase-9 mediated apoptotic cell death in serum starved *ex vivo* granule cell neurons (Bénard *et al.*, 2004). C3a is reported to play a role in the differentiation and maturation of neural progenitor cells *in vitro* (Shinjyo *et al.*, 2009). *In vivo*, C3a knockdown or C3aR blockade results in decreased basal neurogenesis and decreased migration of neuroblasts in models of ischaemia (Rahpeymai *et al.*, 2006).

Supernumerary synapses are generated in the developing brain, which are refined during post-natal development (Hooks and Chen, 2006). Microglia play an important role in refining and shaping the synaptic connectivity during development in an activity and complement dependent manner (Schafer *et al.*, 2012). Engulfment of synapses by microglia is dependent upon C1q, C3 and CR3, the expression of which is regulated in a spatiotemporal manner in the lateral geniculate nucleus and cortex during development and downregulated in the adult brain to prevent excessive synapse stripping (Stevens *et al.*, 2007). This removal of excessive synapses is essential for appropriate signalling within the neuronal circuitry, as demonstrated by the observation of epileptogenesis in mouse models deficient in C1q, due to inefficient refinement of networks in the sensorimotor cortical regions (Chu *et al.*, 2010). This removal of weaker, inappropriate synapses allows the remaining connections to be strengthened. Therefore, in addition to the anti-apoptotic signalling of the anaphylatoxins, a carefully balanced and regulated interplay between complement, neurons and microglia results in the refinement and careful sculpting of spontaneous, immature circuits into organised, experience-based synaptic connections (Katz and Shatz, 1996).

In the adult brain, complement interacts with microglia to ensure that homeostatic conditions are maintained. Through initiating responses to infection and injury, the complement system acts to induce a local inflammatory response in order to promote healing and protection. Despite the risks of causing inflammation and cell damage if activation becomes dysregulated, this local inflammation is key for the removal of cell debris and neurotoxic protein aggregates.

C1q is important for the clearance of misfolded proteins, apoptotic cells and neuronal blebs (Fraser, Pisalyaput and Tenner, 2010) due to its ability to recognise phosphatidylserines exposed on the surface of apoptotic cells, thus flagging them for removal by microglia. This recognition results in downstream complement activation and opsonisation by C3b/iC3b for clearance via phagocytosis (Mevorach *et al.*, 1998) thereby preventing the release of neurotoxic intracellular factors, such as glutamate.

Interactions between complement pattern recognition molecules, complement regulators and opsonins result in the safe removal of apoptotic cells and immune complexes whilst also minimising off target, collateral damage. The ability to differentiate between severe threats and endogenous factors that currently pose no danger, such as apoptotic cells, but could affect cell survival if left unchecked, ensures that responses are appropriate. Residual expression of complement regulators on the surface of apoptotic cells prevents excessive late complement pathway amplification, stopping terminal MAC and induction of inflammatory cytokines (Ricklin *et al.*, 2010).

Therefore, potentially harmful debris is removed without triggering danger signals and exaggerated immune responses. Furthermore, C3b/iC3b and CR3-mediated phagocytosis downregulates IL-12 and oxidative burst responses (Mevorach *et al.*, 1998; Kim, Elkon and Ma, 2004) to safeguard clearance without augmented inflammation. C1q has also been shown to downregulate pro-inflammatory cytokine secretion by monocytes (Fraser *et al.*, 2006). Neurotrophins, such as nerve growth factor (NGF), are important for neuronal survival and function during development and in the adult brain. C5a and C3a induce secretion of NGF by astrocytes and microglia (Heese, Hock and Otten, 1998; Jauneau *et al.*, 2006) therefore these anaphylatoxins may act to preserve neuronal function and abundance in both physiological and pathological conditions.

Thus complement also plays an important role in the adult brain, ensuring that any debris and dying cells that could potentially cause harm are efficiently cleared without initiating any further inflammation whilst also promoting the survival of CNS cells in both physiological conditions and following injury.

Despite evidence suggesting that complement is neuroprotective, there is a significant body of work demonstrating that complement activation paradoxically contributes to the pathogenesis of various neurodegenerative diseases. The role of complement activation in exacerbating neuroinflammatory disease and injury is highlighted by models in which inhibition of complement results in improved responses and decreased pathology; these models include ischaemia and stroke, multiple sclerosis and Alzheimer's disease (Fonseca *et al.*, 2004; Mocco *et al.*, 2006; Elvington *et al.*, 2012; Ramaglia *et al.*, 2012).

Inhibition of the alternative pathway results in improved neurologic function and demyelination in murine ischemic stroke models (Elvington *et al.*, 2012). Additionally, concurrent deficiencies in classical and lectin pathway activators provided protection from cerebral ischemia-reperfusion injuries (Elvington *et al.*, 2012). Disease progression in the EAE model of MS is more rapid and severe in $Crry^{-/-}$ mice (Ramaglia *et al.*, 2012), suggesting that C3 products, the formation of which are negatively regulated Crry activity, the CR1 rodent orthologue, contribute to EAE pathogenesis. Furthermore, $C3^{-/-}$ mice have improved outcomes following focal cerebral ischaemia, including decreased infarct and neurological deficit scores (Mocco *et al.*, 2006). C1q deficient AD mice had decreased loss of the synaptic markers synaptophysin and MAP2 in the CA3 hippocampus compared with controls (Fonseca *et al.*, 2004), suggesting that classical complement activation is detrimental to synapse integrity. C1q is also found to be upregulated in glaucoma (Stasi *et al.*, 2006) and may explain why

extensive synapse loss has been identified in the early stages of disease (Rosen and Stevens, 2010). Dysregulated synapse removal and altered synaptic activity is also found in the early stages of AD (Selkoe, 2002).

In contrast to the pathological effects of complement activation in various disease models, C5a has been shown to be protective against apoptotic cell death in the EAE model of MS (Niculescu *et al.*, 2004) and the kainic acid model of excitotoxicity via Erk1/2 inhibition of Caspase-3 (Osaka *et al.*, 1999). Neurons in C5aR knockout mice are reportedly more vulnerable to glutamate excitotoxicity compared to WT mice due to a lack of C5a regulation of GluR2 subunit expression, resulting in augmented glutamate-mediated apoptosis (Mukherjee, Thomas and Pasinetti, 2008). Complement has also been shown to play a paradoxical and currently unclear role in Alzheimer's disease-associated neuroprotection and pathogenesis, which will be discussed further in the next section. Therefore, different complement components may counteract each other and can be protective and detrimental at different stages of disease and development.

1.5.2 Complement in Alzheimer's Disease

The presence of complement in Alzheimer's pathology is well established; all native complement proteins as well as the terminal MAC are upregulated in the brains of confirmed AD patients (Shen *et al.*, 1997; Yasojima *et al.*, 1999) and C1q and C3c/d, C4c/d, C5-9 have all been found to interact with Aβ plaques (Afagh *et al.*, 1996; Rozemuller *et al.*, 2000). Additionally, neurofibrillary tangles of phosphorylated tau, another classical hallmark of AD, are capable of activating complement via C1q binding (Shen *et al.*, 2001). *In vitro,* it has been demonstrated that Aβ activates both the classical and alternative pathways via C1q and C3 binding (Rogers *et al.*, 1992; Jiang *et al.*, 1994). CR3 has also been shown to bind to Aβ and, in addition to being found to colocalise with Aβ plaques in AD brains (Strohmeyer *et al.*, 2002), is involved in uptake and clearance of Aβ *in vivo* and *in vitro* (Maier *et al.*, 2008; Choucair-Jaafar *et al.*, 2011; Fu *et al.*, 2012). However, conflicting results using models of AD and complement deficiencies mean that it is unclear whether complement has a causative role or is a protective mechanism that is upregulated during the course of the disease.

In the brains of $C1q^{-/-}$ Tg2576 AD mice, a similar Aβ load was found to that in the C1q sufficient mice however there was less microglial recruitment to plaques and decreased levels of synaptic marker loss (Fonseca *et al.*, 2004), suggesting that complement activation in this model is detrimental. In APP23 mice treated with enoxaparin, which inhibits Aβ-induced complement activation, decreased Aβ load was found

(Bergamaschini *et al.*, 2004), which indicates that complement plays a role in mediating neuropathology. The use of the C1 complex inhibitor C1-Inh, which is found at reduced levels in the plasma of AD patients, protected cultured rat hippocampal cells from Aβ-induced classical pathway activated lysis (Sarvari *et al.*, 2003). The inhibitor CD59 is also reduced in the hippocampus and frontal cortex of AD patients (Yang *et al.*, 2000), which would make cells more vulnerable to MAC-induced lysis, suggesting that dysregulation of complement in AD may contribute to neuronal loss. Inhibition of C1q, C3 or CR3 has recently been shown to be protective in models of AD against excessive synaptic removal by microglia in response to Aβ (Hong *et al.*, 2016). Indeed, C1q and CR3 are both necessary for the toxic effects of Aβ on synapse function and long term potentiation in addition to engulfment of synapses, as demonstrated through the use of $C1q^{-/-}$ and $CR3^{-/-}$ AD models (Hong *et al.*, 2016).

Anaphylatoxins are thought to contribute to the neuroinflammatory aspect of Alzheimer's disease due to their recruitment of microglia and astrocytes that, upon activation, release cytokines, proteases and reactive oxygen species that may accelerate neuronal damage and dysfunction. Tight regulation of complement is in place in healthy brains but this may go awry during the course of disease resulting in a neurotoxic microenvironment. Through the same mechanisms that improper synaptic connections are pruned in the developing brain, dysregulated complement could result in the removal of neurons, augmenting the neuronal loss found in Alzheimer's disease.

Despite the body of work suggesting that complement can be detrimental in the progression of AD, there is also evidence that complement plays a neuroprotective role. Complement opsonins play an important role in marking plaques, tangles and apoptotic cells for clearance. This removal of debris and immunogenic fragments from the brain minimises the risk of inappropriate immune responses being raised, which can cause damage to host cells. C3 cleavage products are thought to play an important role in amyloid plaque clearance since $C3^{-/-}$ AD mice have an increased cortical and hippocampal plaque burden as well as increased neuronal loss (Maier *et al.*, 2008). Furthermore, overexpression of Crry, a complement regulating receptor, in mouse AD model lead to increased Aβ pathology (Wyss-Coray *et al.*, 2002).C1q has been found to be upregulated following injury or infection and is neuroprotective against Aβ-induced toxicity and neuronal loss *in vitro* (Pisalyaput and Tenner, 2008) despite the fact that it is the activator of the classical pathway.

Anaphylatoxins are also important for plaque and debris clearance as they recruit phagocytic cells to the area of injury or insult. Both neurons and glia express C5aR, the primary receptor for the potent anaphylatoxin C5a (Woodruff *et al.*, 2010) and, *in vitro*,

C5a has been found to be directly neuroprotective to differentiated SH-SY5Y neuroblastoma cells against Aβ (O'Barr *et al.*, 2001). C5a and C5aR may also contribute to signalling that augments phagocytosis (Lee, Whitfeld and Mackay, 2008; Tsuboi *et al.*, 2011), as well as increasing microglial uptake of glutamate (Persson *et al.*, 2009), a neuroprotective activity.

Conflicting results on the effect of complement activation in AD could be due to the use of different animal modes, cells being at varying stages of differentiation or locations leading to different environmental cues and subtle changes in the net result of toxic and protective consequences of complement (Veerhuis, Nielsen and Tenner, 2011). Expression of all complement components have been found to be upregulated by CNS injury and disease, including AD (Walker and McGeer, 1993), likely in an attempt to increase the activity of neuroprotective factors. However, as pathology worsens and induces dysfunction of complement and complement-producing cells, dysregulation of complement factors to a harmful level could lead to amplification of inflammation and propagation of a neurotoxic environment.

In addition to *in vitro* and *in vivo* studies of complement interactions with AD pathology and the effect of complement knockout in animal models of AD, GWAS have identified common genetic variations in CR1, as a risk factor for the development of late-onset AD along with CLU (Harold *et al.*, 2009; Lambert *et al.*, 2009), which encodes for clusterin, a regulator of MAC. CR1 is a regulator of complement activation and the identification of a genetic link between complement regulators and an increased risk of developing AD further highlights the importance of maintaining the fine balance between the neuroprotective and neurotoxic effects of complement activation.

1.5.3 CR1

Complement receptor type 1 (CR1), also known as CD35 or C3b/C4b receptor, is a single chain, type-1 transmembrane glycoprotein that is expressed widely in erythrocytes, B cells, polymorphonuclear cells and macrophages. CR1 is a multifunctional receptor which acts to clear immune complexes from the blood, induce phagocytosis of immune complexes and inhibit complement activation. The extracellular domain of CR1 is made entirely of 30 short consensus repeats (SCRs), each containing 60-70 amino acids. There is also a transmembrane domain and a short 41 amino acid intracellular domain, which is thought to be too small to be an enzyme but may interact with the cytoskeleton to mediate phagocytosis (Ahearn and Fearon, 1989). Every eighth SCR is a highly homologous repeat so that seven SCRs form a long homologous repeat (LHR). The functions of CR1 are mediated by two

distinct but extremely similar sites, each made up of 3 SCRs (Figure 1.3). The multiple ligand binding sites on the receptor mean that CR1 is well suited for interacting with complexes containing multiple C3b and C4b molecules, such as the polymers of C3b and C4b that cluster on the surface of immune complexes.

In humans, the CR1 gene can be found on chromosome 1q32 on a locus termed the Regulatory of Complement Activation (RCA), alongside the genes for CR2, DAF, C4-binding protein, Factor H and MCP (Ahearn and Fearon, 1989). Host cells express these membrane-bound complement regulatory proteins to prevent complement-mediated autologous tissue damage (Miwa and Song, 2001). These proteins all have C3b/C4b binding properties and the same basic structural element of the SCRs as CR1.

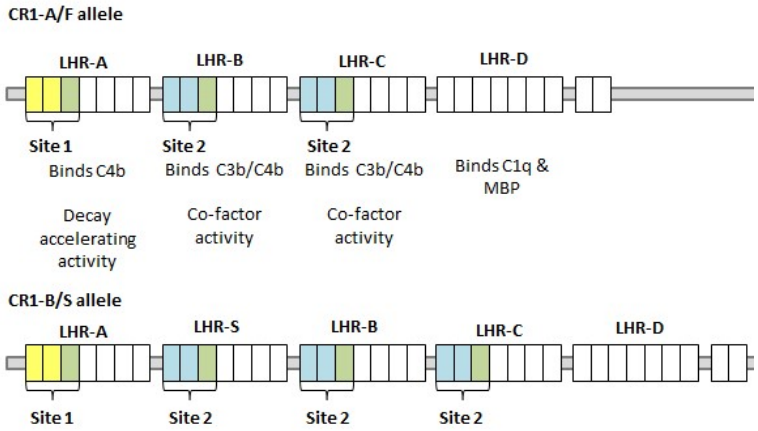

Figure 1.3: Schematic of CR1 A and B allele structures

The CR1 gene is made up of long homologous repeats (LHRs) each composed of seven short consensus repeats (SCRs). CR1-A/F and CR1-B/S are the two most frequently occurring alleles and are defined by the number of LHRs.

CR1 prevents the activation of the alternative pathway at multiple stages (Ross *et al.*, 1982) acting to reduce the formation of the C3b opsonin, which can act as an initiator of further complement activation. Firstly CR1 impairs the uptake of factor B by C3b, minimising the formation of the C3 convertase. It also displaces Bb from the C3 convertase to prevent the cleavage of C3 into more C3b. Finally it promotes factor I cleavage of C3b to the inactive form iC3b, which is unable to sustain or amplify the complement cascade. Therefore, CR1 not only displaces components of the convertases, but irreversibly inactivates them.

In addition to its role in regulation of complement activation, CR1 expression on the surface of erythrocytes is important for the transportation of C3b/C4b opsonised antigens and immune complexes through the blood to the liver and spleen for

clearance, preventing the nonspecific trapping of immune complexes in tissues. CR1 plays a role in neutrophil- and monocyte-mediated phagocytosis by enhancing Fc receptor-dependent phagocytosis of IgG and C3b-opsonised particles and immune complexes, particularly following activation by cytokines (Wright and Silverstein, 1982; Fällman, Andersson and Andersson, 1993). The two receptor types work synergistically as ligation of CR1 by target-bound C3b may direct Fc receptors to sites where an interaction with target-bound IgG is more likely to occur.

There are four different allotypes of CR1, the differences between which are found in the extracellular domain. Each one contains varying numbers of LHRs, hence the difference in size being roughly equivalent to a single LHR (~30kDa or 1.3-1.5kb) (Khera and Das, 2009). The number of LHRs is determined by the number of 18-kb long low-copy repeats (LCRs); the most common allele has LCR1 & LCR2 but CR1-B/S also possesses LCR1' which results in the additional C3b/C4b binding site (see Figure 1.3) (Brouwers *et al.*, 2012). The other isoforms result from a triplication or deletion of one LCR1 copy producing allotypes with varying numbers of C3b/C4b binding sites.

CR1 Allotype	Molecular Weight	Frequency
CR1-C (or F')	190kDa	0.01
CR1-A (or F)	220kDa	0.83
CR1-B (or S)	250kDa	0.15
CR1-D	280kDa	<0.01

Table 1.1 Frequencies and molecular weights of CR1 allotypes

The frequencies of expression within the general population vary between the different CR1 allotypes, with CR1-A/F being the most common (Holers *et al.*, 1987). The molecular weights vary depending on the number of LHR repeats within the gene.

1.5.4 CR1 in Alzheimer's Disease

A GWAS published in 2009 by Lambert et al. first identified a linkage disequilibrium block within CR1 as being associated with increased risk of developing late onset Alzheimer's disease (Lambert *et al.*, 2009). Since then, nine small nuclear polymorphisms (SNPs) in CR1 have been found to be associated with Alzheimer's disease (Harold *et al.*, 2009; Lambert *et al.*, 2009; Carrasquillo *et al.*, 2010; Hollingworth *et al.*, 2011; Naj *et al.*, 2011). Six of these are in the intronic region of CR1 so do not encode for the protein but may function in regulating gene expression levels. The SNP rs6656401 showed the strongest association with AD (odds ratio of 1.21)

(Lambert *et al.*, 2009) and has also been found to be associated with greater cognitive decline and vascular and neuritic plaque Aβ pathology (Chibnik *et al.*, 2011; Biffi *et al.*, 2012; Farfel *et al.*, 2016). Associations of the rs6656401 SNP with AD have been extended beyond European Caucasians and has been found to have an increased OR of 1.31 in East Asian populations (Shen *et al.*, 2015). Lambert et al. showed an interaction between rs6656401 CR1 SNP and APOE genotype, with the strongest association found in APOE ε4 carriers. Another CR1 SNP that has been found to have significant association with AD risk is rs3818361, which had an odds ratio of 1.14, however no association was found between this SNP and APOE ε4 carriers (Jun *et al.*, 2010). In a study investigating associations between AD risk SNPs and disease progression in patients, carriers of the G allele of the rs3818361 SNP had higher rates of medium-term disease progression as measure by annual MMSE loss (Schmidt *et al.*, 2014).

It was thought that CR1 might be involved in clearance of Aβ from the brain since Aβ is known to activate complement by binding to C1q and also binding to C3b opsonins. In plasma, C3b mediates binding of Aβ peptides to erythrocyte-expressed CR1, a process aberrantly regulated in the early stages of AD (Rogers *et al.*, 2006). The peripheral sink hypothesis states that Aβ can be cleared from the brain by Aβ-binding molecules in the periphery, hence CR1 variants may contribute to AD by altering the clearance of Aβ in the periphery or complement activation in the brain.

Further work has shown that the common AD risk association could be explained by expression of the CR1-S allotype, which contains an additional C3b/C4b binding site, as carriers of this longer form of CR1 had around 30% increased risk for AD compared with those expressing CR1-F (Brouwers *et al.*, 2012). CR1-S expression occurs at a frequency of 15% in the population and has an extra C3b/C4b binding site compared to the more common CR1-F. The authors also showed that the LCR (low copy repeat) copy number variation that causes the expression of the longer form of CR1 was in high linkage disequilibrium with the most highly associated risk factor SNP rs6656401, suggesting that that the CR1 association with AD can be explained by the intragenic copy number variation resulting in increased C3b/C4b binding sites in CR1-S compared to CR1-F.

CR1-S, due to its increased cofactor activity sites, may be a more potent inhibitor of complement cascade amplification leading to a reduction in C3b available to opsonise Aβ and also a reduced complement reaction. Studies in mouse AD models have shown that inhibition of complement activation correlated with increased Aβ plaque formation and damage to neurons (Maier *et al.*, 2008). Despite the fact that excessive

complement activation causes neurotoxic inflammation (Afagh *et al.*, 1996; Fonseca *et al.*, 2004), the association between increased AD risk and the longer isoform of CR1 could suggest that the over-inhibition of complement is more damaging.

However, four other SNPs have been linked to elevated cerebrospinal fluid levels of Aβ1-42 in AD patients (Brouwers *et al.*, 2012) suggesting that CR1 variants may be pathogenic via an Aβ-associated effect. It has since been discovered that the CR1-S isoform is expressed at lower protein levels in the brain than CR1-F in both AD patients and controls, with CR1-S AD cases having higher Braak stages than CR1-F homozygous carriers (Hazrati *et al.*, 2012). Analysis of the expression levels of CR1 on erythrocytes of AD patients and controls showed that there was lower surface expression of CR1 in AD cases compared to controls in groups expressing the CR1-S isoform (Mahmoudi *et al.*, 2015). The level of CR1 protein expression on erythrocytes was not the only considerable difference between allotype carriers; individuals with F/S genotype had a 1.8 times increased risk for AD compared to F/F genotype carriers and each genotype had distinct protein expression patterns in neurons. The neuronal CR1 staining in F/F genotype samples was threadlike, filiform profiles in the soma and proximal segments of the dendrites whereas the F/S genotype has vesicular, dot-like punctate profiles. This difference in distribution suggests that the CR1-F may shuttle through protein sorting organelles whilst CR1-S accumulates in the membrane of cytoplasmic vesicles (Hazrati *et al.*, 2012). A decrease in expression levels of CR1 would mean that there are fewer C3b/4b binding sites available on the surface of the cell to bind opsonised Aβ, despite the fact that the few CR1 molecules present each have a greater than average number of binding sites. This could result in impaired clearance of Aβ from both the periphery and the brain, allowing accumulation of neurotoxic fibrils and plaques. Additionally, the reduction in total C3b/C4b binding sites leads to inefficient regulation of complement activation resulting in toxic neuroinflammation that can cause neurodegeneration.

1.5.5 C1q

C1q is a pattern recognition molecule which, through its ability to recognise and bind a wide range of self and non-self ligands, is the initiator of the classical pathway of complement activation. C1q is the first subunit of the C1 complex which is recruited following C1q ligand binding and comprises the C1r and C1s serine proteases. These serine proteases initiate sequential cleavage of various complement proteins generating the components required for the formation of the C3-convertase complex, in addition to the anaphylatoxin C4a. The C3 convertase cleaves C3 into C3a and C3b

which is also a pattern recognition molecule that mediates CR3 phagocytosis as well as contributing to the formation of the C5 convertase, which later forms the terminal MAC complex.

C1q is expressed by a wide variety of cells including macrophages, microglia, mast cells, dendritic cells and oligodendrocytes (Schwaeble *et al.*, 1995; Hosokawa *et al.*, 2003; Färber *et al.*, 2009; Castellano *et al.*, 2010; van Schaarenburg *et al.*, 2016). Furthermore, expression is induced in other cell types, such as astrocytes and neurons during specific stages of development or following infection or injury (Fan and Tenner, 2004; Rambach *et al.*, 2008; Bialas and Stevens, 2013). There are two primary receptors for C1q; calreticulin (cC1qR) which binds the collagen-like, 'stem' domain and gC1qR which binds the globular, 'tulip-head' domains.

In addition to initiating complement cascades through the generation of C3b opsonins, C1q has been shown to play roles in enhancing phagocytic clearance of apoptotic cells (Païdassi *et al.*, 2008) and immune complexes as well as maturation of dendritic cells (Csomor *et al.*, 2007), activation of microglia (Färber *et al.*, 2009) and induction of expression of neuroprotective factors (Benoit and Tenner, 2011). C1q is upregulated in the developing brain (Stevens *et al.*, 2007; Bialas and Stevens, 2013) and plays an essential role in the refinement of synaptic networks during development, as demonstrated by C1q defective mice developing behavioural seizures and epileptoform activity (Chu *et al.*, 2010).

C1q has a hexameric, tulip-like structure comprised of 6 heterotrimeric collagen-like fibres each topped with a C-terminal globular domain. These globular domains mediate C1q's ability to recognise a wide range of ligands including immunoglobulins, altered and misfolded endogenous proteins, such as prion protein, Aβ and apoptotic cells, as well as molecular motifs on bacteria and viruses (Albertí *et al.*, 1993; Stevens *et al.*, 2007; Erlich *et al.*, 2010; Fraser, Pisalyaput and Tenner, 2010; Gaboriaud *et al.*, 2011). The binding of C1q to Fc regions of IgG is strengthened by up to 1000-fold by the presence of multiple, clustered Fc regions, such as those found in immune complexes (Kishore and Reid, 2000).

1.5.6 Complement Receptor 3

The complement receptor 3 (CR3), also known as Mac-1, CD11b/CD18, or integrin αMβ2, is an extremely versatile pattern recognition receptor best known for its role as a phagocytic receptor of C3b/iC3b opsonised particles, however it also regulates cytokine responses, leukocyte trafficking and synapse formation (Whitlock *et al.*, 2000;

Kinashi, 2005; Phillipson *et al.*, 2006; Stevens *et al.*, 2007). It is a member of the β2 integrin family, a family of heterodimeric transmembrane receptors which are all composed of a CD18 β chain associated with a variable α chain, the composition of which defines the receptor. The other members are LFA-1 (CD11a/CD18), CR4 (CD11c/CD18) and a_dβ2 (CD11d/CD18).

CR3 is a pattern recognition receptor with the ability to recognise a vast array of host and non-host ligands including, but not limited to, ICAM-1 (Diamond *et al.*, 1990), fibrinogen (Wright *et al.*, 1988) and LPS (Wright and Jong, 1986). The CD11b I domain binds ICAM-1, iC3b and fibrinogen whilst a lectin-like domain recognises mannose and β-glucans (reviewed by (Ehlers, 2000)). It is expressed on monocytes, macrophages, microglia, dendritic cells and neutrophils.

Information on the multiple roles of CR3 has been ascertained from natural and artificially generated knockouts. LAD syndrome (leukocyte adhesion deficiency) is caused by decreased or total absence of β2 integrin surface expression arising from mutations in CD18 component. Patients present with defective pus formation and wound healing due to defective leukocyte adhesion, migration and phagocytosis (Larson and Springer, 1990; Hogg *et al.*, 1999), highlighting the importance of β2 integrins and CR3 in the response to infection and injury. In order to investigate the effects of mutations on CR3 in isolation from the other β2 integrins, mutations and knockouts of the unique CD11b component of the receptor have been studied. Lupus-associated mutations in CD11b reduced CR3-mediated phagocytosis of iC3b-opsonised particles in monocytes, macrophages and neutrophils (Rhodes *et al.*, 2012; Fossati-Jimack *et al.*, 2013). $CD11b^{-/-}$ models of CR3 knockout have shown that adhesion between neutrophils and epithelial cells during migration is mediated by CR3 (Balsam, Liang and Parkos, 1998) and CR3 is required for maintenance of mast cells for bacterial clearance in a model of acute sepsis (Rosenkranz *et al.*, 1998). Defective phagocytosis has been reported in neutrophils from $CR3^{-/-}$ mice as well as impaired adherence and degranulation (Lu *et al.*, 1997). CR3 also exerts anti-inflammatory effects. CD11b deficiency leads to increased inflammatory cytokine and interferon release following TLR4 stimulation in macrophages (Han *et al.*, 2010) whilst phagocytes downregulate IL-12 and oxidative bursts performing CR3-mediated uptake of C3b/iC3b-opsonised particles (Marth and Kelsall, 1997; Kim, Elkon and Ma, 2004)

CR3 has been reported to phagocytose opsonised and non-opsonised zymosan in type I and type II phagocytosis (Le Cabec *et al.*, 2002). Type 1 phagocytosis is usually mediated by FcγR receptors binding to IgG-coated particles and results in RAC and Cdc42-mediated membrane ruffling to engulf material. Type II involves C3b/iC3b

particles that sink into the membrane and only requires RhoA (Caron and Hall, 1998). It has also been shown to be involved in antibody mediated phagocytosis as CD18-deficient macrophages had reduced phagocytosis of IgM and IgA opsonised *C. neoformans* (Taborda and Casadevall, 2002).

Various studies have indicated that CR3 cooperation with other surface expressed receptors is important for its optimal functioning. In the case of LPS, CR3 can bind particles in both a CD14 independent and dependent manner (Zarewych *et al.*, 1996), resulting in NF-κB signalling and iNOS production by macrophages (Matsuno *et al.*, 1998).CR3 has also been shown to interact with CR1 to induce conversion of particle bound C3b to C3bi for more effective uptake by phagocytosis (Sutterwala, Rosenthal and Mosser, 1996). CR3 also cooperates with FCγRIII to stimulate respiratory burst and antibody-dependent phagocytosis (Krauss *et al.*, 1994; Zhou and Brown, 1994).

1.6 Aims

1) Determine suitability of iPSC-derived microglia-like cells (iPSC-MGLC) as a model of human microglia

- Characterise expression of genes identified as unique to the microglial transcriptome signature (Butovsky et al. 2014).

2) Characterise TREM2 expression in knockdown and mutation-harbouring microglia cell lines

- Characterise CRISPR/Cas9 edited BV2 microglial cell lines in which one or two copies of TREM2 gene have been knocked out
- Assess effects of patient-derived TREM2 mutations on the expression of TREM2 in iPSC-MGLC

3) Identify resultant defective responses following TREM2 loss of function in gene edited cell lines and mutation carrying iPSC-MGLC

- Assess effects on key microglial and TREM2-associated functions including phagocytosis and cytokine secretion

4) Investigate expression of CR1 in human CNS

- Establish expression at both whole tissue and individual cell type level
- Investigate crosstalk between TREM2 and CR1 to further understand potential AD pathogenesis mechanisms

5) Assess suitability of iPSC-MGLC for the study of other microglial genes associated with Alzheimer's disease

2. Materials and Methods

2.1 Materials

A: Adenosine triphosphate disodium salt (ATP, >99% purity, Tocris, Bristol, United Kingdom)

B: Bone morphogenetic protein 4 (BMP-4, human, >98% purity, Peprotech, Rocky Hill, New Jersey, United States), Bovine serum albumin (BSA, Sigma-Aldrich, St. Louis, Missouri, United States), Bradford reagent (Sigma-Aldrich)

C: C1q Human ELISA Kit (Thermo Fisher Scientific, Waltham, Massachusetts, United States), CD14 MicroBeads (human, Miltenyi Biotec, Bergisch Gladbach, Germany), Cell filter (40µm nylon, BD Bioscience Franklin Lakes, New Jersey, United States), Complement component 5a (C5a, mouse, >97% purity, R&D Systems, Minneapolis, Minnesota, United States), CytochalasinD (Santa Cruz Biotechnology, Dallas, Texas, United States)

D: DAB kit (3,3'-diaminobenzidine, Vector Laboratories, Peterborough, United Kingdom), Dextran 500 (Sigma-Aldrich), Duoset ELISA kits (R&D Systems),

E: E8 medium (Thermo Fisher Scientific), Ethylenediaminetetraacetic acid (EDTA, Sigma-Aldrich)

F: Foetal bovine serum (FBS, heat-inactivated, endotoxin free, Thermo Fisher Scientific)

G: Glutamax (Thermo Fisher Scientific),

H: Halt™ Protease and Phosphatase Inhibitor Single-Use Cocktail (100x, Thermo Fisher Scientific), Hanks' balanced saline solution (HBSS, Thermo Fisher Scientific), HiFi HotStart Ready Mix (Roche, Basel, Switzerland), High-capacity RNA-cDNA kit (Thermo Fisher Scientific), Histopaque (Sigma-Aldrich),

I: Interleukin-3 (IL-3, human, >95% purity, Cell Guidance Systems, Cambridge, United Kingdom)

L: Lipopolysaccharide (Sigma-Aldrich)

M: Macrophage colony-stimulating factor (MCSF, human, >98% purity, Peprotech), Macrophage colony-stimulating factor (MCSF, mouse, >98% purity, Peprotech), MACS separator (Miltenyi Biotec), MaxiSORP 96 well plates (Nunc, Roskilde, Denmark), β-mercaptoethanol (Thermo Fisher Scientific), Mini-PROTEAN TGX Precast Gels (Biorad, Hercules, California, United States), miRNeasy mini kit (QIAGEN, Hilden, Germany)

N: Nitrocellulose membrane (Biorad), NucleofectorTM SF-kit (Lonza, Basel, Switzerland), NuPAGE sample reducing agent (10x, Thermo Fisher Scientific)

P: Paraformaldehyde (16% tissue culture grade, Alfa Aesar, Ward Hill, Massachusetts, United States), peptide:N-gycosidase (PNGase, New England Biolabs, Ipswich, Massachusetts, United States), Penicillin/streptomycin (Thermo Fisher Scientific), Phalloidin CF568 (Biotium, Fremont, California, United States), Phosphate-buffered saline (PBS, without calcium chloride and magnesium chloride, Thermo Fisher Scientific), pHrodo green *E. coli* BioParticles conjugated for phagocytosis (Thermo Fisher Scientific), Precision Plus Protein™ All Blue Prestained Protein Standards (Biorad)

Q: QIAzol (QIAGEN)

R: RNase-free DNase set (QIAGEN), RNeasy mini kit (QIAGEN), ROCK inhibitor Y-27632 (Cell Guidance Systems), Roswell Park Memorial Institute medium 1640 (RPMI, Thermo Fisher Scientific)

S: Sample loading buffer (4x, Li-cor, Lincoln, Nebraska, United States), Stem cell factor (SCF, human, >97% purity, Miltenyi Biotec), Streptavidin-HRP (horseradish peroxidase, Thermo Fisher Scientific)

T: TaqMan probes (Thermo Fisher Scientific), TaqMan universal mastermix II (Thermo Fisher Scientific), TMB (3,3',5,5'-tetramethylbenzidine, Thermo Fisher Scientific), TrpLE Express Enzyme (Thermo Fisher Scientific), Tween (Sigma-Aldrich)

V: Vascular endothelial growth factor (VEGF, human, >98% purity, Peprotech), Versene (Lonza), Vectashield antifade mounting medium with DAPI (4',6-diamidino-2-phenylindole, Vector Laboratories), Vectastine Elite ABC HRP kit (horseradish peroxidase, Vector Laboratories)

X: XL cytokine proteome array (mouse, R&D Systems), X-vivo 15 medium (Lonza)

2.2 BV2 Cell Culture & Maintenance

The BV2 cell line is an immortalised murine microglial line generated by transfecting primary microglial cell cultures with a v-raf/v-myc oncogene carrying retrovirus (J2) (Blasi *et al.*, 1990). BV2 cells were obtained from the Banca Biologica and Cell Factory (Genoa, Italy) and cultured according to Blasi et al, 1990. BV2 cells were cultured in T175 culture flasks in Roswell Park Memorial Institute (RPMI) 1640 medium supplemented with 10% heat-inactivated foetal bovine serum (FBS), 100 U/ml penicillin/streptomycin in a humidified incubator at 37°C with 5% CO_2. For passaging and plating cells for experimental procedures, BV2 cells were harvested by washing and incubation with Dulbecco's phosphate buffered saline (PBS, without calcium chloride and magnesium chloride) for 5 minutes at 37°C followed by tapping of the flasks to lift the cells. The cells were then pelleted by centrifugation at 300 *g* for 3 minutes at room temperature (Eppendorf Centrifuge 95 5804R) and resuspended in 10

ml of warmed fresh medium. For quantification of cell number, 10 µl of the cell suspension was administered to a haemocytometer, and cells in four quadrants were counted, which equated to the number of cells present in 0.1 µl of the suspension volume. For experimental procedures, BV2 cells were plated in medium supplemented with FBS in order to encourage cell attachment, which was changed to serum-free medium prior to sample collection where required.

2.3 Primary Cell Culture

2.3.1 Human Neutrophil Isolation

Phlebotomy was performed with 60 ml of blood taken from each subject into heparin coated tubes. This study was approved by University College London (UCL)/UCL Hospitals Joint Research Ethics Committee and all subjects gave informed written consent. Neutrophils were isolated using a standard protocol (Nauseef, 2007). The heparinised blood was mixed at a 2:1 ratio with 3% Dextran 500/HBSS solution in a 50 ml falcon tube and incubated in an upright position for 60 minutes at room temperature upon which two layers will form. The upper, leukocyte-rich plasma layer was collected and cells were pelleted by centrifugation at 4°C for 6 minutes at 460 g. The supernatant was discarded and the cell pellet was resuspended in 25 ml ice-cold PBS (without calcium chloride and magnesium chloride) by gently tapping and swirling the tube. Resuspended cells were gently layered over 15 ml Histopaque and centrifuged at 720 *g for* 20 minutes at room temperature with low acceleration and low brake. Using a pipette, the peripheral blood mononuclear cell (PBMC) layer was collected and saved for monocyte isolation (see 2.3.2 Human Blood-derived Monocyte Isolation). The Histopaque and PBS were removed leaving a cell pellet containing erythrocytes and granulocytes, including neutrophils. In order to lyse the erythrocytes, the pellet was resuspended in 1 ml of ice cold double distilled water (ddH_2O) for 20 seconds, upon which the isotonicity was quickly rebalanced through the addition of 50 ml PBS. The cells were centrifuged at 4°C for 6 minutes at 460 g. If the cell pellet was still red, the lysis and centrifugation steps were repeated until the resulting pellet was white. Cells were then resuspended in pre-warmed RPMI medium and counted prior to lysis in QIAzol for RNA analysis.

2.3.2 Human Blood-derived Monocyte Isolation

The same samples used for the isolation of neutrophils (see 2.3.1 Human Neutrophil Isolation) were used for the isolation of monocytes using standard protocols. Magnetic

CD14 MicroBeads (Miltenyi Biotech) were used to positively select monocytes (Ohradanova-Repic *et al.*, 2016), which highly express CD14 (Haugen *et al.*, 1998), from the PBMC layer generated using Histopaque separation, according to the manufacturer's instructions (Miltenyi Biotech). The samples were centrifuged at 300 g for 10 minutes, the cell pellet was resuspended in 80 µl MACS buffer (PBS, 0.5% bovine serum albumin (BSA) 2mM EDTA) and 20 µl Microbeads per 10^7 cells, and left to incubate at 4°C for 15 minutes. Cells were washed with MACS buffer, centrifuged, resuspended in 500 µl of MACS buffer, and applied to a rinsed MACS LS cell separation column. The column was placed in the magnetic field of a MACS separator in order to positively select the CD14 positive cells. Unlabelled cells passed through the column during the 3 wash steps. The magnetically labelled cells were flushed from the column following the washes using the plunger. CD14 positive monocytes were counted using a haemocytometer and were lysed for RNA analysis or plated to differentiate into monocyte-derived macrophages (see 2.3.3 Human Monocyte-Derived Macrophages).

2.3.3 Human Monocyte-Derived Macrophages

Human blood-derived monocytes (see 2.3.2 Human Blood-derived Monocyte Isolation) were differentiated to generate macrophages using standard protocols (Rey-Giraud *et al.*, 2012; Erbel *et al.*, 2013). Monocytes were plated at a density of 5 x 10^5 in a 6 well plate in X-Vivo medium supplemented with 100 U/ml penicillin/streptomycin, 1% Glutamax and 100 ng/ml human MCSF for 6 days to differentiate into monocyte derived macrophages.

2.4 Generation of human induced Pluripotent Stem Cell-derived Microglia-like Cells (iPSC-MGLC)

For the experiments performed in this thesis, iPSC lines were generated and characterised at the NIHR Cambridge Biomedical Research Centre Human Induced Pluripotent Stem Cells core facility (Cambridge, United Kingdom). iPSCs were differentiated into microglia-like cells (iPSC-MGLC) by Dr Pablo Garcia Reitböck and Dr Thomas Piers, Cell Signalling Lab, UCL Institute of Neurology. Unless otherwise stated, the characterisation and functional experiments using the differentiated cells were performed by me, Alexandra Phillips.

TREM2 mutant primary fibroblast lines were generated from 4mm skin punch biopsies, which were obtained under informed consent. Ethical permission for this study was

obtained from the National Hospital for Neurology and Neurosurgery and the Institute of Neurology joint research ethics committee (study reference 09/H0716/64 for collection of W50C mutant fibroblasts) or approved by the Ethics Committee of Istanbul Faculty of Medicine, Istanbul University (for collection of T66M mutant fibroblasts). iPSC were generated from fibroblast cultures using 4 factor Sendai virus reprogramming and characterised by RT-PCR for plasmid integration, immunofluorescence for expression of pluripotent markers, and 3-germ layer differentiation (Brownjohn et al., in preparation) at the NIHR Cambridge Biomedical Research Centre Human Induced Pluripotent Stem Cells core facility (Cambridge, United Kingdom). Chromosomal abnormalities were also checked for by karyotyping and CNV analysis using OmniExpress-24 chips run on the Illumina Infinum platform by the NIHR Cambridge Biomedical Research Centre Human Induced Pluripotent Stem Cells core facility. The following control iPSC lines were used: CTRL1 (kindly provided by Dr Selina Wray, UCL Institute of Neurology), ND (referred to as CTRL2 in this thesis, from Coriell Institute of Medical Research Biorepository, kindly provided by Dr Rickie Patani, UCL Institute of Neurology), and SFC840 (referred to as CTRL3 in this thesis, kindly provided by Dr Sally Cowley, University of Oxford). iPSC colonies were maintained in E8 medium, and split every 4-5 days using Versene. iPSC colonies were differentiated within 5 passages.

Human iPSC-derived microglia-like cells (iPSC-MGLC) were generated using recently published protocols (Van Wilgenburg *et al.*, 2013), with minor modifications. To generate embryoid bodies at day 0 *in vitro* (D0), iPSC colonies at 60-80% confluence were dissociated for 4 min with TrypLE, collected in 10 x the volume of PBS (without calcium chloride and magnesium chloride), pelleted for 3 min at 300 g and resuspended in 1 ml EBDiff medium (E8 medium with 10 µmol Y27932 ROCK inhibitor, 50 ng/ml BMP-4, 50 ng/ml VEGF, 20 ng/ml SCF). Cells were counted and diluted in EBDiff medium to give a density of 10^5 cells/ml, and 100 µl was added to each well of an ultra-low adherence 96 well plate to give 10^4 cells/well. Plates were centrifuged at 115 g for 3 min, and gently transferred to a tissue culture incubator at 37°C with 5% CO_2. On D2, 50 µl of EBDiff medium was gently added to each well. On D4, embryoid bodies were collected with a P1000 Gilson pipette, transferred into a 15 ml Eppendorf tube, and left to settle at the bottom. The old medium was aspirated and myeloid differentiation medium (X-vivo 15 medium supplemented with 1% Glutamax, 10U Penicillin/Streptomycin and 0.05 mM mercaptoethanol, with 100 ng/ml MCSF and 25 ng/ml IL-3 added. Approximately 150 embryoid bodies were transferred into a 175 cm^2 flask. Myeloid differentiation medium was changed every 5-7 days, making sure that the medium did not become acidotic. After 3-4 weeks, iPSC-MGLC were harvested

once a week by replacing 2/3 of the medium and filtering the cells through a 40µm tube filter. Harvested iPSC-MGLC were further differentiated in X-Vivo 15 medium with 1% Glutamax, 100U Penicillin/Streptomycin and 100 ng/ml MCSF. iPSC-MGLC were used for experiments 7 days post harvesting.

iPSC line	Age	Sex	Clinical Details	TREM2 mutation
CTRL1	78	M	Control	No mutation
CTRL2	64	M	Control	No mutation
CTRL3	31	F	Control	No mutation
T66Mhet1	75	F	Unaffected relative of T66Mhom	Heterozygous T66M
T66Mhet2	47	M	Unaffected relative of T66Mhom	Heterozygous T66M
T66Mhom	51	F	Nasu Hakola disease	Homozygous T66M
W50Chom	36	F	Nasu Hakola disease	Homozygous W50C
R47Hhet1	75	F	Alzheimer's disease	Heterozygous R47H
R47Hhet2	54	F	Possible Alzheimer's disease (MCI, anxiety disorder)	Heterozygous R47H
BionCtrl	19	M	Control	No mutation
BionR47H	19	M	Control modified to insert mutations	Homozygous R47H

Table 2.1 Table of iPSC lines used

2.5 CRISPR/Cas9 Mediated Generation of TREM2 Knockdown and TREM2 Knockout BV2 Cell Lines

CRISPR/Cas9 gene editing technology was used to generate TREM2 knockout lines from mouse BV2 microglial cells by Claudio Villegas-Llerena, Cell Signalling Lab, UCL Institute of Neurology. Characterisation and functional experiments utilising these gene-edited lines were, unless otherwise stated, performed by me, Alexandra Phillips.

BV2 cells were transfected with CRISPR/Cas9n nickase plasmids targeting the second exon of the Trem2 gene (SC-429903-NIC; Santa Cruz Biotechnology Inc.) using the NucleofectorTM SF-Kit for 4DNucleofectorTM according to manufacturer's recommendations. Selection of GFP positive clones and single cell sorting was carried out using a fluorescence activated cell sorter 48 hours post-transfection. Single cell clones were then cultured and expanded with serum containing RPMI (10% FBS) for 2 weeks followed by screening for genetic modifications in *Trem2* by PCR amplification and Sanger sequencing (Source Bioscience). PCR amplification for sequencing analysis was performed in a 25 µl reaction volume. PCR mix was composed of the following; 5µl x 1 µM of each Forward and Reverse primers (Fw-sT2; ACCCAAGGACCAGAACTTATC, Rv-sT2; TCCCATTCCGCTTCTTCAG) 12.5 µl 2x KAPA HiFi HotStart Ready Mix and 2.5 µl of gDNA (~12.5ng). PCR was conducted in a Mastercycler benchtop thermocycler (Eppendorf, Germany). Cycling conditions were as follows: 3 min at 95°C, followed by 35 cycles of amplification (30 sec at 95°C, 30 sec at 62°C and 30 sec at 72°C) and 5 min at 72°C.

No full knockout ($Trem2^{-/-}$) clones were obtained in the first round of CRISPR/Cas9n modification. We obtained 6 cell clones with partial Trem2 knockout, referred to as TREM2 knockdown clones ($Trem2^{+/-}$: 1 allele KO and 1 WT allele); of those we selected two for further experimentation; clones BV2-A7 (4bp deletion) and BV2-C8 (34bp deletion). Confirmation of heterozygous mutations was performed with Single colony Sanger sequencing of PCR products.

A second round of CRISPR/Cas9n modification was carried out using the previously modified clone BV2-C8. The second round of CRISPR/Cas9n modification was performed as described previously. Selection of clones was performed by PCR amplification, enzyme restriction and Sanger sequencing. After selection, we obtained 3 clones with homozygous 23 bp deletions in *Trem2*, rendering these clones complete Trem2 knockout. Two were selected for further experimentation: clones BV2-B5 and BV2-G4.

2.6 Cell Treatments

Cells were routinely plated 24 hours prior to treatment. ATP and MCSF treatments were performed in serum free medium. Cells were treated as follows:

Compound	Final Concentration	Catalogue Number
Lipopolysaccharide (LPS)	1µg/ml for BV2 cells, 100ng/ml for iPSC-MGLC (in ddH_2O)	Sigma #L2880
Mouse macrophage colony stimulating factor (MCSF)	100ng/ml (in ddH_2O)	Peprotech #315-02
Adenosine triphosphate (ATP)	50µM (in ddH_2O)	Tocris #3245
Mouse complement component 5a (C5a)	25ng/ml (in ddH_2O)	R&D Systems #2150-C5
CytochalasinD (CytoD)	10µM (in ddH_2O)	Santa Cruz Biotechnology #SC201442

Table 2.2 Cell culture treatments

2.7 Microscopy

2.7.1 Immunocytochemistry

For immunocytochemical analysis of protein expression, cells were plated on 13mm glass coverslips at a density of 5,000 cells per coverslip. Following the required treatment, cells were washed in PBS, fixed in 4% paraformaldehyde (PFA) for 20 minutes at room temperature and washed again in PBS. Coverslips were stored in PBS at 4°C until use.

For staining, coverslips were quenched with 50 mM ammonium chloride (NH_4CL in PBS) for 10 minutes at room temperature. NH_4CL was aspirated and cells were permeabilised by incubation with 0.2% Triton-X100 for 5 minutes at room temperature, washed 3 times with PBS and blocked for 30 minutes at room temperature with blocking solution (Table 2.3). Primary antibodies were prepared in blocking solution and incubated with the cells for 2 hours at room temperature in a humidified atmosphere with gentle rocking. Primary antibody was aspirated and coverslips were washed 3 times with PBS for 10 minutes per wash. Secondary antibodies were

prepared in PBS and incubated with coverslips for 1 hour at room temperature with gentle shaking, followed by 3 further 10 minute washes. Following the final wash, the coverslips were mounted on slides using Vectashield mounting medium with DAPI for fluorescent staining of nuclei. Coverslips were left to dry overnight and were sealed with nail varnish prior to image acquisition on a Zeiss LSM710 confocal microscope.

Target	Blocking Solution	Primary Antibody	Secondary Antibody
TREM2	5% Normal donkey serum	Mouse: 10µg/ml sheep anti-TREM2 (AF1729, R&D Systems) Human: 10µg/ml goat anti-TREM2 (AF1828, R&D Systems)	Mouse: 1:1000 donkey anti-sheep Alexa Fluor 568 (A-21099, Life Technologies) Human: 1:500 donkey anti-goat Alexa Fluor 568 (A-11057, Life Technologies)
Golgi Complex	3% Bovine Serum Albumin	Mouse: 1:100 rabbit anti-Golgin97 (13192, Cell Signalling Technology) Human: 1:500 mouse anti-Golgin97 (A21270, Life Technologies)	Mouse: 1:1000 goat anti-rabbit Alexa Fluor 488 (R37116, Life Technologies) Human: 1:500 goat anti-mouse Alexa Fluor 568 (A11004, Life Technologies)
Calnexin	3% Bovine Serum Albumin	1:50 mouse anti-Calnexin (sc-23954, Santa Cruz Biotechnology)	1:500 goat anti-mouse Alexa Fluor 568 (A11004, Life Technologies)
Iba1	3% Bovine Serum Albumin	1:500 rabbit anti-Iba1 (019-19741,Wako)	1:1000 goat anti-rabbit Alexa Fluor 488 (R37116, Life Technologies)

Table 2.3 Antibodies used for immunocytochemistry

For golgin97 staining, fixation and permeabilisation using methanol was found to result in improved staining. Instead of using 4% PFA and Triton-X100, cells were fixed and permeabilised in ice-cold methanol for 20 minutes at -20°C. The coverslips were washed, blocked in BSA and the protocol continued as for PFA fixation.

2.7.2 Phalloidin labelling of F-actin

Phalloidin staining was performed using Phalloidin CF568 and a standard protocol (Chazotte, 2010), with adjustments made to concentrations and incubation times according to the manufacturer's instructions (Biotium). Phalloidin, a high affinity actin probe conjugated to a fluorescent dye, was used to study the morphological phenotypes of microglial cells. Cells were plated on 13mm glass coverslips at a density of 5,000 cells per coverslip for BV2 cells. Following treatment with murine macrophage colony-stimulating factor (MCSF, 100ng/ml) or adenosine triphosphate (ATP, 50μM) in serum free RPMI for 5 minutes, cells were washed with PBS and fixed by incubation with 4% PFA for 20 minutes. Cells were washed again and stored in PBS at 4°C until use. Cells were permeabilised with 0.5% Triton-X100 (made up in PBS) at room temperature for 10 minutes. Coverslips were washed 3 times with PBS and incubated with a 1:40 dilution of fluorescent phalloidin at room temperature for 20 minutes, protected from light. Coverslips were washed 3 times with PBS and mounted on slides using Vectashield mounting medium with DAPI for fluorescent staining of nuclei. Coverslips were left to dry overnight and were sealed with nail varnish prior to image acquisition on a Zeiss LSM710 confocal microscope using Zeiss Zen Microscope software.

Cytoskeletal analysis was carried out using ImageJ software (version 1.50). For analysis of filopodia formation, the samples (3 independent experiments, 40-50 cells per sample) underwent blinded measurement of filopodia length and quantification of filopodia number per cell. The samples (5 independent experiments, 40-50 cells per sample) underwent blinded morphological scoring for membrane ruffle formation as: absence, 0, ruffling response 1. Membrane ruffles were defined as wave-like regions of intense F-actin staining at extended cell edges. Immunohistochemistry was performed to confirm that regions counted as ruffles possessed F-actin and Iba1 colocalisation as reported in the literature (Ohsawa *et al.*, 2000).

2.7.3 Immunohistochemistry

Frozen tissue sections were acquired pre-sliced and mounted from the Queen Square Brain Bank (human temporal lobe samples) and from Amsbio (human kidney samples, Abingdon, United Kingdom) and were stored at -80°C until use. Ethical permission for this study was obtained from the National Hospital for Neurology and Neurosurgery and the Institute of Neurology joint research ethics committee (study reference IONMTA19/16 with corresponding RNA samples acquired under study reference IONMTA8/15). Immunohistochemistry performed using standard protocol with fixation modifications due to the use of fresh frozen tissue (Davies *et al.*, 2013). Slides were fixed and permeabilised immediately upon removal from the freezer with ice cold, 100% methanol for 20 minutes at 4°C, followed by 3 x 5 minute PBS washes. Samples were blocked in 5% horse serum for 1 hour at room temperature, followed by primary antibody incubation (1:250 mouse anti-CR1 SC-7308, Santa Cruz) overnight at 4°C. The slides were washed 3 times with PBS prior to treatment with 0.3% hydrogen peroxide (diluted in PBS) for 15 minutes to block endogenous peroxidases found in the tissue. After further 3 x 5 minute PBS washes, biotinylated secondary antibody was added to the slides (1:200 horse anti-mouse, BA-2001, Vector) for an hour at room temperature. DAB visualisation of antibody staining was performed using Vectastine Elite ABC HRP kit followed by DAB kit according to the manufacturer's instructions. The slides were dehydrated in serial alcohol dilutions followed by xylene and were mounted in DPX. Images were acquired on a Zeiss Axiophot light microscope.

2.8 Western Blotting

Western blotting was performed using standard techniques. For samples to be used for western blotting, cells were plated at a density of 8 x 10^4 in 6 well plates. In order to solubilise cellular proteins, medium was aspirated from cells and ice cold lysis buffer (1% NP-40, 150 mM NaCl, 50 mM Tris HCl (pH 7.2) and HaltProtease and Phosphatase Inhibitor (100x)) was added to wells and incubated at 4°C with shaking for 30mins. Lysates were collected and centrifuged at 12,000 g to pellet the nuclear fractions as well as any cellular debris. The supernatant was collected and stored at -20°C until required.

A Bradford protein assay was used to determine the total protein concentration of each cytoplasmic fraction sample using BSA as a standard. The principle of the assay is based upon a colour change shift by an acidic solution of Coomassie dye, from 465 nm to 595 nm, upon binding to proteins (Bradford, 1976). This visible colour change allows

BSA to be used to generate a standard curve to plot known BSA concentrations against absorbance at 595nm, allowing the total protein concentration of a lysate sample to be determined. Samples were run in triplicate in a 96 well plate. Briefly, 200 µl of Bradford reagent was added to 2 µl of sample lysate, as well as to a BSA standard curve, and was mixed on an orbital shaker for 5 minutes. The resultant colour change was measured using a Tecan Genios plate reader on the basis of the greater the concentration of protein, the greater the intensity of the colour shift from brown to blue.

For sodium dodecyl polyacrylamide gel electrophoresis (SDS-PAGE), the volume of lysate sample equivalent to 35 µg of protein was added to 4X protein sample loading buffer + 10% NuPAGE sample reducing agent and denatured by heating at 100°C for 5 minutes. Samples were loaded into gel wells alongside All Blue Prestained Protein Standards molecular weight markers to show the molecular weight of visualised bands. Proteins were separated by SDS-PAGE using 4-20% BIO-RAD mini-PROTEAN TGX Precast Gels in a Bio-Rad mini gel tank filled with running buffer (125mM Tris-Base, 1M glycine, 0.01% SDS) at 120 V until the gel front from the sample buffer reached the bottom of the gel.

Following SDS-PAGE, the gel was removed, trimmed and equilibrated in ice cold transfer buffer for 5 minutes (25mM Tris-Base, 192mM glycine, 20% methanol, 0.01% SDS). 3MM chromatography paper, fibre pads and nitrocellulose membrane cut to the size of the gel were also immersed in ice cold transfer buffer. A sandwich of transfer buffer-soaked fibre pads, 3MM chromatography paper, the gel and the nitrocellulose membrane was constructed on a transfer cassette, ensuring that any air bubbles were removed. The cassette was inserted into a Bio-rad mini gel transfer apparatus and proteins were transferred onto the nitrocellulose membrane for 1.25 hours at 100V.

After transfer, membranes were washed in 1x PBS/0.1% Tween-20 (PBS-T) for 10 minutes and then blocked in 5% non-fat milk solution in PBS-T for 1h at room temperature to reduce non-specific antibody interactions. The membranes were incubated with primary antibody diluted in 5% milk solution overnight at 4°C followed by 3 x 10 minute washes in PBS-T. The membranes were incubated with the appropriate fluorescent secondary antibody (see table) at room temperature for 1 hour and then underwent further 3 x 10min washes. Membranes were visualised using the Odyssey infrared imaging system (Odyssey V3.0 Software) and the resulting bands were subjected to densitometry analysis using ImageJ software. Treatments and conditions were replicated 3 times and quantified for statistical analysis.

In order to accurately quantify the highly glycosylated TREM2 protein, the equivalent volume of 35µg protein was treated with peptide:N-gycosidase (PNGase, according to the manufacturer's instructions) to induce sample deglycosylation. Samples were then prepared for gel electrophoresis as above.

Primary and secondary antibodies were used as follows:

Protein of Interest	Primary Antibody	Secondary Antibody
β-actin	1:10,000 mouse monoclonal anti-β-actin (Sigma #A5441)	1:15,000 Goat anti-Mouse Alexa Fluor 680 conjugate (Life Technologies #A21058)
TREM2 (mouse)	1:500 sheep polyclonal anti-TREM2 (R&D Systems #AF1729)	1:60,000 Donkey Anti-Sheep Alexa Fluor 790 conjugate (Jackson ImmunoResearch 713-655-147)
TREM2 (human)	1:500 goat anti-TREM2 (R&D Systems # AF1828) 1:1000 rabbit anti-TREM2 D8I4C (Cell Signalling Technology #91068)	1:10,000 donkey anti-goat IRDYE 800CW (Li-cor #925-32214) 1:10,000 goat anti-rabbit IRDYE 800CW (Li-cor #925-32211)
Iba1	1:1000 rabbit anti-Iba1 (019-19741,Wako)	1:15,000 Goat-anti rabbit Alexa Fluor 790 conjugate (Life Technologies #A11369)

Table 2.4 Antibodies used for western blotting

2.9 Enzyme-linked Immunosorbent Assay (ELISA)

For ELISAs, BV2 cells were plated at a density of 8 x 10^4 cells per well in a 24 well plate and iPSC-MGLC were plated at a density of 4 x 10^4 cells per well in a 96 well plate, with the exception of supernatants for C1q ELISA which were cultured at a

density of 1 x 1010^5 cells per well in a 6 well plate. BV2 cells were cultured for 24 hours prior to treatment. iPSC-MGLC were differentiated for 7 days prior to treatment. Following treatment, cell culture medium samples were collected and centrifuged at 15,000 *g* for 2 minutes to pellet any cellular debris. All of the supernatants were collected and transferred to new tubes (500 µl)/96 well plates (100 µl), snap frozen on dry ice and stored at -20°C until use. Samples were defrosted and used only once to preserve the integrity of the soluble factors.

2.9.1 ELISA analysis of soluble TREM2 in mouse BV2 cell cultures

Quantification of soluble TREM2 (sTREM2) from mouse cell culture supernatants was performed using an in-house generated ELISA, developed by Dr Matt Butler. MaxiSORP 96 well plates were coated overnight at 4°C with 1 µg/ml rat anti-human/mouse TREM2 monoclonal antibody (R&D Systems; MAB17291) made up in PBS. Plates were washed 3 times with 0.1% PBS-T, blocked with 1% BSA in PBS for 45 minutes at room temperature followed by 3 more washes with 0.1% PBS-T. Recombinant murine TREM2-Fc (R&D Systems; #1729-T2-050) was used to prepare a standard curve to allow the concentration of sTREM2 in the samples to be determined. 100 µl of cell culture supernatants and TREM2 standards were added to the wells and incubated for 2 hours at room temperature with gentle shaking, followed by 3 washes. In order to detect bound sTREM2, 0.2 µg/ml anti-mouse TREM2 biotinylated polyclonal antibody (R&D Systems; #BAF1729) was used as the detecting antibody and was incubated on the plates for 2 hours with gentle shaking at room temperature. Plates underwent 3 further washes with 0.1% PBS-T prior to the addition of 0.1 µg/ml streptavidin-HRP for 45 minutes, with gentle shaking at room temperature. Following 3 washes with 0.1% PBS-T, a chromogenic substance (TMB) was added to the plates. The reaction was stopped with the addition of 0.5M H_2SO_4 in H_2O and absorbance was read at 450 nm (Tecan Genios).

2.9.2 ELISA analysis of soluble TREM2 in human iPSC-MGLC cultures

In order to quantify sTREM2 levels in human samples, the above mouse sTREM2 ELISA protocol (2.9.1 ELISA analysis of soluble TREM2 in mouse BV2 cell cultures) was followed with some modifications. 1 µg/ml of rat anti-mouse/human monoclonal antibody (R&D Systems; clone 237920) and 0.1 µg/ml biotinylated polyclonal goat anti-human TREM2 antibody (R&D Systems BAF1828) were used as the capture and detecting antibody, respectively. Recombinant human TREM2-His (Life Technologies 11084H08H25) was used to generate a standard curve.

2.9.3 Mouse TNFα Cytokine Quantification

Analysis of TNFα secretion by mouse BV2 cells was carried out using a Mouse TNF-alpha Quantikine ELISA Kit (R&D systems, MTA00B) according to the manufacturer's instructions. Briefly, plated cells were either unstimulated or stimulated with 1µg/ml lipopolysaccharide (LPS) for 24 hours. 100 µl cell samples were incubated on the pre-coated plate alongside kit standards in order to determine TNFα concentrations. After 2 hours of incubation, the TNFα conjugate was added to the wells for a further 2 hours. The substrate solution was incubated for 30 minutes and the reaction was stopped through the addition of a stop solution. The resultant colour change was read using a Tecan Genios plate reader.

2.9.4 Human TNFα & IL-6 Cytokine Quantification

Quantification of TNFα and IL-6 secretion by human iPSC-MGLC was conducted using human ELISA kits from DuoSet (R&D systems, DY210 for TNFα and DY206 for IL-6) according to the manufacturer's instructions. Briefly, 100µl of supernatants from cells treated with LPS were added to 96-well plates that had been coated overnight with TNFα capture antibody and blocked with 1% BSA for an hour. Sample supernatants were incubated on the plate alongside serial dilutions of recombinant protein standards for the generation of a standard curve for 2 hours at room temperature. Following 3 PBS-T washes, detection antibody was added for 2 hours at room temperature, followed by 3 further washes and incubation with streptavidin-HRP for 45 minutes. Following 3 final washes with PBS-T, a chromogenic substance (TMB) was added to the plates. The reaction was stopped with the addition of 0.5M H_2SO_4 in H_2O and absorbance was read at 450 nm (Tecan Genios).

2.9.5 Human C1q ELISA

Quantification of human C1q secretion by the iPSC-MGLC was performed using a human C1q ELISA kit (Thermofisher, BMS2099), according to the manufacturer's instructions. Supernatants were collected from unstimulated cells and added to the pre-coated plated alongside diluted C1q standards to provide a standard curve from which the C1q concentration of samples was determined. After 2 hours of incubation, the biotin-conjugate was added for a further hour. Streptavidin-HRP (1:1000) was incubated in the wells for an hour, followed by TMB substrate solution (undiluted). The reaction was stopped with the provided stop solution and absorbance was read at 450 nm (Tecan Genios).

2.9.6 Mouse Cytokine Array

The proteome profiler mouse XL cytokine array (R&D Systems, ARY028) was used to determine the secretion of 111 mouse cytokines in a membrane-based antibody array, according to the manufacturer's instructions. Following treatment with LPS (1µg/ml), BV2 supernatants were collected, centrifuged to remove debris and incubated with the membranes overnight at 4°C. The detection antibody cocktail was added for an hour, followed by streptavidin-HRP. Chemiluminescence was performed to develop the membrane array and the membranes were exposed to autoradiography film. Data were analysed using the Protein Array Analyser Palette plugin (ImageJ), normalising to both reference and negative control points.

2.10 Quantitative Polymerase Chain Reaction (qPCR) for evaluation of mRNA expression levels

For qPCR analysis of mRNA expression levels, BV2 cells were cultured for 24 hours prior to treatment or sample collection and iPSC-MGLC were differentiated for 7 days prior to treatment or sample collection. BV2 cells were lysed and homogenised using QIAzol buffer and total RNA was extracted using miRNeasy mini kit with an additional on-column DNase digestion step using RNase-free DNase set. For human iPSC-MGLCs, cells were lysed and homogenised using RLT buffer (QIAGEN) and total RNA was extracted from cells using an RNeasy minikit according to the manufacturer's instructions, with an on-column DNase digestion step using RNase-free DNase set. The concentration of total RNA extracted was determined using a NanoDrop spectrophotometer. Sample volumes equivalent to 500ng RNA were used to generate complementary DNAs using the High-Capacity RNA-cDNA kit, according to the manufacturer's instructions. Quantitative PCR was conducted using TaqMan Universal Mastermix II in the Stratagene Mx3000p qPCR system and MxPro qPCR software. Expression was normalised to GAPDH and for primers used for mouse and human samples see table below:

Species	Gene name	Primer ID
Human	Aif1	Hs00610419_g1
	Apoe	Hs00171168_m1
	Axl	Hs01064444_m1
	C1qa	Hs00381122_m1
	Cd33	Hs01076281_m1
	Cr1	Hs00559348_m1
	Csf1r	Hs00911250_m1
	Gapdh	Hs0278991_g1
	Gpr34	Hs00758331_m1
	Itgam	Hs00355885_m1
	Itgb2	Hs00164957_m1
	Mertk	Hs01031979_m1
	P2y12	Hs00224470_m1
	Pros1	Hs00165590_m1
	Spi1	Hs02786711_m1
	Tgfβ1	Hs00998133_m1
	Tmem119	Hs01938722_u1
	Trem2	Hs00219132_m1

	Tyrobp	Hs00182426_m1
Mouse	Actb	Mm00607939_s1
	Aif1	Mm00479862_g1
	Gapdh	Mm99999915_g1
	Spi1	Mm00488140_m1
	Tnf	Mm00443258_m1
	Trem2	Mm04209244_g1

Table 2.5 Primer IDs for TaqMan qPCR probes (Thermo Fisher Scientific)

2.11 Analysis of phagocytic activity by flow cytometry

Cells were plated at a density of $1x10^5$ per well in a 24 well plate for 24 hours prior to the assay. As a negative control, cells were pre-incubated with 10μM cytochalasinD for 30 minutes, a potent inhibitor of actin polymerisation, which is vital for the changes in cell structure required for the phagocytosis of particles. Cells were incubated with 50 μg pHrodo green *E. coli* particles for 30 minutes at 37°C, rinsed in PBS and incubated with PBS (without $CaCl_2$ and $MgCl_2$) for 10 minutes to dissociate cells, all conducted whilst taking care to avoid excessive exposure to light. Cells were collected and washed twice in ice cold FACS buffer (0.5% BSA, 0.05% sodium azide and 2mM EDTA in PBS without $CaCl_2$ and $MgCl_2$). Cells were diluted in FACS buffer and were analysed with a BD FACS Calibur flow cytometer and results were analysed with Flowing software (Cell Imaging Core of the Turku Centre for Biotechnology, flowingsoftware.btk.fi). Mean fluorescence intensities were calculated for each sample.

2.12 Statistical Analysis

Results were analysed using Prism software (Version 7, Graphpad). Unless otherwise stated, one-way ANOVA analysis with post-tests, such as Dunnett's multiple comparison test, used as indicated in figure legend.

3. Characterisation of CRISPR/Cas9 TREM2 gene editing in mouse BV2 microglial cell line

In this chapter, the generation of the CRISPR/Cas9 gene edited BV2 cell lines was performed by Claudio Villegas Llerena (UCL Institute of Neurology).

3.1 The generation of TREM2 knockdown and knockout cell lines

Following the identification of TREM2 as a risk factor for Alzheimer's disease (AD), studies have been ongoing to elucidate TREM2 function, as well as dysfunction, in AD pathogenesis. In the healthy central nervous system, TREM2 expression has been found to be limited to microglia (Butovsky *et al.*, 2014); in fact it is one of the highest expressed microglial receptors, ranked at number 31 out of 75 in an analysis of the top 10% of receptors expressed by microglia (Hickman and El Khoury, 2014). The TREM2 mutations associated with Alzheimer's disease are predicted to be loss of function mutations (Kober *et al.*, 2016) and as such are amenable for modelling with knockdown and knockout cell lines. Therefore, in order to further investigate TREM2, CRISPR/Cas9 gene editing technology was used to generate TREM2 knockout lines from the mouse BV2 microglial cell line (performed by C. Villegas Llerena). BV2 cells were transfected with CRIPSR/Cas9 nickase plasmids designed to target exon 2 of the *Trem2* gene (Santa Cruz Biotechnology Inc). Targeting 5' regions of a gene helps to ensure intervention in the translation of the protein of interest at an early stage, thus minimising the likelihood of generating truncated proteins and translating other isoforms. As exon 1 of *Trem2* is only 194bp long, this makes it more difficult to generate guides to compared with exon 2, which is 5472bp long. Transfection with CRIPSR/Cas9 nickase plasmids resulted in the generation of clones with heterozygous *Trem2* knockout (1 allele KO and 1 WT allele): the A7 clone (5bp deletion) and the C8 clone (34bp deletion) (Figure 3.1), henceforth known as TREM2 knockdown lines. A second round of CRISPR Cas9 modification was performed on the C8 clone in order to generate homozygous *Trem2* knockout clones with 34bp deletion in each allele, known as the G4 and B5 cell lines. Single colony Sanger sequencing confirmed the presence of genetic modifications in the *Trem2* gene.

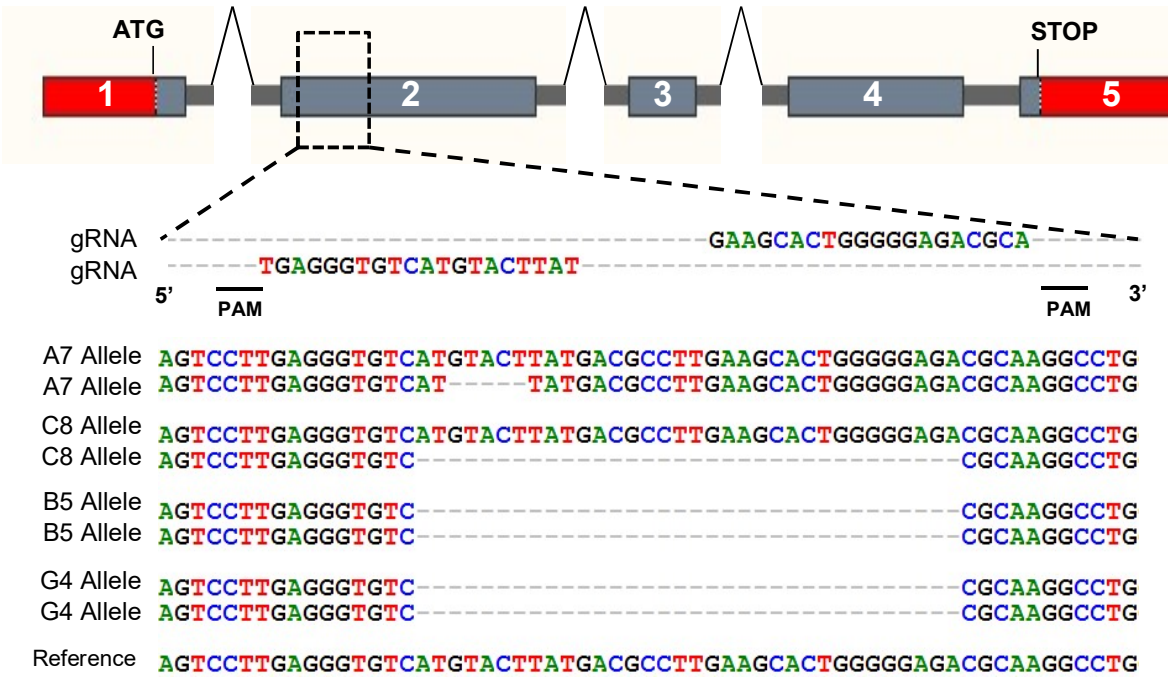

Figure 3.1 CRISPR/Cas9 nickase modification of the *Trem2* gene in BV2 cells

Schematic of the mouse *Trem2* locus and sequence alignment of the WT *Trem2* sequence and *Trem2* CRISPR/Cas9 modified mutants. gRNAs are aligned to their target sequences on exon 2 of the Trem2 gene. Protospacer-adjacent motifs (PAM) for each gRNA are marked with a line. Clones A7 and C8 were obtained during a first round of CRISPR modification, while clones B5 and G4 were obtained during a second round of CRISPR modifications using the clone C8 as the starting cell line. Figure kindly provided by Claudio Villegas Llerena, UCL Institute of Neurology.

qPCR analysis showed that *Trem2* mRNA levels were significantly reduced following TREM2 gene editing in both knockdown (A7 & C8) and knockout (G4 & B5) cell lines (**, $p<0.01$, Figure 3.2a). The resultant effect of decreased levels of *Trem2* mRNA on protein production was assessed by western blotting, ELISA and immunocytochemistry. Prior to western blotting, protein lysates were deglycosylated using PNGaseF as TREM2 exists in forms with varying degrees of glycosylation (Wunderlich et al. 2013; Park et al. 2015a; Kleinberger et al. 2014) resulting in multiple bands of different protein sizes on western blots that are difficult to accurately quantify. Therefore, samples were treated with PNGase to generate one single protein band for quantification of TREM2 expression levels. As shown in the representative western blot and subsequent densitometry quantification (Figure 3.2b and c), TREM2-targeting CRISPR/Cas9 modification resulted in a reduction of TREM2 protein expression to 38% and 15% of WT levels in the A7 and C8 clones respectively (**, $p<0.01$) and to 12% and 14% of WT levels in the knockout G4 and B5 clones (**, $p<0.01$).

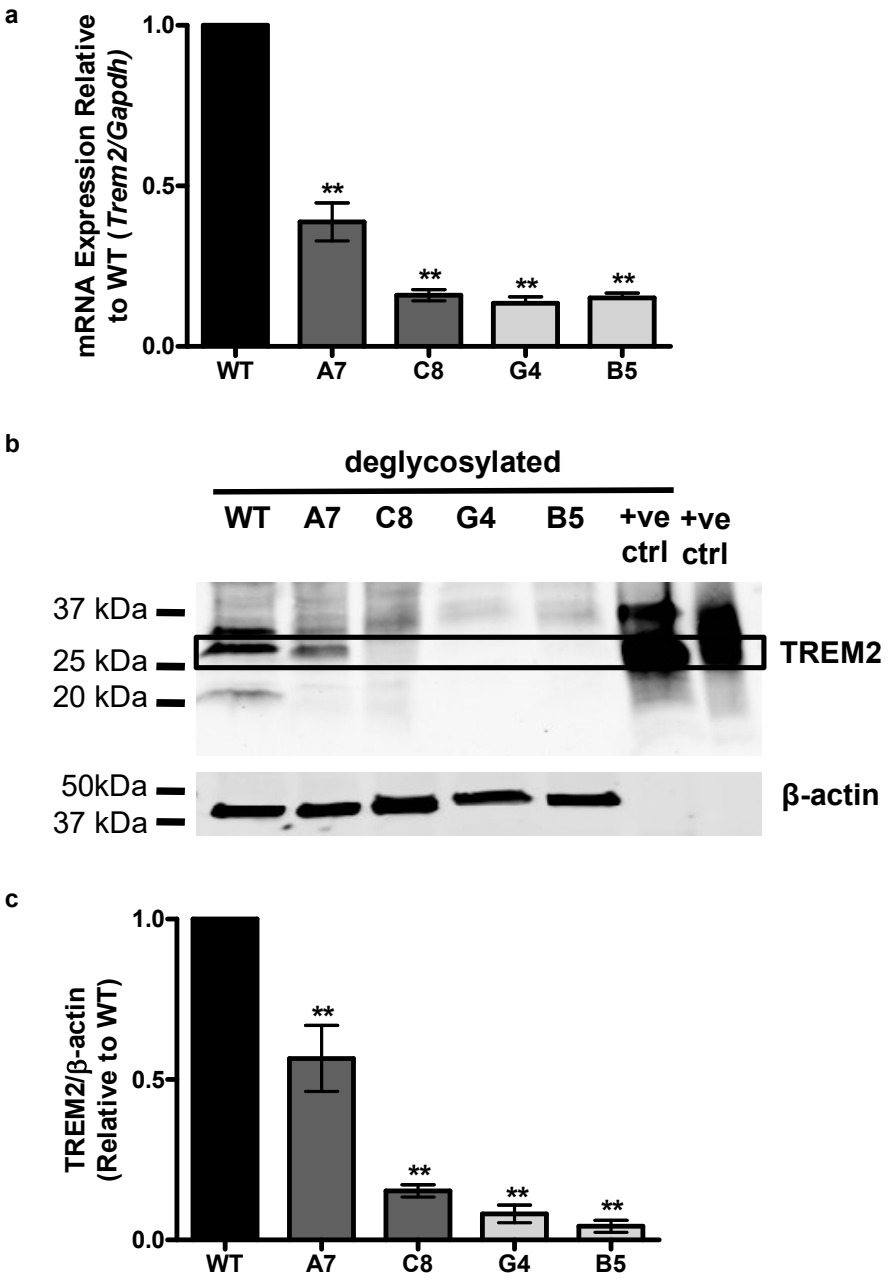

Figure 3.2 Characterisation of TREM2 knockdown and knockout clones generated using CRISPR/Cas9 modification

qPCR used to determine TREM2 mRNA expression levels in wildtype (WT), TREM2 knockdown (A7 and C8) and TREM2 knockout (G4 and B5) CRISPR/Cas9-edited BV2 cell lines (**a**). Graph represents *Trem2* mRNA expression normalised to *Gapdh* mRNA expression. Values relative to WT levels expressed as mean ±SEM for 3 individual experiments (** $p<0.01$; one way ANOVA with Dunnett's multiple comparison test). Representative western blot (**b**) and subsequent densitometric analysis (**c**) of TREM2 expression in WT, TREM2 knockdown (A7 and C8) and knockout (G4 and B5) cells. Lysates were treated with PNGase to deglycosylate proteins to accurately quantify total TREM2 protein levels. Recombinant extracellular mouse TREM2 was used as the positive control. Graph represents protein level relative to WT. Values were normalised to β-actin levels. Values are expressed as mean ±SEM for 3 individual experiments, ** $\rho<0.01$; one way ANOVA with Dunnett's multiple comparison test.

Immunocytochemical analysis of WT BV2 cells indicated that TREM2 protein expression exists as perinuclear puncta that preferentially co-localised with the golgi complex marker golgin97 (Figure 3.3). TREM2 is principally expressed in the golgi complex (Sessa *et al.*, 2004) but is shuttled to the cell surface, where it is readily cleaved by ADAM10-mediated ectodomain shedding (Kleinberger *et al.*, 2014). In the TREM2 knockdown and knockout cell lines, TREM2 staining was not punctate, was less intense and did not colocalise with golgin97 staining (Figure 3.3a & b). Golgin97 staining was not found to be affected by TREM2 knockdown.

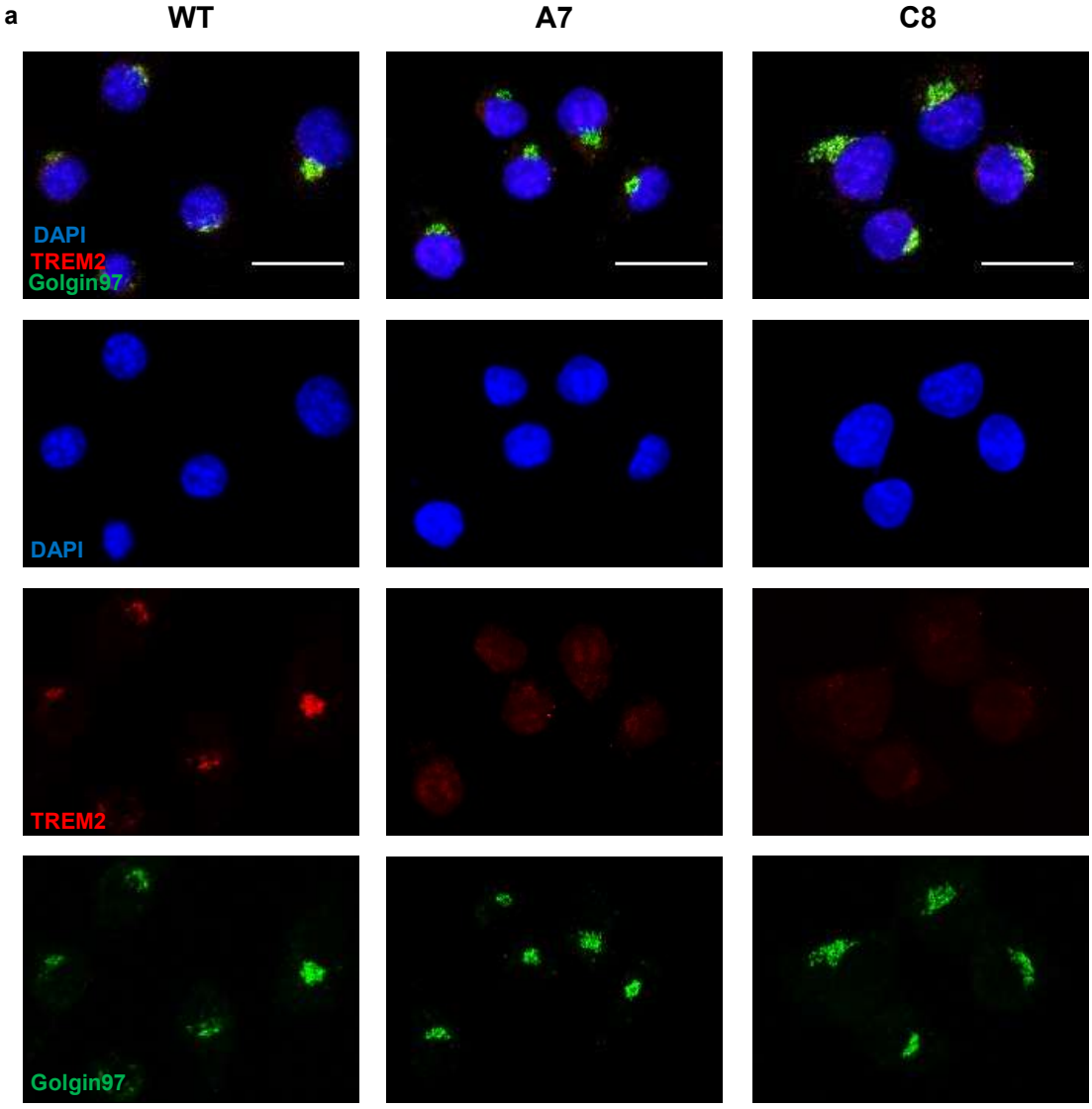

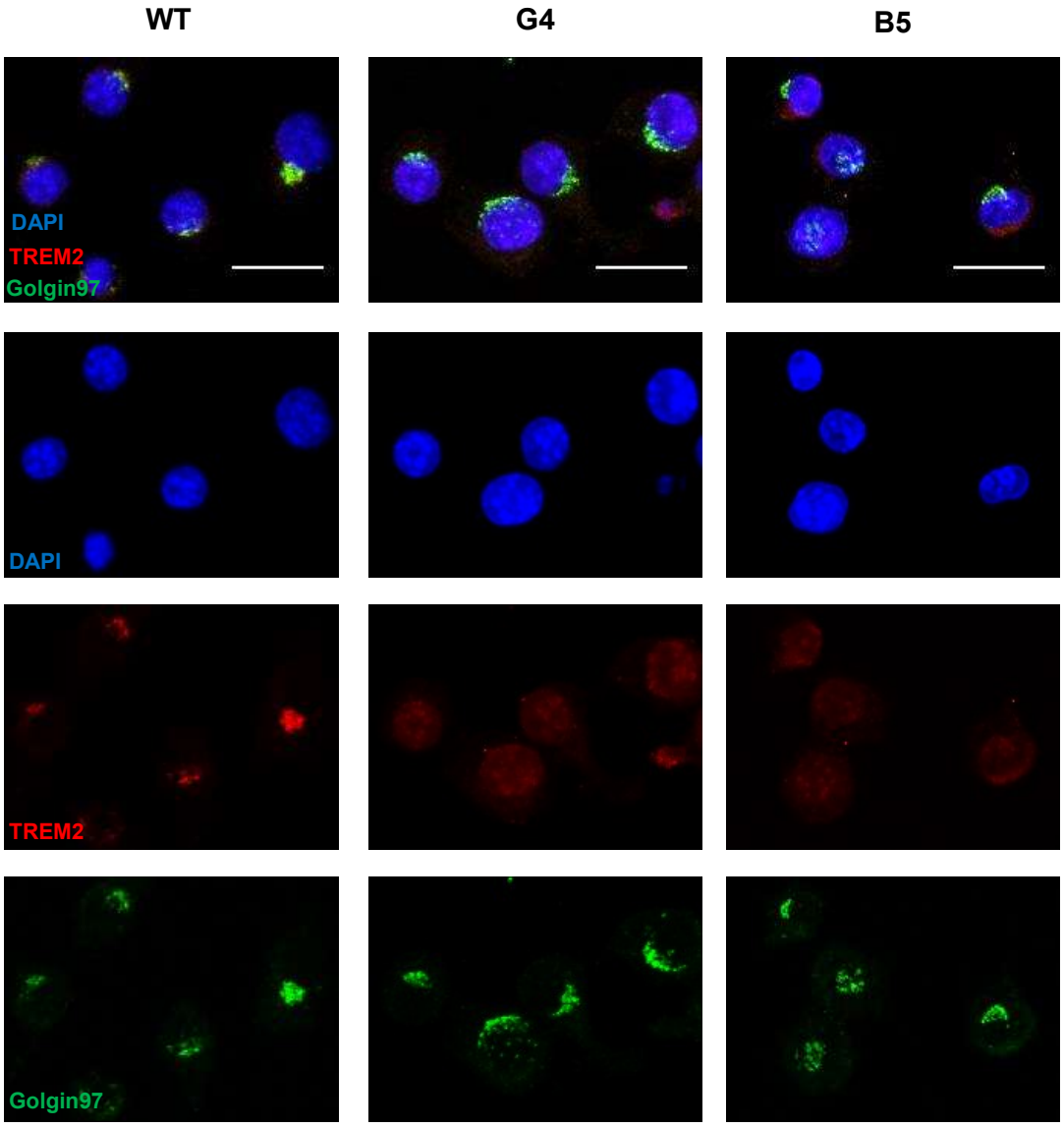

Figure 3.3 Characterisation of TREM2 cellular localisation by immunocytochemistry in WT, knockdown and knockout BV2 clones

Representative images of immunofluorescent labelling of TREM2 (red), golgi complex (green) and DAPI (blue) illustrating the differences in TREM2 staining intensity and cellular localisation in the (**a**) TREM2 knockdown (A7 and C8) and (**b**) TREM2 knockout (G4 and B5) cell lines. Top panel shows merged images. Scale bar represents 25µm.

Interestingly, despite TREM2 being a cell surface receptor, low levels of TREM2 expression at the cell surface were found by immunocytochemistry in all of the BV2 cell lines (Figure 3.3). Following this observation, the levels of soluble TREM2 (sTREM2) secreted into the cell supernatant following cleavage of the receptor at the cell surface were determined by ELISA. sTREM2 production was significantly reduced in the TREM2 modified clones compared with the WT cells (**, $p<0.01$, Figure 3.4) with knockdown and knockout cell lines having similar sTREM2 levels. Despite differences

existing between the western blotting results for the knockdown and the knockout lines regarding protein expression levels, similar levels of sTREM2 may be due to defects in the trafficking of truncated TREM2 protein from the golgi to the surface of the TREM2 knockdown cells, resulting in low surface expression but detectable protein in the cytoplasm.

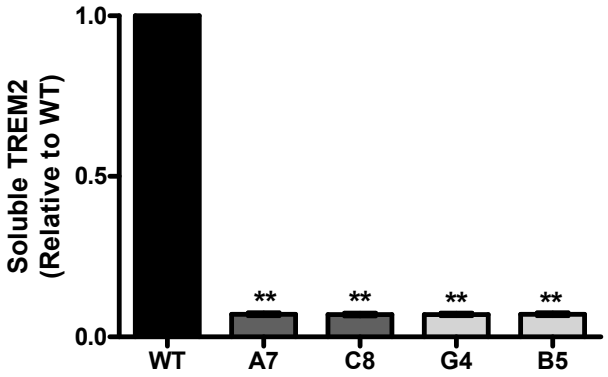

Figure 3.4 Quantification of soluble TREM2 release from WT, TREM2 knockdown and TREM2 knockout BV2 cells by ELISA

Soluble TREM2 (sTREM2) secretion levels determined by ELISA. Graph represents sTREM2 level relative to WT. Values expressed as mean ±SEM for 3 individual experiments (** $p<0.01$; one way ANOVA with Dunnett's multiple comparison test).

3.2 TREM2 knockdown alters LPS-induced TNFα gene transcription

TREM2 is thought to play a role in regulating pro-inflammatory responses in microglia/macrophages, however data demonstrating the directionality of its influence on TNFα production are conflicting (Turnbull *et al.*, 2006; Sieber *et al.*, 2013). Therefore, the effect of TREM2 gene editing on the generation and secretion of the pro-inflammatory cytokine TNFα in response to LPS treatment was assessed in the BV2 cell lines. LPS is a well characterised ligand of the TLR4 receptor, stimulation of which results in robust increases in TNFα secretion in microglia and macrophages. Treatment of WT BV2 cells with 1µg/ml LPS for 2 hours resulted in a 45 fold increase in *Tnf* mRNA expression compared with untreated cells (**, $p<0.01$), with expression remaining augmented 6 hours post-LPS treatment albeit lower than at 2 hours (22 fold increase compared with 45 fold) (Figure 3.5a and b). *Tnf* mRNA expression levels were significantly lower post-LPS treatment in the TREM2 knockdown and knockout cell lines than in the LPS-treated WT cells at both the 2 hour and 6 hour time points (*$p<0.05$, **$p<0.01$, Figure 3.5a and b), with the exception of the heterozygous C8 cell line after 6 hours (ns, $p>0.05$).

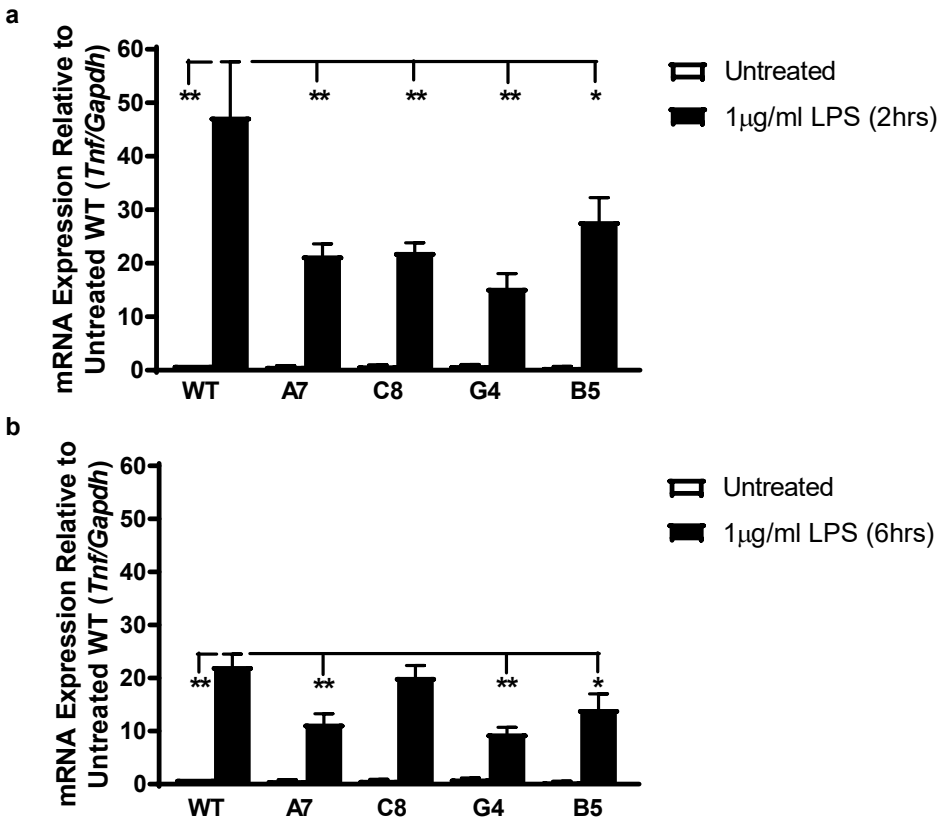

Figure 3.5 Expression of *Tnf* mRNA by WT, TREM2 knockdown and TREM2 knockout cells following 2hr and 6hr of LPS treatment

qPCR used to determine *Tnf* mRNA expression levels following (**a**) 2 hours or (**b**) 6 hours of LPS treatment (1μg/ml) in WT, TREM2 knockdown (A7 and C8) and TREM2 knockout (G4 and B5) BV2 cell lines. Graph represents *Tnf* mRNA expression normalised to *Gapdh* mRNA expression and data are shown relative to untreated WT levels. Values expressed as mean ±SEM for 4 individual experiments (* $p<0.05$, ** $p<0.01$; one way ANOVA with Dunnett's multiple comparison test).

The effect of TREM2 knockdown on the LPS-induced secretion of TNFα protein was further investigated by ELISA. Treatment of cells with 1μg/ml LPS for 24 hours induced a robust release of TNFα from undetectable level to concentrations of approximately 1.8μg/ml (Figure 3.6). With the exception of the G4 knockout cell line, there was no significant difference in the secretion of TNFα following 24 hours of LPS stimulation between WT cells and TREM2 knockdown and knockout cell lines (Figure 3.6). These data conflict with the mRNA results, as one would expect decreased generation of *Tnf* mRNA to result in decreased production of TNFα protein to be released into the cell supernatants.

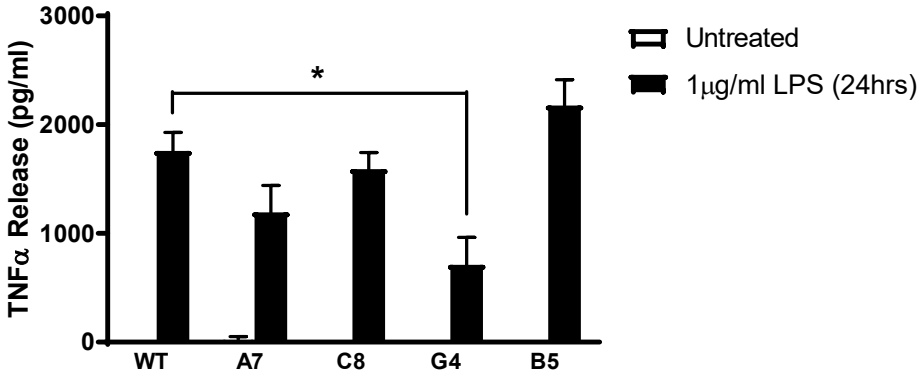

Figure 3.6 ELISA quantification of TNFα secretion by WT, TREM2 knockdown and TREM2 knockout BV2 cells

TNFα secretion following 24 hours of LPS treatment (1μg/ml) in WT, TREM2 knockdown (A7 and C8) and TREM2 knockout (G4 and B5) BV2 cell lines determined by ELISA. Values expressed as mean ±SEM for 4 individual experiments (* p<0.05; one way ANOVA with Dunnett's multiple comparison test).

qPCR analysis of baseline *Tnf* mRNA levels showed that there is no difference between the WT and the TREM2 knockdown lines, and a reduction of 30% in the B5 knockout line (**, p<0.01, Figure 3.7), which concurs with data showing that microglia isolated from TREM2$^{-/-}$ mice have downregulated expression of *Tnf* mRNA (Mazaheri *et al.*, 2017). Therefore, differences in *Tnf* mRNA levels are only found between the WT and knockdown cells following LPS treatment, suggesting that, in heterozygosity, TREM2 has an effect on the LPS-induced expression of *Tnf* rather than baseline expression.

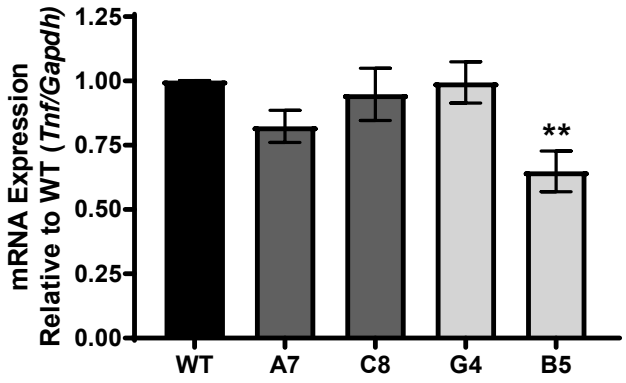

Figure 3.7 Expression of *Tnf* mRNA in untreated WT, TREM2 knockdown and TREM2 knockout cells

Baseline *Tnf* mRNA expression levels assessed using qPCR. Graph represents *Tnf* mRNA expression normalised to *Gapdh* mRNA expression. Data are shown relative to WT levels and values expressed as mean ±SEM for 4 individual experiments (** p<0.01; one way ANOVA with Dunnett's multiple comparison test).

Subsequently, the secretion of TNFα following priming with LPS was also assessed, as defects exist in the transcriptional response to LPS stimulation rather than in untreated cells. A 2 hour pulse of LPS treatment was used to release any existing pools of TNFα from the cells prior to culturing cells with fresh LPS-containing medium for a further 24 hours. The aim of this experiment was to allow the effects of any deficits in LPS-induced *Tnf* mRNA transcription to be seen in the TNFα protein released from the cells. Supernatants were collected after the initial priming 2 hour LPS treatment and TNFα levels were quantified by ELISA (Figure 3.8a). Similar to the ELISA results following 24 hours of treatment without priming (Figure 3.6), the only cell type with a marked difference from WT was the TREM2 knockout G4 line (Figure 3.8a). Primed cells were treated with 1μg/ml LPS for a further 24hours and, following ELISA analysis of the supernatants, the TREM2 knockdown A7 and C8 lines and the G4 knockout lines had significantly reduced levels of TNFα compared with WT (Figure 3.8b), reflecting the lower levels of *Tnf* mRNA found previously by qPCR (Figure 3.5). Interestingly, the levels of TNFα secreted by the knockout B5 cells has remained high at all time points of supernatant analysis both with and without the priming designed to clear existing stores of the cytokine (Figure 3.6, and Figure 3.8a & b). This is in contrast to the significantly decreased levels of *Tnf* mRNA both in baseline conditions and following LPS treatment (Figure 3.5a & b, and Figure 3.7).

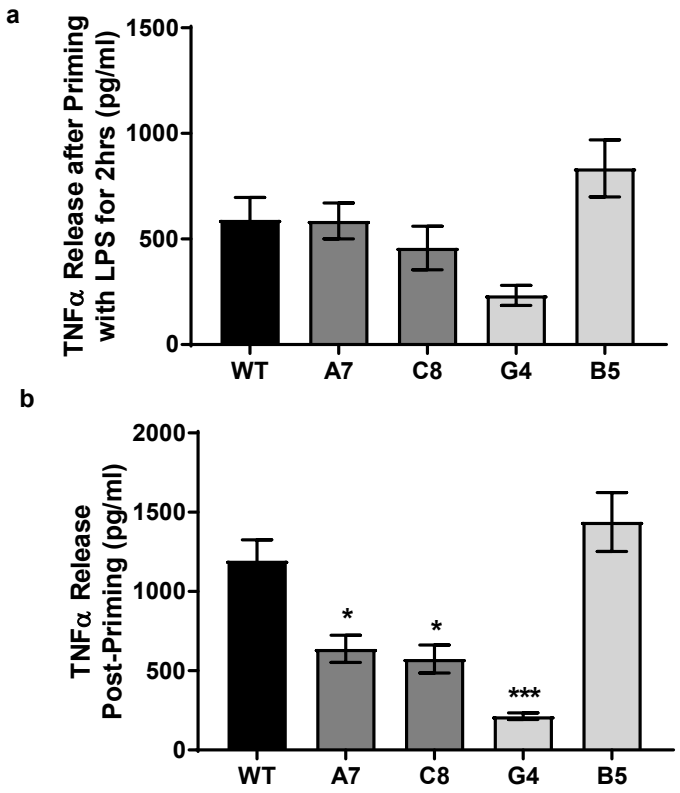

Figure 3.8 ELISA analysis of LPS-induced TNFα secretion after depletion of existing stores

TNFα secretion quantified by ELISA after 2 hours of priming with 1µg/ml LPS (**a**) and following a further 24 hours of treatment with 1µg/ml LPS (**b**) in WT, TREM2 knockdown (A7 and C8) and TREM2 knockout (G4 and B5) BV2 cell lines. Values expressed as mean ±SEM for 3 individual experiments (*p<0.05, ***p<0.001; one way ANOVA with Dunnett's multiple comparison test).

3.3 TREM2 knockdown and knockout microglia have altered actin cytoskeletal structures

Cells with TREM2 gene modifications were observed to have markedly different phenotypes to WT cells, displaying rounded morphology and lacking the extended processes found in WT cells (Figure 3.9). As actin signalling is thought to be downstream of TREM2 receptor activation (Peng *et al.*, 2010), the filamentous actin (F-actin) structures of the cells were investigated using fluorescently-conjugated phalloidin. Phalloidin is high-affinity actin probe derived from a toxin found in *Amanita phalloides* (the death cap mushroom) which binds and stabilises F-actin, preventing depolymerisation (reviewed in Cooper 1987), which when coupled to a fluorescent probe, allows the visualisation of actin cytoskeletal structures of cells

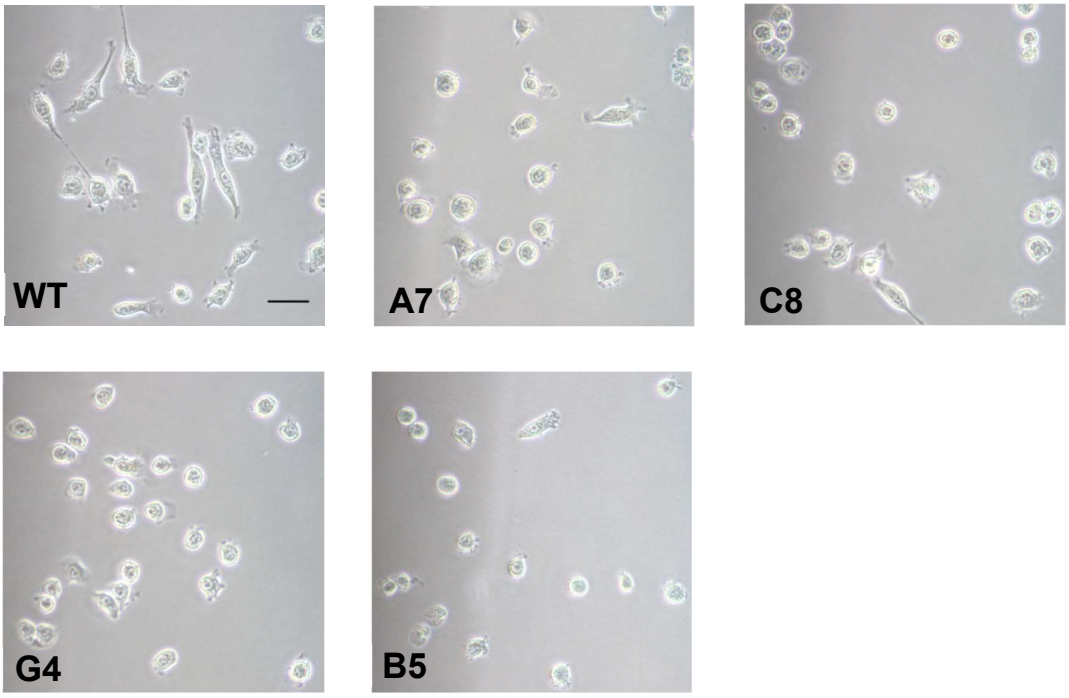

Figure 3.9 The effect of TREM2 knockdown and knockout on the morphology of BV2 cells

Representative phase contrast images of wildtype (WT), TREM2 knockdown (A7 and C8) and TREM2 knockout (G4 and B5) CRISPR/Cas9-edited BV2 cell lines. Scale bar represents 100μm.

Phalloidin staining of BV2 cells revealed the presence of filopodia on the surface of the cells (see arrow heads in Figure 3.10a) which, upon quantification, were found to be significantly shorter on TREM2 knockdown and knockout cell lines than on WT cells (*** $p<0.001$, ****$p<0.0001$, Figure 3.10b). Filopodia are thin, finger-like, plasma-membrane protrusions that are rich in filamentous actin and are thought to play roles in environment sensing, migration and phagocytosis (Pollard and Borisy, 2003; Niedergang and Chavrier, 2004; Chhabra and Higgs, 2007). In addition to the average length of filopodia on TREM2 knockdown and knockout cells being shorter than that on WT cells, the percentage of filopodia that fall in to the medium (6-10μm) or long (10-15μm) length categories was significantly lower following TREM2 modification (** $p<0.01$, Figure 3.10c). There was, however, no statistically significant difference in the average number of filopodia per cell (Figure 3.10d). In order to exclude differential expression of β-actin as a cause for the variation found in actin-rich filopodia formation, the expression levels of *Actb* mRNA in the WT and clone lines was assessed by qPCR. No statistically significant differences in β-actin expression were found although levels appeared to be slightly higher in the B5 knockout cell line (Figure 3.11).

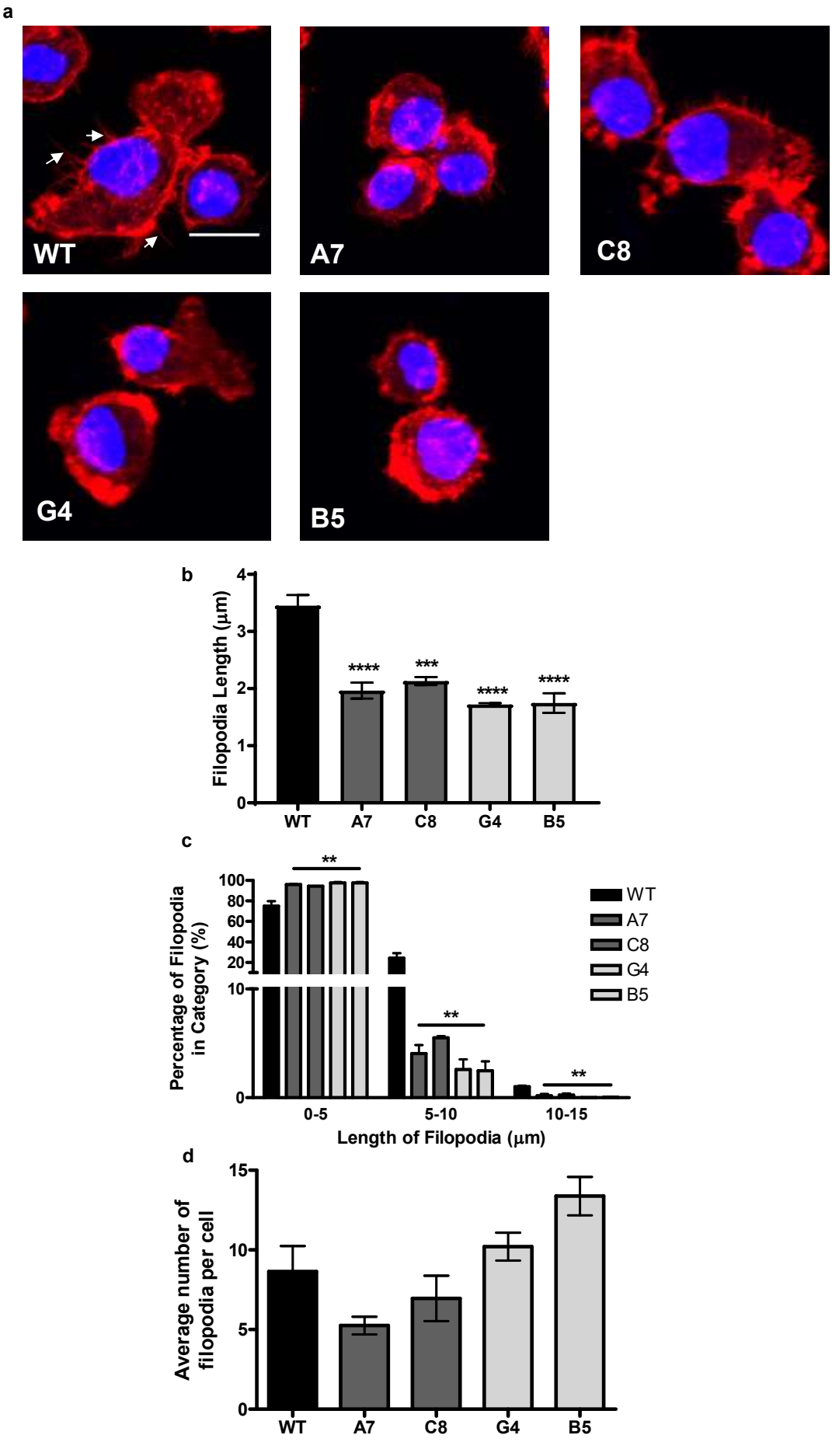
a
WT
A7
C8
G4
B5
b
Filopodia Length (μm)
4
3
2
1
0
****
***
****
****
WT
A7
C8
G4
B5
c
Percentage of Filopodia in Category (%)
100
80
60
40
20
10
0
**
**
**
WT
A7
C8
G4
B5
0-5
5-10
10-15
Length of Filopodia (μm)
d
Average number of filopodia per cell
15
10
5
0
WT
A7
C8
G4
B5

Figure 3.10 The effect of TREM2 knockdown and knockout on filopodia formation by BV2 cells

(**a**) Representative confocal microscopy images of BV2 cell lines labelled with phalloidin-568 (red) to visualise f-actin and DAPI (blue) to visualise the nucleus. Scale bar represents 20µm. Arrow heads showing filopodia. (**b**) Quantification of the length of filopodia on the surface of the cells visualised using phalloidin stain for f-actin. (**c**) Graph showing the percentage of filopodia that fit into the length categories of 0-5µm, 5-10 µm or 10-15µm for each cell line. For the purpose of performing statistical analysis, the percentage of filopodia in each category was tested against the WT values for that length category. (**d**) Quantification of the number of filopodia on the surface of the each cell. For all figures, values expressed as mean ±SEM for 3 individual experiments with a minimum of 5 fields of view analysed per experiment (** p<0.01, *** p<0.001, ****p<0.0001; one way ANOVA with Dunnett's multiple comparison test).

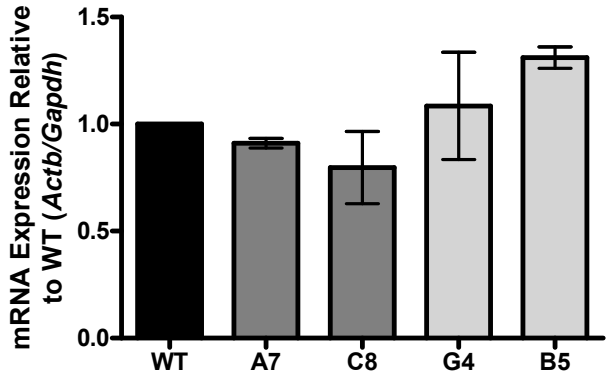

Figure 3.11 Expression of *Actb* mRNA in WT, TREM2 knockdown and TREM2 knockout BV2 cells

qPCR used to determine *Actb* mRNA expression levels in untreated WT, TREM2 knockdown (A7 and C8) and TREM2 knockout (G4 and B5) BV2 cell lines. Graph represents *Actb* mRNA expression normalised to *Gapdh* mRNA expression and data are shown relative to WT levels. Values expressed as mean ±SEM for 3 individual experiments (one way ANOVA with Dunnett's multiple comparison test).

3.4 TREM2 knockdown affects the ability of microglia to alter morphology in response to stimuli

One of the hallmarks of microglia is an ability to make rapid and marked morphological changes in order to respond to injury or potentially noxious stimuli, alongside making alterations to their function and behaviour. Therefore, the morphological responses of the cell lines to various stimuli were assessed to establish whether deletions in the TREM2 gene affected the cytoskeletal reorganisation, which was visualised by phalloidin staining. The WT cells, following stimulation with LPS (1µg/ml, 24 hours), adopted a bipolar morphology, defined as having two symmetrical processes emerging from a smaller cell soma (Figure 3.12a). There was a significantly smaller percentage of cells forming this bipolar morphology post LPS-stimulation in the TREM2 knockdown and knockout cell lines (* p<0.05, ** p<0.01, Figure 3.12b).

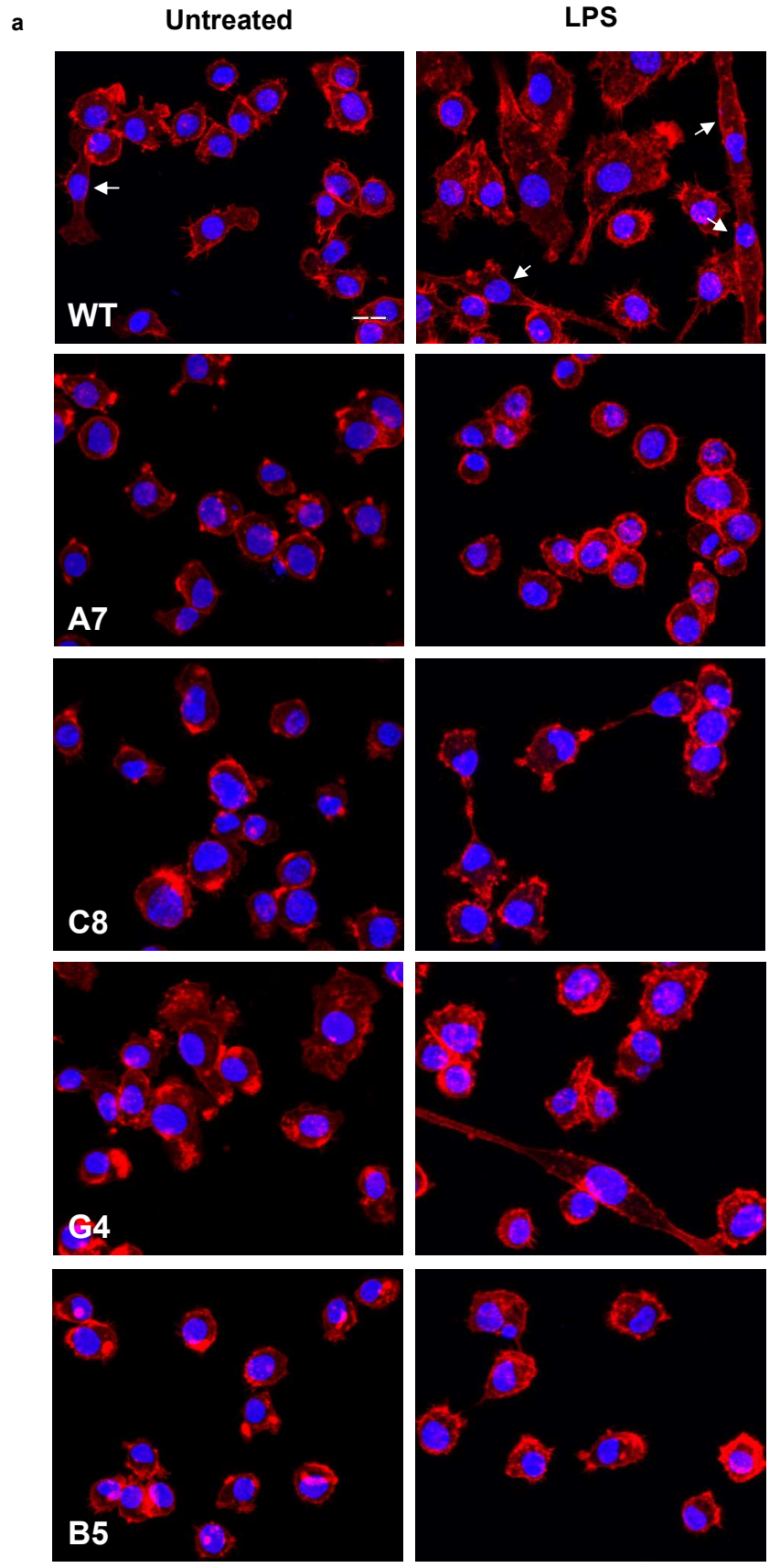
a
Untreated
LPS
WT
A7
C8
G4
B5

b

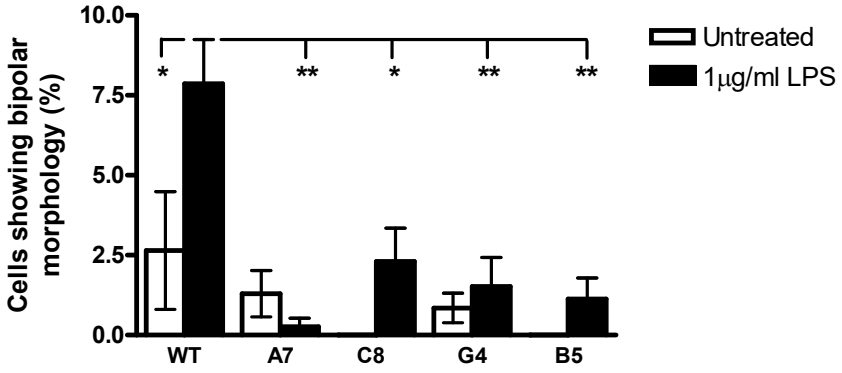

Figure 3.12 The effect of TREM2 knockdown and knockout on cytoskeletal reorganisation in response to LPS treatment in BV2 cells

(**a**) Representative images of immunofluorescent labelling of F-actin using phalloidin (red) and DAPI (blue) in BV2 cells treated with 1µg/ml LPS for 24hours. Scale bar represents 20µm. Arrowheads indicate cells with bipolar morphology. (**b**) Quantification of the percentage of cells with bipolar morphology following 24hours of stimulation with 1µg/ml LPS. Values expressed as mean percentage ±SEM for 3 individual experiments with a minimum of 5 fields of view analysed per experiment (* $p<0.05$, ** $p<0.01$; one way ANOVA with Dunnett's multiple comparison test).

Treatment of BV2 cells with ATP and MCSF also lead to marked morphological changes, namely the formation of membrane ruffles, which are wave-like structures formed by detachment and movement of the extended cell edges (Imai and Kohsaka, 2002). As reported in the literature (Ohsawa *et al.*, 2000), F-actin in the membrane ruffles of WT BV2 cells, which were induced by MCSF treatment, co-localised with Iba1, therefore confirming that the structures seen are indeed membrane ruffles (Figure 3.13).

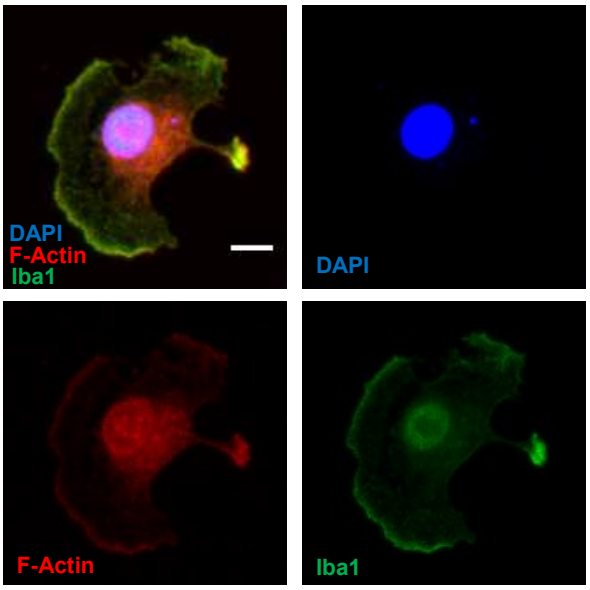

Figure 3.13 Definition of membrane ruffles in BV2 microglial cells

Representative images of immunofluorescent labelling of f-actin(red), Iba1 (green) and DAPI (blue) illustrating the colocalisation of Iba1 in the F-actin rich membrane ruffles in WT BV2 cells stimulated with MCSF (100ng/ml for 5 minutes). Scale bar represents 10µm.

Analysis of cell morphology showed that treatment with ATP (50µM, 5 minutes) or MCSF (100ng/ml, 5 minutes) leads to a significant increase in the number of WT cells with ruffling morphology (** $p<0.01$, Figure 3.14). We therefore wanted to investigate whether similar morphology response defects were found in knockdown and knockout cells in response to ATP and MCSF as those found following LPS treatment. The percentage of TREM2 knockdown and knockout cells displaying ruffling morphology following treatment with ATP was significantly lower than ATP-treated WT cells (* $p<0.05$, **$p<0.01$, Figure 3.14b). Similarly, the cell lines with TREM2 gene modifications also failed to respond to MCSF in the same as the WT cells, with a significantly lower percentage of cells showing ruffling of the cell membrane following stimulation (*$p<0.05$, **$p<0.01$, Figure 3.14c).

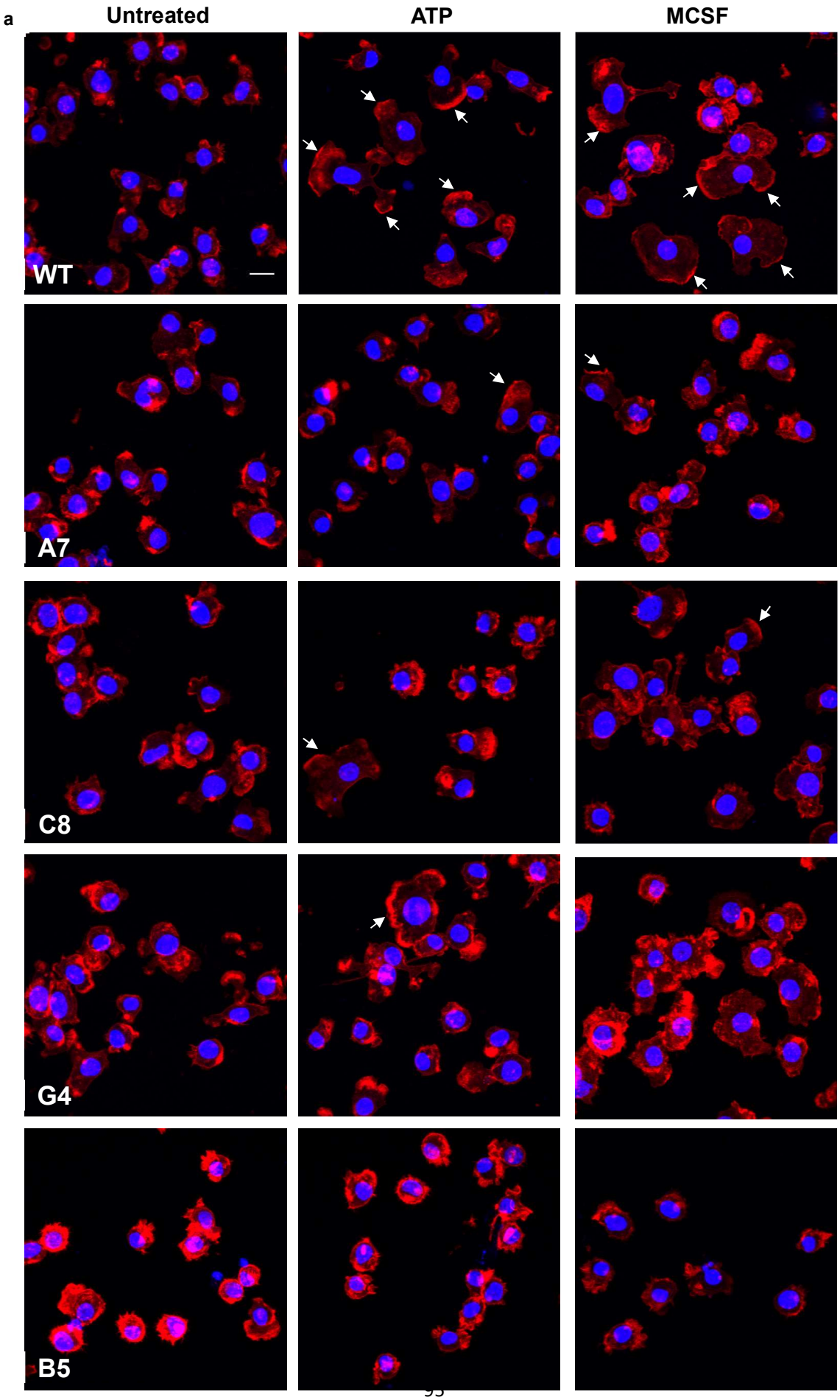
a
Untreated
ATP
MCSF
WT
A7
C8
G4
B5

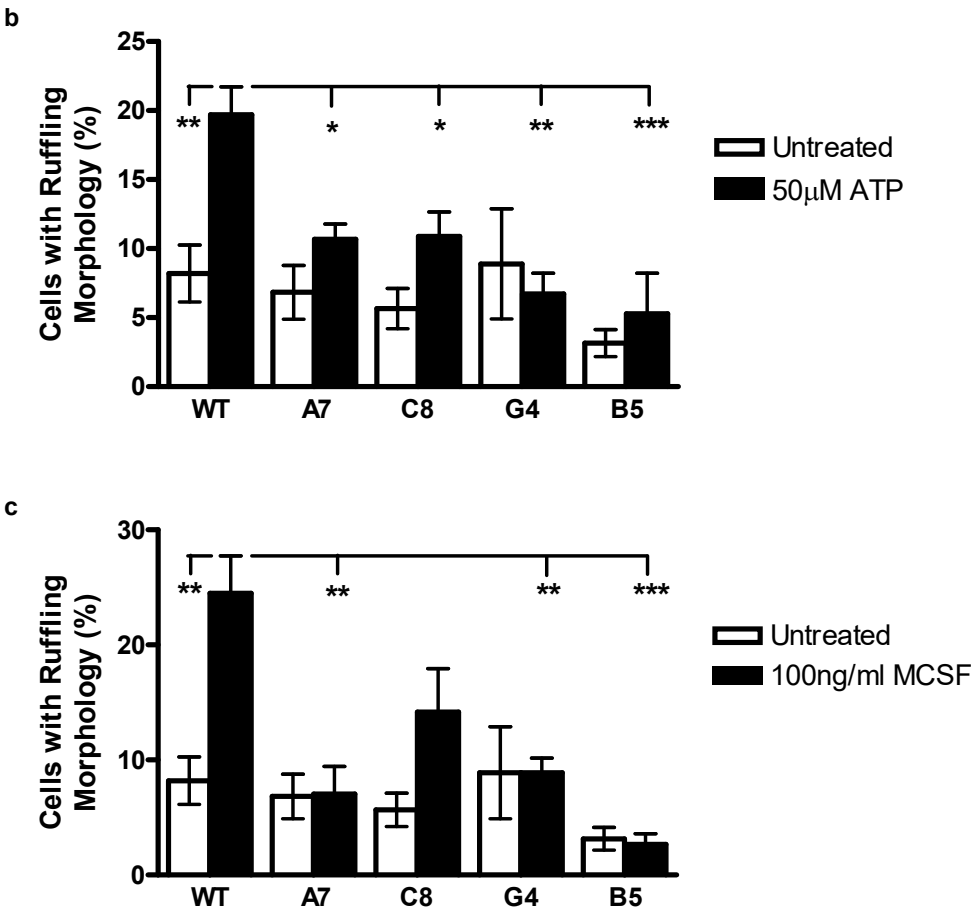

Figure 3.14 The effect of TREM2 knockdown and knockout on membrane ruffling by BV2 cells in response to ATP or MCSF treatment

Representative images of immunofluorescent labelling of F-actin using phalloidin (red) in BV2 cells treated with 50μM ATP or 100ng/ml MCSF for 5 minutes (**a**). Scale bar represents 20μm. Arrowheads indicate membrane ruffles. Quantification of the percentage of cells with membrane ruffling morphology following 5 minutes of stimulation with 50μM ATP (**b**) or 100ng/ml MCSF (**c**). Values expressed as mean percentage ±SEM for 5 individual experiments with a minimum of 5 fields of view analysed per experiment (* P<0.05, **P<0.01; one way ANOVA with Dunnett's multiple comparison test).

Iba1 has been shown to be important for the formation of membrane ruffles (Ohsawa *et al.*, 2000; Sasaki *et al.*, 2001); indeed, overexpression of Iba1 is sufficient for the generation of ruffles in response to growth factors in non-ruffling cells (Kanazawa *et al.*, 2002). Therefore the expression of Iba1 in the TREM2 knockdown and knockout cells was investigated. The TREM2 modified cells have significantly lower levels of *Aif1* mRNA, the gene that encodes for Iba1, than controls (**p<0.01, ***p<0.001, ****p<0.0001, Figure 3.15a). Western blot analysis of Iba1 protein expression concurred with mRNA data, demonstrating that expression was significantly lower in TREM2 knockdown and knockout cells than in controls (**p<0.01, ****p<0.0001, Figure 3.15b & c).

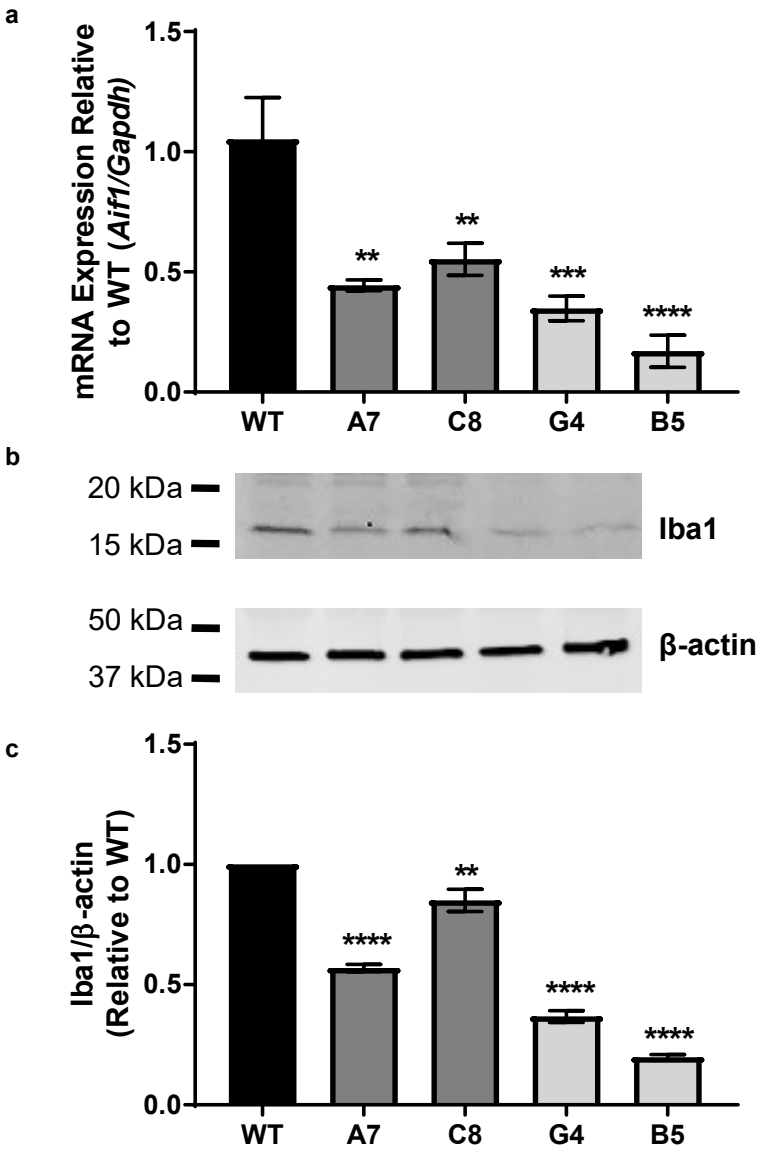

Figure 3.15 The effect of TREM2 knockdown and knockout on the expression of Iba1 in BV2 cells

(**a**) qPCR to determine *Aif1* mRNA expression levels in WT, TREM2 knockdown (A7 and C8) and TREM2 knockout (G4 and B5) BV2 cells. Graph represents *Aif1* mRNA normalised to *Gapdh* mRNA expression, relative to WT levels. Representative western blot (**b**) and subsequent desitometry analysis (**c**) of Iba1 expression in WT, TREM2 knockdown (A7 and C8) and knockout (G4 and B5) cells. Graph represents protein level relative to WT. Values were normalised to β-actin levels. Values are expressed as mean ±SEM for 3 individual experiments, ** ρ<0.01, ***p<0.001, ****p<0.0001; one way ANOVA with Dunnett's multiple comparison test.

3.6 Pre-treatment with sTREM2 does not rescue the morphological defects in the MCSF response found in TREM2 knockout cells

In order to investigate whether any of the phenotypic deficits in the TREM2 knockout cell lines could be rescued through the exposure of cells to sTREM2, the B5 cells, which had the most extreme deficits in membrane ruffling (Figure 3.14), were cultured in microglia conditioned medium (MGCM) from WT cells for 24 hours prior to stimulation with MCSF. MCSF stimulation was chosen as this resulted in higher levels of ruffling in WT cells than ATP treatment (Figure 3.14). sTREM2 is constitutively cleaved from the surface of BV2 cells resulting in concentrations of approximately 150ng/ml in WT MGCM compared with 3ng/ml in B5 MGCM (Figure 3.16a). Neither pre-treatment with WT MGCM nor B5 MGCM could restore the ability to form membrane ruffles in response to MCSF treatment in the B5 cells, with the percentage of cells with ruffling morphology significantly lower than WT cells for all treatment conditions (* $p<0.05$, ***$p<0.001$, Figure 3.16b). Pre-treatment with MGCM from either cell type had no effect on the formation of membrane ruffles by the WT cells.

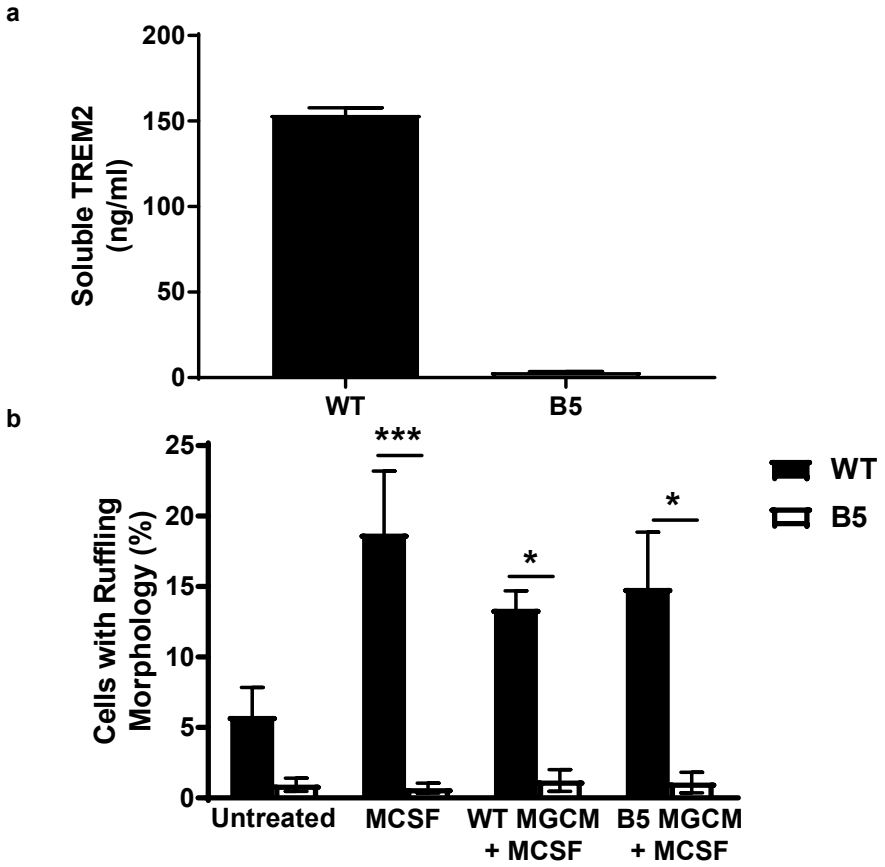

Figure 3.16 Pretreatment with soluble TREM2 does not restore deficits in morphological responses to MCSF

Microglia-conditioned media (MGCM) from WT and TREM2 knockout B5 cells were analysed for soluble TREM2 (sTREM2) levels by ELISA (**a**). WT and B5 cells were pre-treated with WT or B5 MGCM for 18hours prior to stimulation for 5 minutes with 100ng/ml MCSF. The percentage of cells with ruffling morphology was then assessed (**b**). Values expressed as mean percentage ±SEM for 3 individual experiments (* $P<0.05$, ***$P<0.001$; one way ANOVA with Dunnett's multiple comparison test).

3.7 TREM2 knockout cells are less able to phagocytose E.coli particles

In microglia, membrane ruffles and filopodia are thought to be important for cell migration and phagocytosis, therefore the functional implications of reduced formation of these actin structures in the TREM2 knockdown and knockout cell lines were investigated. TREM2 is thought to play a role in phagocytosis (Takahashi, Rochford and Neumann, 2005; Kleinberger *et al.*, 2014) and, since the TREM2 knockdown and knockout cell lines have disrupted actin phenotypes and decreased expression of Iba1, which has also been linked to phagocytic abilities (Ohsawa *et al.*, 2000), the effect of TREM2 modification on the phagocytic ability of the cells was assessed. Uptake of fluorescent pHrodo *E.coli* particles by FACS analysis was performed. The particles only fluoresce in an acidic environment, such as that of a lysosome, which reduces any background signal from cell surface binding by the beads. A further control of cytochalasinD treatment was used, which inhibits actin polymerisation thus preventing the changes in cell structure required for phagocytosis. The TREM2 knockout cell lines G4 and B5 had a significantly lower level of phagocytosis compared with WT cells, as determined by the mean fluorescence signal from FACS analysis of the cells (* $p<0.05$, ** $p<0.01$, Figure 3.17).

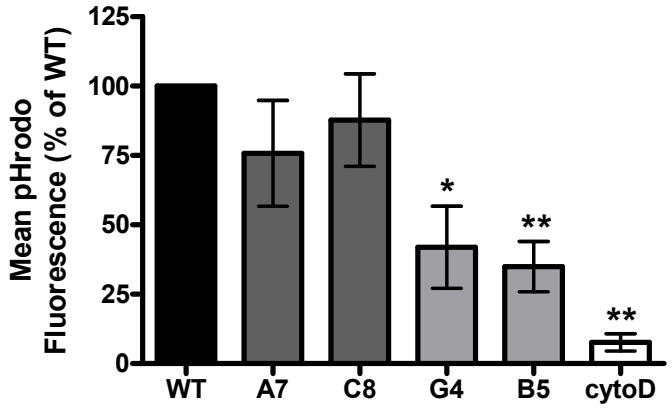

Figure 3.17 The effect of TREM2 knockdown and knockout on the phagocytosis of *E.coli* particles by BV2 cells

FACS analysis of BV2 cell uptake of pHrodo green Ecoli particles as a measure of phagocytosis. CytoD (cytochalasinD) treatment used as a negative control. Graph represents mean fluorescence of individual cells for each cell type expressed as a percentage of WT values. Values expressed as mean ±SEM for 6 individual experiments (* $P<0.05$, ** $P<0.01$; one way ANOVA with Dunnett's multiple comparison test).

3.8 The effect of TREM2 knockdown and knockout expression of chemokines

A proteome array was used in order to identify novel effects of TREM2 gene modulation on cytokine release by BV2 cells. Supernatants were collected from untreated and LPS-treated WT, TREM2 knockdown A7 and TREM2 knockout G4 and B5 cells. Two lines were used for the knockout cells because such large variation was seen between the TNFα levels from these cells in previous ELISA analysis (Figure 3.6). The array is a membrane-based sandwich immunoassay with bound antibodies for 111 cytokines and chemokines, which is visualised by chemiluminescence detection (Figure 3.18). Densitometry was used to analyse the intensity of the resultant dots on the membranes, data from which was used to generate a heat map of expression with cytokine values relative to internal controls and densitometry values normalised between 0 and 1 for comparison.

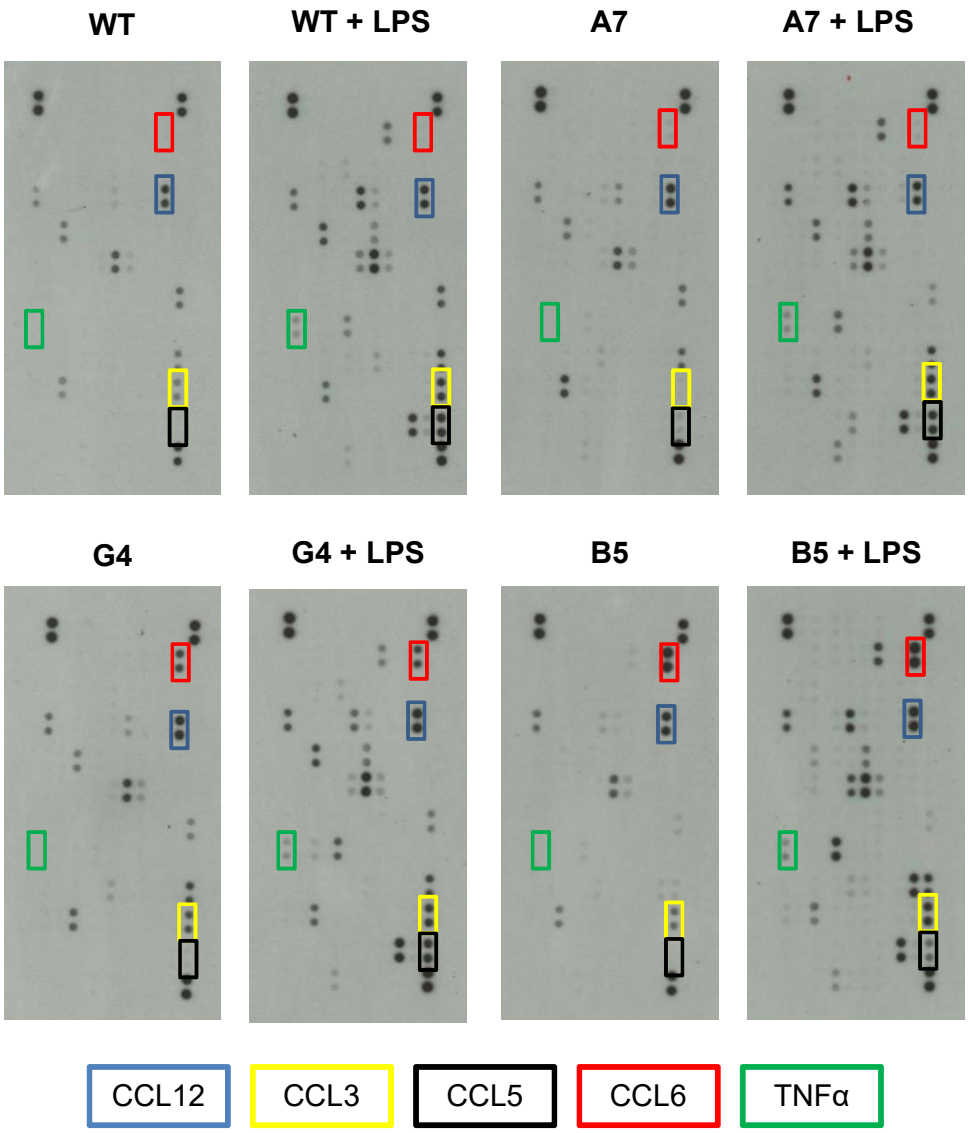

Figure 3.18 Membrane-based proteome array of cytokines and chemokines secreted by untreated and LPS-stimulated BV2 cell lines

WT, TREM2 knockdown A7 and TREM2 knockout G4 and B5 cells were treated with 1µg/ml LPS for 24 hours prior to supernatant collection. Supernatants were analysed using the membrane-based mouse XL proteome array and results visualised by chemiluminescence. Cytokines and chemokines of interest are highlighted in coloured boxes. Two dots are found for each cytokine/chemokine on the membrane.

In the proteome array analysis, the chemokine CCL12 was the highest expressed at baseline levels and, following LPS treatment, the chemokines CCL12, CCL3, and CCL5 were in the top 5 highest expressed factors (Figure 3.19). The chemokine CCL6 was also found to be highly expressed by LPS-treated TREM2 knockout G4 and B5 cells but not by LPS-treated WT and A7 cells. The levels of TNFα secreted following LPS treatment did not appear to differ between the cell types, replicating results found by ELISA analysis previously (Figure 3.6) with the exception of G4 knockout cells which were found by ELISA to secrete significantly less TNFα than controls. The array highlighted the importance of cell recruiting chemokines in the BV2 cells and, since actin regulation and membrane ruffling, both of which are defective in TREM2 knockdown cells, are essential for motility, the motility of these cells should be investigated, as this may be a novel functional defect resulting from TREM2 loss of function.

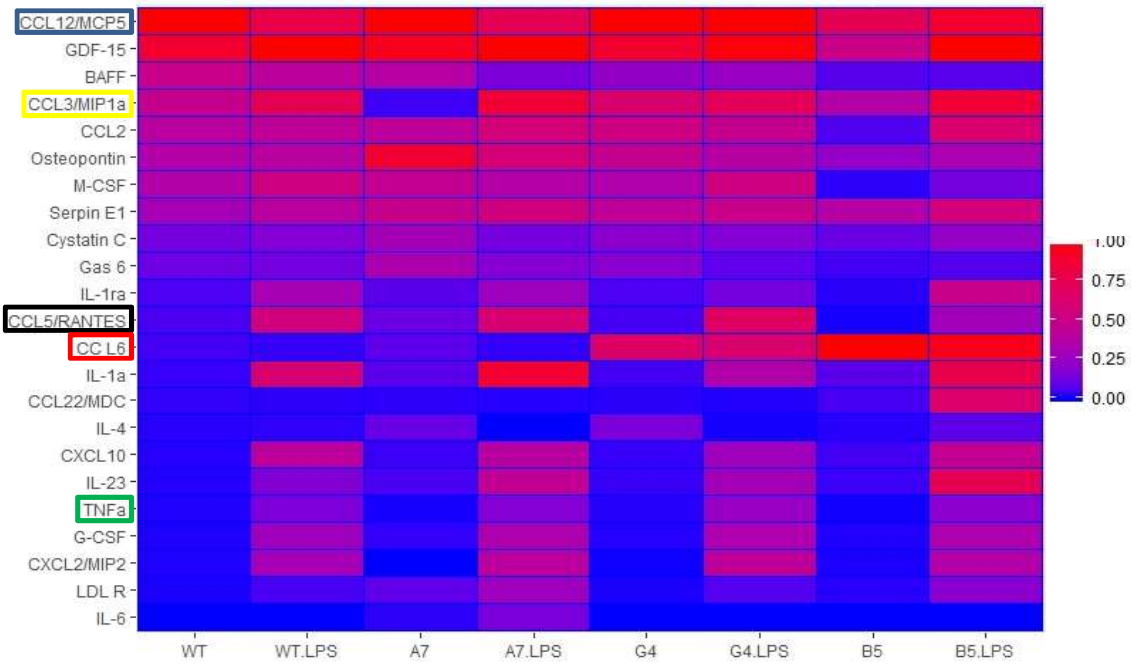

Figure 3.19 Heatmap analysis of cytokines and chemokines secreted by BV2 cells

Heatmap generated from proteome array results from one experiment. Cells were treated with 1µg/ml LPS for 24 hours. Cytokines and chemokines secreted at detectable levels were ranked based on expression levels in untreated WT cells, with the highest scored 1 and the lowest scored 0. Cytokines and chemokines of interested highlighted with coloured boxes.

3.9 Discussion

CRISPR-Cas9 gene editing technology has been successfully used to generate mouse BV2 microglial cell lines with heterozygous or homozygous deletions in the gene encoding for TREM2, a receptor expressed highly in microglia and mutations in which have been found to be associated with Alzheimer's disease. Characterisation of the knockdown and knockout lines demonstrated significant reduction in TREM2 protein expression compared with WT cells, determined by western blotting, immunocytochemistry and ELISA analysis of the cleavage of TREM2 from the surface of the cells. Data from qPCR analysis of TREM2 mRNA levels in the cell lines also indicated that knockdown had been successful.

The generation of these cell lines has provided a valuable tool for studying the role of TREM2 in microglia in the absence of transgenic TREM2$^{-/-}$ mice. These cell lines offer further advantages by generating a high number of available cells for *in vitro* experiments whilst avoiding the use of animals. The gene edits are predicted to result in heterozygous and homozygous loss of function of the receptor, which aims to replicate the heterozygous mutations implicated in Alzheimer's and the more severe homozygous loss of function mutations that cause Nasu Hakola disease.

Despite being described as a cell surface receptor, TREM2 is undetectable at the surface of WT BV2 cells in the immunocytochemistry performed in this study. However, robust TREM2 staining was found in perinuclear regions of the cell cytoplasm that coincided with golgin97 antibody staining for the golgi complex. In other unstimulated microglial cell lines, low levels of TREM2 surface expression have also been reported (Prada *et al.*, 2006) with strong staining in the golgi complex (Sessa *et al.*, 2004) as well as in vesicles that are trafficked to the cell membrane following appropriate stimulation, for example, with interferon-γ (Prada *et al.*, 2006). In the TREM2 knockdown and knockout cells, the TREM2 staining that was found was less intense, more diffuse and no longer punctate. There was also a lack of colocalisation with the golgi complex suggesting that either as the protein is being generated at reduced levels, there is less protein undergoing modification in the golgi or protein that is generated with regions of the gene removed is misfolded and is not being trafficked to the golgi as found with WT TREM2.

Despite low detectable surface expression of the protein, high levels of sTREM2, generated by sequential, proteolytic cleavage of the receptor at the cell surface, were found in the WT cell supernatant. Following TREM2 gene modification, similarly reduced levels of sTREM2 were found in the supernatant of both knockdown and knockout cells despite the knockdown cells still having one unmodified allele and

having higher TREM2 protein and mRNA levels than the knockout cells. This could be attributed to failings in the translocation of the protein to the cell surface due to being truncated or misfolded or feedback mechanisms may be preventing TREM2 protein being translocated to the surface of the cell if low levels exist intracellularly to prevent depletion of stores.

Unexpectedly, some TREM2 mRNA was identified in samples from the knockout G4 and B5 cell line (approximately 20% of the levels found in the WT cells). The CRISPR/Cas9 targeted region of the *Trem2* mouse gene is located in exon 2 and, if the gene editing did not introduce a stop codon to prevent further transcription, truncated TREM2 mRNA could continue to be generated in the knockout cell lines. The primers used to detect for the qPCR analysis span exons 4 and 5 of the TREM2 transcript (Mm04209424_g1, Thermo Fisher Scientific) and thus may be detecting TREM2 mRNA transcripts containing the CRISPR/Cas9-induced indel in the 5' end of the gene. Low levels of TREM2 protein are also detected in the knockout cell lines, which may be due to the generation of truncated mRNA which, following identification of altered protein localisation, almost absent sTREM2 generation and phagocytosis deficits this TREM2 protein, is unlikely to be functional.

When TREM2 mRNA and protein levels are compared between the two different TREM2 knockdown cell lines, A7 and C8, there is markedly lower expression in the C8 line despite both lines expressing one WT TREM2 allele. This could be attributed to gene expression regulation existing on the WT TREM2 allele in the C8 cell line altering the expression of TREM2 mRNA. For example, epigenetic events such as methylation or imprinting could be further contributing to decreases in TREM2 expression resulting in lower levels of mRNA in the C8 line compared with the A7. The regulation of the expression of TREM2 gene in these lines should be investigated further to confirm this hypothesis using techniques such as bisulfite conversion and high resolution melt analysis to determine the methylation state of TREM2 gene.

ELISA data suggest that TREM2 mutations do not have an effect on TNFα secretion following initial stimulation with LPS however, once constitutive stores have been released, TREM2 modulation affects subsequent LPS-induced *Tnf* transcription and protein secretion following secondary stimulation. No difference in baseline *Tnf* mRNA levels were found in TREM2 knockdown cell lines but decreased mRNA post-LPS treatment was found when compared with WT cells. This suggests that TREM2 influences the expression of *Tnf* mRNA in response to LPS treatment but not in unstimulated conditions. Published data have previously indicated that TREM2 acts to decrease TNFα responses following pro-inflammatory microglial activation, with

TREM2 knockout and knockdown models resulting in increased TNFα secretion (Turnbull *et al.*, 2006; Wang *et al.*, 2015; Zheng *et al.*, 2016). However, in this study, the presence of functional TREM2 acted to increase TNFα expression whilst cells with TREM2 mutations expressed lower levels, reflecting data published in a model of stroke where isolated TREM2$^{-/-}$ microglia had decreased TNFα transcription (Sieber *et al.*, 2013).

Despite carrying identical indels in the TREM2 gene, the G4 and B5 knockout cell lines have differential baseline expression of *Tnf* mRNA, TNFα secretion following initial treatment with LPS and TNFα secretion following secondary LPS treatment in priming experiments. The G4 cell line followed similar trends to the A7 and C8 TREM2 knockdown cells but with slightly larger effect sizes, suggesting that the B5 line may be behaving anomalously in regard to *Tnf* transcription and translation. Following the generation of the CRISPR/Cas9 modified cell lines, genes found in the predicted top 10 most likely off target effects of the nickase plasmid were sequenced to confirm that none had been unintentionally modified. The *Tnf* gene was not identified as a top hit by the algorithm but off-target effects of the CRISPR/Cas9 process may explain why the B5 line responds differently to LPS. Interestingly, the *Tnf* mRNA levels following LPS treatment were similar between the G4 and B5 lines. The reduced baseline *Tnf* mRNA levels found in the B5 knockout lines concurred with published data showing that TREM2$^{-/-}$ microglia have downregulated *Tnf* expression (Mazaheri *et al.*, 2017). In that study, TNFα protein was not assessed though so we do not know the implications of this reduced level of *Tnf* mRNA.

We have shown that TREM2 knockout microglial cell lines display defective phagocytosis, resulting in reduced uptake of fluorescent *E.coli* particles compared with WT cells. This result concurs with published data resulting from TREM2 knockdown in cell lines (Takahashi, Rochford and Neumann, 2005; Xiang *et al.*, 2016) as well as primary microglia from TREM2$^{-/-}$ mice (Kleinberger *et al.*, 2014). Furthermore, TREM2 overexpression or blocking of TREM2 cleavage from the surface of cells have been found to ameliorate particle uptake (Takahashi, Rochford and Neumann, 2005; N'Diaye *et al.*, 2009; Kleinberger *et al.*, 2014), demonstrating the importance of TREM2 in phagocytosis. The use of cytochalasinD treatment to block actin polymerisation and pHrodo particles confirmed that the signal measured by FACS was indeed following uptake of the particles rather than passive binding of the particles to the surface of the cells. The importance of a loss of microglial phagocytic ability for the progression of AD is two-fold: firstly, the clearance of apoptotic cells and debris minimises the risk of chronic neuroinflammation, and, secondly, defects in the removal of Aβ may result in

increased plaque load as well as higher concentrations of soluble, neurotoxic Aβ oligomers. Therefore, loss of function mutations in TREM2 may influence pathology by reducing the ability of microglia to clear Aβ as well as allowing the accumulation of debris that may activate microglia resulting in a neurotoxic, inflammatory environment.

The deficiencies in *E.coli* particle uptake exhibited by TREM2 knockout cell lines may be partially attributed to the marked morphological differences identified between WT BV2 cells and cells where indels have been generated in one or both of the TREM2 alleles using CRISPR-Cas9 technology. The TREM2 knockdown and knockout cell lines have significantly shorter filopodia, which are actin-rich projections from the cell membrane. The process of phagocytosis, namely the engulfment, internalisation and degradation of particles, relies entirely upon the ability of the actin cytoskeleton to modify the structure of the plasma membrane (Niedergang and Chavrier, 2004). Filopodia play a vital role in the early steps of engulfment by acting as 'cellular tentacles' that bind particles and drag them towards the cell over distances of up to 10μm (Vonna *et al.*, 2007) and generating forces up to 19pN (Kress *et al.*, 2007). In fact, prevention of filopodia formation in amoebae through depletion of myosin VII results in an ablation of bead uptake, demonstrating the importance of these structures for phagocytosis (Tuxworth *et al.*, 2001). In macrophages and other phagocytes, including microglia, particles are pulled towards the cell by filopodia at rapid speeds resulting from a combination of retrograde actin flow and rotational dynamics (Leijnse, Oddershede and Bendix, 2015). This is followed by slower particle engulfment within the phagocytic cup, which is formed by focal exocytosis of intracellular membrane stores at the cell surface in order to accommodate the necessary membrane extension around the particle (Niedergang and Chavrier, 2004). The phagocytic cup is formed following receptor recognition of particles for phagocytosis and resultant signal transduction for actin polymerisation and membrane extension. Rac and Cdc42 signalling activates the actin nucleating Arp2/3 complex, an essential step for the formation of the phagocytic cup structures (May *et al.*, 2000). Furthermore, the rapid extension and retraction of filopodia from the cell membrane is important for maintaining the high level of resting motility and surveillance performed by microglia (Nimmerjahn, Kirchhoff and Helmchen, 2005), enabling them to monitor their local environment and ensuring the clearance of any debris or infection. Therefore, if TREM2 knockout cells have shorter filopodia, they may be less able to identify, bind to and pull particles towards the cell body for effective phagocytosis.

Accurate and rapid remodelling of the actin cytoskeleton is essential for generating the necessary functional response to stimuli, including phagocytosis and migration, as well

as the constant environmental surveillance performed by microglia. Similar to results reported in the literature in the case of microglia and macrophages, WT BV2 cells underwent actin cytoskeleton remodelling to form membrane ruffles following stimulation with MCSF (Boocock *et al.*, 1989; Ohsawa *et al.*, 2000) and ATP (Honda *et al.*, 2001). Membrane ruffles are wave-like structures found where the cell membrane extends and detaches with high levels of F-actin colocalising with Iba1 expression (Ohsawa *et al.*, 2000). TREM2 knockdown and knockout clones exhibited defective cytoskeletal responses to both ATP and MCSF treatments; there was a significantly lower percentage of cells with ruffling morphology following treatment with both stimuli compared with WT cells.

Despite similar defects in ruffle formation being found in TREM2 mutant cell lines, ATP and MCSF induce membrane ruffling through different signalling pathways (Haynes *et al.*, 2006). Microglia from P2YR12$^{-/-}$ mice did not form membrane ruffles in response to ATP treatment but MCSF-induced ruffling was not affected (Haynes *et al.*, 2006). Defects in two different pathways suggests that it is not detection of stimuli that is ineffective in TREM2 knockdown and knockout cells but more downstream issues in the actin coordination required for ruffle formation. Membrane ruffles have been identified as important actin structures for phagocytosis (Cox *et al.*, 1997; Ohsawa *et al.*, 2000), macropinocytosis (Racoosin and Swanson, 1989) and chemotaxis (Honda *et al.*, 2001). The inability of TREM2 mutant cells to form membrane ruffles and shorter filopodia on the surface of the cells may explain the deficits found in phagocytosis compared with WT cells.

In order to investigate whether treatment with sTREM2 could rescue the morphological defects found following stimulation with MCSF in the TREM2 knockout cell line, B5 cells were treated with conditioned medium collected from WT BV2 cells, which has a high concentration of sTREM2. Although the role of sTREM2 is not yet known, treatment with sTREM2 has been linked to improved microglia viability and survival (Wu *et al.*, 2015; Zhong *et al.*, 2017) as well as influencing inflammatory responses (Zhong *et al.*, 2017). If sTREM2 has a non-autonomous signalling function, one might expect treatment with media containing sTREM2 to improve the functionality of cells in which TREM2 has been knocked out. However, this was not this case as there was no significant difference in the ruffling morphology following MCSF treatment in cells treated with B5-conditioned medium and WT-conditioned medium. This experiment could also be performed with recombinant sTREM2 to ensure that other factors secreted into the conditioned medium are not having an inhibitory effect on cell responses. It has been previously reported that sTREM2 treatment was not effective in

rescuing phagocytic defects in TREM2$^{-/-}$ macrophages (Xiang *et al.*, 2016), suggesting that sTREM2 released from the surface of the cells does not function to induce non-autonomous TREM2 signalling to affect phagocytosis by neighbouring cells.

The altered actin structure formation and subsequent reduced phagocytosis may be due to reduced Iba1 expression found following TREM2 knockdown and knockout. Iba1 (ionized calcium binding adaptor molecule 1) is a microglia/macrophage specific protein that interacts with filamentous actin to form actin bundles (Sasaki *et al.*, 2001) and Rac (Ohsawa *et al.*, 2000), a Rho family small GTPase which has been shown to be essential for the actin reorganisation required for membrane ruffling (Nobes and Hall, 1995). Iba1 and Rac play important roles in membrane ruffling and phagocytosis; in separate studies, one with cells expressing mutant Iba1 (Ohsawa *et al.*, 2000) and another expressing mutant Rac1 (Cox *et al.*, 1997), membrane ruffles fail to form in response to MCSF and decreased phagocytosis is found. Furthermore, expression of inhibitory mutant Iba1 resulted in a failure of actin crosslinking and a decrease in membrane ruffling (Sasaki *et al.*, 2001). Iba1 protein and mRNA expression levels were found to be decreased, in a gene-dose dependent manner, in the TREM2 knockdown and knockout cell lines compared with WT cells. If an interaction is found to exist between TREM2 and Iba1, decreased Iba1 may explain the defects in actin responses and the functional effects of knockdown of TREM2 expression on the phagocytic ability of the cells.

Other downstream effects of defective actin reorganisation should also be investigated for example cell migration as ATP-induced membrane ruffling has been found to precede chemotaxis (Honda *et al.*, 2001; Haynes *et al.*, 2006). P2YR12 is a purinergic receptor expressed on the surface of microglia and, in microglia isolated from P2YR12$^{-/-}$ mice, a decrease in ruffling coincided with a decrease in microglial chemotaxis towards the source of ATP (Haynes *et al.*, 2006). Furthermore, inhibition of Erk1/2, which is a signalling mediator of ATP-induced ruffling, leads to a decrease in membrane ruffles and inefficient chemotaxis (Lee *et al.*, 2012). ATP is released following cell damage so morphological and chemotactic responses to this nucleotide are important for microglial responses to CNS injury. If TREM2 knockdown and knockout cells have altered abilities to generate membrane ruffles in response to ATP stimulation, these cells may be less able to migrate towards the area of CNS damage in order to perform their clearance activity, potentially resulting in the build-up of noxious debris. Filopodia, the generation of which have also been found to be defective in TREM2 modified BV2 cells, have also been shown to play an important role in

motility and chemotactic migration (Xue, Janzen and Knecht, 2010; Boer *et al.*, 2015; Meyen *et al.*, 2015).

It is important to note that we are not proposing that it is the detection of the chemotactic signals that is defective in these cell lines, but that the cytoskeletal responses to the stimuli are lacking. Future investigations into the effect of TREM2 expression manipulation on chemotactic migration and baseline motility should be investigated with transwells, boyden chamber techniques or time lapse, live imaging of cells. Studies in animal models have suggested a decrease in the number of microglia surrounding Aβ plaques in TREM2$^{-/-}$ AD models compared with WT TREM2 models (Ulrich *et al.*, 2014; Jay *et al.*, 2015; Wang *et al.*, 2015), although this could be attributed to decreased microglial survival under stress rather than decreased capacity to migrate towards stimuli. The effect of TREM2 modulation on migration has been investigated in a recent study by Mazarheri et al. which demonstrated reduced migration in TREM2 knockout N9 microglial cells in response to CCL2 and C5a, which was rescued by TREM2 overexpression. Furthermore, baseline motility of ex-vivo microglia was reduced in organotypic brain slices from TREM2$^{-/-}$ mice compared with WT, in addition to impaired wound responses (Mazaheri *et al.*, 2017). In this paper, the authors attribute this delayed response to the TREM2$^{-/-}$ microglia being locked in a resting state from which they are unable to be activated. However this could be due to defective actin structure remodelling resulting in delayed responses in cells lacking functional TREM2.

Proteome analysis of the secretion profiles of unstimulated and LPS-stimulated WT and TREM2 modified cells highlighted the importance of chemokines in both basal and activated cells. Chemokines, including CCL2 which was the highest secreted protein found in the array of 111 cytokines and chemokines, signal via surface receptors and result in downstream signalling that causes actin remodelling in order to migrate towards the source of the chemotactic signal. The release of chemokines is evidently important for microglial function so if responses to these signals are impaired due to actin cytoskeletal issues, this could have a substantial impact of the ability of microglia to function normally.

Rescue experiments should be performed for all assays to ensure that functional effects identified following TREM2 knockdown and knockout are due to loss of function of TREM2 rather than artefacts and off target effects from the CRISPR/Cas9 process. This should be performed using transient overexpression of WT TREM2 protein in the knockdown cells and subsequently ruffling responses, cytokine secretion, phagocytosis

and Iba1 expression should be investigated, with cells expected to act as WT cells if the effects are due to TREM2 knockdown.

It is important to consider that these experiments were performed in cells with removal of significant sections of the TREM2 gene rather than the specific point mutations that are associated with Alzheimer's disease, so cells may not behave in the same way as those expressing endogenous TREM2 levels albeit with point mutations. However, the point mutations found in AD are predicted to be loss of function (Dardiotis *et al.*, 2017), and, as these CRISPR/Cas9 modifications have caused knockdown of protein expression such that the levels of functional protein are significantly reduced, this is a good model of loss of function mutations in the absence of BV2 cells harbouring disease-associated point mutations. Specific editing of the nucleotide required to generate R47H mutations in the BV2 cells was attempted by C. Villegas Llerena as part of this project but, due to the extremely low transfection efficiency found in the BV2 cells, this was not successful. It is likely that highly sensitive microglia become activated upon encountering foreign DNA and, as professional phagocytes, phagocytoses foreign elements thus clearing away and destroying the nucleic acids intended to transfect them.

Although the use of immortalised cell lines, such as BV2s, has many advantages, including convenience, reduced use of animals and high yields, limitations exist in the extent to which they successfully recapitulate the microglia that they are originally derived from. BV2 cells, which were generated from primary mouse microglia transfected with a *v-raf/v-myc* carrying retrovirus (Blasi *et al.*, 1990), carry oncogenes that result in significant differences when compared with primary microglia. They have been shown to have increased proliferation and adhesion (Horvath *et al.*, 2008), which is important to take into account when studying microglia, a cell type known for its slow turnover and low-levels of proliferation in physiological conditions. Furthermore, relative to primary mouse microglia, BV2 cells have a dampened immune response to LPS (Henn *et al.*, 2009), although as many as 90% of the genes induced by LPS in the BV2 cells matched those in primary cultures.

In addition to the limitations of using immortalised cell lines, the suitability of cells of murine origin to study human diseases should also be considered. In the case of studying AD, the inability of a single mouse model to fully recapitulate all aspects of AD pathology, particularly neuronal loss, despite carrying multiple mutations that in isolation are capable of causing disease in humans, suggests that a model for studying AD as a whole is not available yet (reviewed in (Franco Bocanegra, Nicoll and Boche, 2017)). However, analysis of murine and human microglia transcriptome demonstrated

similarities in gene expression, with 13,253 of 15,768 orthologous gene pairs expressed at similar levels (Gosselin *et al.*, 2017). Transcriptional mechanisms that regulate microglial gene expression were also found to be largely conserved between human and mouse microglia (Gosselin *et al.*, 2017), supporting claims that mouse microglia are suitable as a method for studying human microglial expression and function. Therefore murine cells may be suitable for investigating microglial genes associated with AD and their effect on microglia, even though caveats exist for the investigation of these genes in mouse models that aim to recreate AD pathology.

In conclusion, key findings from the use of these TREM2 modified cells have substantiated previous findings from other TREM2 knockdown models including decreased surface expression, decreased sTREM2 generation and a reduction in phagocytosis, which provides evidence that these CRISPR/Cas9-generated lines are a good model of TREM2 loss of function mutations. The observation of a link between TREM2 expression and actin cytoskeleton organisation is a novel finding and could have significant implications for the understanding of the contribution of TREM2 mutations to microglial dysfunction, in particular regarding the ability of microglia to respond to stimuli and to perform phagocytosis. The BV2 cell line has provided a useful tool for studying the effect of TREM2 loss of function but results need to be replicated in cells of human origin, ideally in lines that do not carry oncogenes resulting from immortalisation. The availability of primary human microglia is extremely limited, making conducting these experiments challenging, however the development of human iPSC-derived models of microglia (as discussed in the following chapter) is contributing to overcoming this limiting factor.

4. TREM2 mutations in human iPSC-derived microglia-like cells

The iPSC-derived microglia-like cells used in this chapter were differentiated from iPSC cell lines by Dr Pablo Garcia Reitböck and Dr Thomas Piers (UCL Institute of Neurology).

Microglia are the tissue-resident macrophages of the CNS (central nervous system) and genes expressed by microglia are implicated in a number of neurodegenerative diseases, including Alzheimer's disease (reviewed by (Villegas-Llerena *et al.*, 2016)). However, there are large gaps in our understanding of human microglial activity during homeostasis and their effect on disease due to a lack of reliable, realistic models of microglia, in addition to difficulties in acquiring foetal or adult tissue for the isolation of primary human microglia.

Immortalised cell lines are often used as the first resource for microglial modelling as they yield a large number of cells, are easily maintained and allow more controlled manipulation of specific variables than *in vivo* studies. However, these cells often carry genetic abnormalities derived from the immortalisation process and, as the name suggests, immortalised cell lines are highly proliferative and therefore do not accurately recreate predominantly non-proliferative microglia (Horvath *et al.*, 2008).

The use of animals, particularly mice, provides a readily-available source of brain tissue and also allows investigation into the role of specific genes in disease progression through the generation of genetically modified models. Evolutionarily-conserved similarities found in key biological features of mice and humans, such as metabolic pathways and anatomy, have resulted in the widespread use of mouse models (Chinwalla *et al.*, 2002). However, in the case of AD, difficulties and limitations exist in the use of mouse models as they fail to fully reproduce all of the components of AD pathology, in particular the concurrent deposition of Aβ and tau accumulation, which takes decades to amass in human brains (Bales, 2012; LaFerla and Green, 2012; Franco Bocanegra, Nicoll and Boche, 2017). Additionally, and of particular relevance to the study of microglia, an analysis of the genes expressed in mouse and human brains found that modules of genes involved in immune responses were found to have the highest levels of interspecies divergence (Miller, Horvath and Geschwind, 2010). As well as the divergence of immune-related, microglial genes, Miller et al also identified significant expression differences in the AD-associated genes encoding for tau, presenilin-1 and glycogen synthase kinase 3β. Increasingly identified species-specific differences between rodents and humans, particularly in the case of the

immune system (Franco Bocanegra, Nicoll and Boche, 2017), have highlighted the inadequacies of animal models and the importance of using human models where possible.

Due to the lack of available fresh human brain tissue and the inability of primary microglia to replicate in culture, peripheral blood-derived monocytes and monocyte-derived macrophages are frequently used as *in vitro* human models of microglia. Both cells types can be readily isolated from blood samples and are also myeloid cells like microglia, although as discussed earlier microglia are derived from erythro-myeloid precursors and monocytes are from haematopoietic stem cells (Schulz *et al.*, 2012). Monocyte-derived macrophages are generated by isolating and culturing monocytes in macrophage colony stimulating factor (MCSF) for 7 days. Despite their frequent use as a model of microglia, monocyte-derived macrophages do not accurately recapitulate the yolk-sac derived ontogeny of microglia (Ginhoux *et al.*, 2010, 2013). Furthermore, limitations also exist in the amount of blood that can be collected from donors so animal models are frequently used to provide primary microglia cultures.

The development of protocols to generate renewable, terminally differentiated, human microglia that do not carry the karyotypic abnormalities of immortalised cells lines has the potential to revolutionise our understanding of microglia in both physiological and pathogenic states. Recently a protocol for the generation of human iPSC (induced pluripotent stem cell)-derived macrophages has been published (Van Wilgenburg *et al.*, 2013). This method recapitulates the embryonic ontology of microglia by generating *Myb*-independent myeloid cells (Buchrieser *et al.*, 2017) and, as will be demonstrated in this thesis, following minor modifications, these cells express microglial genes and therefore refer to them as iPSC-derived microglia-like cells (iPSC-MGLC).

4.1 The generation of human iPSC-derived microglia-like cells

A protocol for the culture of iPSC-derived microglia like cells (iPSC-MGLC) was generated by Dr Pablo Garcia Reitböck (UCL Institute of Neurology) using recently developed macrophage differentiation protocols (Van Wilgenburg *et al.*, 2013), with minor modifications in the time points of media changes. Fibroblast cultures were generated from skin punch biopsies, from which iPSC cultures were derived using 4 factor Sendai virus reprogramming at the NIHR Cambridge Biomedical Research Centre (BRC) Human Induced Pluripotent Stem Cells core facility. Characterisation of the iPSC lines was performed by the BRC, including RT-PCR to check for plasmid integration, immunofluorescence to demonstrate expression of pluripotency markers

(Figure 4.1b) and ensuring the ability of the cells to differentiate into the 3 germ layers (Figure 4.1c, Brownjohn et al., manuscript in preparation). iPSCs were harvested and centrifuged to generate large, uniform embryoid bodies (Figure 4.1e). Embryoid bodies were cultured in media supplemented with growth factors that mimic the environmental cues found in the developing embryo in order to encourage haematopoiesis: bone morphogenetic factor 4 (BMP4) to induce cells of mesodermal origin, vascular endothelial growth factor (VEGF) to induce endothelial precursors and stem cell factor (SCF) to induce hematopoietic precursors. After 4 days, embryoid bodies were collected and pooled into a flask, in which directed differentiation was induced through supplementing myeloid progenitor medium with interleukin-3 (IL-3) and macrophage colony stimulating factor (MCSF). Most embryoid bodies floated and generated large cystic structures (Figure 4.1f), which non-adherent cells of small diameter started budding from after 10-14 days post seeding. After approximately 5 weeks, larger cells with fine processes started budding and were able to attach to tissue culture plates. Several million of these cells were able to be harvested from a 175cm^2 flask of ~150 embryoid bodies on a weekly basis. The immature progenitor cells were cultured and matured in medium supplemented with 100 ng/ml MCSF for 7 days resulting in matured, iPSC-microglia like cells (Figure 4.1g & h). In this thesis, one clone from each cell line was used.

1) Generation of iPSCs

- Fibroblast cultures generated from skin punch biopsies
- Reprogrammed using 4 factor Sendai virus
- Pluripotency confirmed by immunofluorescence and scorecard panel
- Normal karyotype confirmed
- iPSCs cultured feeder free in E8 medium

a

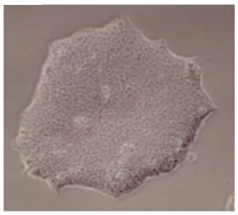

b

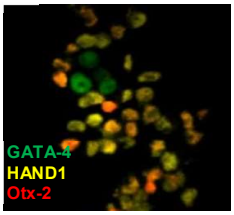

c

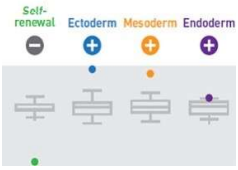

d

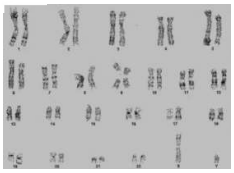

2) Embryoid Body Formation

- E8 medium supplemented with BMP-4, VEGF, SCF and ROCK inhibitor
- Cells were centrifuged to aid embryoid body formation
- Cultured in 96 well plate for 5 days prior to harvesting

e

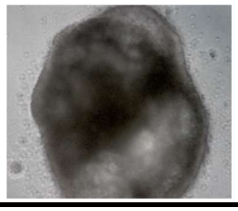

3) Myeloid Progenitor Differentiation

- ~150 embryoid bodies per flask in myeloid progenitor differentiation medium (x-vivo base with β-mercaptoethanol, MCSF and IL3)
- After ~ 4 weeks cells start budding from embryoid bodies
- Budding cells can then be harvested weekly

f

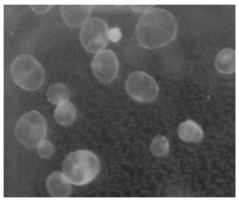

4) Microglia-like Cell Maturation

- Harvested cells are matured for 7 days before being used for experiments in x-vivo medium supplemented with 100ng/ml MCSF

g

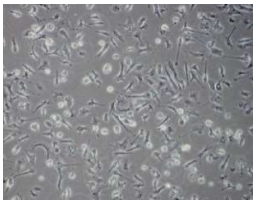

h

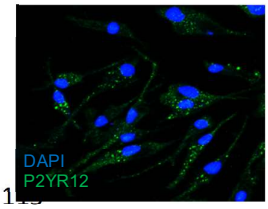

Figure 4.1 The generation and characterisation of iPSC-MGLC

Diagram showing the steps in the generation of iPSC-derived microglia-like cells (iPSC-MGLC). iPSC colonies (a) were generated from fibroblast cultures from donor skin punch biopsies. These iPSCs were characterised by immunofluorescence (b) and gene expression score cards (c) to ensure expression of pluripotency markers. Karyotype was also assessed for abnormalities (d). Brightfield microscopy showing an embryoid body in a 96 well low adherence plate (e) and embryoid bodies forming large cystic structures in myeloid progenitor differentiation medium (f). Brightfield microscopy of iPSC-MGLC following maturation in MCSF and immunofluorescent microscopy showing expression of microglial marker P2YR12 (h). Images kindly provided by Dr Pablo Garcia Reitböck, UCL Institute of Neurology.

4.2 iPSC-MGLC express microglial genes including TREM2

We wanted to investigate whether the expression of various microglial markers by iPSC-MGLCs differed from primary blood derived monocytes and monocyte-derived macrophages through qPCR analysis of mRNA levels. Commercially available human primary microglia cDNA (Sciencell, San Diego, California, United States) was included as a positive control for endogenous microglial expression levels but could not be included in statistical tests as only one sample was available for purchase. This sample was from a single adult donor although further information on the donor's age or cause of death was not provided. The cell surface receptor TMEM119 is a highly expressed microglia-specific receptor, which is reportedly able to distinguish microglia from resident macrophages and infiltrating macrophages following CNS injury and neuroinflammation (Bennett *et al.*, 2016). Indeed, the iPSC-MGLC cells had significantly higher expression levels of *TMEM119* mRNA than the monocytes (*p<0.05, Figure 4.2a), and 5-fold higher expression than the macrophages (p=0.1). Expression of the gene encoding the P2YR12 receptor, preferentially expressed in microglia as opposed to monocytes (Butovsky *et al.*, 2014), was significantly higher in the iPSC-MGLCs than in macrophages (*p<0.05, Figure 4.2b), however the expression in the microglial sample was approximately 4-fold higher than in the iPSC-MGLC samples.

GPR34, PROS1, SPI1, TGFB1 and C1QA were also identified in the Butovksy paper as being highly microglia specific (Butovsky *et al.*, 2014) therefore the expression of these genes compared to monocytes and macrophages was also assessed. The iPSC-MGLC expressed significantly higher levels of C1QA, PROS1 and GPR34 than both monocytes and macrophages (*p<0.05, **p<0.01, ****p<0.0001, Figure 4.2). The expression levels of SPI1 and TGFB1 were found to be consistent across the different myeloid cell types. The iPSC-MGLC had comparable expression levels to microglia in the case of TMEM119 and TGFB1, and, although expression was lower than the

microglia sample for C1QA, GPR34 and P2YR12, the expression was significantly higher than in monocyte-derived macrophages (*p<0.05, **p<0.01, ****p<0.0001, Figure 4.2) therefore the cells can be referred to as 'microglia-like cells'.

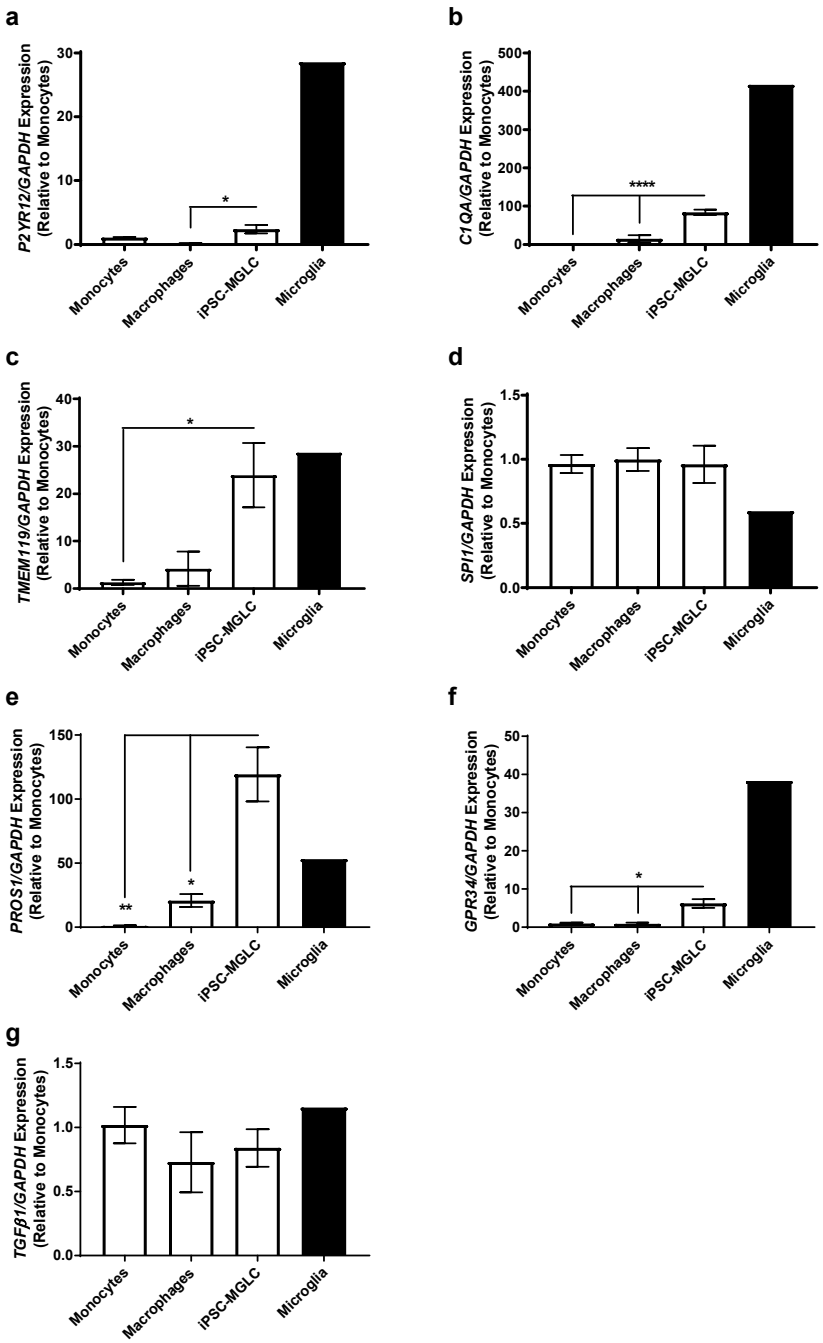

Figure 4.2 Expression of microglial markers by monocytes, macrophages and iPSC-MGLC

qPCR used to determine mRNA expression levels of *P2YR12* (**a**), *C1QA* (**b**), *TMEM119* (**c**), *SPI1* (**d**), *PROS1* (**e**), *GPR34* (**f**), *TGFβ1* (**g**) in iPSC-MGLC compared to monocytes, monocyte-derived macrophages and commercially available cDNA from human microglia (single adult donor obtained from Sciencell). Graph represents gene of interest mRNA expression normalised to *GAPDH* mRNA expression and data is shown relative to monocyte expression levels. Values expressed as mean ± SEM (* p<0.05,**p<0.01, **** p<0.0001; one way ANOVA with Bonferroni's multiple comparison test). n= 5 for

monocyte samples, n=3 for macrophage samples, n=6 for iPSC-MGLC samples and n=1 for microglia samples.

In addition to the microglial markers, the expression of TREM2 by the different cell types was also assessed by qPCR. The iPSC-MGLCs and commercially available microglia cDNA sample expressed similar levels of the gene, which was significantly higher than the monocytes (**p<0.01, Figure 4.3). The iPSC-MGLCs expressed twice as much as the macrophages although there was insufficient power for statistical significance to be achieved (p=0.12). Due to the expression of multiple microglial markers, above levels found in macrophages, and the robust expression of TREM2, the iPSC-MGLCs are a suitable model for studying the role of TREM2 in human microglia.

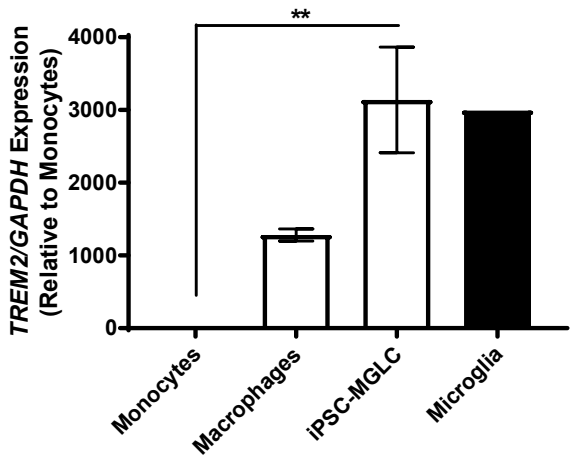

Figure 4.3 Expression of *TREM2* mRNA in iPSC-MGLC

qPCR used to determine mRNA expression levels of *TREM2* in iPSC-MGLC compared to monocytes, monocyte-derived macrophages and microglia. Graph represents *TREM2* mRNA expression normalised to *GAPDH* mRNA expression and data is shown relative to monocyte expression levels. Values expressed as mean ±SEM (** p<0.01; one way ANOVA with Bonferroni's multiple comparison test). n= 6 for monocyte samples, n=3 for macrophage samples, n=6 for iPSC-MGLC samples and n=1 for microglia samples.

4.3 The generation of iPSC-MGLC harbouring TREM2 mutations

One of the main advantages of iPSC technology is the ability to generate patient-derived cell lines from relatively non-invasive skin punch biopsies, providing new opportunities for studying the relationship between disease-associated mutations and pathogenesis. Being able to generate microglia-like cells from iPSCs derived from patients carrying disease modifying mutations allows us to investigate the effect of

these mutations on human microglia function and expression whilst maintaining the patients' genetic background.

For this study into the role of TREM2 in microglia, iPSC-MGLC were generated from a Nasu-Hakola disease (NHD) patient carrying a homozygous *TREM2* T66M mutation, two unaffected relatives carrying a heterozygous *TREM2* T66M mutation, a NHD patient carrying a homozygous *TREM2* W50C mutation and three control cases (Table 4.1). The two cases of NHD have been described previously (Guerreiro et al. 2013b; Dardiotis et al. 2017) and three control iPSC lines were included for comparison. Homozygous *TREM2* mutations are thought to cause NHD (Paloneva *et al.*, 2002) whilst Alzheimer's disease is associated with heterozygous *TREM2* mutations (Guerreiro et al. 2013a; Jonsson et al. 2013). The heterozygous T66M lines may provide information that can be applied to the study of Alzheimer's because, although the most common AD-associated TREM2 mutation is heterozygous R47H, T66M mutations have been found in heterozygosity in some AD cases so the unaffected cases may develop pathology in later life (Guerreiro et al. 2013a). Therefore, the study of these mutations may yield information that can be applied from NHD to AD, two diseases linked to different mutations of the same gene.

iPSC line	Age	Sex	Clinical Details	TREM2 mutation
CTRL1	78	M	Control	No mutation
CTRL2	64	M	Control	No mutation
CTRL3	31	F	Control	No mutation
T66Mhet1	75	F	Unaffected relative of T66Mhom	Heterozygous T66M
T66Mhet2	47	M	Unaffected relative of T66Mhom	Heterozygous T66M
T66Mhom	51	F	Nasu Hakola disease	Homozygous T66M
W50Chom	36	F	Nasu Hakola disease	Homozygous W50C

Table 4.1 Characteristics of TREM2 mutant and control iPSC lines used in this study

4.4 iPSC-MGLC harbouring mutations in TREM2 still express microglial markers

The expression of microglial markers in iPSC-MGLC with mutations in TREM2 was assessed by qPCR to ensure that the mutations had not affected the expression of markers and therefore, not affected how 'microglia-like' these cells are. The expression of *SPI1, PROS1* and *TGFβ1* were found to be the same in the control cells and those with TREM2 mutations (Figure 4.4 d, e, g). The T66Mhet and T66Mhom cells expressed lower levels of *P2YR12* than controls but expression was still detected (Figure 4.4a). The Ct values for *P2YR12* in these cells are usually high (30-35), so decreases identified in expression are exaggerated. The T66Mhom mutant line had significantly higher levels of *TMEM119* than controls (*p<0.05, ****p<0.0001, Figure 4.4b). Levels of *C1QA* and *GPR34* were similar to controls with the exception of the T66M homozygous line (*p<0.05, Figure 4.4c & f).

Following this analysis, we were confident that the mutant lines had maintained their microglial expression signature and could be used to study the effect of TREM2 mutations on microglial function.

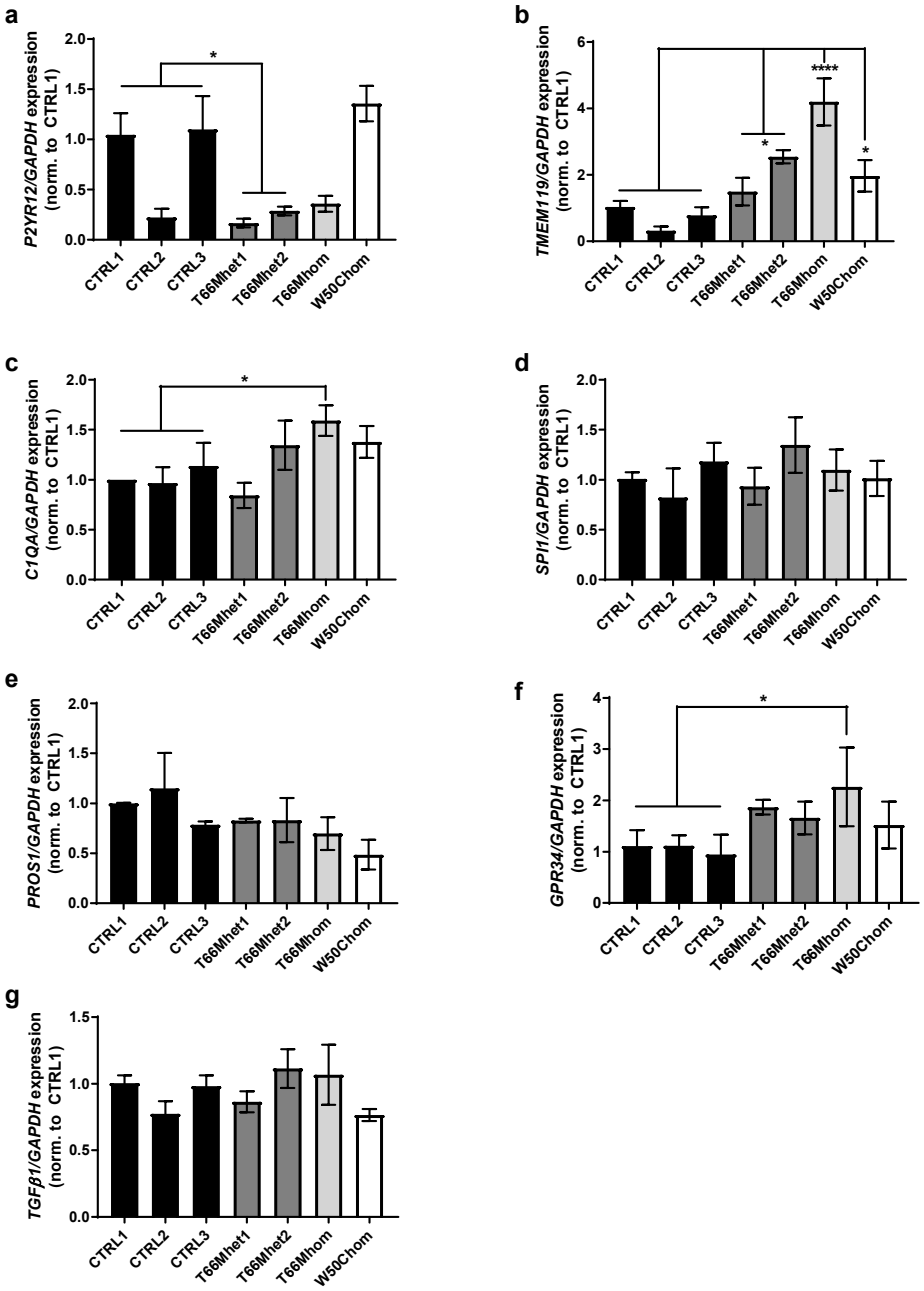

Figure 4.4 Expression of microglial markers in iPSC-MGLC harbouring TREM2 mutations

qPCR used to determine mRNA expression levels of *P2YR12* (**a**), *TMEM119* (**b**), *C1QA* (**c**), *SPI1* (**d**), *PROS1* (**e**), *GPR34* (**f**), *TGFβ1* (**g**) in iPSC-with mutations in TREM2. Graph represents gene of interest mRNA expression normalised to *GAPDH* mRNA expression and data is shown relative to CTRL1 expression levels. Values expressed as mean ±SEM for three individual experiments (* $p<0.05$, **** $p<0.0001$; one way ANOVA with Dunnett's multiple comparison test).

4.5 Reduced TREM2 expression in TREM2 mutant iPSC-MGLC

TREM2 expression levels in the control and TREM2 mutant cells were determined by qPCR and western blotting. There was no statistically significant difference in *TREM2* mRNA levels between the control and heterozygous iPSC-MGLCs, however mRNA levels were significantly lower in both of the lines carrying homozygous TREM2 mutations (** p<0.01,Figure 4.5a). The expression levels of the TREM2 binding partner TYROBP were also assessed by qPCR analysis and no statistically significant differences were found between control and mutant iPSC-MGLC lines (Figure 4.5b).

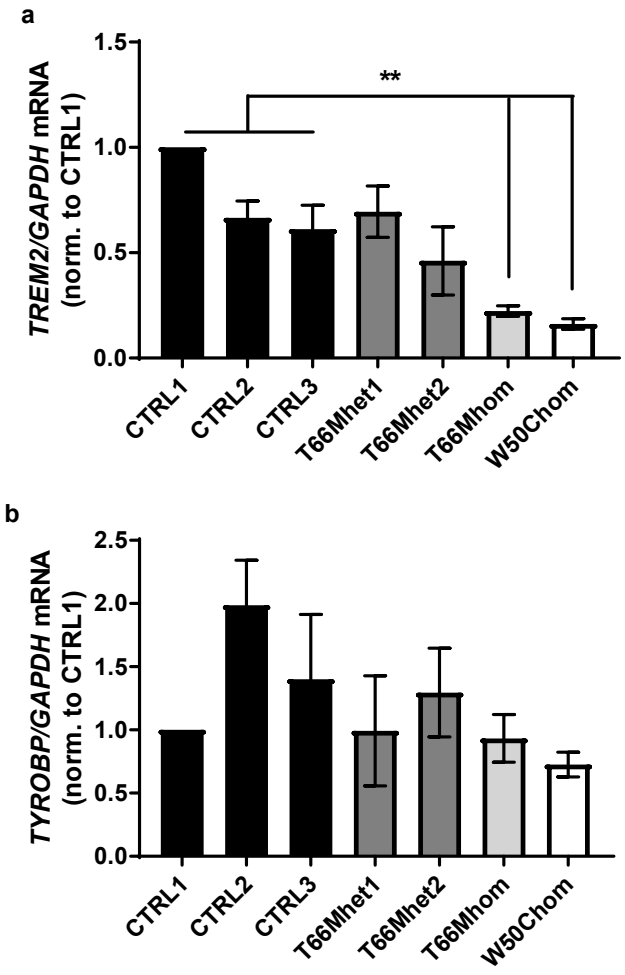

Figure 4.5 The expression of *TREM2* and its signalling partner *TYROBP* in control and TREM2 mutant iPSC-MGLC

qPCR used to determine mRNA expression levels of *TREM2* (a) and *TYROBP* (b) in control and mutant iPSC-MGLC lines. Graph represents gene of interest mRNA expression normalised to *GAPDH* mRNA expression and data is shown relative to CTRL1 expression levels. Values expressed as mean ± SEM (** p<0.01; one way ANOVA with Dunnett's multiple comparison test). Control values (3 groups) and T66M heterozygous values (2 groups) pooled for statistical analysis. N=3 for each cell line.

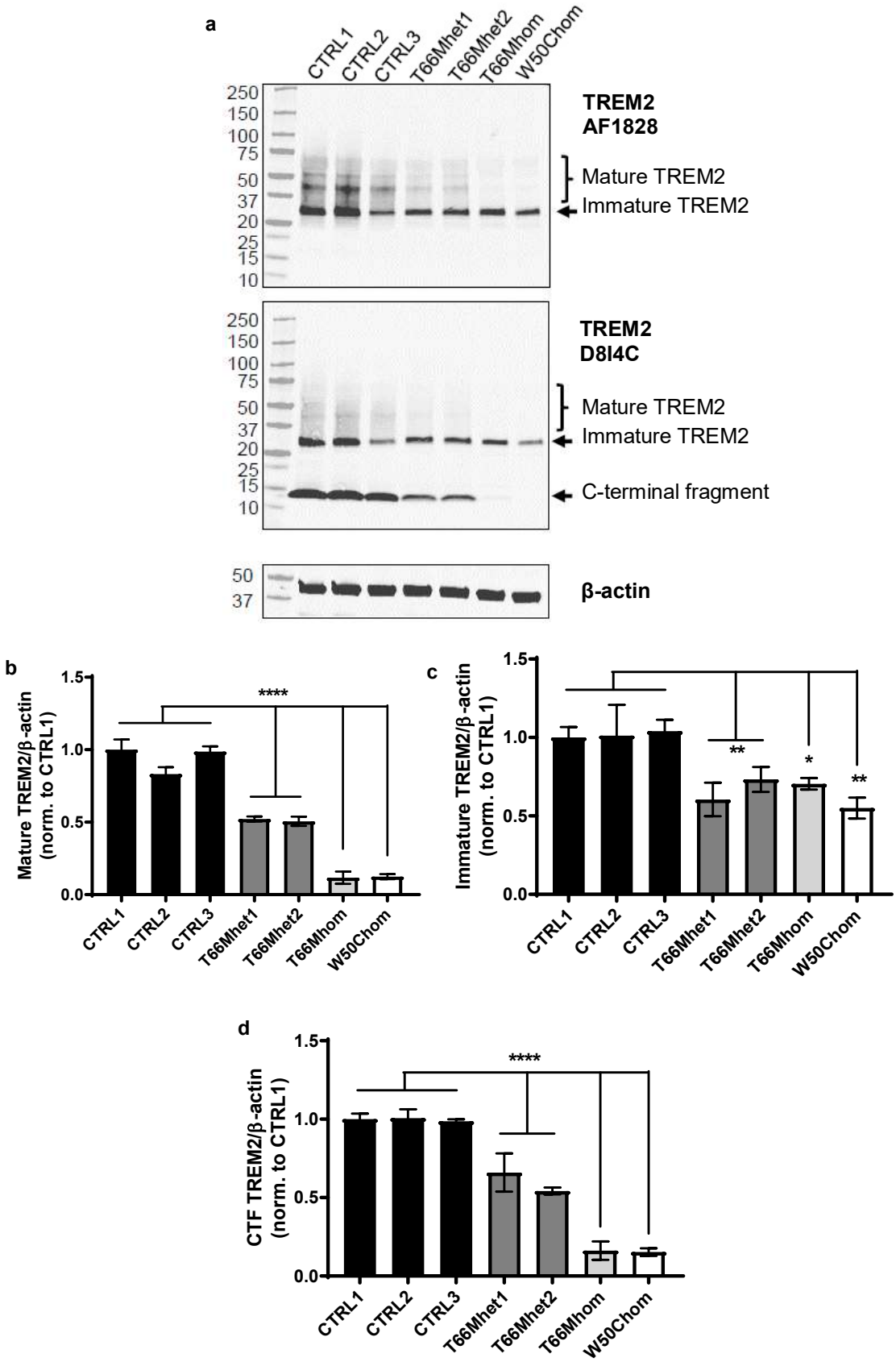
a
CTRL1
CTRL2
CTRL3
T66Mhet1
T66Mhet2
T66Mhom
W50Chom
250
150
100
75
50
37
20
25
15
10
TREM2
AF1828
Mature TREM2
Immature TREM2
TREM2
D8I4C
Mature TREM2
Immature TREM2
C-terminal fragment
50
37
β-actin
b
Mature TREM2/β-actin
(norm. to CTRL1)
1.5
1.0
0.5
0.0
****
c
Immature TREM2/β-actin
(norm. to CTRL1)
**
*
**
d
CTF TREM2/β-actin
(norm. to CTRL1)
****

Figure 4.6 Expression of TREM2 protein in control and TREM2 mutant iPSC-MGLC

Western blot analysis of TREM2 protein expression in control, T66M heterozygous, T66M homozygous and W50C homozygous iPSC-MGLC. Representative blots shown following probing with AF1828 anti-TREM2, D8I4C anti-TREM2 and anti-βactin antibodies (a). Graphs represent protein levels of mature TREM2 (AF1828 antibody)(b), immature TREM2 (AF1828)(c) and TREM2 C-terminal fragment (D8I4C) (d) normalised to β-actin levels. Values relative to CTRL1 and expressed as mean ±SEM for 3 individual experiments (*p<0.05, **p<0.01, ****p<0.0001; one way ANOVA with Dunnett's multiple comparison test). Control values (3 groups) and T66M heterozygous values (2 groups) pooled for statistical analysis. Figure kindly provided by Dr Thomas Piers, UCL Institute of Neurology.

Further evidence of reduced TREM2 expression in the homozygous mutant cells compared with the controls resulted from western blot analysis of TREM2 protein levels. Reduced protein expression was also found in the heterozygous T66Mhet1 and T66Mhet2 cells, which was confirmed with two separate antibodies. The AF1828 and D8I4C anti-TREM2 antibodies allowed the visualisation of mature and immature TREM2 protein, both of which were found at higher levels in control iPSC-MGLC than in the heterozygous and homozygous TREM2 mutation iPSC-MGLC (**p<0.01, ***p<0.001, ****p<0.0001, Figure 4.6b and c). TREM2 is cleaved at the cell membrane by ADAM10 protease activity (Kleinberger *et al.*, 2014) resulting in the secretion of soluble TREM2 (sTREM2) in to the cell supernatant leaving a C-terminal fragment (CTF) tethered to the cell membrane. This CTF is detectable with the D8I4C anti-TREM2 antibody and was found to be significantly lower in the heterozygous and homozygous iPSC-MGLCs than in the control cells (****p<0.0001, Figure 4.6c). Mature TREM2 and TREM2 CTF expression levels were found to be decreased in a gene dose dependent manner; heterozygous cells had approximately 50% of the expression of control cells whilst homozygous cells had approximately 10% of the control cells.

Following the observation of reduced TREM2 protein levels in iPSC-MGLC harbouring TREM2 mutations, the generation of soluble TREM2 (sTREM2) from the surface of the cells was assessed by ELISA analysis. Marked reductions in sTREM2 concentrations in cell supernatants were found in heterozygous iPSC-MGLCs compared with control cells (**p<0.01, Figure 4.7), whilst sTREM2 levels in the supernatants of homozygous T66Mhom and W50Chom cells were almost undetectable (***p<0.001).

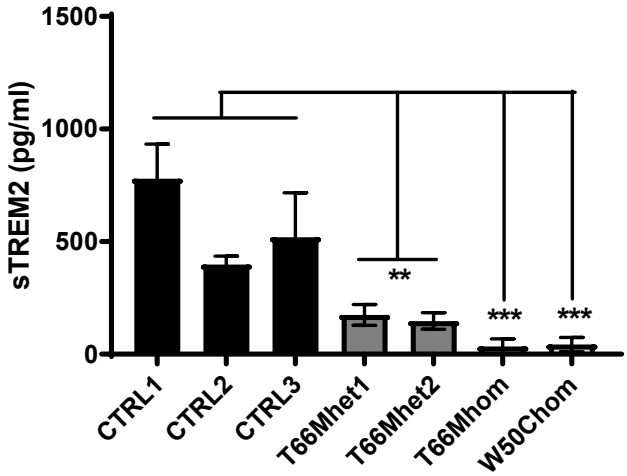

Figure 4.7 Soluble TREM2 release from control and TREM2 mutant iPSC-MGLC

Soluble TREM2 (sTREM2) secretion levels determined by ELISA. Values expressed as mean ±SEM for 3 individual experiments (** $p<0.01$, *** $p<0.001$; one way ANOVA with Dunnett's multiple comparison test). Control values (3 groups) and T66M heterozygous values (2 groups) pooled for statistical analysis.

Immunocytochemical analysis of TREM2 expression in the iPSC-MGLC indicated that, as found by western blotting, TREM2 protein expression is lower in the T66Mhet, T66Mhom and W50Chom cell lines compared with the controls (Figure 4.8a). Preliminary colocalisation analysis was conducted on the control and T66M iPSC-MGLC using antibodies specific to markers of the golgi complex (golgin97) and the endoplasmic reticulum (ER, calnexin) in order to investigate the intracellular localisation of the TREM2 protein. In the control iPSC-MGLC, the highest levels of intracellular TREM2 staining were found in regions that co-stained for golgin97 (Figure 4.8b), indicating that TREM2 protein is primarily found in the golgi, as reported in the literature (Sessa *et al.*, 2004). There did not appear to be significant colocalisation between TREM2 staining and calnexin staining for the ER (Figure 4.8c). In the T66Mhom iPSC-MGLC there was less co-localisation with the golgi (Figure 4.8b), which may suggest that TREM2 protein is not being trafficked through the cell appropriately.

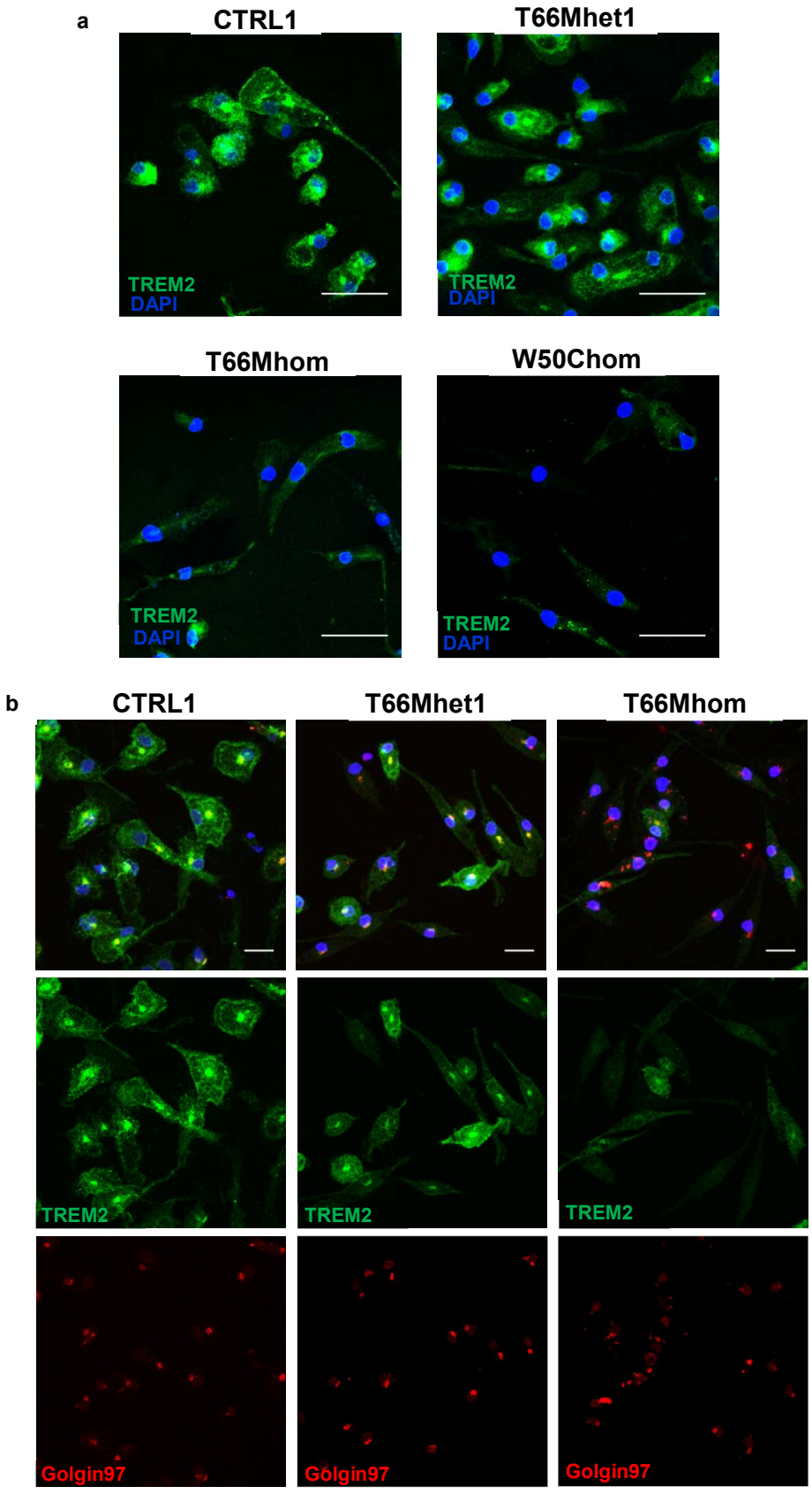
a
CTRL1
T66Mhet1
T66Mhom
W50Chom
TREM2
DAPI
b
CTRL1
T66Mhet1
T66Mhom
TREM2
Golgin97

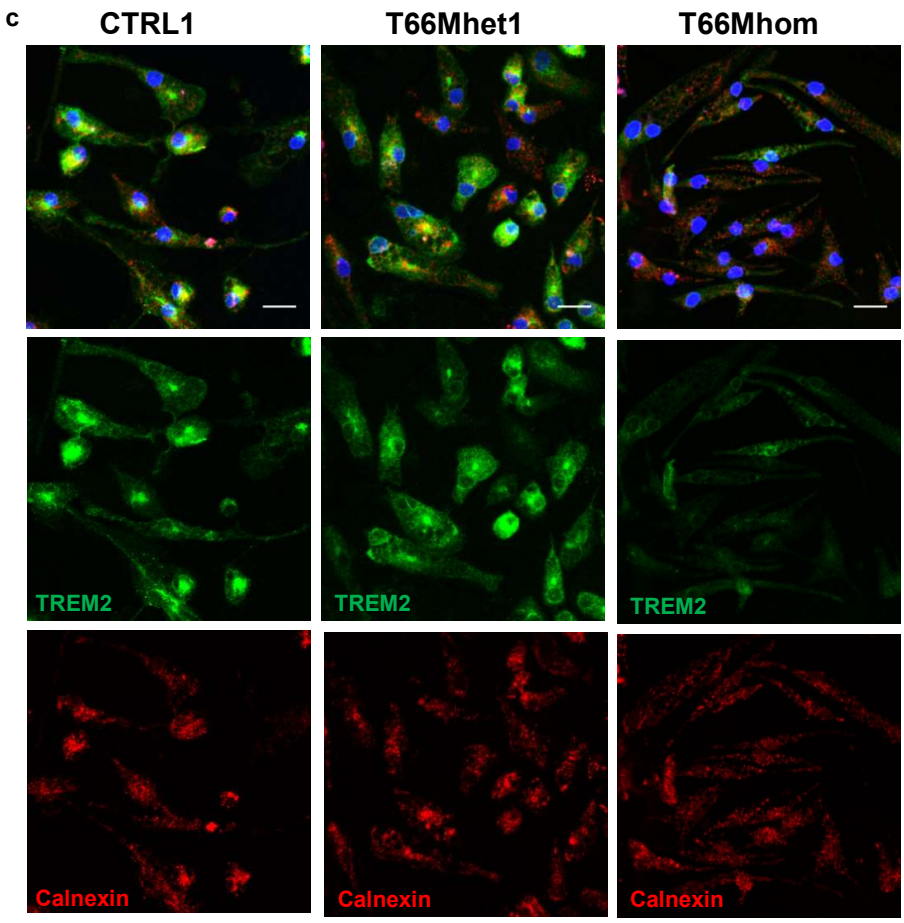

Figure 4.8 Immunocytochemical analysis of TREM2 expression

Representative images of TREM2 immunocytochemical analysis. (**a**) TREM2 expression shown in green merged with DAPI showing nuclear staining in blue. (**b**) Preliminary data showing TREM2 (green), Golgin97 (red, indicating golgi complex) and DAPI (blue). (**c**) Preliminary data showing TREM2 (green), calnexin (red, indicating endoplasmic reticulum) and DAPI (blue). Scale bars represents 50µm.

Mutations in TREM2 alter the expression of TREM2 mRNA, the processing and expression of TREM2 protein and the cleavage of sTREM2 from the surface of the cells, with effects found to be more severe in the homozygous lines than in the heterozygous iPSC-MGLC. Following these observations, the effect of TREM2 mutations on key microglial functions was assessed to understand how these mutations may contribute to pathogenesis.

4.6 The expression of TREM2 T66M homozygous mutations affects phagocytosis by iPSC-MGLC

Modification of TREM2 expression has been shown to affect the phagocytic ability of microglia and macrophages, although the directionality of the effect is disputed (Kleinberger *et al.*, 2014; Wang *et al.*, 2015; Xiang *et al.*, 2016). Therefore the impact of TREM2 mutations on the phagocytic capability of iPSC-MGLC was investigated. Phagocytosis of unstimulated cells was measured using pHrodo *E.coli* particles that are designed to fluoresce in an acidic environment, such as that within a phagosome. Quantification of particle uptake by the control and TREM2 mutant iPSC-MGLC was performed by FACS analysis. CytochalasinD inhibits the cytoskeletal reorganisation required for phagocytosis and therefore was used as a negative control, resulting in almost complete abolishment of fluorescent signal due to inhibition of particle uptake (***$p<0.001$, Figure 4.9). There was no difference in the mean pHrodo fluorescence of T66M heterozygous cells compared with control cells, however, there was a significant decrease in the phagocytosis of *E.coli* particles by T66M homozygous mutant iPSC-MGLC (*$p<0.05$, Figure 4.9).

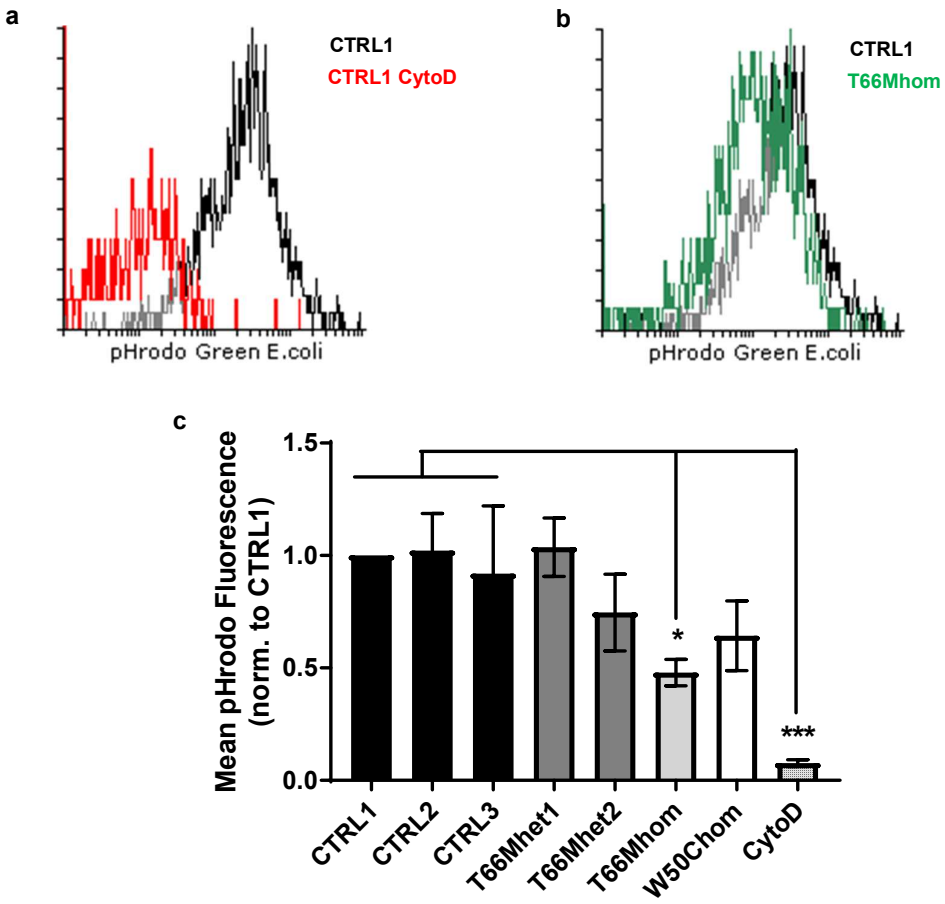

Figure 4.9 The effect of TREM2 mutations on the phagocytosis of pHrodo fluorescent *E.coli* particles by iPSC-MGLC

FACS analysis of iPSC-MGLC uptake of pHrodo green *E.coli* particles after 2 hours of incubation as a measure of phagocytosis. CytochalasinD (cytoD) treatment used as a negative control. Representative histograms showing mean fluorescence plotted against cell number for cytoD (**a**) and T66Mhom (**b**). Graph represents mean fluorescence of individual cells for each cell type normalised to CTRL1 (**c**). Values expressed as mean ±SEM for 3 individual experiments (* $p<0.05$, *** $p<0.001$; one way ANOVA with Dunnett's multiple comparison test). Control values (3 groups) and T66M heterozygous values (2 groups) pooled for statistical analysis.

In addition to being a component of the molecular signature that is enriched in microglia populations relative to other myeloid cells (Butovsky *et al.*, 2014), MerTK is a member the Tyro3, Axl, and MerTK (TAM) family of tyrosine kinase receptors. This group of receptors are important phagocytosis receptors that function to clear apoptotic cells, membranes and myelin, whilst downregulating pro-inflammatory responses (Lemke, 2013). In order to investigate the reason for the decreased phagocytosis found in T66M homozygous mutant iPSC-MGLC, and to confirm that defects were due to reduced altered TREM2 expression rather than reduced expression of other phagocytosis receptors, the expression of MERTK and AXL was assessed by qPCR. No significant differences in MERTK or AXL mRNA levels were identified in control or TREM2 mutant iPSC-MGLC (Figure 4.10).

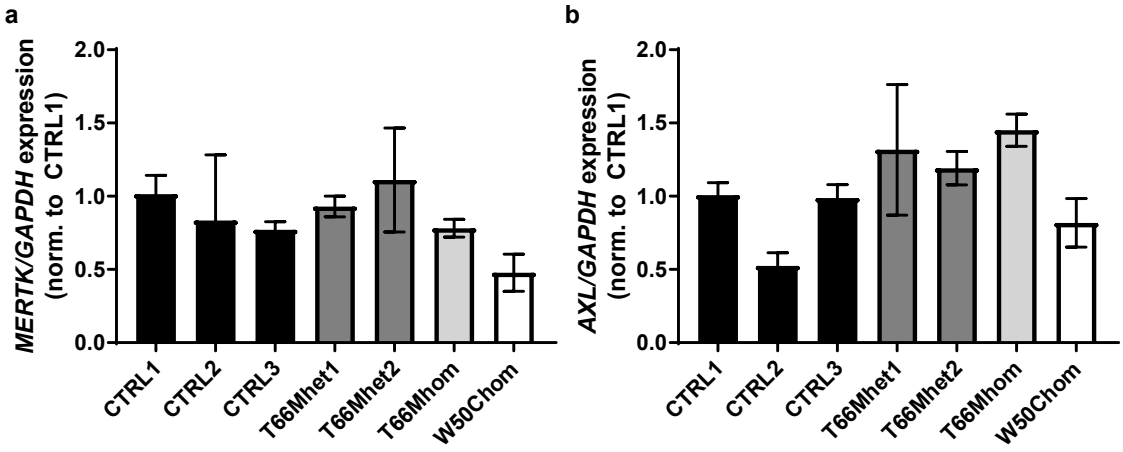

Figure 4.10 Expression of *MERTK* and *AXL* in iPSC-MGLC

qPCR used to determine mRNA expression levels of *MERTK* (a) and *AXL* (b) in control and mutant iPSC-MGLC lines. Graph represents gene of interest mRNA expression normalised to *GAPDH* mRNA expression and data is shown relative to CTRL1 expression levels. Values expressed as mean ±SEM (one way ANOVA with Dunnett's multiple comparison test). Control values (3 groups) and T66M heterozygous values (2 groups) pooled for statistical analysis. N=3 for each cell line.

4.7 Homozygous TREM2 mutant iPSC-MGLC secrete more TNFα in response to LPS than controls

The inflammatory aspects of many neurodegenerative diseases, including Alzheimer's disease, are often attributed to the release of proinflammatory cytokines and immune cell-recruiting chemokines by activated microglia. Published data regarding TNFα release following pro-inflammatory stimulation in TREM2 knockout mice and TREM2 knockdown cell lines are conflicting (Turnbull *et al.*, 2006; Sieber *et al.*, 2013). Therefore, the secretion of TNFα by control and TREM2 mutation-carrying iPSC-MGLC was assessed by ELISA. The cells were stimulated for 18 hours with 100ng/ml LPS, a well characterised TLR-4 ligand known to activate microglia, prior to collection of supernatants. LPS treatment resulted in increased TNFα secretion in all cell lines compared to basal levels, however only T66Mhom had significantly higher TNFα concentrations in the cell supernatant than the control lines (**$p<0.01$, Figure 4.11). No statistically significant difference was found in the T66M heterozygous and W50C homozygous iPSC-MGLC lines.

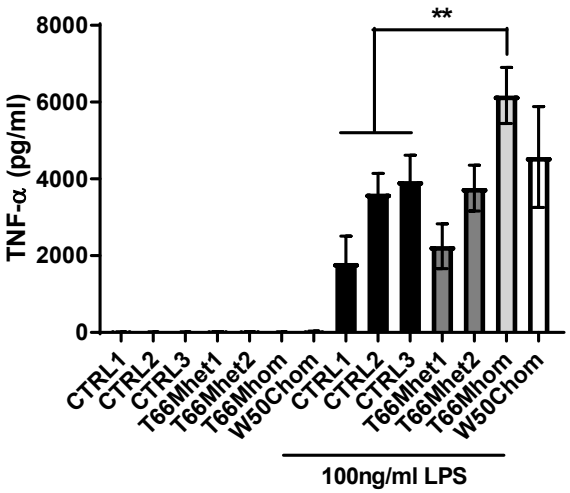

Figure 4.11 ELISA quantification of TNFα secretion by iPSC-MGLC

TNFα secretion following 18 hours of LPS treatment (100ng/ml). Values expressed as mean ±SEM for 3 individual experiments (* $p<0.05$, *** $p<0.001$; one way ANOVA with Dunnett's multiple comparison test). Control values (3 groups) and T66M heterozygous values (2 groups) pooled for statistical analysis.

Interleukin-6 (IL-6) has previously been reported to be modulated by TREM2 expression (Turnbull *et al.*, 2006; Jay *et al.*, 2015; Zhong *et al.*, 2015) so it was also selected for further ELISA analysis. However, baseline levels and LPS-evoked IL-6 secretion levels did not differ between control and TREM2 mutant iPSC-MGLCs (Figure 4.12).

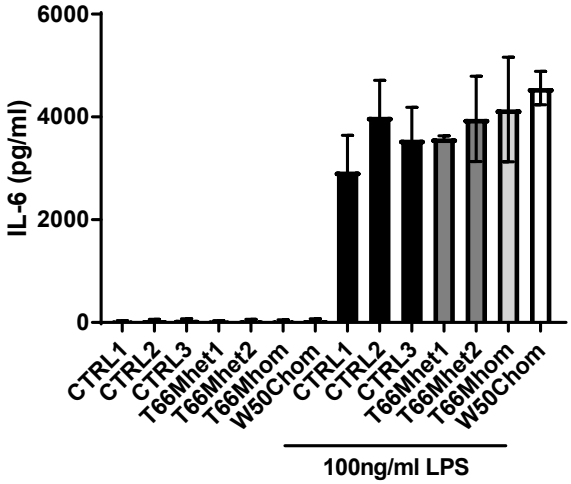

Figure 4.12 ELISA quantification of IL-6 secretion by iPSC-MGLC

IL-6 secretion following 18 hours of LPS treatment (100ng/ml). Values expressed as mean ±SEM for 3 individual experiments (one way ANOVA with Dunnett's multiple comparison test). Control values (3 groups) and T66M heterozygous values (2 groups) pooled for statistical analysis.

4.8 iPSC-MGLC express other dementia-associated microglial genes

Several other microglial genes have been identified as having a genetic association with AD and other neurodegenerative diseases, including *CSF1R, CD33, APOE* and *SPI1*. The ε4 allele of the apolipoprotein APOE is the strongest risk factor for developing AD and, in the brain, is mainly expressed by astrocytes and microglia (Zhang *et al.*, 2014). Different SNPs in the *CD33* gene have been associated with both increased and decreased risk of AD (Griciuc *et al.*, 2013; Malik *et al.*, 2013), and in human monocytes CD33 has been found to modulate TREM2 expression (Chan *et al.*, 2015). A common haplotype that lowers the expression of Pu.1, encoded for by *SPI1*, has been found to delay AD onset (Huang *et al.*, 2017) and mutations in the MCSF receptor CSF1R have been found to cause leukoencephalopathy with axonal spheroids (Rademakers *et al.*, 2011). The expression of these genes in the iPSC-MGLC was investigated to determine whether these cells lines would be suitable models for the study of microglia and genetic risk factors for other neurodegenerative diseases.

Expression levels of *CSF1R* and *SPI1* were found to be similar in monocytes, macrophages and iPSC-MGLC, with expression slightly lower in the microglia sample (Figure 4.13 a & d). iPSC-MGLC also expressed similar levels of *CD33* and *APOE* to microglia (Figure 4.13 b & c), indicating that the iPSC-MGLC cell lines are suitable models for studying these genes and the subsequent protein products in microglia.

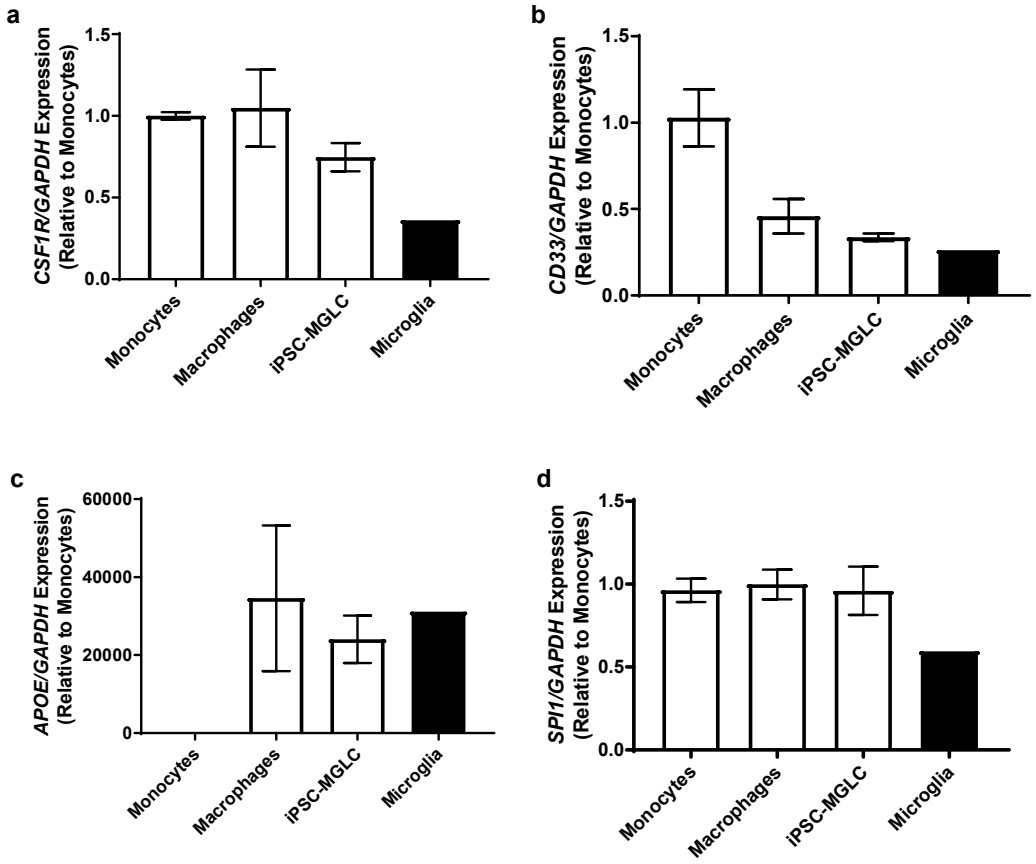

Figure 4.13 Expression of neurodegenerative disease risk factors in iPSC-MGLC

qPCR used to determine mRNA expression levels of *CSF1R* (**a**), *CD33* (**b**), *APOE* (**c**), *SPI1* (**d**) in iPSC-MGLC compared to monocytes, monocyte-derived macrophages and microglia. Graph represents gene of interest mRNA expression normalised to *GAPDH* mRNA expression and data is shown relative to monocyte expression levels. Values expressed as mean ±SEM n= 5 for monocyte samples, n=3 for macrophage samples, n=6 for iPSC-MGLC samples and n=1 for microglia samples.

4.9 The expression of TREM2 T66M and W50C mutations affects the expression of dementia-associated microglial genes

The expression of these neurodegenerative disease risk factors in iPSC-MGLC carrying TREM2 mutations was assessed to investigate whether TREM2 mutations have any effect on these risk genes. All genes were found to be expressed in the iPSC-MGLC and no differences were found in the mRNA levels of *CSF1R*, *SPI1* or *CD33* between control and TREM2 mutant iPSC-MGLCs (Figure 4.14a, b & c). Interestingly, *APOE* expression levels were found to be lower in the W50C homozygous iPSC-MGLC compared to the controls (*$p<0.05$, Figure 4.14d). Therefore, as the cells express these neurodegeneration-associated genes, they would be suitable models for the further study of the role of these genes in human microglia. TREM2 mutations do not affect the expression of *CSF1R, SPI1* or *CD33* but, in this case, may alter the expression levels

of the *APOE*, which is the highest risk factor for the development of late onset Alzheimer's disease.

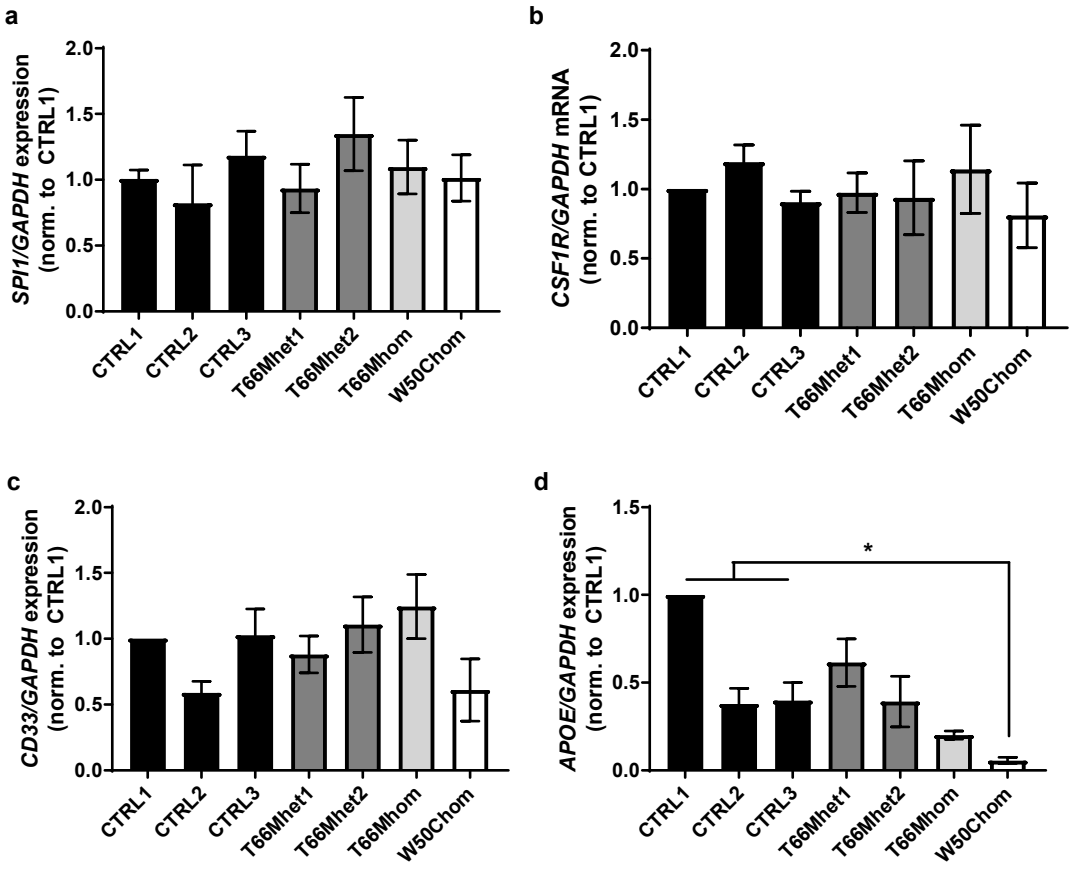

Figure 4.14 Expression of neurodegenerative disease risk factors in TREM2 mutant iPSC-MGLC

qPCR used to determine mRNA expression levels of *SPI1* (**a**), *CSF1R* (**b**), *CD33* (**c**), *APOE* (**d**) in control and mutant iPSC-MGLC lines. Graph represents gene of interest mRNA expression normalised to *GAPDH* mRNA expression and data is shown relative to CTRL1 expression levels. Values expressed as mean ±SEM (*p<0.01; one way ANOVA with Dunnett's multiple comparison test). Control values (3 groups) and T66M heterozygous values (2 groups) pooled for statistical analysis. N=3 for each cell line.

4.10 Discussion

It has been shown in this thesis that iPSC-derived macrophages cultured by other members of the lab (Dr Pablo Garcia Reitböck and Dr Thomas Piers) can, after minor protocol modifications, express key microglial marker genes, with these cells henceforth known as iPSC-derived microglia-like cells (iPSC-MGLC). The iPSC-MGLC express higher levels of microglial markers than monocytes and monocyte-derived macrophages, and are able to function as phagocytes that respond appropriately to pro-inflammatory stimuli, thus making them a valuable model of human microglia.

Genome-wide association studies continue to link microglia-expressed genes and neurodegenerative disease, particularly Alzheimer's disease (Villegas-Llerena *et al.*, 2016), resulting in more demand than ever for appropriate human models to study these cells. Primary microglia isolated from rodent brain tissue had previously been seen as the best model of brain resident microglia, however as limitations in the use of rodents as suitable models for the study of immune responses in human CNS health and disease continue to be recognised (Miller, Horvath and Geschwind, 2010; Franco Bocanegra, Nicoll and Boche, 2017), it is increasingly important to utilise human-derived cells for these studies. Primary microglia can be isolated from brain tissue but, whilst tissue from resective epilepsy surgery can occasionally be obtained at the Institute of Neurology, it is difficult to obtain sufficient cell numbers for most experimental techniques, and furthermore information on the expression of any AD-associated mutations is not provided, so these cells do not provide the additional benefits of the iPSCs derived from AD patients. Additionally, due to the plastic nature of microglia, the process of acquiring and culturing primary cells has been shown to significantly alter the expression of key microglial markers and disease risk-factor genes in these cells (Gosselin *et al.*, 2017). Gosselin et al showed that culturing *ex vivo* primary human microglia resulted in upregulation of 300 genes by 10 fold, including inflammatory and stress response genes, and downregulation of 700 by 10 fold, including immune cell function associated genes. Furthermore, with 31% of genes associated with AD found to be modified by at least twofold (Gosselin *et al.*, 2017), this highlights the limitations of using *ex vivo* culturing of such responsive cell types, particularly for the study of AD.

In light of this, modifications to a protocol designed for the generation of iPSC-derived macrophages (Van Wilgenburg *et al.*, 2013) were made in order to produce iPSC-derived microglia-like cells. This protocol provides many benefits over culturing primary cells, in addition to avoiding isolation steps where expression changes are found. In the

iPSC-generation process, fibroblast cultures from donor skin punch biopsies are reprogrammed to form iPSCs, providing a starting material that has unlimited capacity for self-renewal, normal karyotype, is amenable to genetic modification and can be patient derived and thus carry disease-associated mutations. This protocol utilises fully defined culture conditions that do not require serum, a potential source of variability due to batch effects, ensuring more consistent results across multiple differentiation runs. Furthermore, progenitor cells can be harvested for several weeks providing a high yield of cells, allowing the application of a range of experimental techniques with every batch.

Recent deciphering of microglial ontogeny allows us to accurately recapitulate microglial development in order to appropriately model these cells. Yolk sac-derived primitive macrophages populate the developing mouse brain between embryonic days E7.5-E8.2, where they develop into microglial progenitors that proliferate slowly, develop ramified process and become mature microglia, the resident tissue macrophages of the brain and CNS (Ginhoux *et al.*, 2010, 2013). These cells are *Myb*-independent and PU.1-dependent, in contrast to the blood monocytes-derived macrophages which are constantly renewed in a *Myb*-dependent manner by hematopoietic stem cells. These *Myb*-dependent cells only populate the fetal liver and bone marrow at day E10.5, after the closure of the blood brain barrier (Ginhoux *et al.*, 2010; Hoeffel *et al.*, 2015). In homeostatic conditions, microglia self-renew and are not replenished by peripheral monocytes and macrophages, although infiltration of these cells has been reported following infection, injury and neurodegenerative disease (El Khoury *et al.*, 2007; Ajami *et al.*, 2011; Menasria *et al.*, 2015; Ritzel *et al.*, 2015). The precursors to the iPSC-MGLCs generated by this protocol have been shown to be *Myb* independent and PU.1 dependent (Vanhee *et al.*, 2015; Buchrieser *et al.*, 2017) and therefore recapitulate the embryonic ontogeny of microglia.

This faithful recreation of yolk sac primitive macrophage ontogeny combined with modifications to existing macrophage protocols have resulted in the generation of iPSC-MGLC that express various key microglial markers. When compared with monocytes and monocyte-derived macrophages, the iPSC-MGLC were found to express higher levels of the microglial markers *C1QA*, *TMEM119, P2YR12, GPR34* and *PROS1,* showing that the modifications to the iPSC-derived macrophage protocol produced “microglia-like” cells. These markers have been identified as key components of the molecular signature of microglia and are capable of distinguishing microglia from the circulating macrophages and monocytes that are recruited into the CNS during neuroinflammatory disease (Butovsky *et al.*, 2014). The availability of commercially-

sourced microglial cDNA as an indicator of the physiological expression of microglia markers provided a useful extra tool for evaluating the iPSC-MGLC as a model of microglia. The iPSC-MGLC and microglia sample expressed similar levels of *TMEM119* and *TGFβ1,* with expression levels of *SPI1* and *PROS1* found to be higher in the iPSC-MGLC than in the microglia. Although the inclusion of this human microglial sample is useful for comparing expression levels of microglial markers in a range of cell types which are used as models of microglial to varying levels of accuracy, it is worth noting that there are limitations in the comparisons that can be drawn between these *in vitro* and *ex vivo* samples. The monocyte, and presumably the microglial, although this cannot be confirmed, samples were prepared for RNA isolation immediately after isolation so are likely to represent *in vivo* expression most closely. The macrophages were cultured for 7 days prior to RNA extraction so are unlikely to maintain their *in vivo* expression profile, along with the *in vitro* iPSC-MGLC. The different culture methods should therefore be taken into account when comparing expression levels in these samples. It is also important to consider how accurately the microglia sample represents true, physiological microglial expression. The sample was collected from a "healthy" brain however this was likely to be an autopsy sample with no specific information provided on the time of isolation. The cause of death of the donor is also unknown so pre-symptomatic pathology may have existed in the brain that altered microglial expression. Furthermore, the process of microglial isolation reportedly activates microglia and alters their expression (Gosselin *et al.*, 2017), therefore although this sample is useful as it gives an indication of microglial marker expression, it is unlikely to represent resting microglia.

The iPSC-MGLC expressed microglial markers at levels greater than those found in the macrophage samples, in addition to exhibiting similar expression levels of *TREM2* as those found in the human primary microglia sample. This demonstrates the usefulness of the iPSC-MGLC as a model for studying the role of TREM2 in microglia. iPSC-based models allow the study of disease risk factors at their correct gene dosage, avoiding artefacts from protein overexpression systems. Furthermore they can provide high numbers of relevant cell types expressing patient-specific mutations that can be studied at an endogenous level rather than studying loss of function via whole gene knockouts, as typically found in animal models.

This study is the first model of NHD utilising iPSC-derived microglia-like cells generated from homozygous T66M TREM2 mutation-carrying patients and unaffected relatives harbouring heterozygous TREM2 mutations. It is also the first to investigate functional effects of homozygous TREM2 W50C mutation, initially reported by Dardiotis et al.

NHD is characterised by bone cysts and fractures, followed by frontal lobe syndrome and progressive presenile dementia (Paloneva *et al.*, 2001). It is an autosomal recessive genetic disease caused by mutations in either *TREM2* or in the gene encoding the TREM2-signalling partner, DAP12 (Paloneva *et al.*, 2002). Patients with homozygous T66M TREM2 mutations have presented with frontotemporal dementia-like syndrome-behavioural variant without bone involvement (Guerreiro et al. 2013b), whilst in heterozygosity, the mutation has been associated with a behavioural variant of frontotemporal dementia (Borroni *et al.*, 2014) and also found in rare Alzheimer's cases (Guerreiro et al. 2013a). The development of protocols to generate human microglial models harbouring these homozygous and heterozygous TREM2 mutations has therefore provided a valuable tool for studying multiple neurodegenerative diseases, linked by mutations in the same gene.

The expression of microglial markers was assessed in the TREM2 mutation carrying iPSC-MGLC to ensure that the expression of mutations does not affect how "microglia-like" the cells are. The expression of homozygous and heterozygous TREM2 mutations did not alter the expression of *SPI1, PROS1* and *TGFβ1*, demonstrating the consistency of the reprogramming and differentiation of this protocol, in addition to confirming that TREM2 mutations do not affect the expression of several key microglial markers. Compared with the control lines, the TREM2 heterozygous and homozygous iPSC-MGLC had significantly higher levels of *TMEM119,* a cell surface receptor that is used to distinguish between CNS-resident microglia and infiltrating macrophages after CNS injury and inflammation (Bennett *et al.*, 2016). In the mouse brain, TMEM119 is undetectable until postnatal days 3-6, but once established it remains at a constant level in the adult brain, with all microglia expressing TMEM119 by postnatal day 14 (Bennett *et al.*, 2016). Treatment of an immortalised human microglial cell line with 'classical' activation stimuli LPS and IFNγ or 'alternative' activation stimuli IL-4 and IL-13 did not elevate the expression levels of *TMEM119* (Satoh *et al.*, 2016), although mRNA was found to be increased in AD brains compared with controls (Satoh *et al.*, 2016). Although the function of this receptor is not yet known, these data suggest that expression is not associated with a particular microglial activation state but may be altered by disease. Once more information is known about the function of this receptor, the changes in expression in TREM2 mutation harbouring iSPC-MGLC could prove to be very interesting.

The expression of *P2YR12* was found to be highly varied between the different control lines and significantly lower in the T66M heterozygous and homozygous iPSC-MGLC lines than in the controls. This variability in expression levels may have been because

the Ct values obtained in the qPCR were high so differences are magnified on the logarithmic scale. Alternatively, *P2YR12* expression has been shown to be modulated by microglial activation state, with alternative activation elevating expression levels (Moore *et al.*, 2015), so perhaps this decreased expression is due to the cells existing in a more pro-inflammatory state. Increased expression of *GPR34* was found in the T66Mhom line compared with the controls, which could be explained by the location of the *GPR34* gene on the X chromosome. Two of the controls are from male donors so one would expect expression to be lower in these cells versus those from female donors, such as the T66Mhom patient.

The homozygous TREM2 mutations had a significant effect on the expression levels of *TREM2* mRNA in the iPSC-MGLC; T66M homozygous and W50C homozygous iPSC-MGLC expressed significantly less mRNA than the control lines contrasted to the T66M heterozygous lines where no effect was observed. Western blot analysis indicated that, in control iPSC-MGLC, TREM2 protein exists in three main forms: highly glycosylated mature TREM2 (~37-60kDa), immature TREM2 (~28kDa) and a C-terminal fragment (CTF, ~14kDa). TREM2 contains a large number of N-glycosylation sites and is modified as it is processed through the endoplasmic reticulum (ER) and the golgi apparatus, before being trafficked to the cell membrane. Gene dose-dependent reductions in the expression of mature TREM2 protein and CTF were found in the T66M heterozygous, T66M homozygous and W50C homozygous iPSC-MGLC. Overall, decreased levels of TREM2 protein in the T66Mhet, T66Mhom and W50Chom iPSC-MGLC were also identified by immunocytochemistry. If less mature TREM2 protein expressed at the cell surface, decreased levels of sTREM2 production would be predicted as there is less TREM2 available for cleavage by ADAM10 proteases. As expected, and similar to protein expression patterns, heterozygous T66M iPSC-MGLC generated lower concentrations of sTREM2 than control cells, with concentrations from homozygous mutation-harbouring cells even further reduced. The heterozygous TREM2 iPSC-MGLC cells displayed dramatic reductions in sTREM2 levels despite western blotting indicating that the cells expressed 50% of the protein levels of control cells suggesting that defects in TREM2 processing and trafficking to the cell membrane where cleavage occurs is contributing to low TREM2 shedding, in addition to overall lower expression levels.

TREM2 protein from cells expressing T66M mutations has been reported to accumulate in the ER, resulting in a failure in trafficking to the Golgi apparatus and subsequent targeting to the plasma membrane (Park et al. 2015a). Furthermore, protein structure modelling predictions have suggested that the side chains of the T66

site are found within the core of the Ig fold, mutations in which are predicted to disrupt the stability of packing in the protein core (Kober *et al.*, 2016). The threonine found at position 66 in TREM2 is fully conserved in many mammalian species (Kleinberger *et al.*, 2017) and the T66M point mutation results in an amino acid shift from polar threonine to non-polar methionine, causing a polarity shift in the extracellular domain (Dardiotis *et al.*, 2017). Retained T66M TREM2 protein has been found to be misfolded and results in increased expression of markers of the unfolded stress response (Park et al. 2015a). These data therefore suggest that, in addition to decreased surface expression of TREM2, the T66M harbouring TREM2 protein may be further contributing to microglial dysfunction by inducing ER stress. Indeed, preliminary immunohistochemical analysis of TREM2 localisation in the T66Mhom iPSC-MGLC indicated that TREM2 did not co-localise with the golgi, as found in the control cells, which indicates that the misfolded protein may not traffic to the cell membrane correctly. Analysis of the cellular localisation of TREM2 in W50Chom lines should also be performed as well as analysis of potential ER stress, for example by assessment of CHOP expression or PERK eIF2α kinase activity (Ubeda and Habener, 2000; Yan *et al.*, 2002).

In addition to reduced expression of mature TREM2 protein, the mutant lines generate significantly lower levels of TREM2 CTF. This concurs with data from HeLa cells transfected with human TREM2 plasmids which show that T66M mutations result in CTF formation deficits attributed to failures in the trafficking of misfolded TREM2 protein to the Golgi apparatus, where CTFs are generated (Park et al. 2015a). This provides further evidence of TREM2 protein modification and trafficking issues arising from mutations. Due to the fact that the proteins were denatured during the western blotting process, it is unlikely that the decreased protein detection is due to antibody recognition failures arising from TREM2 mutant protein being misfolded. Mutations may affect the epitope of monoclonal antibody leading to changes in binding affinity, but the AF1828 is polyclonal, and the D8I4C monoclonal shows a similar expression pattern so the decreased TREM2 protein detection is likely not due to antibody specificity deficits. The *TREM2* mRNA data, which does not rely on conformation specific identification, also demonstrates reduced levels in mutants compared with control iPSC-MGLC.

Key findings from these experiments have been replicated in studies utilising BV2 mouse microglia cells and human HeLa cells expressing human TREM2 with T66M mutations (Kleinberger et al. 2014; Park et al. 2015a) and homozygous T66M knock in mice (Kleinberger *et al.*, 2017). Similarly to our iPSC-MGLC, these cells showed reduced levels of mature TREM2 protein and reduced sTREM2 shedding in T66M

mutants compared to controls. This study is the first report of sTREM2 secretion in human iPSC-MGLCs expressing endogenous levels of mutant TREM2 protein and the decreased generation of sTREM2 mimics results found in patients carrying homozygous T66M mutations where sTREM2 is undetectable in plasma and CSF samples (Kleinberger *et al.*, 2014; Piccio *et al.*, 2016).

The loss of function from protein misfolding and a lack of trafficking to the cell membrane may contribute to disease progression as the receptor will not be able to fully function if not expressed at the cell surface, although intracellular signalling may be able to continue without impediment. Furthermore, the role of sTREM2 is not yet known but this decreased availability of the TREM2 protein at the surface for cleavage is likely to modulate sTREM2 functionality. sTREM2 has been linked to microglia viability and survival (Wu *et al.*, 2015; Zhong *et al.*, 2017) as well as influencing inflammatory responses (Zhong *et al.*, 2017) so the effect of misfolded protein on sTREM2 generation may explain some of the functional effects of the T66M mutation. Indeed, bone marrow-derived macrophages from T66M knock in mouse models had decreased survival, slower proliferation and increased Caspase3/7 activation compared to WT cells (Kleinberger *et al.*, 2017) so the effect of T66M mutations and the contribution of sTREM2 secretion levels on iPSC-MGLC survival and proliferation should be investigated. The weekly yield from the embryoid body flasks did not vary between controls and mutation-carrying cells (data not shown) but differences in the survival of the progenitors once differentiated into iPSC-MGLC is yet to be assessed.

The functional effects of reduced TREM2 expression levels in iPSC-MGLC carrying TREM2 mutations were then investigated. One of the primary activities of microglia is constant surveillance of their environment and the clearance by phagocytosis of any debris or pathogens that they encounter. TREM2 has been reported to influence microglial phagocytosis, however published data on the effect of TREM2 mutations on phagocytosis are inconsistent; microglia and macrophages from TREM2 knockout mouse models have exhibited both decreased phagocytosis compared to WT (Kleinberger *et al.*, 2014; Xiang *et al.*, 2016) and undetectable differences (Wang *et al.*, 2015). Furthermore, brain Aβ loads in AD TREM2$^{-/-}$ mouse models, which are used as a measure of phagocytic activity by microglia, are conflicting (Jay *et al.*, 2015; Wang *et al.*, 2015). However, in these studies, different AD mouse models and time points were investigated, which limits the usefulness of comparing these cases.

The phagocytic activity of the iPSC-MGLC was investigated by assessing the uptake of fluorescent *E.coli*, which has been shown to bind to TREM2 resulting in phagocytosis in a TREM2/DAP12-dependent manner (N'Diaye *et al.*, 2009). The T66M homozygous

iPSC-MGLC exhibited decreased levels of phagocytosis compared to control iPSC-MGLC, however no effect was found in heterozygous T66M mutant cells. The homozygous W50C mutation resulted in a decrease in particle uptake but this was not statistically significant. In support of this result, T66M mutations in TREM2 have been previously shown to exert a negative effect on *E.coli* particle uptake relative to WT controls in HEK cells expressing mutated human TREM2 (Kleinberger *et al.*, 2014) and in macrophages from T66M knock in mice (Kleinberger *et al.*, 2017). Low sTREM2 and decreased surface expression of TREM2, as found in T66M iPSC-MGLC, have been found to correlate with reduced phagocytosis of E.coli particles (Kleinberger *et al.*, 2014); indeed inhibition of ADAM protease activity allowed receptor accumulation at the cell surface and rescued phagocytosis (Kleinberger *et al.*, 2014). This decreased TREM2 expression may explain the phagocytic deficits found in the homozygous T66M iPSC-MGLC. The phagocytic ability of cells may be important for disease progression both through the clearance of debris to limit chronic inflammation and the clearance of Aβ in the toxic oligomeric seed formation as well as in the plaque-associated formation.

This is the first investigation of functional effects arising from TREM2 W50C mutations in microglia. Compared to controls, W50C homozygous iPSC-MGLC exhibited decreased *TREM2* mRNA levels, reduced TREM2 protein expression including mature, immature and CTF formations, almost undetectable levels of sTREM2 generation and decreased phagocytosis (although statistical significance was not achieved). The phagocytic ability of monocytes and neutrophils isolated from a patient carrying a homozygous W50C mutation have previously been assessed and no difference was found compared to heterozygous relatives and controls (Dardiotis *et al.*, 2017), although these cell types are not the most disease relevant for studying the effect of the mutation on a neurodegenerative disease. The W50C mutation is found in the extracellular domain of the protein and causes an amino acid substitution from tryptophan to cysteine. Due to the fact that the mutation is located in an evolutionary conserved region and results in changes in the receptor region where interaction with extracellular molecules for downstream signalling occurs, it has been predicted to result in loss of function and may be the reason for disease pathogenesis (Dardiotis *et al.*, 2017). Other NHD-associated mutations, including T66M have been predicted to alter protein stability and folding, whilst AD-linked mutations are expected to alter ligand binding (Kober *et al.*, 2016).

It is interesting that, despite significant decreases being found in the TREM2 expression at both protein and mRNA levels, there is no functional effect of the heterozygous T66M mutations on phagocytosis in the iPSC-MGLC. Kleinberger et al.,

2014 reported only modest differences in phagocytosis between WT and TREM2$^{-/-}$ mouse microglia, however, with increased *E.coli* load, differences in uptake were greater. Therefore, differences between control and heterozygous iPSC-MGLCs, as well as W50C cells, may be more marked if the particle concentration was more saturated. It would also be important to assess phagocytic ability with more disease relevant substrates such as Aβ or apoptotic neurons in order to draw conclusions on the effect of these mutations on Alzheimer's disease pathogenesis.

To evaluate the effect of TREM2 mutations on cytokine release by iPSC-MGLC, the secretion of TNFα and IL-6 following activation with LPS was assessed by ELISA. TREM2 is reported to exert an anti-inflammatory influence upon TLR stimulation in microglia/macrophages (Turnbull *et al.*, 2006; Ito and Hamerman, 2012). Evidence for this comes from studies utilising knockdown of TREM2 by siRNA in primary microglia (Zheng *et al.*, 2016) or in microglia/macrophages isolated from TREM2$^{-/-}$ mice (Turnbull *et al.*, 2006; Wang *et al.*, 2015; Zheng *et al.*, 2016), to demonstrate that LPS treatment results in increased TNFα release in the absence of TREM2.

T66M homozygous iPSC-MGLC had an augmented TNFα response following LPS treatment compared to control and heterozygous cells. Microglia-derived TNFα has been shown to induce apoptosis of mature neurons and neuronal precursors (Talley *et al.*, 1995; Combs *et al.*, 2001; Guadagno *et al.*, 2013), thus contributing to further cell death. This result has been reported previously in T66M knock in mice brain tissue following LPS treatment (Kleinberger *et al.*, 2017) and LPS-stimulated TREM2$^{-/-}$ mouse macrophages and microglia (Turnbull *et al.*, 2006; Wang *et al.*, 2015; Zheng *et al.*, 2016). In models where AD relevant stimuli are utilised, such as Aβ and apoptotic cells, TREM2 loss of function also results in heightened pro-inflammatory responses. Increased TNFα secretion is found following co-culture with apoptotic neurons in primary mouse microglia treated with TREM2-targeting shRNAs relative to controls (Takahashi, Rochford and Neumann, 2005). Moreover, TREM2 expression levels also alter cytokine responses to Aβ, as TREM2 knockdown in primary mouse microglia leads to increased levels of TNFα, IL-1β, IL-6 and iNOS following stimulation with Aβ1-42 (Jiang et al. 2014b). In mouse models of AD and aging, TREM2 knockdown results in augmented pro-inflammatory cytokine release (Jiang et al. 2015; Jiang et al. 2014a) whilst TREM2 overexpression reverses these responses (Jiang et al. 2014b; Jiang et al. 2015). In light of this data, it would be interesting to stimulate the iPSC-MGLC with apoptotic cells or Aβ to establish whether more marked effects of TREM2 mutations on cytokine release can be found.

Treatment of microglia with TNFα has been shown to reduce phagocytic uptake of Aβ (Hickman, Allison and El Khoury, 2008). The combination of multiple TREM2 defects in phagocytosis and anti-inflammatory signalling found in T66M homozygous iPSC-MGLC could result in the generation of a self-perpetuating cycle of microglial dysfunction. As T66M homozygous iPSC-MGLC have defects in phagocytosis, microglia with TREM2 mutations may be less able to clear apoptotic cells and Aβ in the brain resulting in an accumulation of neurotoxic stimuli known to induce microglial expression of TNFα. Furthermore, as these cells also have augmented TNFα secretion following pro-inflammatory stimulation, there may be increased secretion of TNFα into the extracellular space resulting in a cytotoxic, neuroinflammatory environment that further propagates phagocytic dysfunction and microglial over-activation, summarised in Figure 4.15.

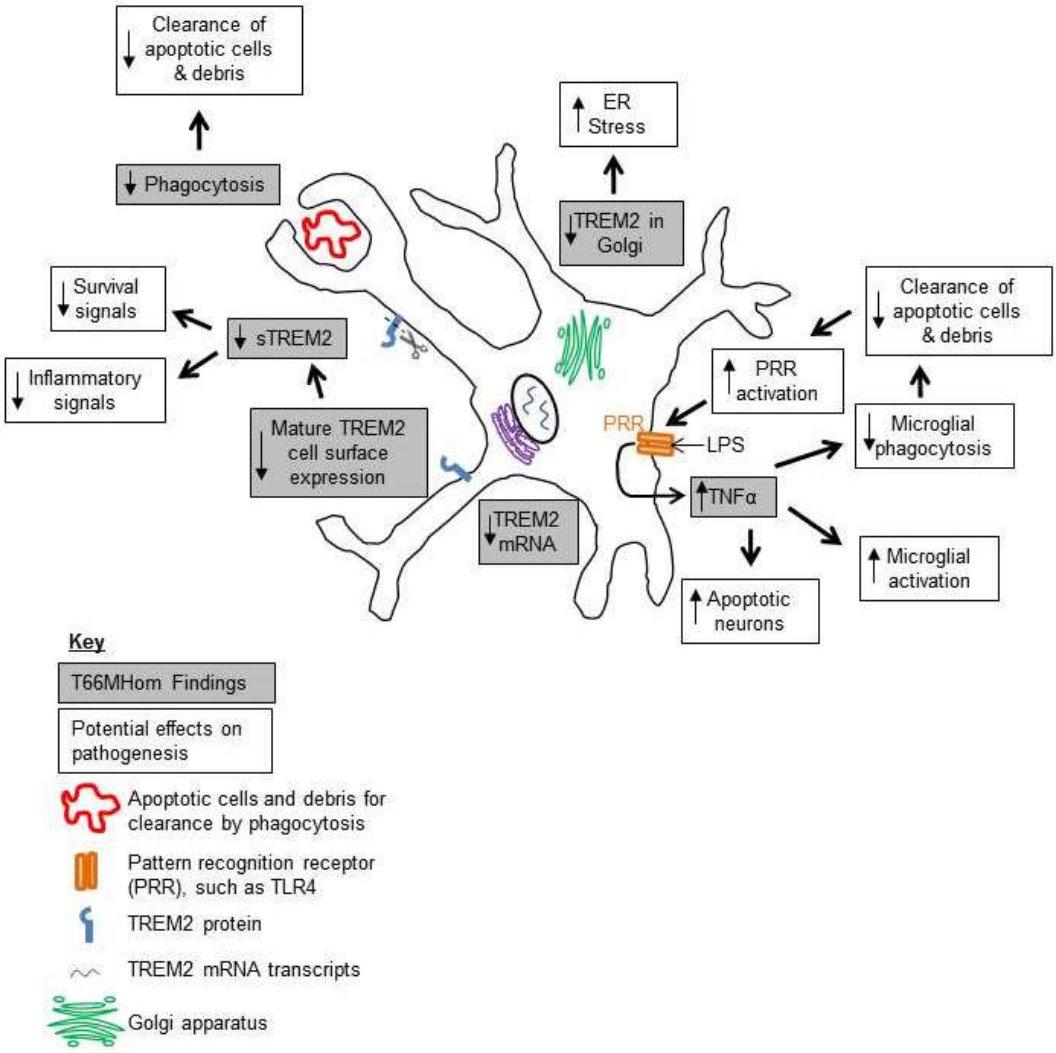

Figure 4.15 Summary of findings in T66M homozygous iPSC-MGLC and potential effects on pathogenesis

Despite reports in the literature of TREM2 loss of function causing increased IL-6 secretion following LPS stimulation (Turnbull *et al.*, 2006; Zhong *et al.*, 2015), no effect of TREM2 mutations on IL-6 release by iPSC-MGLC was found in this study. This may be because the timing of sample collection for cytokine secretion analysis can significantly alter the results found; in the peritoneal lavage fluid of TREM2$^{-/-}$ mice, IL-6 levels were increased compared to WT after 6hours of LPS treatment however, at 20hours, IL-6 concentrations were lower vs controls (Gawish *et al.*, 2015). Therefore, an effect of TREM2 mutations on IL-6 secretion, as reported in the literature (Turnbull *et al.*, 2006; Jay *et al.*, 2015; Zhong *et al.*, 2015), may have been found if more time points for sample collection had been tested.

The iPSC-MGLC were found to express similar levels of various other microglia-expressed, neurodegenerative disease risk factors to those found in human primary microglia. These results indicate that this model of iPSC-derived human microglia is applicable for the study of other neurodegenerative diseases in which the dysfunction of microglia has been implicated. This protocol is currently being utilised to generate iPSC-MGLC from AD patients harbouring heterozygous R47H mutations, which carries similar odds ratio for the development of late onset AD as the APOE ε4 genotype. These cells will be useful for further investigation into the role of TREM2 mutations in AD pathogenesis.

The expression of the neurodegenerative disease risk factors was assessed in the heterozygous and homozygous TREM2 mutation iPSC-MGLC to establish whether mutations in TREM2 alter the expression of other microglial genes linked to neurodegenerative disease. Considerable variation was found in *APOE* expression levels in the control lines and expression was significantly lower in the W50C homozygous line. The APOE ε4 status of the donors is not known and may contribute to the variability that was found in the different cell lines. LPS treatment induces expression of *APOE* in monocyte cell lines but reduces expression of *APOE* mRNA in macrophage cell lines and murine peritoneal macrophages (Gafencu *et al.*, 2007). Therefore the expression of *APOE* may also be altered by the activation state of the iPSC-MGLC. Interestingly, *TREM2* expression has also been shown to be reduced by TLR4-mediated signalling (Turnbull *et al.*, 2006; Owens *et al.*, 2017) suggesting a link between TREM2 and APOE mRNA expression; both have been shown to be downregulated by classical microglial activation states thus the reduction of two protective factors in disease-associated activation conditions could contribute to AD-associated microglial dysfunction.

A significant limitation of this study is the low power from only two homozygous mutant samples being studied, with only one line generated per patient. Work is ongoing to collect samples for iPSC generation from more patients carrying homozygous mutations and more lines are being generated from existing patient samples to minimise the effect of inter-individual and intra-individual variability, in the hopes of resolving this lack of power. Increased sample sizes will allow any subtle differences that may exist between the heterozygous and homozygous lines, or between the control and heterozygous lines, to be identified, as there is currently an unexpected lack of functional effect of TREM2 mutations when found in heterozygosity.

The cells that bud from the embryoid bodies in this protocol resemble primitive tissue macrophages so we need to continue to make improvements in recapitulating endogenous environments to drive cells to differentiate into a mature, tissue-specific state of microglia rather than microglia-like cells or microglia progenitors. Exposure to neuronal factors during differentiation and maturation steps is likely to encourage the development of more matured, ramified, functional morphology resulting in cells that more accurately represent the microglia of adult brains rather than immature progenitors. Despite these limitations, the availability of any type of human microglia to study function and disease is an additional tool with advantages over the use of blood-derived cells or rodent microglia.

Since the commencement of this work, other protocols for the generation of iPSC-derived microglia have been published, attempting to closely mimic the environment of microglia in the developing and adult brain in order to generate a more accurate model of this cell type. It has been shown that microglia are able to develop normally in MCSF deficient transgenic mice due to the fact that IL-34 and MCSF can act similarly to regulate CSF-1R expressing cells (Wei *et al.*, 2010; Wang *et al.*, 2012). New protocols are now utilising this alternative CSF-1R ligand by differentiating iPSC-microglia in IL-34 and low MCSF defined medium in order to model the CNS environment more closely (Muffat *et al.*, 2016; Haenseler *et al.*, 2017). The importance of TGFβ1 in maintaining the microglial transcriptome signature has been recently highlighted by Butovsky et al, which is now being incorporated as a growth factor in differentiation protocols (Abud *et al.*, 2017). Co-culturing techniques are increasingly being used (Haenseler *et al.*, 2017) to try to generate more functional, ramified microglia, which also allows the study of the interactions between microglia and neurons, a model which could prove to be particularly useful if patient-derived cells for particular diseases are employed.

Gosselin et al showed that iPSC-derived microglia, despite avoiding the isolation-associated gene transcription changes resulting from the culture of primary microglia, have expression patterns more similar to *in vitro* cultured cells than freshly isolated brain cells. The use of 3D cultures with multiple CNS cell types is suggested to improve the gene profiles of the iPSC-derived cells (Gosselin *et al.*, 2017). Similar gene expression changes were identified in isolated murine microglia, in which genes associated with mature microglia were particularly affected, however the expression profile was restored upon transplantation into a mouse brain (Bohlen *et al.*, 2017), demonstrating the plasticity of these cells and the importance of CNS environmental signals for influencing expression of mature microglia. The application of 3D co-cultures has demonstrated the ability of iPSC-microglia to mature and function as predicted into highly ramified, resting cells that dynamically survey their environment through branch extension and retraction (Muffat *et al.*, 2016; Abud *et al.*, 2017). Combining various components of different protocols to incorporate knowledge of essential growth factors, co-culture conditions and microglial ontogeny would help to further improve iPSC-MGLC differentiation protocols to increase the likelihood of generating *bona fide* microglia that consistently express the signature microglial transcriptome. In addition to gene expression analysis to confirm differentiation of microglia-like cells, functional assays should be conducted to demonstrate that these iPSC-derived cells also act like microglia. Examples of these functional experiments include assessing appropriate cytokine release following inflammatory stimulation, migration in response to chemokine exposure, appropriate transient calcium responses and the phagocytosis of both pathogenic particles and host cell debris.

The ability to generate cells from patient-derived iPSCs has provided a valuable opportunity to avoid many of the current pitfalls of isolating primary rodent microglia while allowing the possibility to investigate the links between genetic risk factors and the development of disease. Through the generation of Nasu-Hakola disease-patient derived iPSC-MGLC, the effect of TREM2 mutations on microglial TREM2 expression and the functional implications of decreased expression of this receptor have been assessed. The availability of a family of individuals with heterozygous and homozygous mutations is useful for studying the effects of specific mutations on similar genetic backgrounds. TREM2 in AD and Nasu-Hakola is interesting as different mutations in the same gene lead to the development of neurodegenerative diseases of varying severity. iPSC-MGLC with homozygous T66M mutations had significantly reduced surface and total expression of TREM2 and exhibited defects in phagocytosis and augmented TNFα responses following LPS stimulation, suggestive of aberrant TREM2 anti-inflammatory signalling. In addition to modifying iPSC differentiation protocols to

further improve the expression of microglial markers, more disease-relevant stimuli should be employed that may result in the detection of functional deficits in patients and lines harbouring heterozygous TREM2 mutations.

5. CR1 and Complement in Human Microglia

Since the initial identification of Complement Receptor 1 (CR1) as a genetic risk factor for late onset Alzheimer's disease (Lambert *et al.*, 2009), further studies have gone on to confirm the association of polymorphisms in the *CR1* gene with AD. Of the 10 CR1 SNPs found to be associated with Alzheimer's disease in GWAS, meta-analyses and case-control studies, 8 are intronic (rs6656401 (Lambert *et al.*, 2009), rs3818361 (Carrasquillo *et al.*, 2010; Jun *et al.*, 2010), rs1408077 (Kok *et al.*, 2011), rs48744610 (Hazrati *et al.*, 2012), rs646817 (Brouwers *et al.*, 2012), rs12034383 (Brouwers *et al.*, 2012), rs6701713 (Jun *et al.*, 2010) and rs6701710 (Wijsman *et al.*, 2011)) and 2 are found in coding regions (rs116806456 and rs6691117 (Ma *et al.*, 2014)). Interactions between CR1 and C3b-opsonised Aβ and cellular debris, in addition to robust expression of the CR1 orthologue Crry (complement receptor 1-related gene/protein Y) on rodent microglia (Davoust *et al.*, 1999), have resulted in the hypothesis that CR1 mutations may increase the risk of AD by affecting clearance of Aβ and pro-inflammatory debris (Crehan, Hardy and Pocock, 2012). Furthermore, CR1 regulates complement activation so mutations may alter the inhibitory activity of this receptor, resulting in neuroinflammation, which is frequently attributed to microglial activation.

Despite mouse Crry being used to predict functions of human CR1, key differences exist in the structure and functions of Crry compared to hCR1. Both hCR1 and Crry act as C3 convertase inhibitors with decay accelerating and cofactor properties (Molina *et al.*, 1992) however, only hCR1 acts as a receptor for C3b/C4b (Kim *et al.*, 1995), which is key for binding and clearance of opsonised particles. Mice also express murine CR1, which is of similar size to hCR1, although its expression is much more limited and its absence from erythrocytes and platelets suggests that it may not play an important role in immune adherence and clearance (Miwa and Song, 2001).

Despite confirmation of rodent microglial expression of Crry and mCR1 (Davoust *et al.*, 1999; Crehan, Hardy and Pocock, 2013), there is little published evidence indicating that CR1 is expressed by human microglia. In fact, data regarding the expression of CR1 in other cells of the human CNS are conflicting. Singhrao et al., have published a series of papers demonstrating that *in vivo and in vitro* samples of human neurons, astrocytes and microglia lack CR1 expression at the mRNA and protein level (Singhrao *et al.*, 1999, 2000). It has also been reported that human oligodendrocytes do not express CR1 (Scolding, Morgan and Compston, 1998). However, other studies have published expression of CR1 in human astrocytes (Gasque, Fontaine and Morgan, 1995; Gasque *et al.*, 1996; Fonseca *et al.*, 2016) and neurons (Hazrati *et al.*, 2012). As

AD is a disease of the CNS, and limitations of animal models for studying CNS inflammatory diseases, including AD, continue to be identified (Franco Bocanegra, Nicoll and Boche, 2017), it is of great importance to establish how proteins of interest are expressed in disease relevant tissues and cells both in health and disease.

Multiple GWAS studies have demonstrated an association between AD and CR1, however little is known about the role of CR1 in Alzheimer's pathogenesis. The availability of human iPSC-derived microglia-like cells (iPSC-MGLC) is an extremely useful tool for further investigations of this receptor's expression and function.

5.1 *CR1* mRNA is undetectable in control human temporal lobe

Due to a lack of published data confirming the expression of CR1 in the human brain, experiments were conducted to establish whether *CR1* mRNA could be detected in human control brain samples. RNA was isolated from temporal lobe samples of five control adult brains and expression of *CR1* mRNA was assessed by qPCR. The temporal lobe was used to investigate *CR1* expression as this brain region has a dense microglial population, the CNS cell type where CR1 is postulated to be expressed. The levels of *CR1* mRNA in the control human brain samples were found to be almost undetectable (Figure 5.1, Ct values>35), particularly when compared to the levels of *TREM2*, *P2YR12* and *AIF1*, which are known to be expressed on human microglia. The detectable expression of these other microglial markers suggest that the indiscernible level of *CR1* mRNA is not due to an absence of microglia.

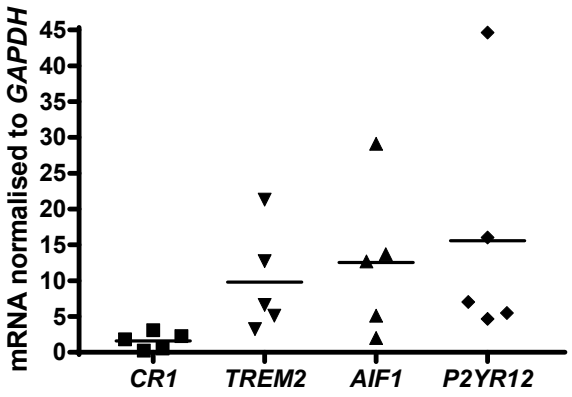

Figure 5.1 mRNA expression of CR1 and microglial makers in control human temporal lobe

qPCR analysis of the expression of *CR1, TREM2, AIF1* and *P2YR12* in RNA extracted from control human temporal lobe samples. Graph represents expression levels of genes of interest normalised to *GAPDH*. Data plotted represents 1/Ct value so high values indicate high expression. N=5

5.2 RNA expression databases indicate that *CR1* expression is undetectable in human brain

The Protein Atlas database (www.proteinatlas.org) holds data on protein expression from antibody-based analysis of control human tissue, in addition to pooling together multiple online RNAseq databases, to provide expression and localisation information on the majority of human protein-coding genes. This tool is valuable for supporting the mRNA expression data generated from our small pilot study into the expression of *CR1* in the human brain.

The HPA RNA-seq dataset (Figure 5.2a) included 3 samples of cerebral cortex in which an average *CR1* abundance score of 0.9 TPM (transcripts per million) was detected. The threshold level to detect the presence of a gene transcript is set to ≥1 TPM, therefore *CR1* was undetectable in this cerebral cortex dataset.

The Genotype-Tissue Expression project (www.gtexportal.org) dataset found that *CR1* expression was undetectable in the cerebral cortex, hypothalamus, caudate and cerebellum (Figure 5.2b). *CR1* mRNA transcripts in the pituitary gland (n=103) and hippocampus (n=94) were only detected at an average of 0.1 RPKM (reads per kilobase per million mapped reads), however this is well below the 0.5 RPKM threshold set for detection.

The Functional Annotation of Mammalian Genomes 5 (fantom.gsc.riken.jp/5/) dataset has a cut off for detection of ≥1 TPM. However the 0.2 TPM in the pituitary gland, 0.2 TPM in the total brain, 0.3 TPM in the hippocampus, 0.5 TPM in the caudate and 0.1 TPM in the cerebellum (Figure 5.2c) were all found to be below the threshold of confident detection of expression.

The RNA expression data from these online datasets concur with the qPCR analysis of *CR1* expression performed in this study; CR1 mRNA levels are found below the confident threshold of expression in control human brain samples.

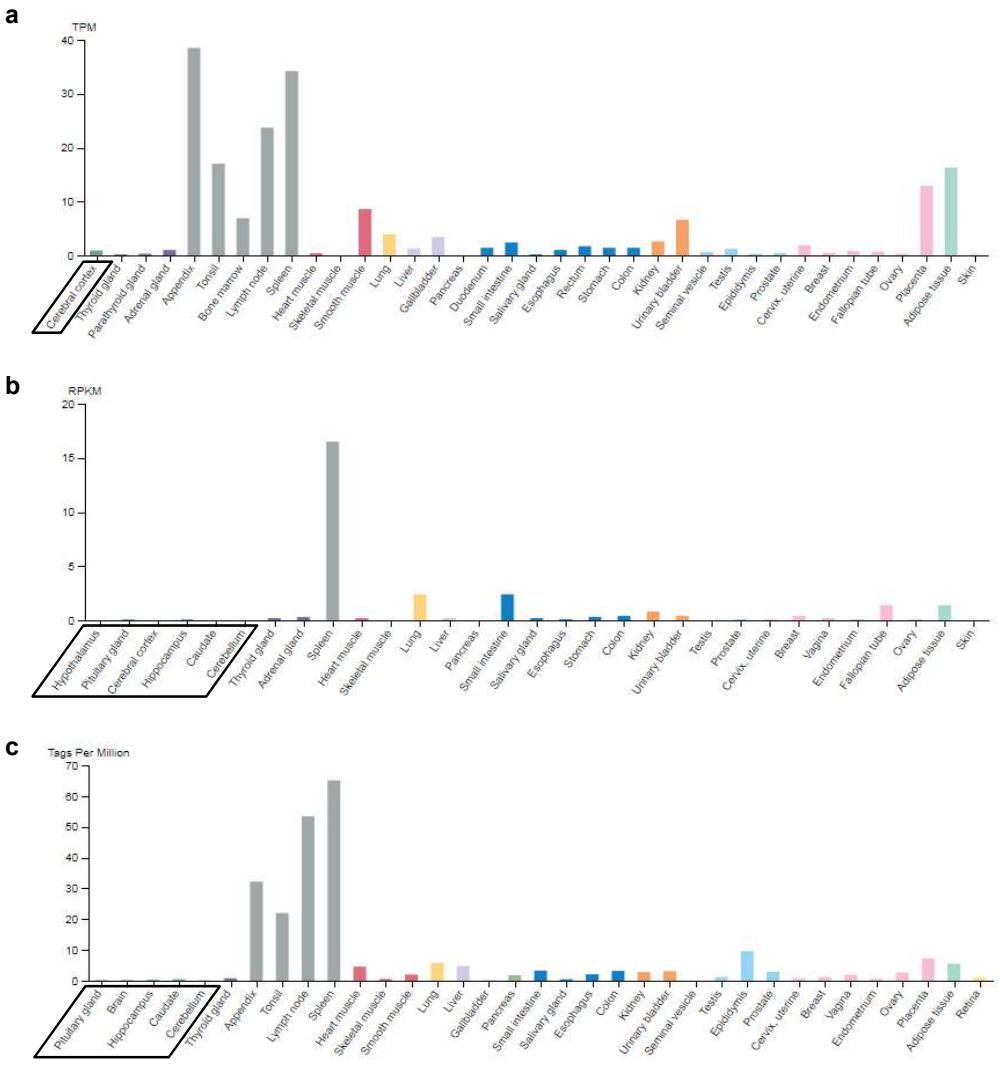

Figure 5.2 Expression of *CR1* in human brain according to RNA-seq databases

Figures adapted from Protein Atlas Database (http://www.proteinatlas.org/ENSG00000203710-CR1/tissue) showing expression of *CR1* in human brain regions. Figures created using data from (**a**) HPA, (**b**) GTex and (**c**) FANTOM5 datasets with RNA-seq tissue data reported as mean TPM (transcripts per million) or median RPKM (reads per kilobase per million mapped reads).

5.3 Protein expression database suggests that CR1 protein is not detectable in human brain

The Protein Atlas database provides information on the expression of CR1 protein in different cell types of various brain regions resulting from immunohistochemical analysis using 5 different antibodies. The antibody staining score describes the level of antibody staining observed in the cell types, which are categorised based on staining intensity and fraction of stained cells: not detected (n), low (l), medium (m) or high (h).

Overall, CR1 protein expression was found to be 'not detected' in the cerebral cortex, hippocampus, caudate and cerebellum (Figure 5.3a). Further analysis of different cell types showed some 'low' CR1 expression in neuronal and epithelial cells (Figure 5.3b), but this was not confirmed with all of the antibodies.

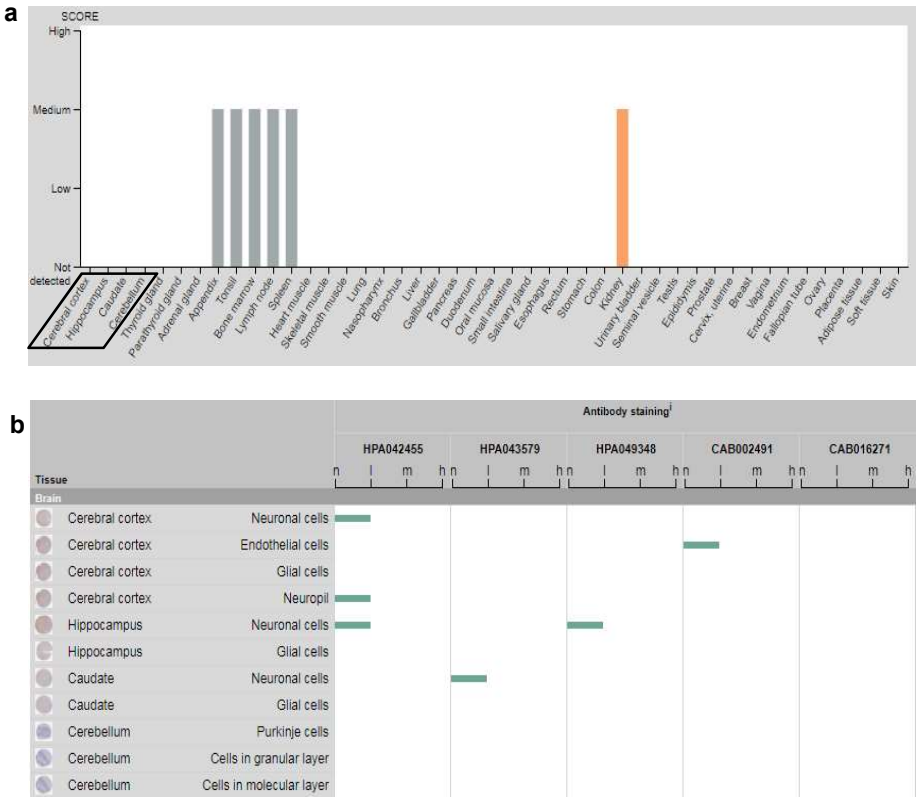

Figure 5.3 Expression of CR1 in human brain according to Protein Atlas expression database

Figures adapted from Protein Atlas Database (http://www.proteinatlas.org/ENSG00000203710-CR1/tissue) showing expression of CR1 protein in human brain regions. Expression analysis conducted using 5 anti-CR1 antibodies for immunohistochemistry of different tissue samples (**a**). Expression within different cell types of brain regions were assessed (**b**), with staining scored as not detected (n), low (l), medium (m) or high (h).

5.4 *CR1* mRNA is almost undetectable in microglia and iPSC-derived microglia-like cells

Following the observation that *CR1* mRNA could not be detected at the whole brain level, the expression of CR1 at the cellular level was investigated, with particular interest in whether CR1 is expressed by human microglia. RNA was extracted from various cell types used to model microglia including blood-derived monocytes, monocyte-derived macrophages and iPSC-derived microglia-like cells (iPSC-MGLCs).

Commercially available human microglial cDNA (Sciencell Online), generated from RNA extracted from microglia isolated from a healthy brain, was also assessed. Neutrophils were included as a positive control for CR1 expression in addition to iPSC-derived astrocytes (kind gift from G. Tyzack, UCL), since some studies have indicated that CR1 may be expressed on astrocytes (Gasque *et al.*, 1996; Fonseca *et al.*, 2016). Robust levels of *CR1* mRNA expression were found in neutrophils but, in comparison, *CR1* was found to be low in monocytes and monocyte-derived macrophages and almost undetectable in microglia, iPSC-MGLCs and iPSC-astrocytes (Figure 5.4).

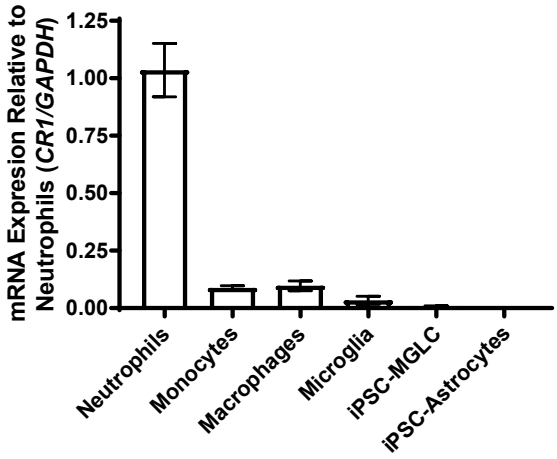

Figure 5.4 Expression of *CR1* mRNA in CNS and immune cells

qPCR analysis to determine CR1 mRNA levels in human neutrophils, monocytes, monocyte-derived macrophages, microglia, iPSC-derived microglia-like cells (iPSC-MGLC) and iPSC-derived astrocytes. Graph represents *CR1* expression normalised to *GAPDH*. Values relative to neutrophil expression levels expressed as mean ±SEM. N=1 microglia and iPSC-astrocytes, n=3 monocytes and macrophages, n=4 neutrophils and n=6 for iPSC-MGLC.

5.5 RNA expression database concurs with very low levels of CR1 mRNA in microglia

The Barres Brain RNA seq database provides transcriptomic data for different cell types of the CNS (http://web.stanford.edu/group/barres_lab/brain_rnaseq.html,, (Zhang *et al.*, 2014)). The database showed very low levels of *CR1* expression in all of the analysed cell types (Figure 5.5), however the highest expression was found in microglia/macrophages at a level of 0.15 FPKM (fragments per kilobase of exon per million reads mapped). Typically a cut-off of 0.5 FPKM is applied, suggesting that *CR1* is not expressed in these CNS cell types, including microglia.

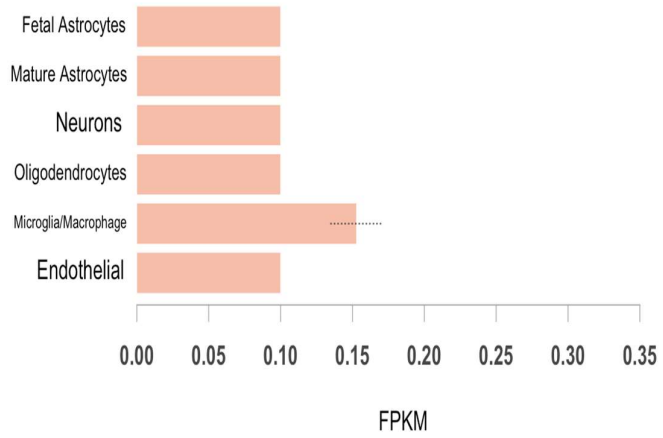

Figure 5.5 Expression of CR1 in CNS cells according to Barres Brain RNA seq database

Figure adapted from http://web.stanford.edu/group/barres_lab/brain_rnaseq.html showing CR1 expression in human CNS cells in the Barres Brain RNA seq database. Expression reported as FPKM (fragments per kilobase of exon per million reads mapped).

5.6 CR1 mRNA expression is upregulated in pre-AD temporal lobe

In addition to RNA samples from control brains, RNA samples from 'pre-AD' brains were also acquired for analysis from the Queen Square Brain Bank (UCL, London). These samples had been collected from donors with no apparent cognitive impairment who, upon post-mortem histopathological examination, were found to have Aβ deposits at Braak stage III or IV and thus have been described here as 'pre-AD' cases. The majority of cases also underwent ABC scoring of AD neuropathological change (Montine *et al.*, 2012), which incorporates histolopathological results for **A**β plaque score using the Thal method (Thal *et al.*, 2002), neurofibrillary tangle stage using the **B**raak method (Braak and Braak, 1991) and **C**ERAD scoring of neuritic plaques (Mirra *et al.*, 1991). The individual scores for each category are combined and transformed into one of four levels of AD neuropathological change: 'not', 'low', 'intermediate' or 'high'. All of the control cases were categorised as 'not' or 'low' neuropathological change whilst the pre-AD samples were all of 'intermediate' AD neuropathological change (Table 5.1). As well as the temporal lobe samples, an area of the brain which has high AD pathology burden and denser microglial populations, samples from the occipital lobe were also assessed as a control for inter-individual expression levels. Compared with control brains, *CR1* expression was higher in pre-AD temporal and occipital lobe samples, although statistical significance was only achieved in the temporal lobe (*$p<0.05$, Figure 5.6c). The expression levels of the microglia specific marker *P2YR12* were also assessed as this would provide information on changes in

the microglia population in these brain regions during the early stages of disease pathology. In both regions *P2YR12* expression was found to be higher in pre-AD samples than controls (Figure 5.6b and d), however this was not statistically significant likely due to large variation in expression between the samples and the small sample size.

Sample	Gender	Age	Braak Score	Neuropathological Change	A Score	B Score	C score
Control 1	F	86	0	Not	0	0	0
Control 2	F	91	0	Low	1	1	1
Control 3	M	71	0	Not	0	1	0
Control 4	M	95	I	N/A			
Control 5	F	87	I	Low	1	1	1
Pre – AD 1	F	95	IV	Intermediate	3	2	2
Pre – AD 2	F	99	IV	Intermediate	2	2	2
Pre – AD 3	F	92	III	Intermediate	2	2	1
Pre – AD 4	F	93	III	Intermediate	2	2	2
Pre – AD 5	M	89	III	Intermediate	2	2	1
AD 1	F	73	VI	High	3	3	3
AD 2	M	85	VI	N/A			
AD 3	F	86	V	N/A			
AD 4	M	76	V	N/A			
AD 5	F	88	V	N/A			

Table 5.1 Pathological details of human control, pre-AD and AD samples

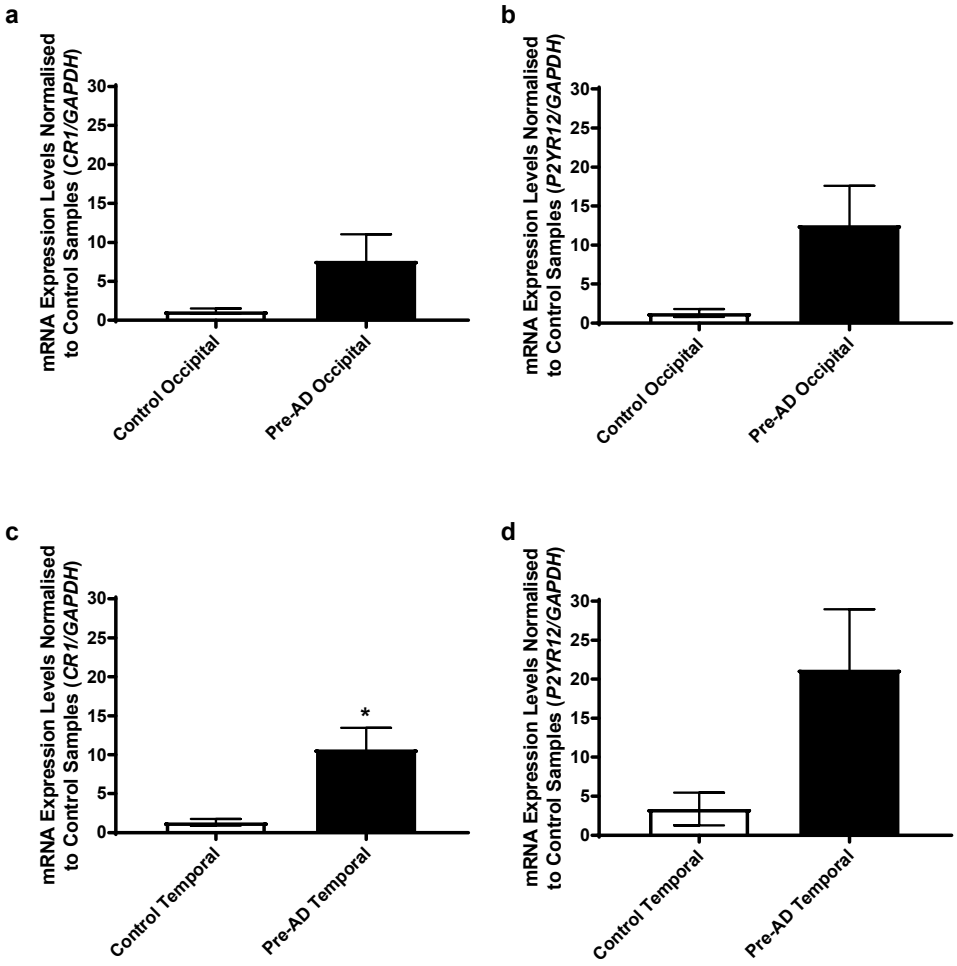

Figure 5.6 Expression of *CR1* and *P2YR12* in temporal and occipital lobes of control and pre-AD cases

qPCR analysis of *CR1* and *P2YR12* mRNA levels in the occipital lobe and temporal lobe of control (n=5) and pre-AD cases (n=5). Graph represents gene of interest expression normalised to *GAPDH*. Values relative to expression levels in controls expressed as mean ±SEM (* $p<0.05$, un-paired t-test).

Recently published data have suggested that neutrophils, a cell type that expresses high levels of CR1, infiltrate the brain during the early stages of AD and are found in areas with Aβ deposits (Zenaro *et al.*, 2015). In light of this report, the expression of the neutrophil marker *ELANE* was assessed in these samples, in order to confirm the presence of neutrophils in the CNS parenchyma of our pre-AD samples. However, in the control and pre-AD samples from both the occipital and temporal lobes, the expression of *ELANE* was undetectable (Ct>40, data not shown), suggesting the increased expression of CR1 in pre-AD brains was not due to the presence of neutrophils.

5.7 Preliminary immunohistochemical analysis of CR1 expression indicates upregulation with AD progression

A small preliminary study into the expression of CR1 protein in human temporal lobe tissue sections by immunohistochemistry was conducted, with 5 samples from control, pre-AD and AD patient groups (see Table 5.1). The ABC score of neuropathological scoring of all of the AD samples had not yet been performed so the groups were assigned according to their Braak staging of disease pathology as follows: I-II controls, III-IV pre AD, V-VI AD. The temporal lobe was chosen as this was shown to have higher expression of *CR1* mRNA than the occipital lobe. Prior to staining for CR1 in human brain tissue samples, the antibody was tested in human kidney tissue samples. CR1 has been shown to be expressed in human glomerulus (Fischer *et al.*, 1986), in particular the epithelial podocyte cells (Appay *et al.*, 1990), thus kidney tissue was chosen as a positive control for CR1 immunohistochemistry. Clear staining of the glomeruli was found (Figure 5.7a and c) with little non-specific staining in the no primary antibody control (Figure 5.7b) therefore we were confident with the suitability of the antibody for probing the brain samples for CR1 expression.

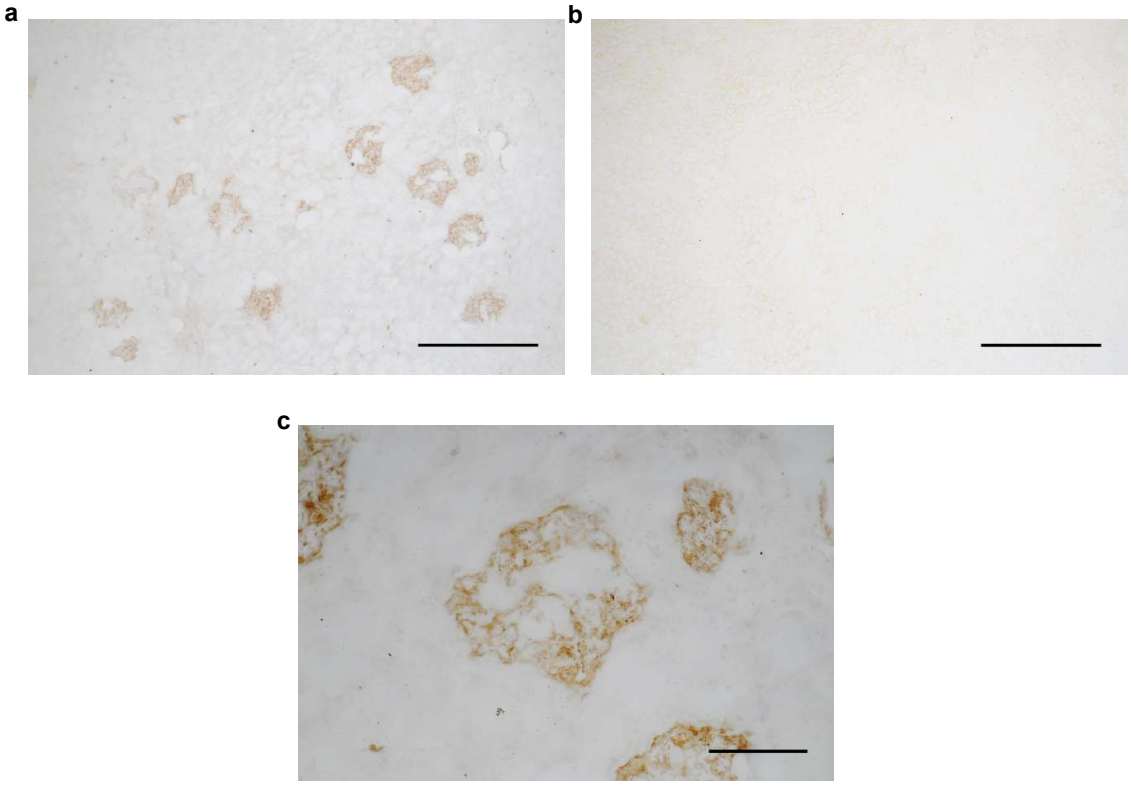

Figure 5.7 Testing of CR1 antibody in human kidney tissue

Representative images from testing the specificity of anti-CR1 antibody in human kidney tissue. Positively stained glomeruli shown at 10x (**a**) and 40x (**c**) magnification. Representative images of no primary antibody negative control at 10x magnification shows secondary antibody specificity (**b**). Scale bars represent 500µm in 10x images and 100µm in 40x images.

In the control brain samples, positive staining for CR1 was present (Figure 5.8a) but this was at a lower level to those found in the pre-AD and AD samples (Figure 5.8b and c). Upon quantification, CR1 positive staining was found to be similar in pre-AD and AD samples, both of which were higher than in the control samples (Figure 5.8e). This increase in CR1 was not significant however, likely due to the small sample size of each group (n=5).

CR1 is a cell surface receptor, however the morphology of the staining found did not indicate that a particular cell type was the source of the expression (Figure 5.9a). Indeed, in a few cases the staining morphology was markedly different with some showing long, vessel-like staining (Figure 5.9c) whereas other staining indicated dark, rounded cells or nuclei (Figure 5.9b). The increase in CR1 protein between control and pre-AD cases supports CR1 mRNA data found in the same samples. Immuno-colocalisation studies would need to be performed to establish whether this increased CR1 is due to upregulation of expression in CNS resident cells, including microglia, or because of infiltration of cells from the periphery. Furthermore, a larger investigation with more samples per group should also be conducted to confirm the increase in expression with the onset of pathology that has been found in this preliminary study.

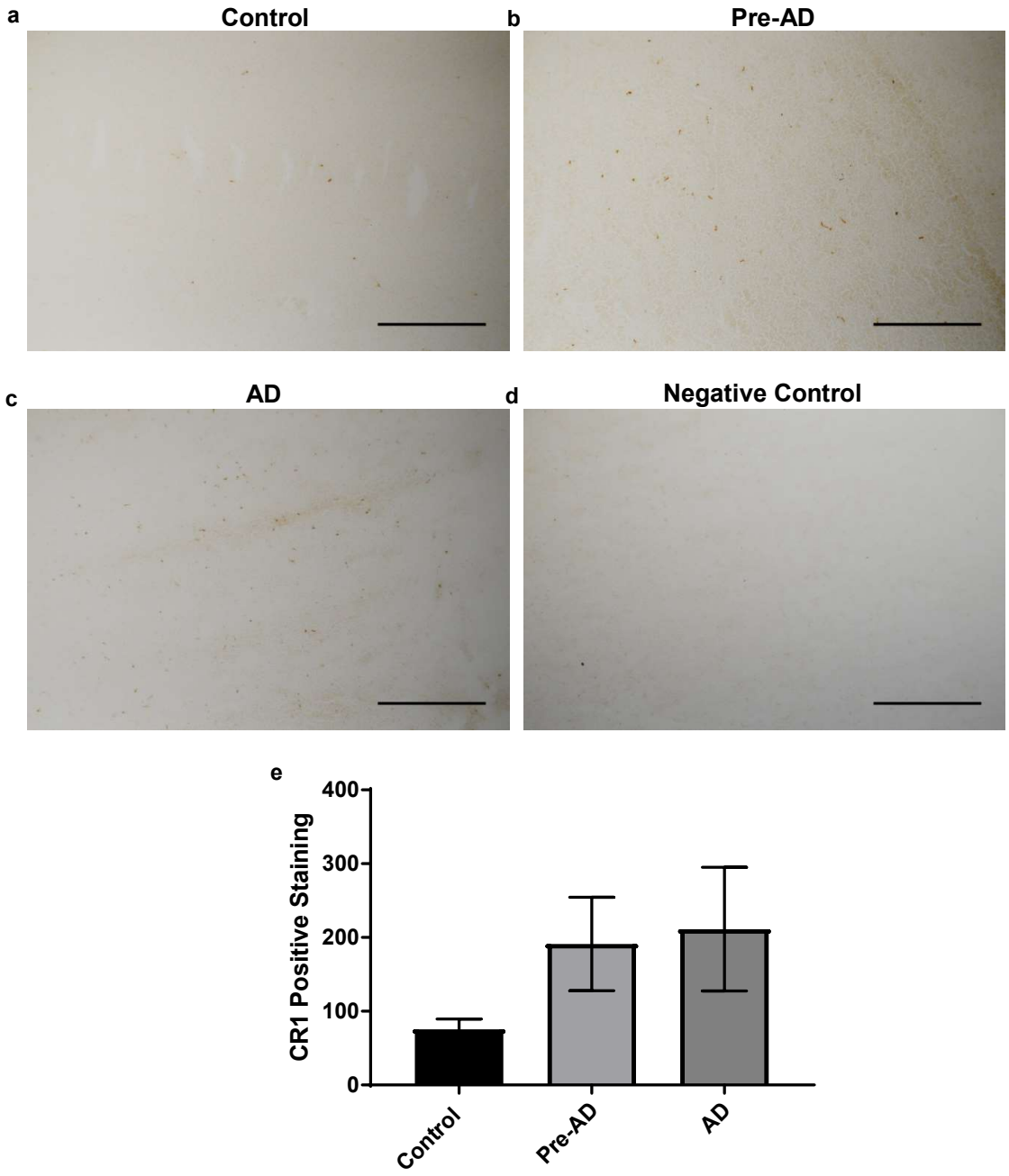

Figure 5.8 Expression of CR1 in control, pre-AD and AD temporal lobes

Representative images from the assessment of CR1 expression in human temporal lobe samples from control (**a**), pre-AD (**b**) and AD (**c**) cases by immunohistochemistry. No primary antibody control representative image is also shown (**d**). 10x magnification, scale bar represents 500µm. CR1-positive staining from three randomly selected fields of view per slide (n=5 per condition) was quantified blinded (**e**).

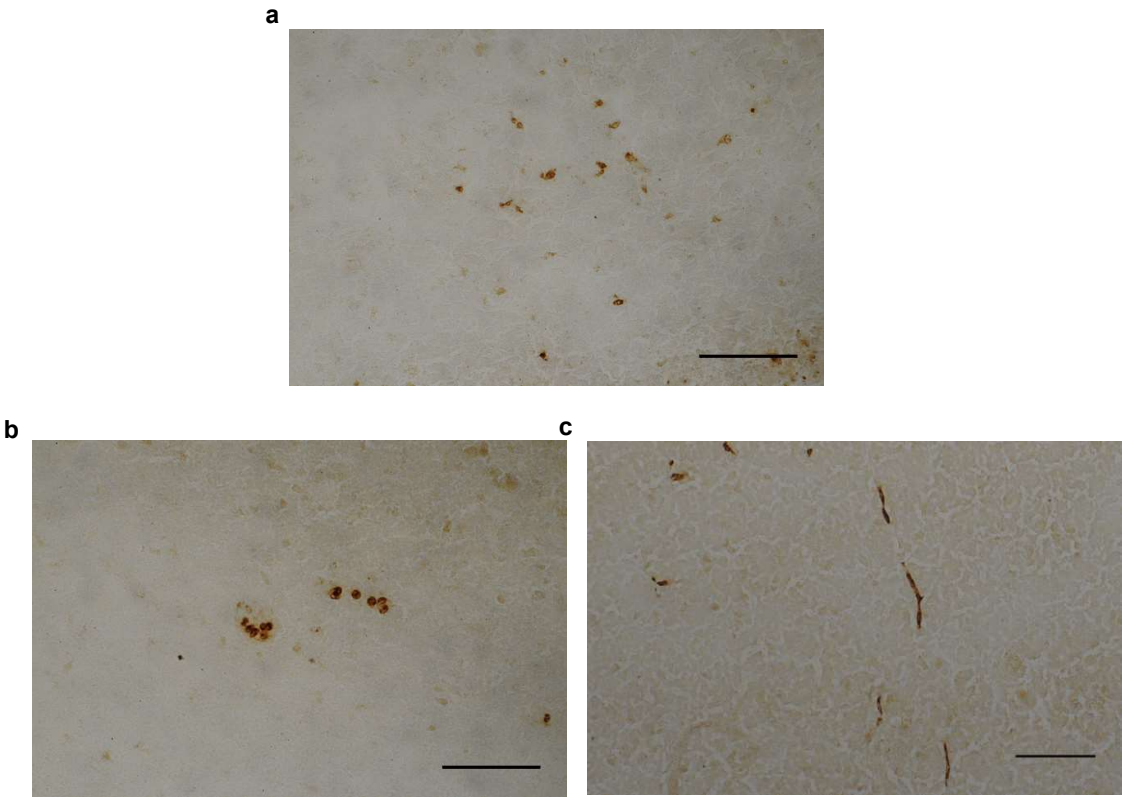

Figure 5.9 Varied morphology of CR1-positive staining

Immunohistochemical analysis of CR1 staining in AD (**a**, **b**) and pre-AD (**c**) temporal lobes revealed varied morphology of positively-stained cells. Images acquired at 40x magnification, scale bar represents 100µm.

5.8 Microglia and iPSC-MGLC express other complement factors linked to Alzheimer's disease

Despite the fact that microglia and iPSC-MGLC have been found to not express CR1, at least in the context of a healthy brain or in an unstimulated state, microglia express other complement factors that have been identified as playing a role in the synaptic loss found in the early stages of disease in AD models. The complement opsonin and classical pathway activator C1q, and the phagocytosis receptor CR3 have been recently shown to mediate oligomeric Aβ-induced dysregulation of synapse pruning by microglia (Hong *et al.*, 2016). It had been planned that the iPSC-MGLC described in Chapter 4 would be used to investigate the role of CR1 in human microglia however, since microglia and the iPSC-MGLC have been found to not express this receptor, the expression of C1q and CR3 by iPSC-MGLC was assessed by qPCR analysis of mRNA levels. The expression in three different control lines of iPSC-MGLC was compared to levels found in a primary human microglia sample from a healthy donor. *C1QA* mRNA was easily detectable at similar levels across the different iPSC-MGLC lines, with

expression in the microglia sample approximately 2.5 fold higher than in the iPSC-MGLC (Figure 5.10a). The CR3 receptor is composed of CD11b and CD18, encoded for by *ITGAM* and *ITGB2* respectively, which were found at twice the level found in the microglial sample (Figure 5.10b and c). Therefore this iPSC-derived model of human microglia was found to be suitable for the study of C1q and CR3, with the aim of investigating their role in AD.

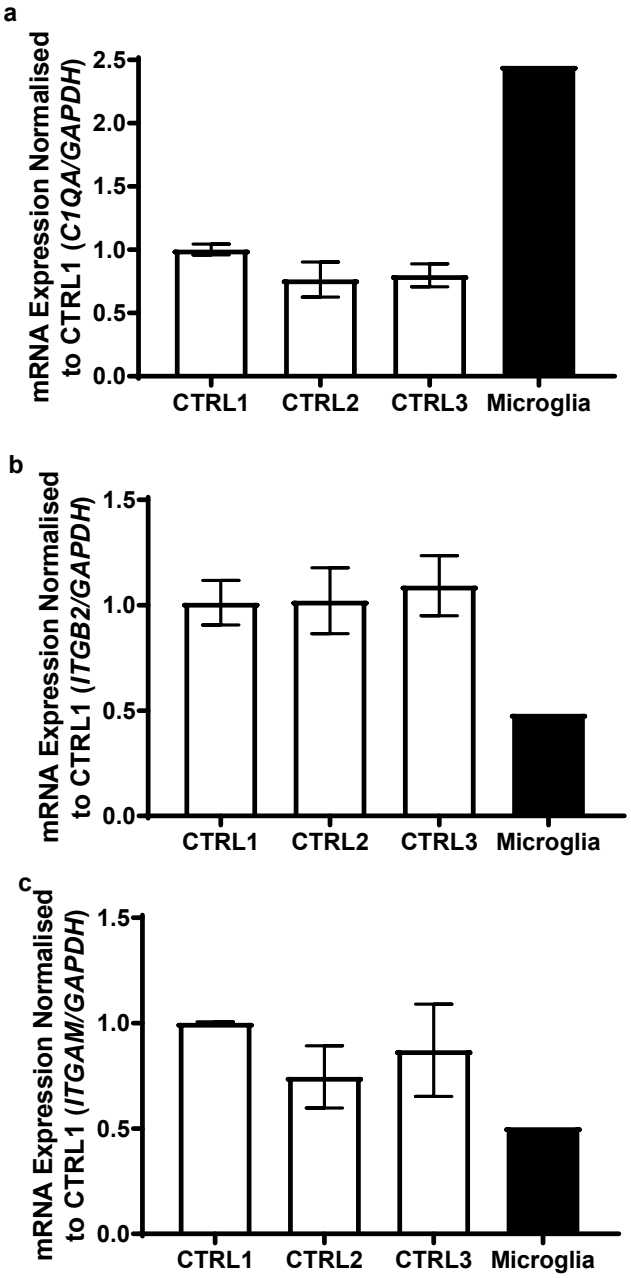

Figure 5.10 Expression of AD-linked complement factors by iPSC-MGLC and microglia

qPCR analysis of *C1QA* (**a**), *ITGB2* (**b**) and *ITGAM* (**c**) expression in iPSC-MGLC compared with microglia. Graph represents gene of interest expression normalised to *GAPDH*. Values relative to expression levels in CTRL1 iPSC-MGLC line expressed as mean ±SEM (n=3 for each iPSC-MGLC line, n=1 for microglia sample).

5.9 Mutations in TREM2 alter the mRNA expression levels of AD-linked complement factors

In addition to the Nasu-Hakola and FTD-associated T66M and W50C TREM2 mutation-harbouring iPSC lines described in Chapter 4, two lines carrying heterozygous R47H TREM2 mutations were also generated (See Chapter 2 Materials and Methods, table 2.1). Rare missense mutations resulting in an R47H substitution in the TREM2 gene have been found to be associated with the development of late onset AD (Guerreiro et al. 2013a; Jonsson et al. 2013), with an odds ratio similar to that of the APOE ε4 allele. Microglia-like cells were generated from these patient-derived, TREM2 mutation-harbouring iPSCs and the expression of *C1QA* and CR3 genes was assessed to investigate whether any links exist between *TREM2* and other AD-associated genes.

Both of the R47H heterozygous iPSC-MGLC were found to have significantly decreased expression of *C1QA* compared with control lines (*** $p<0.001$, Figure 5.11a), with cells expressing only 20% of the mRNA found in controls. Expression of *ITGB2*, which encodes for the CD18 component of the CR3 receptor, was reduced in the T66M homozygous, W50C homozygous and both R47H heterozygous iPSC-MGLC (** $p<0.01$, **** $p<0.0001$, Figure 5.11b) versus controls. In addition to this, expression of *ITGAM* encoding the CD11b subunit of CR3 was also reduced in the W50C homozygous lines compared to controls, alongside the heterozygous T66M iPSC-MGLC (*$p<0.05$). Expression of *ITGAM* was also reduced in T66M homozygous lines but this was not statistically significant ($p=0.076$, Figure 5.11c). These results suggest that expression of the CD18 subunit of CR3 is affected by mutations in multiple sites of the *TREM2* gene, whilst both of the CR3 subunits are downregulated in iPSC-MGLC carrying homozygous W50C mutations.

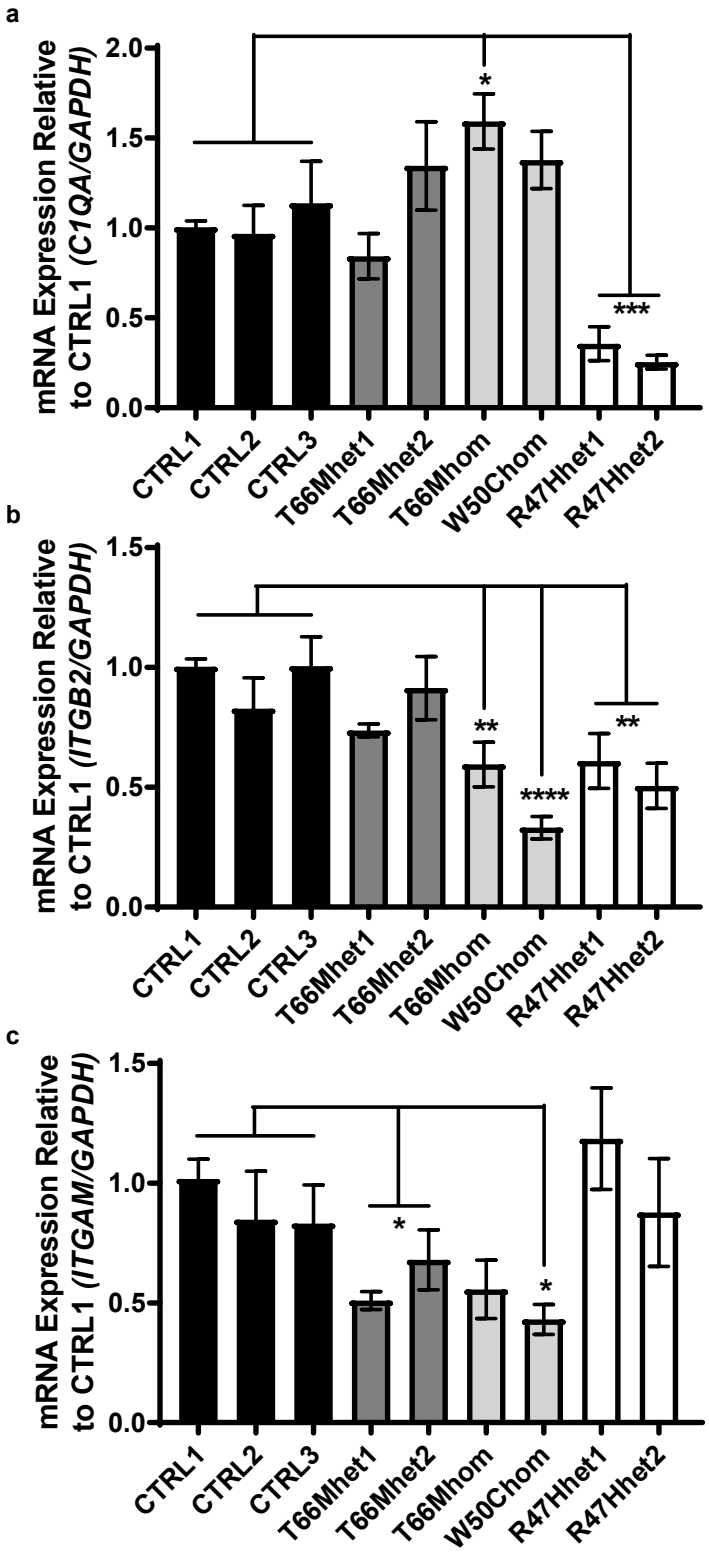

Figure 5.11 TREM2 mutations alter complement factor expression in iPSC-MGLC

qPCR analysis of *C1QA* (**a**), *ITGB2* (**b**) and *ITGAM* (**c**) expression in iPSC-MGLC carrying TREM2 mutations. Graph represents gene of interest expression normalised to *GAPDH*. Values relative to expression levels in CTRL1 expressed as mean ±SEM for 3 individual experiments (*p<0.05, **p<0.01, ***p<0.001, ****p<0.0001; one way ANOVA with Dunnett's multiple comparison test).

5.10 TREM2 R47H mutations affect the secretion of C1q by iPSC-MGLC

The effect of significantly lower *C1QA* mRNA levels found in the R47H iPSC-MGLC on the generation of C1q protein was investigated by assessing the secretion of C1q from these cells. C1q is generated by neurons, astrocytes and microglia, and is secreted in order to perform its function of recognising antibodies, Aβ, pathogen-associated ligands or particles for clearance. This results in the activation of the classical complement pathway leading to C3b generation or induction of phagocytosis through gC1qR (calreticulin) or cC1qR (α2β1 integrin) receptor binding. The levels of C1q protein in the supernatants of R47H mutant and control iPSC-MGLC were determined by ELISA. Interestingly, despite decreased levels of *C1QA* mRNA being found in R47H iPSC-MGLC, these cells secreted greater concentrations of C1q than controls (**p<0.01, Figure 5.12).

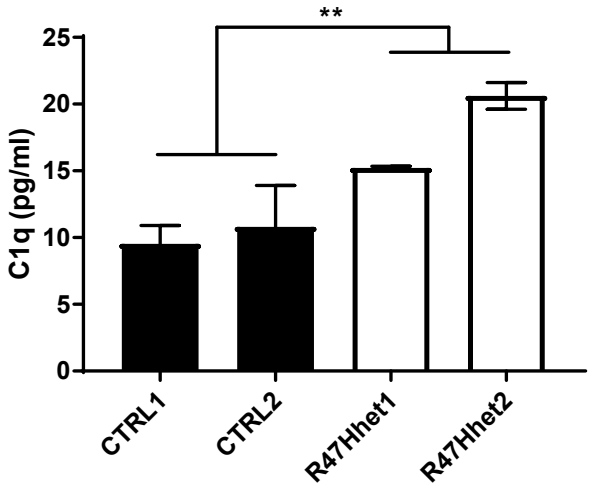

Figure 5.12 ELISA analysis of C1q secretion by control and R47H TREM2 iPSC-MGLC

Baseline C1q secretion in control and iPSC-MGLC carrying heterozygous R47H mutations determined by ELISA. Values relative to expression levels in CTRL1 expressed as mean ±SEM for 3 individual experiments (**p<0.01; unpaired t test).

Another line of iPSC cells carrying R47H TREM2 mutations was available to further investigate the effect of this AD-associated mutation on C1q. The BionCtrl iPSC line was generated from fibroblasts donated by a 19 year old male with no TREM2 mutations, from which a homozygous R47H line was created using CRISPR/Cas9 technology. Therefore, the BionCtrl and BionR47H lines are genetically identical with the exception of the codon at position 47 in the TREM2 gene. iPSC-MGLC were differentiated from these lines providing an extremely valuable tool for studying the effect of this point mutation in isolation on microglial expression and function.

The effect of R47H mutations in the Bion cells on C1QA expression and C1q secretion were therefore investigated. Quantification of C1q release by ELISA demonstrated that the homozygous R47H mutations had no effect on the C1q secretion by the BionR47H line compared with both the BionCtrl and the other control iPSC-MGLC (Figure 5.13a). This suggests that the R47H TREM2 mutations in the R47H heterozygous iPSC-MGLC are not the sole cause of the increased C1q concentrations found in the ELISA analysis (Figure 5.12). Preliminary analysis of *C1QA* mRNA expression levels in the Bion iPSC-MGLC also suggested that there is no difference in the expression of C1q between the BionCTRL and BionR47H cells (Figure 5.13b).

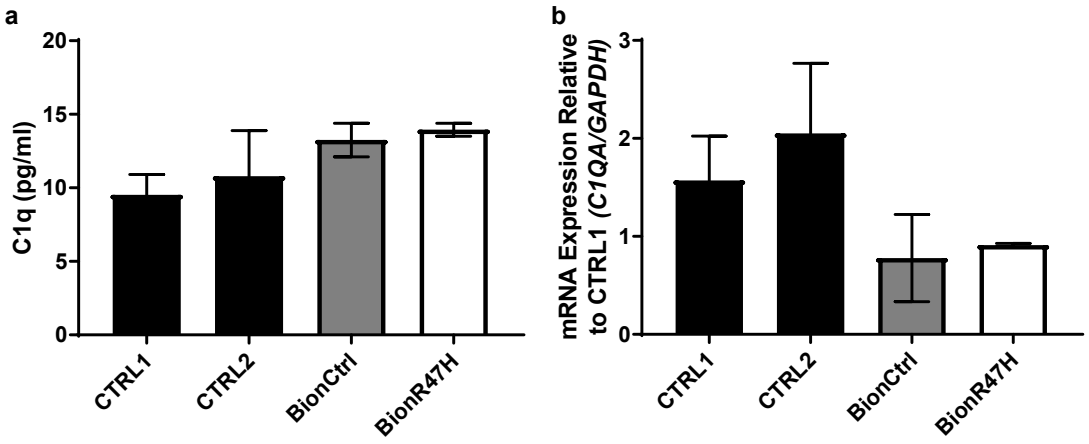

Figure 5.13 Analysis of C1q mRNA expression and secretion by control, Bion control and Bion R47H iPSC-MGLC

(a)Baseline C1q secretion in control and iPSC-MGLC carrying homozygous R47H mutations determined by ELISA. Values relative to expression levels in CTRL1 expressed as mean ± SEM for 3 individual experiments. (b) Preliminary results from qPCR analysis of *C1QA* expression relative to *GAPDH* for 2 individual experiments

5.12 Discussion

Polymorphisms in the gene encoding CR1 have been identified as risk factors for the development of late-onset Alzheimer's disease (Lambert *et al.*, 2009), however the evidence for its expression in the human CNS is unclear. Rodent cultures have been used to demonstrate microglial expression of the murine CR1 orthologue Crry (Davoust *et al.*, 1999; Crehan, Hardy and Pocock, 2013), however, since significant differences exist between human and murine complement receptor expression and function, particularly in the case of CR1 (Jacobson and Weis, 2008), it is important the CR1 expression in human microglial and brain tissue is established. Analysis of RNA isolated from the temporal lobe, a region with relatively dense microglial population, of healthy human brains has shown that almost undetectable levels of *CR1* expression are found, particularly when compared with *TREM2*, *P2YR12* and *AIF1*, which are expressed by human microglia. This is backed up by data from various online RNA sequencing databases which find extremely low CR1 RNA and protein expression levels in the healthy human brain.

Since *CR1* could not be detected at the whole tissue level, *CR1* expression was investigated at a cellular level using RNA that had been extracted from human peripheral blood mononuclear cells and microglia-like iPSC-derived cells, in addition to commercially available microglial cDNA. Robust *CR1* expression was found in neutrophils but was very low in monocytes and macrophages, and levels were almost undetectable in the microglia and iPSC-MGLC samples. This lack of expression in human microglia despite high levels of CR1 orthologs in rodents highlights the importance of understanding the differences between rodent and human systems before drawing conclusions on the role of a protein or an effect of a mutation from studies conducted in just one species. iPSC-derived astrocytes were included in the analysis as CR1 protein has been reported in human control brains by western blotting of total brain lysates and immunohistochemical analysis that indicated expression by astrocytes (Hazrati *et al.*, 2012; Fonseca *et al.*, 2016). However, *CR1* mRNA was undetectable in our analysis of astrocytic cells. This discrepancy could be attributed to different subtypes of astrocytes being analysed, the accuracy in which this iPSC model recapitulates human astrocytes or issues with the specificity of the antibodies used to detect CR1 protein expression, as the published data did not include analysis of RNA expression by techniques, such as qPCR or in-situ hybridisation, which have fewer antibody specificity-associated limitations.

Following the observation that *CR1* mRNA could hardly be detected in control brains or found in brain RNA seq and protein expression databases, the expression of CR1 in

disease was investigated in a small study of RNA and tissue samples from early pathology stage pre-AD and later stage AD cases. The donors of the pre-AD samples had not presented with any clinical symptoms of AD but were found to have 'intermediate' scores of AD neuropathological change according to the ABC scoring system (Montine *et al.*, 2012). This system takes into account previously used scoring for Aβ deposits, neurofibrillary tangles and neuritic plaques in order to report on the presence and extent of pathology rather than cognitive state. Minimum sampling of brain regions and lesions is required and results in a scoring system that provides more information on the full range of AD-associated pathology.

RNA analysis found an upregulation of *CR1* expression in pre-AD temporal and occipital lobes relative to healthy controls, although found to a lesser degree in the occipital lobe. Similarly, CR1 protein levels determined by immunohistochemistry were higher in pre-AD samples than in controls. For the immunohistochemistry, AD samples were also available which demonstrated increased expression relative to controls at an equivalent level to those found in the pre-AD tissue. This suggests that CR1 increases in the early stages of AD, during or following the initial deposition of Aβ plaques and neurofibrillary tangles. In this small, preliminary study, CR1 expression did not change with worsening pathology but there are currently insufficient numbers to make concrete conclusions. This study should be extended to include RNA samples from AD cases for analysis of mRNA expression levels, lysates for analysis of protein expression by western blotting, as well as increasing the sample size of the groups for both RNA and protein analysis. It should be noted that there is no way of knowing that the pre-AD patients, those who did not present with symptoms but upon post mortem analysis were found to have low levels of AD pathology, would have gone on to develop AD and therefore may not truly represent the early stages of disease.

The lack of *CR1* mRNA expression in control brains poses interesting questions for the role of CR1 in the development of AD, given that the mutation effect size and frequency are sufficient for it to be detected as a hit in GWAS studies of a disease of a tissue where it is not found in homeostasis. The fact that CR1 expression in the brain is only detectable after the onset of pathology suggests that increases in *CR1* mRNA transcripts may be a consequence rather than a primary cause of disease. Whether the increase in CR1 expression is due to an upregulation of expression by resident cells of the CNS or due to infiltration through an increasingly leaky blood brain barrier by cells from the periphery needs to be investigated further. Immunohistochemical colocalisation studies need to be performed to ascertain the identity of the cells that express CR1 protein in the human temporal lobe samples used in this study.

Zenaro et al report that neutrophils, a cell type that expresses high levels of CR1, which I have confirmed through mRNA analysis, infiltrate the brain in the early stage of disease in AD models, particularly in areas with Aβ deposits. Following analysis of human AD brains, neutrophils were found to be present at levels up to 10x greater than those in controls, with cells observed in vessels and the parenchyma (Zenaro *et al.*, 2015). The effect of increased neutrophil numbers in AD brains is not yet known but inhibiting neutrophil extravasation by blocking the receptor required for neutrophil trafficking resulted in an amelioration of Aβ load and improvements in cognitive performance (Zenaro *et al.*, 2015). As neutrophils robustly express CR1, the infiltration in the early stages of AD found in the mouse models could explain the increased expression of CR1 mRNA and protein found in the pre-AD cases. Furthermore, vessel-like staining was found in some samples from pre-AD and AD cases, mimicking the presence of neutrophils in the venules found in the Zenaro study. However, the inability to detect the neutrophil marker ELANE in the control and pre-AD samples contradicts this hypothesis. Perhaps evidence of neutrophils could be found if more markers were investigated or expression of neutrophil elastase, encoded for by the ELANE gene, was assessed at the protein level by immunohistochemistry or western blotting as neutrophils are small and thus have low RNA levels relative to other cell types. As stated previously, increased sample numbers would need to be analysed with extensive investigations required into the cell types expressing the CR1 detected in the pre-AD and AD samples before conclusions can be drawn.

Treatment of human neutrophils with TNFα and IFNγ have been shown to upregulate expression of CR1 (Limb *et al.*, 1991; Arora *et al.*, 2007). Both of these cytokines have been found to be increased in models of AD (Benzing *et al.*, 1999; Abbas *et al.*, 2002; Hickman, Allison and El Khoury, 2008), so perhaps the inflammatory environment resulting from Aβ accumulation and glial dysfunction induces augmented CR1 expression in the brain. In order to investigate this hypothesis, iPSC-MGLC could be treated with these cytokines and mRNA analysis of *CR1* expression could be undertaken. Alternatively, several studies have indicated that peripheral blood cells infiltrate the brain during AD, including T cells, monocytes and neutrophils (Togo *et al.*, 2002; Michaud *et al.*, 2013; Baik *et al.*, 2014), which could contribute to the expression of CR1 in the pre-AD and AD brain and could be investigated by immunohistochemical analysis.

As CR1 is not expressed in the healthy brain, mutations in the receptor may be exerting an effect on AD pathogenesis from the periphery, rather than increasing risk due to activity in the CNS. Erythrocytes are the most abundant CR1-expressing cells

and CR1 surface expression binds opsonised particulate enabling trafficking to, and clearance within, the liver and the spleen. The peripheral sink hypothesis posits that Aβ in the brain can be cleared by Aβ-binding molecules in the periphery disrupting the equilibrium found in brain and periphery Aβ levels (Reviewed by Zhang & Lee 2011). Indeed, Aβ has been shown to bind erythrocyte CR1 via the complement C3b opsonin (Rogers *et al.*, 2006), thus defects in CR1 immune adherence on the surface of erythrocytes may affect AD pathology in the CNS. Rogers et al suggest that decreased efficiency of Aβ binding by complement opsonisation mechanisms in plasma may be associated with worsened cognition, as measured by MMSE. It has also been shown that peripheral administration of anti-Aβ antibodies resulted in the clearance of Aβ from the brain in AD mouse models (DeMattos *et al.*, 2001).

However, analysis of the associations of CR1 polymorphisms and CSF Aβ levels has cast doubt over this hypothesis. A CR1 SNP that is in high linkage disequilibrium with CR1 polymorphisms affecting receptor density on the surface of erythrocytes was not associated with AD risk nor with CSF Aβ levels (Brouwers *et al.*, 2012). The longer form of CR1, which has more C3b binding sites, is the most strongly associated with AD risk, contradicting the hypothesis that increased ability of CR1 to bind C3b-tagged Aβ in the periphery is protective. Furthermore, studies into enzymatic clearance of peripheral Aβ using neprilysin in mouse (Walker *et al.*, 2013), rat and cynomologous monkey (Henderson *et al.*, 2014) studies have cast doubt over the peripheral sink hypothesis, as significant decreases in plasma Aβ levels had no effect on the levels of Aβ in the CSF or brain.

Following the observation that *CR1* was undetectable in control human primary and iPSC-derived microglia, the expression of other microglial genes that link complement and AD was investigated. Hong et al., have recently shown that in the early stages of mouse models of AD, C1q and CR3 are necessary for the Aβ oligomer-induced synapse loss that results from dysregulated microglial pruning. The expression of *C1QA, ITGAM* and *ITGB2*, the genes encoding these complement cascade components, in human iPSC-MGLC and microglia was confirmed. iPSC lines derived from individuals carrying homozygous and heterozygous T66M mutations, as described in Chapter 4, were differentiated into microglia-like cells in order to investigate the effect of TREM2 mutations on C1q and CR3 expression. In addition to these Nasu-Hakola and frontotemporal dementia-associated mutation-harbouring cells, two lines carrying heterozygous R47H mutations, which are associated with an increased risk for the development of late onset AD (Guerreiro et al. 2013a; Jonsson et al. 2013), were also available for analysis.

The iPSC-MGLC carrying the homozygous W50C mutation were found to have significantly lower levels of *ITGB2* and *ITGAM* than control lines, indicating that expression of the mRNA encoding both components of the CR3 receptor are reduced in these cells. The homozygous T66M iPSC-MGLC also had a statistically significant reduction in the expression of *ITGB2* and a trend towards decreased levels of *ITGAM* (p=0.07) suggesting that homozygous mutations in TREM2 alter the expression of the mRNA of the CR3 components CD11b and CD18. iPSC-MGLC with heterozygous T66M mutations were also found to have decreased *ITGAM* expression levels relative to controls. These data together indicate that TREM2 mutations alter the expression of the CR3 receptor.

CR3, also known as Mac-1, is a heterodimeric transmembrane receptor that is expressed on macrophages, microglia, monocytes, dendritic cells and neutrophils and plays a role in phagocytosis as well as regulating cytokine secretion, leukocyte trafficking and synapse formation (Whitlock *et al.*, 2000; Kinashi, 2005; Phillipson *et al.*, 2006). In addition to binding the complement opsonin C3b/iC3b (Beller, Springer and Schreiber, 1982), CR3 ligands include ICAM-1 (Diamond *et al.*, 1990), fibrinogen (Wright *et al.*, 1988) and LPS (Wright and Jong, 1986) however phagocytosis is most effective when particles are opsonised with C3b/iC3b (Mevorach *et al.*, 1998). The CR3 components CD18 and CD11b have been shown to accumulate in the phagocytic cup of a macrophage cell line (Jongstra-Bilen, Harrison and Grinstein, 2003) whilst knockout of CR3 expression in transgenic mice decreased C3b/iC3b mediated phagocytosis in neutrophils (Lu *et al.*, 1997). Treatment with a CR3-blocking antibody has also been shown to reduce phagocytosis by macrophages (Taborda and Casadevall, 2002).

Due to the importance of CR3 in phagocytosis, the decreased expression of the two CR3 component genes may result in a reduction in the phagocytic ability of the iPSC-MGLC. Indeed macrophages from *ITGB2*$^{-/-}$ mice have been shown to have decreased levels of phagocytosis (Taborda and Casadevall, 2002). Heterozygous, lupus-associated mutations in *ITGAM* result in impaired phagocytosis by mutation expressing T cell and monocyte lines (MacPherson *et al.*, 2011) and in monocytes and macrophages from patients carrying the risk-associated mutation (Rhodes *et al.*, 2012). This mutation was also found to impair the phagocytosis of C3b/iC3b coated particles by monocytes, macrophages and neutrophils (Fossati-Jimack *et al.*, 2013).

In addition to effects on phagocytosis, CR3 signalling has been shown to be anti-inflammatory (Marth and Kelsall, 1997; Han *et al.*, 2010). Monocytes and macrophages downregulate pro-inflammatory responses such as IL-12 expression and oxidative

bursts as phagocytosis of C3b/iC3b-opsonised particles occurs, in order to minimise inflammation and damage to neighbouring cells (Marth and Kelsall, 1997; Kim, Elkon and Ma, 2004). The use of *ITGAM*$^{-/-}$ mice has shown that CD11b functions as a negative regulator of TLR-mediated, pro-inflammatory cytokine and interferon release in macrophages (Han *et al.*, 2010).

As CR3 has been shown to play a role in the clearance of apoptotic cells (Mevorach *et al.*, 1998) and Aβ (Choucair-Jaafar *et al.*, 2011; Fu *et al.*, 2012), as well as being found to co-localise with Aβ plaques in AD patient brains (Strohmeyer *et al.*, 2002), decreased expression of *ITGAM* or *ITGB2* due to TREM2 mutations may result in decreased ability of cells to clear neurotoxic Aβ and cellular debris, augmenting the neuroinflammatory environment and contributing to cell death. CR3$^{-/-}$ mice have decreased levels of synapse engulfment by microglia following treatment with oligomeric Aβ (Hong *et al.*, 2016), suggesting CR3 is important for Aβ-induced microglial removal of synapses in the early stages of AD pathology. Furthermore, the role of CR3 in limiting pro-inflammatory responses could lead to increased cytokine secretion in the cells with downregulated expression of this receptor. However, results from studies carried out in CR3 transgenic mice should be carefully considered in the light of identified interspecies differences in the expression of CR1.

In this thesis, it has been shown that iPSC-MGLC with TREM2 mutations cells have downregulated expression of two phagocytic receptors, CR3 and TREM2, which will likely affect the phagocytic capabilities of these microglia-like cells. The functional implications of decreased TREM2 expression on phagocytosis by these cells has already been assessed (see chapter 4), however the effects of decreased CR3 should also be investigated. CR3-mediated phagocytosis is much more effective in the presence of the complement factors C3b/iC3b (Mevorach *et al.*, 1998) so the uptake of complement-opsonised particles by CR3 in the TREM2 mutant iPSC-MGLC should be assessed by incubating fluorescent particles in human serum as a source of complement opsonins.

The expression of the complement opsonin and classical pathway activator C1q was also investigated in the TREM2 mutation harbouring iPSC-MGLC. In the CNS, C1q is secreted by astrocytes and microglia and released into the extracellular space, where it binds to immune complexes and initiates classical pathway through activation of various complement proteases resulting in the formation of the C3 convertase complex. C1q is capable of recognising and binding a range of self and non-self ligands including synapses, apoptotic cells, Aβ, immunoglobulin-containing complexes and PAMPs on the surface of viruses and bacteria (Albertí *et al.*, 1993; Stevens *et al.*, 2007; Fraser,

Pisalyaput and Tenner, 2010; Gaboriaud *et al.*, 2011) and regulates clearance via phagocytosis both with and without complement activation. *C1QA* mRNA levels were found to be significantly lower in both heterozygous R47H mutation iPSC-MGLC lines compared with controls. The R47H mutation is found in the extracellular domain of the TREM2 receptor and is thought to affect TREM2 ligand binding efficiencies (Atagi *et al.*, 2015; Bailey, DeVaux and Farzan, 2015; Poliani *et al.*, 2015). Interestingly, when the secretion of C1q protein was investigated by ELISA, supernatants from R47H iPSC-MGLC were found to contain greater concentrations of C1q versus control iPSC-MGLC, contradicting the typical view that decreased mRNA levels result in lower levels of protein generation.

There are various reasons for this unexpected discrepancy in mRNA and protein levels; a study conducted showed that only 40% of variation in protein expression levels is due to variation in the abundance of the respective mRNA (Vogel and Marcotte, 2012). The remaining 60% is due to post-transcriptional variation consisting of a balance of transcript stability, translational regulation (RNA processing, RNA stability and regulatory elements) and protein degradation. Low *C1QA* mRNA levels may be found in R47H iPSC-MGLC due to decreased stability of the RNA leading to faster degradation and reduced half-life. Intracellular signalling and activity can alter regulation of translation (Sonenberg and Hinnebusch, 2009; Roux and Topisirovic, 2012), generating greater protein despite low levels of mRNA, as single mRNA transcripts can be translated multiple times. In the future, western blotting and immunocytochemistry should be performed to establish whether TREM2 mutations alter the size of the intracellular pool of C1q protein because, if a protein product is designed to be release from the cell, the correlation between intracellular protein levels and mRNA levels can be lost. Alternatively, R47H mutations may alter the mechanisms and signalling pathways regulating the release of C1q from iPSC-MGLC resulting in augmented release despite low mRNA levels relative to controls. Alterations in C1q expression could lead to effects via classical complement activation, such as phagocyte recruitment, synapse removal, immune regulation and cell lysis or via non-classical pathways including phagocytosis, immune regulation, neuroprotection and cognitive aging (Stephan *et al.*, 2013). Baseline expression of C1q mRNA and protein is different between R47H mutant iPSC-MGLC and controls, however expression following activation of iPSC-MGLC should be assessed to establish whether differences between R47H and control iPSC-MGLC are also found in these conditions.

Links between TREM2 and C1q have been identified previously. Alveolar macrophages from TREM2$^{-/-}$ mice had increased levels of C1q protein, although this was also

associated with increased C1qa mRNA levels (Sharif *et al.*, 2014), unlike the expression found in these TREM2 mutant iPSC-MGLC. The *C1Q* gene, as well as the gene encoding C3, have been identified as a 'core' TREM2-related hub gene within the 'Fc-gamma R-mediated phagocytosis' pathway of human and mouse brains (Forabosco *et al.*, 2013; Matarin *et al.*, 2015), which could explain why altered C1q expression is found in iPSC-MGLC carrying TREM2 mutations.

Analysis of the C1q secretion by BionCtrl and BionR47H iPSC-MGLC suggest that R47H TREM2 mutations alone do not in fact alter the secretion of C1q. This is backed up by preliminary data from qPCR analysis of *C1QA* mRNA levels (n=2), which currently suggest that there is no difference in expression of *C1QA* between BionCtrl and BionR47H.The Bion cell lines were generated from fibroblasts from a healthy 19 year old donor who does not harbour TREM2 mutations, in contrast to the R47H heterozygous lines which were donated by a 75 year old and a 54 year old presenting with symptoms of AD. Homozygous R47H mutations were inserted into the TREM2 gene of the BionCtrl line using CRISPR/Cas9 technology in order to generate a tool for unravelling the specific effects of this AD-associated mutation on cells of identical genetic backgrounds. No significant difference in the secretion of C1q was found between BionCtrl iPSC-MGLC and BionR47H iPSC-MGLC suggesting that the augmented C1q secretion identified in AD patient-derived R47H heterozygous iPSC-MGLC compared to controls is not due to the R47H mutation in TREM2. Both heterozygous R47H iPSC-MGLC were found to have increased secretion, which reduces the likelihood of unrelated C1q mutations being the cause of the augmented secretion. The epigenetic memory of the fibroblasts from which the iPSC were generated could therefore be the cause of this altered C1q expression. Epigenetic modifications accumulate with age (Li *et al.*, 2009; Mahmoudi and Brunet, 2012; Fernández-Santiago and Ezquerra, 2016) and can be modified by disease (Wang, Oelze and Schumacher, 2008), potentially altering the expression of genes associated with AD.

Indeed, expression of C1q increases in the aging brain of humans and mice (Reichwald *et al.*, 2009; Stephan *et al.*, 2013), with reports of up to 300 fold increases in transcript levels (Stephan *et al.*, 2013). Perhaps environmental cues related to age alter the epigenetic regulation of the transcription of C1q, which is expressed by fibroblasts (Al-Adnani and O'D McGee, 1976), or the stability of C1q mRNA resulting in increased secretion of C1q in the older, AD patient-derived R4H heterozygous iPSC-MGLC. C1q is upregulated in response to various CNS insults and injuries, including viral infection, ischemia/reperfusion, kainic acid treatment, stroke and Aβ treatment of

organotypic brain slices (Dietzschold *et al.*, 1995; Goldsmith *et al.*, 1997; Huang *et al.*, 1999; Fan and Tenner, 2004) resulting in improved neuronal viability and neurite outgrowth (Pisalyaput and Tenner, 2008), suggesting that it may act as a protective response to injury (Benoit and Tenner, 2011). Of particular importance to the role of C1q in AD, C1q found in the absence of complement activation has been shown to interact with and prevent toxicity from fibrillary and oligomeric Aβ (Pisalyaput and Tenner, 2008; Benoit *et al.*, 2013) and induce neuronal expression of neuroprotective factors including nerve growth factor and neurotrophin-3 (Benoit and Tenner, 2011). C1q enhances microglial phagocytosis of Aβ (Webster *et al.*, 2000) and binds to phosphatidylserines exposed by apoptotic cells for early and efficient removal of these cells via 'eat me' signals (Païdassi *et al.*, 2008). Therefore, C1q may be upregulated in the R47H iPSC-MGLC as a response to both age and disease-associated conditions in order to protect surrounding neurons.

Classical complement activation via C1q and C3b has been shown to be essential during development, as a lack of C1q results in defective anatomic refinement of synaptic connections causing excessive innervation, enhanced synaptic connectivity and epileptogensis (Stevens *et al.*, 2007; Chu *et al.*, 2010). The expression of C3 and its products including the opsonin C3b/iC3b is high during development but decreases and remains low during adult life and normal aging (Stephan *et al.*, 2013). Indeed, despite high levels of C1q found in healthy aged mice brains, C3 was found to be low and no particular synapse loss was detected despite C1q colocalising with synapses (Stephan *et al.*, 2013). Interestingly, C1q was found to negatively affect synaptic plasticity and contribute to cognitive decline in aged animals that were otherwise healthy (Stephan *et al.*, 2013). However, in the models of AD where aged brains are put under additional stresses from the generation and accumulation of Aβ, C1q and C3 levels were augmented and found to be involved in synapse loss arising from Aβ-induced microglial dysfunction (Hong *et al.*, 2016). In this study, Hong and colleagues showed that microglia and complement pathways become inappropriately activated in AD leading to synaptic loss through microglial priming. Following treatment with Aβ or in mouse models of AD, microglial generation of C1q is induced by Aβ oligomers resulting in deposition on synapses. Downstream of C1q deposition and activation, increases in C3 product generation are found which result in tagging of synapses for phagocytosis by CR3 causing subsequent LTP impairment (Hong *et al.*, 2016). Inhibition of C1q and the use of $C1QA^{-/-}$ mice showed that C1q is a key mediator of oligomeric Aβ-induced synaptic loss and LTP dysfunction (Hong *et al.*, 2016). Therefore, in the healthy aging brain, increased levels of C1q may act to be neuroprotective and important for homeostasis. However, in the presence of Aβ-

induced microglial dysfunction, C1q can contribute to disease progression through aberrant induction of complement activation and synaptic damage. In the case of the AD patient-derived iPSC-MGLC, increased C1q secretion may be a result of neuroprotective efforts or due to epigenetic modification of expression in response to microglial activation by Aβ, which could have detrimental effects on synapse function.

C1q has also been implicated in the synaptic alterations found in the hippocampus of multiple sclerosis patients (Michailidou *et al.*, 2015) indicating that C1q dysfunction is not solely an AD-associated phenomenon and other cell stresses found in the neuroinflammatory diseases may also result in unregulated synapse disruption. The studies into the various protective and neurotoxic effects of C1q activity suggest that a fine balance must be found between effective removal of potential sources of injury, such as apoptotic cells and Aβ, and excessive synapse removal following injury induced activation of microglia and complement signalling. In order to study the effect of the R47H heterozygous iPSC-MGLC on this equilibrium, co-culture experiments utilising iPSC-derived neurons could be performed to investigate the effect of increased microglial C1q on neurons; whether increased C1q induces the expression of neuroprotective factors or results in excessive and detrimental synapse stripping should be investigated.

The availability of the Bion cell line from a young donor for analysis of the effect of R47H mutations in TREM2 on gene expression, receptor function and cellular phenotypes has been extremely valuable in highlighting the importance of cell donor age and disease background in the generation of iPSC lines from AD cases and controls. In theory, transcription factor reprogramming using the Yamanaka factors should reset the methylation and epigenetic regulation of the genome of the reprogrammed cell type although some epigenetic memory of the somatic tissue of origin has been found to exist in iPSC lines (Kim *et al.*, 2010). Epigenetics are heritable changes in gene expression that occur independently of nucleotide sequence changes, resulting in alterations in the accessibility of the DNA for transcription through DNA methylation or alter expression post translationally through histone acetylation and methylation or via non-coding RNAs (Fernández-Santiago and Ezquerra, 2016). Changes in epigenetic signatures or ‘epigenetic drift’ from the original epigenome has been reported during aging (Hannum *et al.*, 2013) and also in sporadic diseases, including AD (Wang, Oelze and Schumacher, 2008) which could be contributing to disease development. Interestingly, fibroblasts from sporadic AD cases have been reported to have alterations in oxidative stress responses (Ramamoorthy *et al.*, 2012) which, upon reprogramming and differentiation into a more disease-relevant cell type

such as microglia, may have an even more marked effect on disease-associated phenotypes. Therefore, differences in C1q expression between AD patient-derived iPSC-MGLC and iPSC-MGLC from a 19 year old donor with the disease mutations inserted could be explained by age and disease-associated changes to gene expression levels.

The age of sources of fibroblasts for reprogramming should also be considered due to variations in the reprogramming efficiency of young and aged cells. Age-dependent declines in reprogramming efficiencies have been identified in murine fibroblasts, with strong effects of age even seen in 'middle aged' donors (Mahmoudi and Brunet, 2012). These differences in aged cells could be attributed to higher densities of senescent and pre-dysfunctional cells present in cell populations obtained from older donors. Aged cells have increased expression levels of Ink4 and Arf, two anti-proliferative genes which have been shown to decrease the efficiency and fidelity of reprogramming (Li *et al.*, 2009). Furthermore, the tissue source of material for reprogramming has also been found to affect efficiency, with keratinocytes found to be more readily reprogrammed than fibroblasts (Maherali *et al.*, 2008).

Serial reprogramming has been shown to be effective in reducing the epigenetic memory of cells (Kim *et al.*, 2010), particularly related to biases in lineage differentiation propensities based on the lineage of the original cell type. However, one's area of research interest may alter one's opinion on whether epigenetic memory is a disadvantageous artefact of reprogramming or a useful source of information on disease pathogenesis, particularly in the case of a disease where the greatest risk factor is age. If one is focussed on the effects of specific point mutations on defined cells for the development of disease, it may be more useful to use CRISPR/Cas9 technology to generate the desired point mutations in control cell lines or to repair disease associated mutations in patient-derived cells. This would generate the necessary controls for establishing whether altered phenotypes and genotypes are due to the mutation of interest. Conversely, incomplete eradication of epigenetic signatures may be a valuable opportunity for investigating epigenetic changes to chromatin during disease providing information on pathogenesis, particularly in the case of sporadic rather than monogenic diseases. The fact that the epigenetic memory is not completely wiped during reprogramming reinforces the importance of utilising aged matched controls, considering the effect of age on the epigenome. In order to overcome this issue to establish the effect of R47H mutations in the TREM2 gene on C1q expression and secretion, the point mutation should be repaired to generate controls with identical

genetic background. Any variations found in C1q in the R47Hhet iPSC-MGLC could therefore be confidently attributed to the mutation in TREM2.

In summary, I have shown using RNA analysis and an investigation of online databases that under physiological conditions CR1 is not detectable in human microglia and is found at extremely low levels in the human brain. Expression is upregulated in the early stages of AD pathology although the source of this RNA and protein expression needs to be established. Other complement components linked to AD, C1q and CR3, are expressed by microglia and have been shown to be modulated by the expression of TREM2 mutations in human iPSC-MGLC. The functional implications of altered expression of multiple components of the innate immune response system in the brain should be assessed as predicted effects upon the phagocytic ability of microglia could have significant implications for development as well as the response to AD pathogenesis and other CNS insults and infections.

6. Conclusions

Since their initial identification by Franz Nissl in 1899, opinions on the functions of microglia in the CNS have evolved. Once viewed as merely support cells, the use of transgenic animal models have demonstrated that microglia are essential for fully functional development and maintenance of neuronal networks, whilst the use of GWAS and gene expression network analyses have identified roles of microglia-expressed genes in many neurodegenerative diseases, including AD. The ability to accurately model these low frequency but highly active cells has also progressed, allowing us to further understand their role in physiology and pathogenesis. GWAS and exome sequencing studies have identified AD-associated genes that would never have been discovered by genetic linkage analysis alone, such as TREM2 and CR1, as well as identifying core pathways that appear to play roles in AD pathogenesis. Two consistently identified pathways are those involved in the immune system and inflammatory responses, which in the brain, primarily point to the involvement of microglia.

In this thesis, models have been characterised that have been generated using two techniques, iPSC and CRISPR/Cas9 technologies, that, in the decade since their conception, have had ground-breaking effects on basic biological research as well as translational medicine and biotechnology. Gene and protein expression dynamics and phenotypic changes in CRISPR/Cas9-generated TREM2 null BV2 microglia, and iPSC-derived microglial-like cells from patients harbouring TREM2 mutations were investigated. Both models showed that these predicted loss of function mutations resulted in aberrant TREM2 protein expression and localisation, a lack of sTREM2 generation and decreased phagocytosis. This consistency between models and the generation of results concurs with published data and suggests that these models are reliable for the study of the effects of mutations in this receptor.

The generation of a microglial model harbouring TREM2 T66M mutations has value beyond the study of Nasu-Hakola disease alone. T66M mutations have also been identified in FTD-like syndrome-behavioural variant, FTD, and AD cases, indicating the range of contexts in which this model could be useful. Also, although T66M heterozygous mutations are only found in a few rare cases of AD (Guerreiro et al. 2013a), an R47H mutation in TREM2 is one of the largest genetic risk factors for the development of late onset AD, second only to APOE genotype. Therefore this tool for studying TREM2 dysfunction could provide valuable information for the investigation of

all pathologies in which altered TREM2 activity may contribute, regardless of the mutations associated.

Although the characterised iPSC-derived microglia-like cells already express many of the genes identified as key features of the microglial transcriptome signature identified by Butovsky et al, 2014 which currently acts as the gold standard for microglial models, our model of microglia-like cells is still in its infancy. As CNS environmental factors continue to be identified as important for directing microglial differentiation and homeostasis, the culture conditions used in our model will continue to evolve in order to more accurately recapitulate those found physiologically, with the aim of creating the most microglia-like phenotype. Microglial differentiation in the presence of neuronal- and astrocytic-derived factors is becoming more commonplace and should be incorporated into our protocol. This could be achieved through supplementing media with factors produced endogenously by these cell types, the use of neuron/astrocyte-conditioned medium or through 3D co-culture with iPSC-derived astrocytes and neurons.

The ability to generate microglia-like cells from patient-derived fibroblasts has the potential to revolutionise therapies for the multitude of neurodegenerative diseases in which microglia have been implicated. Through the combination of iPSC technology and CRISPR/Cas9, disease-modifying mutations could be repaired in patient-derived fibroblasts prior to differentiation into microglia. Once the safety of the transplantation process has been confirmed, the 'repaired' microglia could be used as a cell therapy to populate the brain, with the aim that 'repaired' microglia are less vulnerable to pathology-associated dysfunction and act in a more neuroprotective manner than the existing pool of microglia. Proof of concept for the use of iPSC-derived cells as a cell therapy for neurodegenerative diseases has been recently published; it was demonstrated that iPSC-derived dopaminergic neuron progenitors could be safely transplanted into non-human primates, resulting in successful engraftment and improved motor function in the absence of rejection or tumour formation (Kikuchi *et al.*, 2017).

The need to apply the use of iPSC technology to generate co-cultures for studying the interactions between dysfunctional microglia and neurons has been emphasised by results suggesting a link between TREM2 mutations and alterations in expression of C1q and CR3. These complement components have been shown to be essential for optimising neuronal networks during development but also implicated in the synapse loss found in the early stages of AD. Investigating the functional effects of the identified alterations in expression in a more disease relevant context would provide valuable

information on the contributions of TREM2 mutations to neurodegenerative disease pathogenesis.

In the case of all findings identified using the patient-derived iPSC-MGLC, a lack of power from the use of only one line from one or two patients puts considerable limitations on the conclusions that can be drawn. Therefore, in order to improve the statistical power of these results and allow more confident suggestions to be made regarding the effects of TREM2 mutations, extra lines should be generated from existing donor samples and ongoing work to recruit and generate iPSCs from additional carriers of TREM2 mutations should continue. The investigation into complement expression in microglia and the brain highlighted two significant caveats to further consider when modelling disease: the implications of species specific differences in gene expression and the importance of using aged matched controls.

The identification of a lack of expression of CR1, an AD-risk associated gene, in control brains and in unstimulated human microglia has significant implications for the current working hypothesis that CR1 contributes to AD through altered complement regulation and Aβ clearance by microglia. With our preliminary study, we have shown that expression of CR1 is found in the brains of AD patients and in donors without cognitive deficits but with early stages of pathology identified post mortem. Whether the increased expression is due to upregulation of CR1 expression by microglia activated by Aβ or from infiltration of CR1 expressing cells into the brain parenchyma is not yet known. This result was identified in disease relevant tissue samples, rather than in an AD model, and thus would be a priority to investigate further to elucidate the effect of AD-associated SNPs in the CR1 gene on pathogenesis.

In conclusion, data have been presented demonstrating the suitability of iPSC-derived microglia like cells for the study of microglia in the context of neurodegeneration. These studies have also highlighted some weaknesses of current modelling techniques that need to be overcome. Due to small sample sizes, concrete conclusions regarding the effect of TREM2 mutations on microglial dysfunction and the expression of CR1 in control and AD human brains cannot yet be drawn, but the results presented herein have interesting implications for the understanding of these recently identified AD-associated mutations in pathogenesis, which should be investigated further.

7. References

Abbas, N. *et al.* (2002) 'Up-regulation of the inflammatory cytokines IFN-gamma and IL-12 and down-regulation of IL-4 in cerebral cortex regions of APP(SWE) transgenic mice.', *Journal of neuroimmunology*, 126(1–2), pp. 50–7.

Abud, E. M. *et al.* (2017) 'iPSC-Derived Human Microglia-like Cells to Study Neurological Diseases.', *Neuron*, 94(2), p. 278–293.e9.

Afagh, A. *et al.* (1996) 'Localization and cell association of C1q in Alzheimer's disease brain', *Exp Neurol*, 138(1), pp. 22–32.

Ahearn, J. M. and Fearon, D. T. (1989) 'Structure and function of the complement receptors, CR1 (CD35) and CR2 (CD21).', *Advances in immunology*, 46, pp. 183–219.

Ajami, B. *et al.* (2007) 'Local self-renewal can sustain CNS microglia maintenance and function throughout adult life', *Nature Neuroscience*, 10(12), pp. 1538–1543.

Ajami, B. *et al.* (2011) 'Infiltrating monocytes trigger EAE progression, but do not contribute to the resident microglia pool', *Nature Neuroscience*, 14(9), pp. 1142–1149.

Al-Adnani, M. S. and O'D McGee, J. (1976) 'C1q production and secretion by fibroblasts', *Nature*, 263(5573), pp. 145–146.

Albertí, S. *et al.* (1993) 'C1q binding and activation of the complement classical pathway by Klebsiella pneumoniae outer membrane proteins.', *Infection and immunity*, 61(3), pp. 852–60.

Alliot, F., Godin, I. and Pessac, B. (1999) 'Microglia derive from progenitors, originating from the yolk sac, and which proliferate in the brain.', *Brain research. Developmental brain research*, 117(2), pp. 145–52.

Almeida, S. *et al.* (2012) 'Induced pluripotent stem cell models of progranulin-deficient frontotemporal dementia uncover specific reversible neuronal defects.', *Cell reports*, 2(4), pp. 789–98.

Apostolou, E. and Hochedlinger, K. (2013) 'Chromatin dynamics during cellular reprogramming', *Nature*, 502(7472), pp. 462–471.

Appay, M.-D. *et al.* (1990) 'Expression of CR1 (CD35) mRNA in podocytes from adult and fetal human kidneys', *Kidney International*, 38(2), pp. 289–293.

Areschoug, T. and Gordon, S. (2009) 'Scavenger receptors: role in innate immunity

and microbial pathogenesis.', *Cellular microbiology*, 11(8), pp. 1160–9.

Arnett, H. A. *et al.* (2001) 'TNF alpha promotes proliferation of oligodendrocyte progenitors and remyelination.', *Nature neuroscience*, 4(11), pp. 1116–22.

Arora, V. *et al.* (2007) 'Modulation of CR1 transcript in systemic lupus erythematosus (SLE) by IFN-gamma and immune complex.', *Molecular immunology*, 44(7), pp. 1722–8.

Atagi, Y. *et al.* (2015) 'Apolipoprotein E Is a Ligand for Triggering Receptor Expressed on Myeloid Cells 2 (TREM2)', *Journal of Biological Chemistry*, 290(43), pp. 26043–26050.

Azevedo, F. A. C. *et al.* (2009) 'Equal numbers of neuronal and nonneuronal cells make the human brain an isometrically scaled-up primate brain.', *The Journal of comparative neurology*, 513(5), pp. 532–41.

Baik, S. H. *et al.* (2014) 'Migration of neutrophils targeting amyloid plaques in Alzheimer's disease mouse model.', *Neurobiol Aging*, 35(6).

Bailey, C. C., DeVaux, L. B. and Farzan, M. (2015) 'The Triggering Receptor Expressed on Myeloid Cells 2 Binds Apolipoprotein E', *Journal of Biological Chemistry*, 290(43), pp. 26033–26042.

Bales, K. R. (2012) 'The value and limitations of transgenic mouse models used in drug discovery for Alzheimer's disease: an update', *Expert Opinion on Drug Discovery*, 7(4), pp. 281–297.

Balsam, L. B., Liang, T. W. and Parkos, C. A. (1998) 'Functional mapping of CD11b/CD18 epitopes important in neutrophil-epithelial interactions: a central role of the I domain.', *Journal of immunology,* 160(10), pp. 5058–65.

Barger, S. W. *et al.* (2007) 'Glutamate release from activated microglia requires the oxidative burst and lipid peroxidation.', *Journal of neurochemistry*, 101(5), pp. 1205–13.

Barnum, S. R., Jones, J. L. and Benveniste, E. N. (1992) 'Interferon-gamma regulation of C3 gene expression in human astroglioma cells', *J Neuroimmunol*, 38(3), pp. 275–282.

Barrangou, R. *et al.* (2007) 'CRISPR Provides Acquired Resistance Against Viruses in Prokaryotes', *Science*, 315(5819), pp. 1709–1712.

Barres, B. A. *et al.* (2008) 'The Mystery and Magic of Glia: A Perspective on Their Roles in Health and Disease', *Neuron*, 60(3), pp. 430–440.

Beers, D. R. *et al.* (2006) 'Wild-type microglia extend survival in PU.1 knockout mice with familial amyotrophic lateral sclerosis.', *Proceedings of the National Academy of Sciences of the United States of America*, 103(43), pp. 16021–6.

Beller, D. I., Springer, T. A. and Schreiber, R. D. (1982) 'Anti-Mac-1 selectively inhibits the mouse and human type three complement receptor.', *The Journal of experimental medicine*, 156(4), pp. 1000–9.

Bénard, M. *et al.* (2004) 'Characterization of C3a and C5a receptors in rat cerebellar granule neurons during maturation. Neuroprotective effect of C5a against apoptotic cell death.', *The Journal of biological chemistry*, 279(42), pp. 43487–96.

Bennett, M. L. *et al.* (2016) 'New tools for studying microglia in the mouse and human CNS', *Proceedings of the National Academy of Sciences*, 113(12), pp. E1738–E1746.

Benoit, M. E. *et al.* (2013) 'C1q-induced LRP1B and GPR6 Proteins Expressed Early in Alzheimer Disease Mouse Models, Are Essential for the C1q-mediated Protection against Amyloid-β Neurotoxicity', *Journal of Biological Chemistry*, 288(1), pp. 654–665.

Benoit, M. E. and Tenner, A. J. (2011) 'Complement Protein C1q-Mediated Neuroprotection Is Correlated with Regulation of Neuronal Gene and MicroRNA Expression', *Journal of Neuroscience*, 31(9).

Benzing, W. C. *et al.* (1999) 'Evidence for glial-mediated inflammation in aged APP(SW) transgenic mice.', *Neurobiology of aging*, 20(6), pp. 581–9.

Bergamaschini, L. *et al.* (2004) 'Peripheral treatment with enoxaparin, a low molecular weight heparin, reduces plaques and beta-amyloid accumulation in a mouse model of Alzheimer's disease.', *The Journal of neuroscience*, 24(17), pp. 4181–6.

Bernardino, L. *et al.* (2005) 'Modulator Effects of Interleukin-1 and Tumor Necrosis Factor- on AMPA-Induced Excitotoxicity in Mouse Organotypic Hippocampal Slice Cultures', *Journal of Neuroscience*, 25(29), pp. 6734–6744.

Bhattacharjee, S. *et al.* (2016) 'microRNA-34a-Mediated Down-Regulation of the Microglial-Enriched Triggering Receptor and Phagocytosis-Sensor TREM2 in Age-Related Macular Degeneration', *PLOS ONE*, 11(3), p. e0150211.

Bhaya, D., Davison, M. and Barrangou, R. (2011) 'CRISPR-Cas Systems in Bacteria and Archaea: Versatile Small RNAs for Adaptive Defense and Regulation', *Annual Review of Genetics*, 45(1), pp. 273–297.

Bialas, A. R. and Stevens, B. (2013) 'TGF-β signaling regulates neuronal C1q expression and developmental synaptic refinement.', *Nature neuroscience*, 16(12), pp. 1773–82.

Bianchin, M. M. *et al.* (2004) 'Nasu-Hakola disease (polycystic lipomembranous osteodysplasia with sclerosing leukoencephalopathy--PLOSL): a dementia associated with bone cystic lesions. From clinical to genetic and molecular aspects.', *Cellular and molecular neurobiology*, 24(1), pp. 1–24.

Biffi, A. *et al.* (2012) 'Genetic variation at CR1 increases risk of cerebral amyloid angiopathy.', *Neurology*, 78(5), pp. 334–41.

Blasi, E. *et al.* (1990) 'Immortalization of murine microglial cells by a v-raf / v-myc carrying retrovirus', *Journal of Neuroimmunology*, 27(2–3), pp. 229–237.

Bock, V. *et al.* (2013) 'Polycystic Lipomembranous Osteodysplasia with Sclerosing Leukoencephalopathy (PLOSL): a new report of an Italian woman and review of the literature.', *Journal of the neurological sciences*, 326(1–2), pp. 115–9.

Boer, E. F. *et al.* (2015) 'Fascin1-Dependent Filopodia are Required for Directional Migration of a Subset of Neural Crest Cells', *PLOS Genetics*, 11(1), p. e1004946.

Bohlen, C. J. *et al.* (2017) 'Diverse Requirements for Microglial Survival, Specification, and Function Revealed by Defined-Medium Cultures', *Neuron*, 94(4), p. 759–773.e8.

Boocock, C. A. *et al.* (1989) 'Colony-stimulating factor-1 induces rapid behavioural responses in the mouse macrophage cell line, BAC1.2F5', *Journal of Cell Science*, 93(3).

Borroni, B. *et al.* (2014) 'Heterozygous TREM2 mutations in frontotemporal dementia', *Neurobiology of Aging*, 35(4), p. 934.e7-934.e10.

Bouchon, A. *et al.* (2001) 'A Dap12-Mediated Pathway Regulates Expression of Cc Chemokine Receptor 7 and Maturation of Human Dendritic Cells', *Journal of Experimental Medicine*, 194(8).

Braak, H. and Braak, E. (1991) 'Neuropathological stageing of Alzheimer-related changes.', *Acta neuropathologica*, 82(4), pp. 239–59.

Bradford, M. M. (1976) 'A rapid and sensitive method for the quantitation of microgram quantities of protein utilizing the principle of protein-dye binding', *Analytical Biochemistry*, 72(1–2), pp. 248–254.

Brouwers, N. *et al.* (2012) 'Alzheimer risk associated with a copy number variation in the complement receptor 1 increasing C3b/C4b binding sites.', *Molecular psychiatry*, 17(2), pp. 223–33.

Brown, G. C. and Neher, J. J. (2014) 'Microglial phagocytosis of live neurons', *Nature Reviews Neuroscience*, 15(4), pp. 209–216.

Buchrieser, J. *et al.* (2017) 'Human Induced Pluripotent Stem Cell-Derived Macrophages Share Ontogeny with MYB-Independent Tissue-Resident Macrophages', *Stem Cell Reports*, 8(2), pp. 334–345.

Buganim, Y. *et al.* (2012) 'Single-Cell Expression Analyses during Cellular Reprogramming Reveal an Early Stochastic and a Late Hierarchic Phase', *Cell*, 150(6), pp. 1209–1222.

Butovsky, O. *et al.* (2014) 'Identification of a unique TGF-β-dependent molecular and functional signature in microglia.', *Nature neuroscience*, 17(1), pp. 131–43.

Le Cabec, V. *et al.* (2002) 'Complement receptor 3 (CD11b/CD18) mediates type I and type II phagocytosis during nonopsonic and opsonic phagocytosis, respectively.', *Journal of immunology*, 169(4), pp. 2003–9.

Cady, J. *et al.* (2014) 'TREM2 variant p.R47H as a risk factor for sporadic amyotrophic lateral sclerosis.', *JAMA neurology*, 71(4), pp. 449–53.

Cardona, S. M. *et al.* (2015) 'Disruption of Fractalkine Signaling Leads to Microglial Activation and Neuronal Damage in the Diabetic Retina.', *ASN neuro*, 7(5).

Caron, E. and Hall, A. (1998) 'Identification of two distinct mechanisms of phagocytosis controlled by different Rho GTPases.', *Science*, 282(5394), pp. 1717–21.

Carrasquillo, M. M. *et al.* (2010) 'Replication of CLU, CR1, and PICALM Associations With Alzheimer Disease', *Archives of Neurology*, 67(8), pp. 961–4.

Castellano, G. *et al.* (2010) 'Infiltrating dendritic cells contribute to local synthesis of C1q in murine and human lupus nephritis', *Molecular Immunology*, 47(11–12), pp. 2129–2137.

Van Cauwenberghe, C., Van Broeckhoven, C. and Sleegers, K. (2016) 'The genetic landscape of Alzheimer disease: clinical implications and perspectives.', *Genetics in medicine*, 18(5), pp. 421–30.

Chan, G. *et al.* (2015) 'CD33 modulates TREM2: convergence of Alzheimer loci', *Nature Neuroscience*, 18(11), pp. 1556–1558.

Chazotte, B. (2010) 'Labeling Cytoskeletal F-Actin with Rhodamine Phalloidin or Fluorescein Phalloidin for Imaging', *Cold Spring Harbor Protocols*, 2010(5), p. pdb.prot4947-prot4947.

Chen, Q. *et al.* (2013) 'Triggering Receptor Expressed on Myeloid Cells-2 Protects against Polymicrobial Sepsis by Enhancing Bacterial Clearance', *American Journal of Respiratory and Critical Care Medicine*, 188(2), pp. 201–212.

Chhabra, E. S. and Higgs, H. N. (2007) 'The many faces of actin: matching assembly factors with cellular structures', *Nature Cell Biology*, 9(10), pp. 1110–1121.

Chibnik, L. B. *et al.* (2011) 'CR1 is associated with amyloid plaque burden and age-related cognitive decline.', *Annals of neurology*, 69(3), pp. 560–9.

Chinwalla, A. T. *et al.* (2002) 'Initial sequencing and comparative analysis of the mouse genome', *Nature*, 420(6915), pp. 520–562.

Cho, S. W. *et al.* (2014) 'Analysis of off-target effects of CRISPR/Cas-derived RNA-guided endonucleases and nickases.', *Genome research*, 24(1), pp. 132–41.

Choucair-Jaafar, N. *et al.* (2011) 'Complement receptor 3 (CD11b/CD18) is implicated in the elimination of β-amyloid peptides.', *Fundamental & clinical pharmacology*, 25(1), pp. 115–22.

Chu, Y. *et al.* (2010) 'Enhanced synaptic connectivity and epilepsy in C1q knockout mice', *Proceedings of the National Academy of Sciences*, 107(17), pp. 7975–7980.

Citri, A. and Malenka, R. C. (2008) 'Synaptic Plasticity: Multiple Forms, Functions, and Mechanisms', *Neuropsychopharmacology*, 33(1), pp. 18–41.

Collingridge, G. L. and Peineau, S. (2014) 'Strippers reveal their depressing secrets: removing AMPA receptors.', *Neuron*, 82(1), pp. 3–6.

Colonna, M. and Butovsky, O. (2017) 'Microglia Function in the Central Nervous System During Health and Neurodegeneration', *Annual Review of Immunology*, 35(1), pp. 441–468.

Colton, C. A. (2009) 'Heterogeneity of Microglial Activation in the Innate Immune Response in the Brain', *Journal of Neuroimmune Pharmacology*, 4(4), pp. 399–418.

Combs, C. K. *et al.* (2001) 'β-Amyloid Stimulation of Microglia and Monocytes Results in TNFα-Dependent Expression of Inducible Nitric Oxide Synthase and Neuronal Apoptosis', *Journal of Neuroscience*, 21(4).

Cooper, J. A. (1987) 'Effects of cytochalasin and phalloidin on actin.', *The Journal of cell biology*, 105(4), pp. 1473–8.

Corder, E. H. *et al.* (1993) 'Gene dose of apolipoprotein E type 4 allele and the risk of Alzheimer's disease in late onset families.', *Science*, 261(5123), pp. 921–3.

Cox, D. *et al.* (1997) 'Requirements for both Rac1 and Cdc42 in membrane ruffling and phagocytosis in leukocytes.', *The Journal of experimental medicine*, 186(9), pp. 1487–

94.

Crehan, H., Hardy, J. and Pocock, J. (2012) 'Microglia, Alzheimer's disease, and complement', *Int J Alzheimers Dis*, 2012, p. 983640.

Crehan, H., Hardy, J. and Pocock, J. (2013) 'Blockage of CR1 prevents activation of rodent microglia.', *Neurobiology of disease*, 54, pp. 139–49.

Csomor, E. *et al.* (2007) 'Complement protein C1q induces maturation of human dendritic cells', *Molecular Immunology*, 44(13), pp. 3389–3397.

Cunningham, C. L., Martínez-Cerdeño, V. and Noctor, S. C. (2013) 'Microglia Regulate the Number of Neural Precursor Cells in the Developing Cerebral Cortex', *Journal of Neuroscience*, 33(10).

Daneman, R. (2012) 'The blood-brain barrier in health and disease.', *Annals of neurology*, 72(5), pp. 648–72.

Dardiotis, E. *et al.* (2017) 'A novel mutation in TREM2 gene causing Nasu-Hakola disease and review of the literature', *Neurobiology of Aging*, 53, p. 194.e13-194.e22.

Davalos, D. *et al.* (2005) 'ATP mediates rapid microglial response to local brain injury in vivo', *Nature Neuroscience*, 8(6), pp. 752–758.

Davies, A. L. *et al.* (2013) 'Neurological deficits caused by tissue hypoxia in neuroinflammatory disease', *Annals of Neurology*, 74(6), pp. 815–825.

Davis, R. L., Weintraub, H. and Lassar, A. B. (1987) 'Expression of a single transfected cDNA converts fibroblasts to myoblasts.', *Cell*, 51(6), pp. 987–1000.

Davoust, N. *et al.* (1999) 'Expression of the murine complement regulatory protein crry by glial cells and neurons.', *Glia*, 27(2), pp. 162–70.

Daws, M. R. *et al.* (2001) 'Cloning and characterization of a novel mouse myeloid DAP12-associated receptor family.', *European journal of immunology*, 31(3), pp. 783–91.

Daws, M. R. *et al.* (2003) 'Pattern recognition by TREM-2: binding of anionic ligands.', *Journal of immunology*, 171(2), pp. 594–9.

Deane, R. *et al.* (2008) 'apoE isoform–specific disruption of amyloid β peptide clearance from mouse brain', *Journal of Clinical Investigation*, 118(12), pp. 4002–4013.

DeMattos, R. B. *et al.* (2001) 'Peripheral anti-A beta antibody alters CNS and plasma A beta clearance and decreases brain A beta burden in a mouse model of Alzheimer's disease.', *Proceedings of the National Academy of Sciences of the United States of America*, 98(15), pp. 8850–5.

Diamond, M. S. *et al.* (1990) 'ICAM-1 (CD54): a counter-receptor for Mac-1 (CD11b/CD18).', *The Journal of cell biology*, 111(6 Pt 2), pp. 3129–39.

Dietzschold, B. *et al.* (1995) 'Expression of C1q, a subcomponent of the rat complement system, is dramatically enhanced in brains of rats with either Borna disease or experimental allergic encephalomyelitis.', *Journal of the neurological sciences*, 130(1), pp. 11–6.

Dissing-Olesen, L. *et al.* (2014) 'Activation of neuronal NMDA receptors triggers transient ATP-mediated microglial process outgrowth.', *The Journal of neuroscience*, 34(32), pp. 10511–27.

Dunkelberger, J. R. and Song, W. C. (2010) 'Role and mechanism of action of complement in regulating T cell immunity', *Mol Immunol*, 47(13), pp. 2176–2186.

Ehlers, M. R. (2000) 'CR3: a general purpose adhesion-recognition receptor essential for innate immunity.', *Microbes and infection*, 2(3), pp. 289–94.

Eikelenboom, P. *et al.* (2006) 'The significance of neuroinflammation in understanding Alzheimer's disease.', *Journal of neural transmission*, 113(11), pp. 1685–95.

Elliott, M. R. *et al.* (2009) 'Nucleotides released by apoptotic cells act as a find-me signal to promote phagocytic clearance.', *Nature*, 461(7261), pp. 282–6.

Elmore, M. R. P. *et al.* (2014) 'Colony-Stimulating Factor 1 Receptor Signaling Is Necessary for Microglia Viability, Unmasking a Microglia Progenitor Cell in the Adult Brain', *Neuron*, 82(2), pp. 380–397.

Elvington, A. *et al.* (2012) 'The Alternative Complement Pathway Propagates Inflammation and Injury in Murine Ischemic Stroke', *The Journal of Immunology*, 189(9), pp. 4640–4647.

Erbel, C. *et al.* (2013) 'An in vitro model to study heterogeneity of human macrophage differentiation and polarization.', *Journal of visualized experiments : JoVE*, (76), p. e50332.

Erlich, P. *et al.* (2010) 'Complement Protein C1q Forms a Complex with Cytotoxic Prion Protein Oligomers', *Journal of Biological Chemistry*, 285(25), pp. 19267–19276.

Evans, M. J. and Kaufman, M. H. (1981) 'Establishment in culture of pluripotential cells

from mouse embryos.', *Nature*, 292(5819), pp. 154–6.

Fällman, M., Andersson, R. and Andersson, T. (1993) 'Signaling properties of CR3 (CD11b/CD18) and CR1 (CD35) in relation to phagocytosis of complement-opsonized particles.', *Journal of immunology*, 151(1), pp. 330–8.

Fan, R. and Tenner, A. J. (2004) 'Complement C1q expression induced by Abeta in rat hippocampal organotypic slice cultures.', *Experimental neurology*, 185(2), pp. 241–53.

Färber, K. *et al.* (2009) 'C1q, the recognition subcomponent of the classical pathway of complement, drives microglial activation', *Journal of Neuroscience Research*, 87(3), pp. 644–652.

Farfel, J. M. *et al.* (2016) 'Relation of genomic variants for Alzheimer disease dementia to common neuropathologies', *Neurology*, 87(5), pp. 489–496.

Fernández-Santiago, R. and Ezquerra, M. (2016) 'Epigenetic Research of Neurodegenerative Disorders Using Patient iPSC-Based Models.', *Stem cells international*, 2016, p. 9464591.

Fischer, E. *et al.* (1986) 'Characterization of the human glomerular C3 receptor as the C3b/C4b complement type one (CR1) receptor.', *Journal of immunology*, 136(4), pp. 1373–7.

Fleisher-Berkovich, S. *et al.* (2010) 'Distinct modulation of microglial amyloid β phagocytosis and migration by neuropeptides (i).', *Journal of neuroinflammation*, 7(1), p. 61.

Fonseca, M. I. *et al.* (2004) 'Absence of C1q leads to less neuropathology in transgenic mouse models of Alzheimer's disease', *J Neurosci*, 24(29), pp. 6457–6465.

Fonseca, M. I. *et al.* (2016) 'Analysis of the Putative Role of CR1 in Alzheimer's Disease: Genetic Association, Expression and Function.', *PloS one*, 11(2), p. e0149792.

Forabosco, P. *et al.* (2013) 'Insights into TREM2 biology by network analysis of human brain gene expression data.', *Neurobiology of aging*, 34(12), pp. 2699–714.

Fossati-Jimack, L. *et al.* (2013) 'Phagocytosis Is the Main CR3-Mediated Function Affected by the Lupus-Associated Variant of CD11b in Human Myeloid Cells', *PLoS ONE*, 8(2), p. e57082.

Frakes, A. E. *et al.* (2014) 'Microglia induce motor neuron death via the classical NF-κB pathway in amyotrophic lateral sclerosis.', *Neuron*, 81(5), pp. 1009–23.

Franco Bocanegra, D. K., Nicoll, J. A. R. and Boche, D. (2017) 'Innate immunity in Alzheimer's disease: the relevance of animal models?', *Journal of neural transmission*.

Frank, S. *et al.* (2008) 'TREM2 is upregulated in amyloid plaque-associated microglia in aged APP23 transgenic mice.', *Glia*, 56(13), pp. 1438–47.

Fraser, D. A. *et al.* (2006) 'C1q and MBL, components of the innate immune system, influence monocyte cytokine expression.', *Journal of leukocyte biology*, 80(1), pp. 107–16.

Fraser, D. A., Pisalyaput, K. and Tenner, A. J. (2010) 'C1q enhances microglial clearance of apoptotic neurons and neuronal blebs, and modulates subsequent inflammatory cytokine production', *J Neurochem*, 112(3), pp. 733–743.

Fricker, M. *et al.* (2012) 'MFG-E8 Mediates Primary Phagocytosis of Viable Neurons during Neuroinflammation', *Journal of Neuroscience*, 32(8), pp. 2657–2666.

Fu, H. *et al.* (2012) 'Complement component C3 and complement receptor type 3 contribute to the phagocytosis and clearance of fibrillar Aβ by microglia', *Glia*, 60(6), pp. 993–1003.

Fusaki, N. *et al.* (2009) 'Efficient induction of transgene-free human pluripotent stem cells using a vector based on Sendai virus, an RNA virus that does not integrate into the host genome.', *Proceedings of the Japan Academy*, 85(8), pp. 348–62.

Gaboriaud, C. *et al.* (2011) 'The human c1q globular domain: structure and recognition of non-immune self ligands.', *Frontiers in immunology*, 2, p. 92.

Gafencu, A. V *et al.* (2007) 'Inflammatory signaling pathways regulating ApoE gene expression in macrophages.', *The Journal of biological chemistry*, 282(30), pp. 21776–85.

Gardai, S. J. *et al.* (2005) 'Cell-Surface Calreticulin Initiates Clearance of Viable or Apoptotic Cells through trans-Activation of LRP on the Phagocyte', *Cell*, 123(2), pp. 321–334.

Garton, K. J. *et al.* (2001) 'Tumor necrosis factor-alpha-converting enzyme (ADAM17) mediates the cleavage and shedding of fractalkine (CX3CL1).', *The Journal of biological chemistry*, 276(41), pp. 37993–8001.

Gasque, P. *et al.* (1996) 'Identification and characterization of complement C3 receptors on human astrocytes.', *The Journal of Immunology*, 156(6).

Gasque, P., Fontaine, M. and Morgan, B. P. (1995) 'Complement expression in human brain. Biosynthesis of terminal pathway components and regulators in human glial cells

and cell lines.', *Journal of immunology*, 154(9), pp. 4726–33.

Gasque, P. and Morgan, B. P. (1996) 'Complement regulatory protein expression by a human oligodendrocyte cell line: cytokine regulation and comparison with astrocytes', *Immunology*, 89(3), pp. 338–347.

Gatz, M. *et al.* (2006) 'Role of Genes and Environments for Explaining Alzheimer Disease', *Archives of General Psychiatry*, 63(2), p. 168.

Gawish, R. *et al.* (2015) 'Triggering receptor expressed on myeloid cells-2 fine-tunes inflammatory responses in murine Gram-negative sepsis.', *FASEB journal*, 29(4), pp. 1247–57.

Ginhoux, F. *et al.* (2010) 'Fate Mapping Analysis Reveals That Adult Microglia Derive from Primitive Macrophages', *Science*, 330(6005), pp. 841–845.

Ginhoux, F. *et al.* (2013) 'Origin and differentiation of microglia.', *Frontiers in cellular neuroscience*, 7, p. 45.

Giraldo, M. *et al.* (2013) 'Variants in triggering receptor expressed on myeloid cells 2 are associated with both behavioral variant frontotemporal lobar degeneration and Alzheimer's disease.', *Neurobiology of aging*, 34(8), p. 2077.e11-8.

Goate, A. *et al.* (1991) 'Segregation of a missense mutation in the amyloid precursor protein gene with familial Alzheimer's disease', *Nature*, 349(6311), pp. 704–706.

Goldsmith, S. K. *et al.* (1997) 'Kainic acid and decorticating lesions stimulate the synthesis of C1q protein in adult rat brain.', *Journal of neurochemistry*, 68(5), pp. 2046–52.

Gosselin, D. *et al.* (2017) 'An environment-dependent transcriptional network specifies human microglia identity', *Science*, 356(6344), p. eaal3222.

Griciuc, A. *et al.* (2013) 'Alzheimer's disease risk gene CD33 inhibits microglial uptake of amyloid beta.', *Neuron*, 78(4), pp. 631–43.

Griffin, W. S. *et al.* (1989) 'Brain interleukin 1 and S-100 immunoreactivity are elevated in Down syndrome and Alzheimer disease.', *Proceedings of the National Academy of Sciences of the United States of America*, 86(19), pp. 7611–5.

Griffin, W. S. *et al.* (1994) 'Microglial interleukin-1 alpha expression in human head injury: correlations with neuronal and neuritic beta-amyloid precursor protein expression.', *Neuroscience letters*, 176(2), pp. 133–6.

Guadagno, J. *et al.* (2013) 'Microglia-derived TNFα induces apoptosis in neural precursor cells via transcriptional activation of the Bcl-2 family member Puma', *Cell Death and Disease*, 4(3), p. e538.

Guerreiro, R. *et al.* (2013a) 'TREM2 variants in Alzheimer's disease.', *The New England journal of medicine*, 368(2), pp. 117–27.

Guerreiro, R. and Hardy, J. (2014) 'Genetics of Alzheimer's disease.', *Neurotherapeutics*, 11(4), pp. 732–7.

Guerreiro, R. J. *et al.* (2013b) 'Using exome sequencing to reveal mutations in TREM2 presenting as a frontotemporal dementia-like syndrome without bone involvement.', *JAMA neurology*, 70(1), pp. 78–84.

Guerreiro, R. J., Gustafson, D. R. and Hardy, J. (2012) 'The genetic architecture of Alzheimer's disease: beyond APP, PSENs and APOE.', *Neurobiology of aging*, 33(3), pp. 437–56.

Gurdon, J. B. (1962) 'Adult frogs derived from the nuclei of single somatic cells.', *Developmental biology*, 4, pp. 256–73.

Haenseler, W. *et al.* (2017) 'A Highly Efficient Human Pluripotent Stem Cell Microglia Model Displays a Neuronal-Co-culture-Specific Expression Profile and Inflammatory Response.', *Stem cell reports*, 8(6), pp. 1727–1742.

Hamerman, J. A. *et al.* (2006) 'Cutting Edge: Inhibition of TLR and FcR Responses in Macrophages by Triggering Receptor Expressed on Myeloid Cells (TREM)-2 and DAP12', *The Journal of Immunology*, 177(4), pp. 2051–2055.

Hamerman, J. A. *et al.* (2009) 'The expanding roles of ITAM adapters FcRgamma and DAP12 in myeloid cells.', *Immunological reviews*, 232(1), pp. 42–58.

Han, C. *et al.* (2010) 'Integrin CD11b negatively regulates TLR-triggered inflammatory responses by activating Syk and promoting degradation of MyD88 and TRIF via Cbl-b', *Nature Immunology*, 11(8), pp. 734–742.

Hanayama, R. *et al.* (2002) 'Identification of a factor that links apoptotic cells to phagocytes.', *Nature*, 417(6885), pp. 182–7.

Hannum, G. *et al.* (2013) 'Genome-wide Methylation Profiles Reveal Quantitative Views of Human Aging Rates', *Molecular Cell*, 49(2), pp. 359–367.

Hardy, J. A. and Higgins, G. A. (1992) 'Alzheimer's disease: the amyloid cascade hypothesis.', *Science*, 256(5054), pp. 184–5.

Harold, D. *et al.* (2009) 'Genome-wide association study identifies variants at CLU and PICALM associated with Alzheimer's disease', *Nat Genet*, 41(10), pp. 1088–1093.

Haugen, T. S. *et al.* (1998) 'CD14 Expression and Binding of Lipopolysaccharide to Alveolar Macrophages and Monocytes', *Inflammation*, 22(5), pp. 521–532.

Haynes, S. E. *et al.* (2006) 'The P2Y12 receptor regulates microglial activation by extracellular nucleotides.', *Nature neuroscience*, 9(12), pp. 1512–9.

Hazrati, L.-N. *et al.* (2012) 'Genetic association of CR1 with Alzheimer's disease: a tentative disease mechanism.', *Neurobiology of aging*, 33(12), p. 2949.e5-2949.e12.

Heese, K., Hock, C. and Otten, U. (1998) 'Inflammatory signals induce neurotrophin expression in human microglial cells.', *Journal of neurochemistry*, 70(2), pp. 699–707.

Henderson, S. J. *et al.* (2014) 'Sustained peripheral depletion of amyloid-β with a novel form of neprilysin does not affect central levels of amyloid-β.', *Brain,* 137(Pt 2), pp. 553–64.

Heneka, M. T. *et al.* (2015) 'Neuroinflammation in Alzheimer's disease', *The Lancet Neurology*, 14(4), pp. 388–405.

Henn, A. *et al.* (2009) 'The suitability of BV2 cells as alternative model system for primary microglia cultures or for animal experiments examining brain inflammation.', *ALTEX*, 26(2), pp. 83–94.

Heppner, F. L., Ransohoff, R. M. and Becher, B. (2015) 'Immune attack: the role of inflammation in Alzheimer disease', *Nature Reviews Neuroscience*, 16(6), pp. 358–372.

Heslegrave, A. *et al.* (2016) 'Increased cerebrospinal fluid soluble TREM2 concentration in Alzheimer's disease', *Molecular Neurodegeneration*, 11(1), p. 3.

Hickman, S. E., Allison, E. K. and El Khoury, J. (2008) 'Microglial dysfunction and defective beta-amyloid clearance pathways in aging Alzheimer's disease mice.', *The Journal of neuroscience*, 28(33), pp. 8354–60.

Hickman, S. E. and El Khoury, J. (2014) 'TREM2 and the neuroimmunology of Alzheimer's disease.', *Biochemical pharmacology*, 88(4), pp. 495–8.

Hockemeyer, D. and Jaenisch, R. (2016) 'Induced Pluripotent Stem Cells Meet Genome Editing', *Cell Stem Cell*, 18(5), pp. 573–586.

Hoeffel, G. *et al.* (2015) 'C-Myb+ Erythro-Myeloid Progenitor-Derived Fetal Monocytes

Give Rise to Adult Tissue-Resident Macrophages', *Immunity*, 42(4), pp. 665–678.

Hogg, N. *et al.* (1999) 'A novel leukocyte adhesion deficiency caused by expressed but nonfunctional beta2 integrins Mac-1 and LFA-1.', *The Journal of clinical investigation*, 103(1), pp. 97–106.

Holers, V. M. *et al.* (1987) 'Human complement C3b/C4b receptor (CR1) mRNA polymorphism that correlates with the CR1 allelic molecular weight polymorphism.', *Proceedings of the National Academy of Sciences of the United States of America*, 84(8), pp. 2459–63.

Hollingworth, P. *et al.* (2011) 'Common variants at ABCA7, MS4A6A/MS4A4E, EPHA1, CD33 and CD2AP are associated with Alzheimer's disease', *Nat Genet*, 43(5), pp. 429–435.

Honda, S. *et al.* (2001) 'Extracellular ATP or ADP induce chemotaxis of cultured microglia through Gi/o-coupled P2Y receptors.', *The Journal of neuroscience*, 21(6), pp. 1975–82.

Hong, H. S. *et al.* (2003) 'Interferon gamma stimulates beta-secretase expression and sAPPbeta production in astrocytes.', *Biochemical and biophysical research communications*, 307(4), pp. 922–7.

Hong, S. *et al.* (2016) 'Complement and microglia mediate early synapse loss in Alzheimer mouse models', *Science*, 352(6286), pp. 712–716.

Hooks, B. M. and Chen, C. (2006) 'Distinct Roles for Spontaneous and Visual Activity in Remodeling of the Retinogeniculate Synapse', *Neuron*, 52(2), pp. 281–291.

Horvath, R. J. *et al.* (2008) 'Differential migration, LPS-induced cytokine, chemokine, and NO expression in immortalized BV-2 and HAPI cell lines and primary microglial cultures.', *Journal of neurochemistry*, 107(2), pp. 557–69.

Hosokawa, M. *et al.* (2003) 'Expression of complement messenger RNAs and proteins by human oligodendroglial cells', *Glia*, 42(4), pp. 417–423.

Hsieh, C. L. *et al.* (2009) 'A role for TREM2 ligands in the phagocytosis of apoptotic neuronal cells by microglia.', *Journal of neurochemistry*, 109(4), pp. 1144–56.

Hu, N. *et al.* (2014) 'Increased expression of TREM2 in peripheral blood of Alzheimer's disease patients.', *Journal of Alzheimer's disease*, 38(3), pp. 497–501.

Huang, J. *et al.* (1999) 'Neuronal protection in stroke by an sLex-glycosylated complement inhibitory protein.', *Science*, 285(5427), pp. 595–9.

Huang, K.-L. *et al.* (2017) ‘A common haplotype lowers PU.1 expression in myeloid cells and delays onset of Alzheimer’s disease.’, *Nature neuroscience*.

Huang, Y. (2006) ‘Molecular and cellular mechanisms of apolipoprotein E4 neurotoxicity and potential therapeutic strategies.’, *Current opinion in drug discovery & development*, 9(5), pp. 627–41.

Huang, Y. and Mucke, L. (2012) ‘Alzheimer mechanisms and therapeutic strategies.’, *Cell*, 148(6), pp. 1204–22.

Humphrey, M. B. *et al.* (2006) ‘TREM2, a DAP12-associated receptor, regulates osteoclast differentiation and function.’, *Journal of bone and mineral research*, 21(2), pp. 237–45.

Imai, Y. and Kohsaka, S. (2002) ‘Intracellular signaling in M-CSF-induced microglia activation: Role of Iba1’, *Glia*, 40(2), pp. 164–174.

Imbimbo, B. P. (2009) ‘An update on the efficacy of non-steroidal anti-inflammatory drugs in Alzheimer’s disease.’, *Expert opinion on investigational drugs*, 18(8), pp. 1147–68.

Ito, H. and Hamerman, J. A. (2012) ‘TREM-2, triggering receptor expressed on myeloid cell-2, negatively regulates TLR responses in dendritic cells.’, *European journal of immunology*, 42(1), pp. 176–85.

Jacobson, A. C. and Weis, J. H. (2008) ‘Comparative functional evolution of human and mouse CR1 and CR2.’, *Journal of immunology*, 181(5), pp. 2953–9.

Jauneau, A. *et al.* (2006) ‘Interleukin-1beta and anaphylatoxins exert a synergistic effect on NGF expression by astrocytes.’, *Journal of neuroinflammation*, 3(1), p. 8.

Jay, T. R. *et al.* (2015) ‘TREM2 deficiency eliminates TREM2+ inflammatory macrophages and ameliorates pathology in Alzheimer’s disease mouse models’, *Journal of Experimental Medicine*, 212(3), pp. 287–95.

Jay, T. R. *et al.* (2017a) ‘Disease Progression-Dependent Effects of TREM2 Deficiency in a Mouse Model of Alzheimer’s Disease’, *The Journal of Neuroscience*, 37(3), pp. 637–647.

Jay, T. R., von Saucken, V. E. and Landreth, G. E. (2017b) ‘TREM2 in Neurodegenerative Diseases’, *Molecular Neurodegeneration*, 12(1), p. 56.

Jendresen, C. *et al.* (2017) ‘The Alzheimer’s disease risk factors apolipoprotein E and TREM2 are linked in a receptor signaling pathway.’, *Journal of neuroinflammation*, 14(1), p. 59.

Jiang, H. *et al.* (1994) ‘beta-Amyloid activates complement by binding to a specific region of the collagen-like domain of the C1q A chain.’, *Journal of immunology*, 152(10), pp. 5050–9.

Jiang, T. *et al.* (2013) ‘Epidemiology and etiology of Alzheimer’s disease: from genetic to non-genetic factors.’, *Current Alzheimer research*, 10(8), pp. 852–67.

Jiang, T., Yu, J.-T., *et al.* (2014a) ‘Triggering receptor expressed on myeloid cells 2 knockdown exacerbates aging-related neuroinflammation and cognitive deficiency in senescence-accelerated mouse prone 8 mice.’, *Neurobiology of aging*, 35(6), pp. 1243–51.

Jiang, T., Tan, L., *et al.* (2014b) ‘Upregulation of TREM2 Ameliorates Neuropathology and Rescues Spatial Cognitive Impairment in a Transgenic Mouse Model of Alzheimer’s Disease’, *Neuropsychopharmacology*, 39(13), pp. 2949–2962.

Jiang, T. *et al.* (2015) ‘Silencing of TREM2 exacerbates tau pathology, neurodegenerative changes, and spatial learning deficits in P301S tau transgenic mice’, *Neurobiology of Aging*, 36(12), pp. 3176–3186.

Jiang, T., Tan, L., *et al.* (2016a) ‘A rare coding variant in TREM2 increases risk for Alzheimer’s disease in Han Chinese’, *Neurobiology of Aging*, 42, p. 217.e1-217.e3.

Jiang, T., Zhang, Y.-D., *et al.* (2016b) ‘TREM2 modifies microglial phenotype and provides neuroprotection in P301S tau transgenic mice.’, *Neuropharmacology*, 105, pp. 196–206.

Jin, S. C. *et al.* (2014) ‘Coding variants in TREM2 increase risk for Alzheimer’s disease.’, *Human molecular genetics*, 23(21), pp. 5838–46.

Jin, S. C. *et al.* (2015) ‘TREM2 is associated with increased risk for Alzheimer’s disease in African Americans’, *Molecular Neurodegeneration*, 10(1), p. 19.

Jinek, M. *et al.* (2012) ‘A Programmable Dual-RNA–Guided DNA Endonuclease in Adaptive Bacterial Immunity’, *Science*, 337(6096).

Jongstra-Bilen, J., Harrison, R. and Grinstein, S. (2003) ‘Fcgamma-receptors induce Mac-1 (CD11b/CD18) mobilization and accumulation in the phagocytic cup for optimal phagocytosis.’, *The Journal of biological chemistry*, 278(46), pp. 45720–9.

Jonsson, T. *et al.* (2013) ‘Variant of TREM2 associated with the risk of Alzheimer’s disease.’, *The New England journal of medicine*, 368(2), pp. 107–16.

Jun, G. *et al.* (2010) ‘Meta-analysis confirms CR1, CLU, and PICALM as alzheimer disease risk loci and reveals interactions with APOE genotypes.’, *Archives of*

neurology. American Medical Association, 67(12), pp. 1473–84.

Jung, S. *et al.* (2000) 'Analysis of fractalkine receptor CX(3)CR1 function by targeted deletion and green fluorescent protein reporter gene insertion.', *Molecular and cellular biology*, 20(11), pp. 4106–14.

Kanazawa, H. *et al.* (2002) 'Macrophage/microglia-specific protein Iba1 enhances membrane ruffling and Rac activation via phospholipase C-gamma -dependent pathway.', *The Journal of biological chemistry*, 277(22), pp. 20026–32.

Katz, L. C. and Shatz, C. J. (1996) 'Synaptic activity and the construction of cortical circuits.', *Science (New York, N.Y.)*, 274(5290), pp. 1133–8.

Kawabori, M. *et al.* (2015) 'Triggering receptor expressed on myeloid cells 2 (TREM2) deficiency attenuates phagocytic activities of microglia and exacerbates ischemic damage in experimental stroke.', *The Journal of neuroscience*, 35(8), pp. 3384–96.

Khera, R. and Das, N. (2009) 'Complement Receptor 1: disease associations and therapeutic implications.', *Molecular immunology*, 46(5), pp. 761–72.

El Khoury, J. *et al.* (2007) 'Ccr2 deficiency impairs microglial accumulation and accelerates progression of Alzheimer-like disease.', *Nature medicine*, 13(4), pp. 432–8.

Kichev, A. *et al.* (2017) 'Implicating Receptor Activator of NF-kB (RANK)/RANK Ligand Signalling in Microglial Responses to Toll-Like Receptor Stimuli', *Developmental Neuroscience*, 39(1–4), pp. 192–206.

Kikuchi, T. *et al.* (2017) 'Human iPS cell-derived dopaminergic neurons function in a primate Parkinson's disease model.', *Nature*, 548(7669), pp. 592–596.

Kim, D. *et al.* (2009a) 'Generation of Human Induced Pluripotent Stem Cells by Direct Delivery of Reprogramming Proteins', *Cell Stem Cell*, 4(6), pp. 472–476.

Kim, J., Basak, J. M. and Holtzman, D. M. (2009b) 'The Role of Apolipoprotein E in Alzheimer's Disease', *Neuron*, 63(3), pp. 287–303.

Kim, K. *et al.* (2010) 'Epigenetic memory in induced pluripotent stem cells.', *Nature*. NIH Public Access, 467(7313), pp. 285–90.

Kim, S., Elkon, K. B. and Ma, X. (2004) 'Transcriptional Suppression of Interleukin-12 Gene Expression following Phagocytosis of Apoptotic Cells', *Immunity*, 21(5), pp. 643–653.

Kim, Y. U. *et al.* (1995) 'Mouse complement regulatory protein Crry/p65 uses the

specific mechanisms of both human decay-accelerating factor and membrane cofactor protein.', *The Journal of experimental medicine*, 181(1), pp. 151–9.

Kinashi, T. (2005) 'Intracellular signalling controlling integrin activation in lymphocytes.', *Nature reviews. Immunology*, 5(7), pp. 546–59.

Kishore, U. and Reid, K. B. . (2000) 'C1q: Structure, function, and receptors', *Immunopharmacology*, 49(1–2), pp. 159–170.

Kleinberger, G. *et al.* (2014) 'TREM2 mutations implicated in neurodegeneration impair cell surface transport and phagocytosis.', *Science translational medicine*, 6(243), p. 243ra86.

Kleinberger, G. *et al.* (2017) 'The FTD-like syndrome causing TREM2 T66M mutation impairs microglia function, brain perfusion, and glucose metabolism', *The EMBO Journal*, p. e201796516.

Kober, D. L. *et al.* (2016) 'Neurodegenerative disease mutations in TREM2 reveal a functional surface and distinct loss-of-function mechanisms.', *eLife*, 5.

Kok, E. H. *et al.* (2011) 'CLU, CR1 and PICALM genes associate with Alzheimer's-related senile plaques.', *Alzheimer's research & therapy*, 3(2), p. 12.

Kopec, K. K. and Carroll, R. T. (1998) 'Alzheimer's beta-amyloid peptide 1-42 induces a phagocytic response in murine microglia.', *Journal of neurochemistry*, 71(5), pp. 2123–31.

Korvatska, O. *et al.* (2015) 'R47H Variant of TREM2 Associated With Alzheimer Disease in a Large Late-Onset Family: Clinical, Genetic, and Neuropathological Study.', *JAMA neurology*, 72(8), pp. 920–7.

Kotter, M. R. *et al.* (2005) 'Macrophage-depletion induced impairment of experimental CNS remyelination is associated with a reduced oligodendrocyte progenitor cell response and altered growth factor expression', *Neurobiology of Disease*, 18(1), pp. 166–175.

Krauss, J. C. *et al.* (1994) 'Reconstitution of antibody-dependent phagocytosis in fibroblasts expressing Fc gamma receptor IIIB and the complement receptor type 3.', *Journal of immunology*, 153(4), pp. 1769–77.

Kress, H. *et al.* (2007) 'Filopodia act as phagocytic tentacles and pull with discrete steps and a load-dependent velocity', *Proceedings of the National Academy of Sciences*, 104(28), pp. 11633–11638.

de la Rosa, E. J. and de Pablo, F. (2000) 'Cell death in early neural development:

beyond the neurotrophic theory.', *Trends in neurosciences*, 23(10), pp. 454–8.

LaFerla, F. M. and Green, K. N. (2012) 'Animal models of Alzheimer disease.', *Cold Spring Harbor perspectives in medicine*, 2(11).

Lambert, J. C. *et al.* (2009) 'Genome-wide association study identifies variants at CLU and CR1 associated with Alzheimer's disease', *Nat Genet*, 41(10), pp. 1094–1099.

Lambert, J. C. *et al.* (2013) 'Meta-analysis of 74,046 individuals identifies 11 new susceptibility loci for Alzheimer's disease.', *Nature genetics*, 45(12), pp. 1452–8.

Larson, R. S. and Springer, T. A. (1990) 'Structure and function of leukocyte integrins.', *Immunological reviews*, 114, pp. 181–217.

Lawson, L. J. *et al.* (1990) 'Heterogeneity in the distribution and morphology of microglia in the normal adult mouse brain.', *Neuroscience*, 39(1), pp. 151–70.

Lee, C. Y. D. and Landreth, G. E. (2010) 'The role of microglia in amyloid clearance from the AD brain.', *Journal of neural transmission*, 117(8), pp. 949–60.

Lee, H., Whitfeld, P. L. and Mackay, C. R. (2008) 'Receptors for complement C5a. The importance of C5aR and the enigmatic role of C5L2.', *Immunology and cell biology*, 86(2), pp. 153–60.

Lee, S.-H. *et al.* (2012) 'β-arrestin 2-dependent activation of ERK1/2 is required for ADP-induced paxillin phosphorylation at Ser83 and microglia chemotaxis', *Glia*, 60(9), pp. 1366–1377.

Lehnardt, S. (2010) 'Innate immunity and neuroinflammation in the CNS: the role of microglia in Toll-like receptor-mediated neuronal injury.', *Glia*, 58(3), pp. 253–63.

Leijnse, N., Oddershede, L. B. and Bendix, P. M. (2015) 'An updated look at actin dynamics in filopodia', *Cytoskeleton*, 72(2), pp. 71–79.

Lemke, G. (2013) 'Biology of the TAM receptors.', *Cold Spring Harbor perspectives in biology*. Cold Spring Harbor Laboratory Press, 5(11), p. a009076.

Li, H. *et al.* (2009) 'The Ink4/Arf locus is a barrier for iPS cell reprogramming.', *Nature*, 460(7259), pp. 1136–9.

Liang, K. J. *et al.* (2009) 'Regulation of Dynamic Behavior of Retinal Microglia by CX3CR1 Signaling', *Investigative Opthalmology & Visual Science*, 50(9), p. 4444.

Liao, Y.-F. *et al.* (2004) 'Tumor necrosis factor-alpha, interleukin-1beta, and interferon-gamma stimulate gamma-secretase-mediated cleavage of amyloid precursor protein through a JNK-dependent MAPK pathway.', *The Journal of biological chemistry*, 279(47), pp. 49523–32.

Limb, G. A. *et al.* (1991) 'Selective up-regulation of human granulocyte integrins and complement receptor 1 by cytokines.', *Immunology*, 74(4), pp. 696–702.

Lu, H. *et al.* (1997) 'LFA-1 is sufficient in mediating neutrophil emigration in Mac-1-deficient mice.', *Journal of Clinical Investigation*, 99(6), pp. 1340–1350.

Lu, Y., Liu, W. and Wang, X. (2015) 'TREM2 variants and risk of Alzheimer's disease: a meta-analysis.', *Neurological sciences*, 36(10), pp. 1881–8.

Lue, L.-F. *et al.* (2015) 'TREM2 Protein Expression Changes Correlate with Alzheimer's Disease Neurodegenerative Pathologies in Post-Mortem Temporal Cortices.', *Brain pathology*, 25(4), pp. 469–80.

Lue, L. F. *et al.* (2001) 'Inflammatory repertoire of Alzheimer's disease and nondemented elderly microglia in vitro.', *Glia*, 35(1), pp. 72–9.

Ma, X.-Y. *et al.* (2014) 'Missense variants in CR1 are associated with increased risk of Alzheimer' disease in Han Chinese.', *Neurobiology of aging*, 35(2), p. 443.e17-21.

Mack, C. L. *et al.* (2003) 'Microglia are activated to become competent antigen presenting and effector cells in the inflammatory environment of the Theiler's virus model of multiple sclerosis.', *Journal of neuroimmunology*, 144(1–2), pp. 68–79.

MacPherson, M. *et al.* (2011) 'A systemic lupus erythematosus-associated R77H substitution in the CD11b chain of the Mac-1 integrin compromises leukocyte adhesion and phagocytosis.', *The Journal of biological chemistry*, 286(19), pp. 17303–10.

Maffei, A. *et al.* (2006) 'Potentiation of cortical inhibition by visual deprivation', *Nature*, 443(7107), pp. 81–84.

Magnus, T. *et al.* (2001) 'Microglial phagocytosis of apoptotic inflammatory T cells leads to down-regulation of microglial immune activation.', *Journal of immunology*, 167(9), pp. 5004–10.

Maherali, N. *et al.* (2008) 'A High-Efficiency System for the Generation and Study of Human Induced Pluripotent Stem Cells', *Cell Stem Cell*, 3(3), pp. 340–345.

Mahmoudi, R. *et al.* (2015) 'Alzheimer's disease is associated with low density of the long CR1 isoform.', *Neurobiology of aging*, 36(4), p. 1766.e5-1766.e12.

Mahmoudi, S. and Brunet, A. (2012) 'Aging and reprogramming: a two-way street', *Current Opinion in Cell Biology*, 24(6), pp. 744–756.

Maier, M. *et al.* (2008) 'Complement C3 deficiency leads to accelerated amyloid beta plaque deposition and neurodegeneration and modulation of the microglia/macrophage phenotype in amyloid precursor protein transgenic mice', *J Neurosci*, 28(25), pp. 6333–6341.

Malik, M. *et al.* (2013) 'CD33 Alzheimer's risk-altering polymorphism, CD33 expression, and exon 2 splicing.', *The Journal of neuroscience*, 33(33), pp. 13320–5.

Malone, K. E. *et al.* (2008) 'Induction of class I antigen processing components in oligodendroglia and microglia during viral encephalomyelitis.', *Glia*, 56(4), pp. 426–35.

Marín-Teva, J. L. *et al.* (2004) 'Microglia promote the death of developing Purkinje cells.', *Neuron*, 41(4), pp. 535–47.

Marth, T. and Kelsall, B. L. (1997) 'Regulation of interleukin-12 by complement receptor 3 signaling.', *The Journal of experimental medicine*, 185(11), pp. 1987–95.

Martin, G. R. (1981) 'Isolation of a pluripotent cell line from early mouse embryos cultured in medium conditioned by teratocarcinoma stem cells.', *Proceedings of the National Academy of Sciences of the United States of America*, 78(12), pp. 7634–8.

Martinez, F. O. and Gordon, S. (2014) 'The M1 and M2 paradigm of macrophage activation: time for reassessment', *F1000Prime Reports*, 6, p. 13.

Mason, J. L. *et al.* (2001) 'Interleukin-1beta promotes repair of the CNS.', *The Journal of neuroscience*, 21(18), pp. 7046–52.

Masuch, A. *et al.* (2016) 'Mechanism of microglia neuroprotection: Involvement of P2X7, TNFα, and valproic acid', *Glia*, 64(1), pp. 76–89.

Matarin, M. *et al.* (2015) 'A Genome-wide Gene-Expression Analysis and Database in Transgenic Mice during Development of Amyloid or Tau Pathology', *Cell Reports*, 10(4), pp. 633–44.

Matsuno, R. *et al.* (1998) 'Contribution of CR3 to nitric oxide production from macrophages stimulated with high-dose of LPS.', *Biochemical and biophysical research communications*, 244(1), pp. 115–9.

May, R. C. *et al.* (2000) 'Involvement of the Arp2/3 complex in phagocytosis mediated by FcgammaR or CR3.', *Nature Cell Biology*, 2(4), pp. 246–248.

Mazaheri, F. *et al.* (2014) 'Distinct roles for BAI1 and TIM-4 in the engulfment of dying neurons by microglia.', *Nature communications*, 5, p. 4046.

Mazaheri, F. *et al.* (2017) 'TREM2 deficiency impairs chemotaxis and microglial responses to neuronal injury', *EMBO reports*, p. e201743922.

McKercher, S. R. *et al.* (1996) 'Targeted disruption of the PU.1 gene results in multiple hematopoietic abnormalities.', *The EMBO journal*, 15(20), pp. 5647–58.

McVicar, D. W. and Trinchieri, G. (2009) 'CSF-1R, DAP12 and β-catenin: a ménage à trois', *Nature Immunology*, 10(7), pp. 681–683.

Meda, L. *et al.* (1999) 'Proinflammatory profile of cytokine production by human monocytes and murine microglia stimulated with beta-amyloid[25-35].', *Journal of neuroimmunology*, 93(1–2), pp. 45–52.

Melchior, B. *et al.* (2010) 'Dual induction of TREM2 and tolerance-related transcript, Tmem176b, in amyloid transgenic mice: implications for vaccine-based therapies for Alzheimer's disease.', *ASN neuro*, 2(3), p. e00037.

Menasria, R. *et al.* (2015) 'Infiltration Pattern of Blood Monocytes into the Central Nervous System during Experimental Herpes Simplex Virus Encephalitis', *PLOS ONE*, 10(12), p. e0145773.

Mevorach, D. *et al.* (1998) 'Complement-dependent clearance of apoptotic cells by human macrophages.', *The Journal of experimental medicine*, 188(12), pp. 2313–20.

Meyen, D. *et al.* (2015) 'Dynamic filopodia are required for chemokine-dependent intracellular polarization during guided cell migration in vivo.', *eLife*, 4.

Michailidou, I. *et al.* (2015) 'Complement C1q-C3-associated synaptic changes in multiple sclerosis hippocampus', *Annals of Neurology*, 77(6), pp. 1007–1026.

Michaud, J.-P. *et al.* (2013) 'Real-Time In Vivo Imaging Reveals the Ability of Monocytes to Clear Vascular Amyloid Beta', *Cell Reports*, 5(3), pp. 646–653.

Mildner, A. *et al.* (2007) 'Microglia in the adult brain arise from Ly-6ChiCCR2+ monocytes only under defined host conditions', *Nature Neuroscience*, 10(12), pp. 1544–1553.

Miller, J. A., Horvath, S. and Geschwind, D. H. (2010) 'Divergence of human and mouse brain transcriptome highlights Alzheimer disease pathways', *Proceedings of the National Academy of Sciences*, 107(28), pp. 12698–12703.

Mills, C. D. *et al.* (2000) 'M-1/M-2 macrophages and the Th1/Th2 paradigm.', *Journal of immunology*, 164(12), pp. 6166–73.

Mirra, S. S. *et al.* (1991) 'The Consortium to Establish a Registry for Alzheimer's Disease (CERAD). Part II. Standardization of the neuropathologic assessment of Alzheimer's disease.', *Neurology*, 41(4), pp. 479–86.

Miwa, T. and Song, W.-C. C. (2001) 'Membrane complement regulatory proteins: insight from animal studies and relevance to human diseases.', *International immunopharmacology*, 1(3), pp. 445–459.

Mocco, J. *et al.* (2006) 'Complement component C3 mediates inflammatory injury following focal cerebral ischemia.', *Circulation research*, 99(2), pp. 209–17.

Molina, H. *et al.* (1992) 'Distinct receptor and regulatory properties of recombinant mouse complement receptor 1 (CR1) and Crry, the two genetic homologues of human CR1.', *The Journal of experimental medicine*, 175(1), pp. 121–9.

Montine, T. J. *et al.* (2012) 'National Institute on Aging–Alzheimer's Association guidelines for the neuropathologic assessment of Alzheimer's disease: a practical approach', *Acta Neuropathologica*, 123(1), pp. 1–11.

Moore, C. S. *et al.* (2015) 'P2Y12 expression and function in alternatively activated human microglia', *Neurology: Neuroimmunology & Neuroinflammation*, 2(2), pp. e80–e80.

Mrak, R. E. (2012) 'Microglia in Alzheimer brain: a neuropathological perspective.', *International journal of Alzheimer's disease*, 2012, p. 165021.

Muffat, J. *et al.* (2016) 'Efficient derivation of microglia-like cells from human pluripotent stem cells.', *Nature medicine*, 22(11), pp. 1358–1367.

Mukherjee, P., Thomas, S. and Pasinetti, G. M. (2008) 'Complement anaphylatoxin C5a neuroprotects through regulation of glutamate receptor subunit 2 in vitro and in vivo.', *Journal of neuroinflammation*, 5(1), p. 5.

N'Diaye, E.-N. *et al.* (2009) 'TREM-2 (triggering receptor expressed on myeloid cells 2) is a phagocytic receptor for bacteria.', *The Journal of cell biology*, 184(2), pp. 215–23.

Nagai, A. *et al.* (2001) 'Generation and characterization of immortalized human microglial cell lines: expression of cytokines and chemokines.', *Neurobiology of disease*, 8(6), pp. 1057–68.

Naj, A. C. *et al.* (2011) 'Common variants at MS4A4/MS4A6E, CD2AP, CD33 and EPHA1 are associated with late-onset Alzheimer's disease', *Nat Genet*, 43(5), pp. 436–

441.

Nakajima, K. *et al.* (2001) 'Ability of rat microglia to uptake extracellular glutamate.', *Neuroscience letters*, 307(3), pp. 171–4.

Nauseef, W. M. (2007) 'Isolation of Human Neutrophils From Venous Blood', in *Neutrophil Methods and Protocols*, pp. 15–20.

Neher, J. J. *et al.* (2011) 'Inhibition of Microglial Phagocytosis Is Sufficient To Prevent Inflammatory Neuronal Death', *The Journal of Immunology*, 186(8), pp. 4973–4983.

Neniskyte, U., Neher, J. J. and Brown, G. C. (2011) 'Neuronal death induced by nanomolar amyloid β is mediated by primary phagocytosis of neurons by microglia.', *The Journal of biological chemistry*, 286(46), pp. 39904–13.

Neumann, H., Kotter, M. R. and Franklin, R. J. M. (2009) 'Debris clearance by microglia: an essential link between degeneration and regeneration.', *Brain*, 132(Pt 2), pp. 288–95.

Niculescu, T. *et al.* (2004) 'Effects of complement C5 on apoptosis in experimental autoimmune encephalomyelitis.', *Journal of immunology*, 172(9), pp. 5702–6.

Niedergang, F. and Chavrier, P. (2004) 'Signaling and membrane dynamics during phagocytosis: Many roads lead to the phagos(R)ome', *Current Opinion in Cell Biology*, pp. 422–428.

Nimmerjahn, A., Kirchhoff, F. and Helmchen, F. (2005) 'Resting microglial cells are highly dynamic surveillants of brain parenchyma in vivo.', *Science*, 308(5726), pp. 1314–8.

Nobes, C. D. and Hall, A. (1995) 'Rho, rac, and cdc42 GTPases regulate the assembly of multimolecular focal complexes associated with actin stress fibers, lamellipodia, and filopodia.', *Cell*, 81(1), pp. 53–62.

O'Barr, S. A. *et al.* (2001) 'Neuronal Expression of a Functional Receptor for the C5a Complement Activation Fragment', *The Journal of Immunology*, 166(6), pp. 4154–4162.

Ohradanova-Repic, A. *et al.* (2016) 'Differentiation of human monocytes and derived subsets of macrophages and dendritic cells by the HLDA10 monoclonal antibody panel', *Clinical & Translational Immunology*, 5(1), p. e55.

Ohsawa, K. *et al.* (2000) 'Involvement of Iba1 in membrane ruffling and phagocytosis of macrophages/microglia.', *Journal of cell science*, pp. 3073–84.

Oppenheim, R. W. (1991) 'Cell Death During Development of the Nervous System', *Annual Review of Neuroscience*, 14(1), pp. 453–501.

Osaka, H. *et al.* (1999) 'Complement-derived anaphylatoxin C5a protects against glutamate-mediated neurotoxicity.', *Journal of cellular biochemistry*, 73(3), pp. 303–11.

Osenkowski, P. *et al.* (2008) 'Direct and Potent Regulation of γ-Secretase by Its Lipid Microenvironment', *Journal of Biological Chemistry*, 283(33), pp. 22529–22540.

Otero, K. *et al.* (2009) 'Macrophage colony-stimulating factor induces the proliferation and survival of macrophages via a pathway involving DAP12 and beta-catenin.', *Nature immunology*, 10(7), pp. 734–43.

Otero, K. *et al.* (2012) 'TREM2 and β-catenin regulate bone homeostasis by controlling the rate of osteoclastogenesis.', *Journal of immunology*, 188(6), pp. 2612–21.

Ousman, S. S. and Kubes, P. (2012) 'Immune surveillance in the central nervous system.', *Nature neuroscience*, 15(8), pp. 1096–101.

Owens, R. *et al.* (2017) 'Divergent Neuroinflammatory Regulation of Microglial TREM Expression and Involvement of NF-κB', *Frontiers in Cellular Neuroscience*, 11, p. 56.

Païdassi, H. *et al.* (2008) 'C1q binds phosphatidylserine and likely acts as a multiligand-bridging molecule in apoptotic cell recognition.', *Journal of immunology*, 180(4), pp. 2329–38.

Pakkenberg, B. and Gundersen, H. J. (1997) 'Neocortical neuron number in humans: effect of sex and age.', *The Journal of comparative neurology*, 384(2), pp. 312–20.

Paloneva, J. *et al.* (2001) 'CNS manifestations of Nasu-Hakola disease: a frontal dementia with bone cysts.', *Neurology*, 56(11), pp. 1552–8.

Paloneva, J. *et al.* (2002) 'Mutations in Two Genes Encoding Different Subunits of a Receptor Signaling Complex Result in an Identical Disease Phenotype', *The American Journal of Human Genetics*, 71(3), pp. 656–662.

Paloneva, J. *et al.* (2003) 'DAP12/TREM2 deficiency results in impaired osteoclast differentiation and osteoporotic features.', *The Journal of experimental medicine*, 198(4), pp. 669–75.

Panaretakis, T. *et al.* (2009) 'Mechanisms of pre-apoptotic calreticulin exposure in immunogenic cell death.', *The EMBO journal*, 28(5), pp. 578–90.

Paolicelli, R. C. *et al.* (2011) 'Synaptic pruning by microglia is necessary for normal

brain development.', *Science*, 333(6048), pp. 1456–8.

Park, J.-S. *et al.* (2015a) 'Disease-Associated Mutations of TREM2 Alter the Processing of N-Linked Oligosaccharides in the Golgi Apparatus', *Traffic*, 16(5), pp. 510–518.

Park, M. *et al.* (2015b) 'Triggering receptor expressed on myeloid cells 2 (TREM2) promotes adipogenesis and diet-induced obesity.', *Diabetes*, 64(1), pp. 117–27.

Parkhurst, C. N. *et al.* (2013) 'Microglia Promote Learning-Dependent Synapse Formation through Brain-Derived Neurotrophic Factor', *Cell*, 155(7), pp. 1596–1609.

Patel, N. S. *et al.* (2005) 'Inflammatory cytokine levels correlate with amyloid load in transgenic mouse models of Alzheimer's disease.', *Journal of neuroinflammation*, 2(1), p. 9.

Peng, Q. *et al.* (2010) 'TREM2- and DAP12-Dependent Activation of PI3K Requires DAP10 and Is Inhibited by SHIP1', *Science Signaling*, 3(122), p. ra38-ra38.

Peng, Q. *et al.* (2013) 'A Physical Interaction Between the Adaptor Proteins DOK3 and DAP12 Is Required to Inhibit Lipopolysaccharide Signaling in Macrophages', *Science Signaling*, 6(289), p. ra72-ra72.

Perez, S. E. *et al.* (2017) 'Neocortical and hippocampal TREM2 protein levels during the progression of Alzheimer's disease.', *Neurobiology of aging*, 54, pp. 133–143.

Persson, M. *et al.* (2009) 'The complement-derived anaphylatoxin C5a increases microglial GLT-1 expression and glutamate uptake in a TNF-alpha-independent manner', *Eur J Neurosci*, 29(2), pp. 267–274.

Phillipson, M. *et al.* (2006) 'Intraluminal crawling of neutrophils to emigration sites: a molecularly distinct process from adhesion in the recruitment cascade', *Journal of Experimental Medicine*, 203(12).

Piccio, L. *et al.* (2016) 'Cerebrospinal fluid soluble TREM2 is higher in Alzheimer disease and associated with mutation status', *Acta Neuropathologica*, 131(6), pp. 925–933.

Pickering, M., Cumiskey, D. and O'Connor, J. J. (2005) 'Actions of TNF-α on glutamatergic synaptic transmission in the central nervous system', *Experimental Physiology*, 90(5), pp. 663–670.

Pisalyaput, K. and Tenner, A. J. (2008) 'Complement component C1q inhibits beta-amyloid- and serum amyloid P-induced neurotoxicity via caspase- and calpain-independent mechanisms.', *Journal of neurochemistry*, 104(3), pp. 696–707.

Pocock, J. M. and Kettenmann, H. (2007) 'Neurotransmitter receptors on microglia', *Trends in Neurosciences*, 30(10), pp. 527–535.

Poliani, P. L. *et al.* (2015) 'TREM2 sustains microglial expansion during aging and response to demyelination.', *The Journal of clinical investigation*, 125(5), pp. 2161–70.

Pollard, T. D. and Borisy, G. G. (2003) 'Cellular motility driven by assembly and disassembly of actin filaments.', *Cell*, 112(4), pp. 453–65.

Prada, I. *et al.* (2006) 'Triggering receptor expressed in myeloid cells 2 (TREM2) trafficking in microglial cells: continuous shuttling to and from the plasma membrane regulated by cell stimulation.', *Neuroscience*, 140(4), pp. 1139–48.

Priller, J. *et al.* (2001) 'Targeting gene-modified hematopoietic cells to the central nervous system: use of green fluorescent protein uncovers microglial engraftment.', *Nature Medicine*, 7(12), pp. 1356–1361.

Qi, X. *et al.* (2004) 'BMP4 supports self-renewal of embryonic stem cells by inhibiting mitogen-activated protein kinase pathways.', *Proceedings of the National Academy of Sciences of the United States of America*, 101(16), pp. 6027–32.

Racoosin, E. L. and Swanson, J. A. (1989) 'Macrophage colony-stimulating factor (rM-CSF) stimulates pinocytosis in bone marrow-derived macrophages.', *The Journal of experimental medicine*, 170(5), pp. 1635–48.

Rademakers, R. *et al.* (2011) 'Mutations in the colony stimulating factor 1 receptor (CSF1R) gene cause hereditary diffuse leukoencephalopathy with spheroids', *Nature Genetics*, 44(2), pp. 200–205.

Raha, A. A. *et al.* (2017) 'Neuroprotective Effect of TREM-2 in Aging and Alzheimer's Disease Model.', *Journal of Alzheimer's disease*, 55(1), pp. 199–217.

Rahpeymai, Y. *et al.* (2006) 'Complement: a novel factor in basal and ischemia-induced neurogenesis', *EMBO J*, 25(6), pp. 1364–1374.

Rajagopalan, P., Hibar, D. and Thompson, P. (2013) 'TREM2 and Neurodegenerative Disease', *New England Journal of Medicine*, 369(16), pp. 1564–1570.

Ramaglia, V. *et al.* (2012) 'C3-dependent mechanism of microglial priming relevant to multiple sclerosis.', *Proceedings of the National Academy of Sciences of the United States of America*, 109(3), pp. 965–70.

Ramamoorthy, M. *et al.* (2012) 'Sporadic Alzheimer disease fibroblasts display an oxidative stress phenotype', *Free Radical Biology and Medicine*, 53(6), pp. 1371–1380.

Rambach, G. *et al.* (2008) 'Complement induction and complement evasion in patients with cerebral aspergillosis', *Microbes and Infection*, 10(14–15), pp. 1567–1576.

Ransohoff, R. M. (2016) 'A polarizing question: do M1 and M2 microglia exist?', *Nature Neuroscience*, 19(8), pp. 987–991.

Rappert, A. *et al.* (2004) 'CXCR3-Dependent Microglial Recruitment Is Essential for Dendrite Loss after Brain Lesion', *Journal of Neuroscience*, 24(39), pp. 8500–8509.

Rayaprolu, S. *et al.* (2013) 'TREM2 in neurodegeneration: evidence for association of the p.R47H variant with frontotemporal dementia and Parkinson's disease.', *Molecular neurodegeneration*, 8, p. 19.

Reemst, K. *et al.* (2016) 'The Indispensable Roles of Microglia and Astrocytes during Brain Development.', *Frontiers in human neuroscience*, 10, p. 566.

Reichwald, J. *et al.* (2009) 'Expression of complement system components during aging and amyloid deposition in APP transgenic mice', *Journal of Neuroinflammation*, 6(1), p. 35.

Rey-Giraud, F. *et al.* (2012) 'In Vitro Generation of Monocyte-Derived Macrophages under Serum-Free Conditions Improves Their Tumor Promoting Functions', *PLoS ONE*, 7(8), p. e42656.

Rhodes, B. *et al.* (2012) 'The rs1143679 (R77H) lupus associated variant of ITGAM (CD11b) impairs complement receptor 3 mediated functions in human monocytes', *Annals of the Rheumatic Diseases*, 71(12), pp. 2028–2034.

Ricklin, D. *et al.* (2010) 'Complement: a key system for immune surveillance and homeostasis', *Nat Immunol*, 11(9), pp. 785–797.

Righi, M. *et al.* (1989) 'Monokine production by microglial cell clones.', *European journal of immunology*, 19(8), pp. 1443–8.

Ritzel, R. M. *et al.* (2015) 'Functional differences between microglia and monocytes after ischemic stroke.', *Journal of neuroinflammation*, 12(1), p. 106.

Rogaeva, E. (2002) 'The solved and unsolved mysteries of the genetics of early-onset Alzheimer's disease.', *Neuromolecular medicine*, 2(1), pp. 1–10.

Rogers, J. *et al.* (1992) 'Complement activation by beta-amyloid in Alzheimer disease.', *Proceedings of the National Academy of Sciences of the United States of America*. National Academy of Sciences, 89(21), pp. 10016–20.

Rogers, J. *et al.* (2006) 'Peripheral clearance of amyloid beta peptide by complement C3-dependent adherence to erythrocytes.', *Neurobiology of aging*, 27(12), pp. 1733–9.

Rogers, J. T. *et al.* (2011) 'CX3CR1 deficiency leads to impairment of hippocampal cognitive function and synaptic plasticity.', *The Journal of neuroscience*, 31(45), pp. 16241–50.

Rosen, A. M. and Stevens, B. (2010) 'The role of the classical complement cascade in synapse loss during development and glaucoma.', *Advances in experimental medicine and biology*, 703, pp. 75–93.

Rosenkranz, A. R. *et al.* (1998) 'Impaired mast cell development and innate immunity in Mac-1 (CD11b/CD18, CR3)-deficient mice.', *Journal of immunology*, 161(12), pp. 6463–7.

Ross, G. D. *et al.* (1982) 'Generation of three different fragments of bound C3 with purified factor I or serum. I. Requirements for factor H vs CR1 cofactor activity.', *Journal of immunology*, 129(5), pp. 2051–60.

Roussos, P. *et al.* (2015) 'The triggering receptor expressed on myeloid cells 2 (TREM2) is associated with enhanced inflammation, neuropathological lesions and increased risk for Alzheimer's dementia.', *Alzheimer's & dementia*, 11(10), pp. 1163–70.

Roux, P. P. and Topisirovic, I. (2012) 'Regulation of mRNA translation by signaling pathways.', *Cold Spring Harbor perspectives in biology*, 4(11).

Rozemuller, A. J. *et al.* (2000) 'Activated microglial cells and complement factors are unrelated to cortical Lewy bodies', *Acta Neuropathol*, 100(6), pp. 701–708.

Saber, M. *et al.* (2017) 'Triggering Receptor Expressed on Myeloid Cells 2 Deficiency Alters Acute Macrophage Distribution and Improves Recovery after Traumatic Brain Injury.', *Journal of neurotrauma*, 34(2), pp. 423–435.

Sarma, J. V and Ward, P. A. (2011) 'The complement system', *Cell Tissue Res*, 343(1), pp. 227–235.

Sarvari, M. *et al.* (2003) 'Inhibition of C1q-beta-amyloid binding protects hippocampal cells against complement mediated toxicity', *J Neuroimmunol*, 137(1–2), pp. 12–18.

Sasaki, A. *et al.* (2015) 'Variable expression of microglial DAP12 and TREM2 genes in Nasu-Hakola disease', *neurogenetics*, 16(4), pp. 265–276.

Sasaki, Y. *et al.* (2001) 'Iba1 is an actin-cross-linking protein in macrophages/microglia.', *Biochemical and biophysical research communications*,

286(2), pp. 292–7.

Satoh, J. *et al.* (2011) 'Immunohistochemical characterization of microglia in Nasu-Hakola disease brains', *Neuropathology*, 31(4), pp. 363–375.

Satoh, J. *et al.* (2016) 'TMEM119 marks a subset of microglia in the human brain', *Neuropathology*, 36(1), pp. 39–49.

Saunders, A. M. *et al.* (1993) 'Association of apolipoprotein E allele epsilon 4 with late-onset familial and sporadic Alzheimer's disease.', *Neurology*, 43(8), pp. 1467–72.

Savage, J. C. *et al.* (2015) 'Nuclear receptors license phagocytosis by trem2+ myeloid cells in mouse models of Alzheimer's disease.', *The Journal of neuroscience*, 35(16), pp. 6532–43.

van Schaarenburg, R. A. *et al.* (2016) 'The production and secretion of complement component C1q by human mast cells', *Molecular Immunology*, 78, pp. 164–170.

Schafer, D. P. *et al.* (2012) 'Microglia sculpt postnatal neural circuits in an activity and complement-dependent manner.', *Neuron*, 74(4), pp. 691–705.

Schmidt, C. *et al.* (2014) 'CR1 is potentially associated with rate of decline in sporadic Alzheimer's disease.', *Journal of clinical neuroscience*, 21(10), pp. 1705–8.

Schulz, C. *et al.* (2012) 'A Lineage of Myeloid Cells Independent of Myb and Hematopoietic Stem Cells', *Science*, 336(6077), pp. 86–90.

Schwab, M. E. (2004) 'Nogo and axon regeneration.', *Current opinion in neurobiology*, 14(1), pp. 118–24.

Schwaeble, W. *et al.* (1995) 'Follicular dendritic cells, interdigitating cells, and cells of the monocyte-macrophage lineage are the C1q-producing sources in the spleen. Identification of specific cell types by in situ hybridization and immunohistochemical analysis.', *The Journal of Immunology*, 155(10).

Scolding, N. J., Morgan, B. P. and Compston, D. A. (1998) 'The expression of complement regulatory proteins by adult human oligodendrocytes.', *Journal of neuroimmunology*, 84(1), pp. 69–75..

Segawa, K. *et al.* (2014) 'Caspase-mediated cleavage of phospholipid flippase for apoptotic phosphatidylserine exposure', *Science*, 344(6188), pp. 1164–1168.

Selkoe, D. J. (2002) 'Alzheimer's Disease Is a Synaptic Failure', *Science*, 298(5594), pp. 789–791.

Sessa, G. *et al.* (2004) 'Distribution and signaling of TREM2/DAP12, the receptor system mutated in human polycystic lipomembraneous osteodysplasia with sclerosing leukoencephalopathy dementia', *European Journal of Neuroscience*, 20(10), pp. 2617–2628.

Sharif, O. *et al.* (2014) 'The Triggering Receptor Expressed on Myeloid Cells 2 Inhibits Complement Component 1q Effector Mechanisms and Exerts Detrimental Effects during Pneumococcal Pneumonia', *PLoS Pathogens*, 10(6), p. e1004167.

Shen, B. *et al.* (2014) 'Efficient genome modification by CRISPR-Cas9 nickase with minimal off-target effects', *Nature Methods*, 11(4), pp. 399–402.

Shen, N. *et al.* (2015) 'An Updated Analysis with 85,939 Samples Confirms the Association Between CR1 rs6656401 Polymorphism and Alzheimer's Disease.', *Molecular neurobiology*, 51(3), pp. 1017–23.

Shen, Y. *et al.* (1997) 'Neuronal expression of mRNAs for complement proteins of the classical pathway in Alzheimer brain.', *Brain research*, 769(2), pp. 391–5.

Shen, Y. *et al.* (2001) 'Complement activation by neurofibrillary tangles in Alzheimer's disease', *Neurosci Lett*, 305(3), pp. 165–168.

Sheng, J. G., Mrak, R. E. and Griffin, W. S. (1998) 'Enlarged and phagocytic, but not primed, interleukin-1 alpha-immunoreactive microglia increase with age in normal human brain.', *Acta neuropathologica*, 95(3), pp. 229–34.

Sherrington, R. *et al.* (1995) 'Cloning of a gene bearing missense mutations in early-onset familial Alzheimer's disease', *Nature*, 375(6534), pp. 754–760.

Sherrington, R. *et al.* (1996) 'Alzheimer's disease associated with mutations in presenilin 2 is rare and variably penetrant.', *Human molecular genetics*, 5(7), pp. 985–8.

Shinjyo, N. *et al.* (2009) 'Complement-derived anaphylatoxin C3a regulates in vitro differentiation and migration of neural progenitor cells.', *Stem cells*, 27(11), pp. 2824–32.

Sieber, M. W. *et al.* (2013) 'Attenuated inflammatory response in triggering receptor expressed on myeloid cells 2 (TREM2) knock-out mice following stroke.', *PloS one*, 8(1), p. e52982.

Sierra, A. *et al.* (2010) 'Microglia Shape Adult Hippocampal Neurogenesis through Apoptosis-Coupled Phagocytosis', *Cell Stem Cell*, 7(4), pp. 483–495.

Singhrao, S. K. *et al.* (1999) 'Differential expression of individual complement

regulators in the brain and choroid plexus.', *Laboratory investigation*, 79(10), pp. 1247–59.

Singhrao, S. K. *et al.* (2000) 'Spontaneous classical pathway activation and deficiency of membrane regulators render human neurons susceptible to complement lysis.', *The American journal of pathology*, 157(3), pp. 905–18.

Slattery, C. F. *et al.* (2014) 'R47H TREM2 variant increases risk of typical early-onset Alzheimer's disease but not of prion or frontotemporal dementia.', *Alzheimer's & dementia*, 10(6), p. 602–608.e4.

Ślusarczyk, J. *et al.* (2016) 'Fractalkine Attenuates Microglial Cell Activation Induced by Prenatal Stress', *Neural Plasticity*, 2016, pp. 1–11.

Smith, A. G. *et al.* (1988) 'Inhibition of pluripotential embryonic stem cell differentiation by purified polypeptides.', *Nature*, 336(6200), pp. 688–90.

Sokolowski, J. D. *et al.* (2014) 'Fractalkine is a "find-me" signal released by neurons undergoing ethanol-induced apoptosis.', *Frontiers in cellular neuroscience*, 8, p. 360.

Sonenberg, N. and Hinnebusch, A. G. (2009) 'Regulation of Translation Initiation in Eukaryotes: Mechanisms and Biological Targets', *Cell*, 136(4), pp. 731–745.

Song, W. *et al.* (2017) 'Alzheimer's disease-associated TREM2 variants exhibit either decreased or increased ligand-dependent activation', *Alzheimer's & Dementia*, 13(4), pp. 381–387.

Stahel, P. F. *et al.* (1997) 'TNF-alpha-mediated expression of the receptor for anaphylatoxin C5a on neurons in experimental Listeria meningoencephalitis', *J Immunol*, 159(2), pp. 861–869.

Stahel, P. F. and Barnum, S. R. (1997) 'Bacterial meningitis: complement gene expression in the central nervous system', *Immunopharmacology*, 38(1–2), pp. 65–72.

Stasi, K. *et al.* (2006) 'Complement Component 1Q (C1Q) Upregulation in Retina of Murine, Primate, and Human Glaucomatous Eyes', *Investigative Opthalmology & Visual Science*, 47(3), p. 1024.

Stephan, A. H. *et al.* (2013) 'A dramatic increase of C1q protein in the CNS during normal aging.', *The Journal of neuroscience*, 33(33), pp. 13460–74.

Stevens, B. *et al.* (2007) 'The classical complement cascade mediates CNS synapse elimination', *Cell*, 131(6), pp. 1164–1178.

Strobel, S. *et al.* (2015) ‘Changes in the expression of genes related to neuroinflammation over the course of sporadic Alzheimer’s disease progression: CX3CL1, TREM2, and PPARγ.’, *Journal of neural transmission*, 122(7), pp. 1069–76.

Strohmeyer, R. *et al.* (2002) ‘Association of factor H of the alternative pathway of complement with agrin and complement receptor 3 in the Alzheimer’s disease brain.’, *Journal of neuroimmunology*, 131(1–2), pp. 135–46.

Suárez-Calvet, M. *et al.* (2016a) ‘Early changes in CSF sTREM2 in dominantly inherited Alzheimer’s disease occur after amyloid deposition and neuronal injury.’, *Science translational medicine*, 8(369), p. 369ra178.

Suárez-Calvet, M. *et al.* (2016b) ‘sTREM2 cerebrospinal fluid levels are a potential biomarker for microglia activity in early-stage Alzheimer’s disease and associate with neuronal injury markers’, *EMBO Molecular Medicine*, 8(5), pp. 466–476.

Sutterwala, F. S., Rosenthal, L. A. and Mosser, D. M. (1996) ‘Cooperation between CR1 (CD35) and CR3 (CD 11b/CD18) in the binding of complement-opsonized particles.’, *Journal of leukocyte biology*, 59(6), pp. 883–90.

Taborda, C. P. and Casadevall, A. (2002) ‘CR3 (CD11b/CD18) and CR4 (CD11c/CD18) are involved in complement-independent antibody-mediated phagocytosis of Cryptococcus neoformans.’, *Immunity*, 16(6), pp. 791–802.

Takahashi, K. *et al.* (2007a) ‘Induction of Pluripotent Stem Cells from Adult Human Fibroblasts by Defined Factors’, *Cell*, 131(5), pp. 861–872.

Takahashi, K. *et al.* (2007b) ‘TREM2-Transduced Myeloid Precursors Mediate Nervous Tissue Debris Clearance and Facilitate Recovery in an Animal Model of Multiple Sclerosis’, *PLoS Medicine*, 4(4), p. e124.

Takahashi, K., Rochford, C. D. P. and Neumann, H. (2005) ‘Clearance of apoptotic neurons without inflammation by microglial triggering receptor expressed on myeloid cells-2.’, *The Journal of experimental medicine*, 201(4), pp. 647–57.

Takahashi, K. and Yamanaka, S. (2006) ‘Induction of Pluripotent Stem Cells from Mouse Embryonic and Adult Fibroblast Cultures by Defined Factors’, *Cell*, 126(4), pp. 663–676.

Takeuchi, H. *et al.* (2006) ‘Tumor necrosis factor-alpha induces neurotoxicity via glutamate release from hemichannels of activated microglia in an autocrine manner.’, *The Journal of biological chemistry*, 281(30), pp. 21362–8.

Talley, A. K. *et al.* (1995) ‘Tumor necrosis factor alpha-induced apoptosis in human neuronal cells: protection by the antioxidant N-acetylcysteine and the genes bcl-2 and crmA.’, *Molecular and cellular biology*, 15(5), pp. 2359–66.

Thal, D. R. *et al.* (2002) 'Phases of A beta-deposition in the human brain and its relevance for the development of AD.', *Neurology*, 58(12), pp. 1791–800.

Thelen, M. *et al.* (2014) 'Investigation of the role of rare TREM2 variants in frontotemporal dementia subtypes.', *Neurobiology of aging*, 35(11), p. 2657.e13-9.

Thomas, A. *et al.* (2000) 'Expression of a complete and functional complement system by human neuronal cells in vitro', *Int Immunol*, 12(7), pp. 1015–1023.

Thomson, J. A. *et al.* (1998) 'Embryonic stem cell lines derived from human blastocysts.', *Science (New York, N.Y.)*, 282(5391), pp. 1145–7.

Thrash, J. C., Torbett, B. E. and Carson, M. J. (2009) 'Developmental Regulation of TREM2 and DAP12 Expression in the Murine CNS: Implications for Nasu-Hakola Disease', *Neurochemical Research*, 34(1), pp. 38–45.

Togo, T. *et al.* (2002) 'Occurrence of T cells in the brain of Alzheimer's disease and other neurological diseases.', *Journal of neuroimmunology*, 124(1–2), pp. 83–92.

Tremblay, M.-E. *et al.* (2011) 'The Role of Microglia in the Healthy Brain', *Journal of Neuroscience*, 31(45), pp. 16064–16069.

Tremblay, M.-È., Lowery, R. L. and Majewska, A. K. (2010) 'Microglial interactions with synapses are modulated by visual experience.', *PLoS biology*, 8(11), p. e1000527.

Tsuboi, N. *et al.* (2011) 'Regulation of human neutrophil Fcγ receptor IIa by C5a receptor promotes inflammatory arthritis in mice', *Arthritis & Rheumatism*, 63(2), pp. 467–478.

Turnbull, I. R. *et al.* (2006) 'Cutting Edge: TREM-2 Attenuates Macrophage Activation', *The Journal of Immunology*, 177(6), pp. 3520–3524.

Turner, M. and Billadeau, D. D. (2002) 'VAV proteins as signal integrators for multi-subunit immune-recognition receptors', *Nature Reviews Immunology*, 2(7), pp. 476–486.

Tuxworth, R. I. *et al.* (2001) 'A role for myosin VII in dynamic cell adhesion.', *Current biology*, 11(5), pp. 318–29.

Tyurina, Y. Y. *et al.* (2007) 'Nitrosative stress inhibits the aminophospholipid translocase resulting in phosphatidylserine externalization and macrophage engulfment: implications for the resolution of inflammation.', *The Journal of biological chemistry*, 282(11), pp. 8498–509.

Ubeda, M. and Habener, J. F. (2000) 'CHOP gene expression in response to endoplasmic-reticular stress requires NFY interaction with different domains of a conserved DNA-binding element.', *Nucleic acids research*, 28(24), pp. 4987–97.

Ueno, M. *et al.* (2013) 'Layer V cortical neurons require microglial support for survival during postnatal development.', *Nature neuroscience*, 16(5), pp. 543–51.

Ulrich, J. D. *et al.* (2014) 'Altered microglial response to Aβ plaques in APPPS1-21 mice heterozygous for TREM2.', *Molecular neurodegeneration*, 9, p. 20.

Valente, T. *et al.* (2010) 'Immunohistochemical analysis of human brain suggests pathological synergism of Alzheimer's disease and diabetes mellitus', *Neurobiology of Disease*, 37(1), pp. 67–76.

Vanhee, S. *et al.* (2015) 'In vitro human embryonic stem cell hematopoiesis mimics MYB-independent yolk sac hematopoiesis', *Haematologica*, 100(2), pp. 157–166.

Veerhuis, R. *et al.* (1998) 'Complement C1-inhibitor expression in Alzheimer's disease', *Acta Neuropathol*, 96(3), pp. 287–296.

Veerhuis, R., Nielsen, H. M. and Tenner, A. J. (2011) 'Complement in the brain', *Mol Immunol*, 48(14), pp. 1592–1603.

Vezzani, A. and Viviani, B. (2015) 'Neuromodulatory properties of inflammatory cytokines and their impact on neuronal excitability', *Neuropharmacology*, 96(Pt A), pp. 70–82.

Villegas-Llerena, C. *et al.* (2016) 'Microglial genes regulating neuroinflammation in the progression of Alzheimer's disease.', *Current opinion in neurobiology*, 36, pp. 74–81.

Vogel, C. and Marcotte, E. M. (2012) 'Insights into the regulation of protein abundance from proteomic and transcriptomic analyses', *Nature Reviews Genetics*, 13(4), pp. 227–32.

Vonna, L. *et al.* (2007) 'Micromechanics of filopodia mediated capture of pathogens by macrophages.', *European biophysics journal : EBJ*, 36(2), pp. 145–51.

Wake, H. *et al.* (2009) 'Resting Microglia Directly Monitor the Functional State of Synapses In Vivo and Determine the Fate of Ischemic Terminals', *Journal of Neuroscience*, 29(13), pp. 3974–3980.

Wakselman, S. *et al.* (2008) 'Developmental neuronal death in hippocampus requires the microglial CD11b integrin and DAP12 immunoreceptor', *The Journal of neuroscience*, 28(32), pp. 8138–43.

Walker, D. G., Kim, S. U. and McGeer, P. L. (1995) 'Complement and cytokine gene expression in cultured microglial derived from postmortem human brains', *J Neurosci Res*, 40(4), pp. 478–493.

Walker, D. G. and McGeer, P. L. (1993) 'Complement gene expression in neuroblastoma and astrocytoma cell lines of human origin', *Neurosci Lett*, 157(1), pp. 99–102.

Walker, J. R. *et al.* (2013) 'Enhanced proteolytic clearance of plasma Aβ by peripherally administered neprilysin does not result in reduced levels of brain Aβ in mice.', *The Journal of neuroscience*, 33(6), pp. 2457–64.

Walport, M. J. (2001) 'Complement', *New England Journal of Medicine*, 344(14), pp. 1058–1066.

Wang, S.-C., Oelze, B. and Schumacher, A. (2008) 'Age-Specific Epigenetic Drift in Late-Onset Alzheimer's Disease', *PLoS ONE*. Edited by A. E. Toland, 3(7), p. e2698.

Wang, Y. *et al.* (2012) 'IL-34 is a tissue-restricted ligand of CSF1R required for the development of Langerhans cells and microglia', *Nature Immunology*, 13(8), pp. 753–760.

Wang, Y. *et al.* (2015) 'TREM2 Lipid Sensing Sustains the Microglial Response in an Alzheimer's Disease Model', *Cell*, 160(6), pp. 1061–1071.

Wang, Y. *et al.* (2016) 'TREM2-mediated early microglial response limits diffusion and toxicity of amyloid plaques.', *The Journal of experimental medicine*, 213(5), pp. 667–75.

Warren, L. *et al.* (2010) 'Highly Efficient Reprogramming to Pluripotency and Directed Differentiation of Human Cells with Synthetic Modified mRNA', *Cell Stem Cell*, 7(5), pp. 618–630.

Webster, S. D. *et al.* (2000) 'Complement Component C1q Modulates the Phagocytosis of Aβ by Microglia', *Experimental Neurology*, 161(1), pp. 127–138.

Wei, S. *et al.* (2010) 'Functional overlap but differential expression of CSF-1 and IL-34 in their CSF-1 receptor-mediated regulation of myeloid cells', *Journal of Leukocyte Biology*, 88(3), pp. 495–505.

Wes, P. D. *et al.* (2016) 'Next generation transcriptomics and genomics elucidate biological complexity of microglia in health and disease.', *Glia*, 64(2), pp. 197–213.

Whitlock, B. B. *et al.* (2000) 'Differential Roles for αMβ2 Integrin Clustering or Activation in the Control of Apoptosis via Regulation of Akt and ERK Survival

Mechanisms', *The Journal of Cell Biology*, 151(6).

Wiedenheft, B., Sternberg, S. H. and Doudna, J. A. (2012) 'RNA-guided genetic silencing systems in bacteria and archaea', *Nature*, 482(7385), pp. 331–338.

Wijsman, E. M. *et al.* (2011) 'Genome-wide association of familial late-onset Alzheimer's disease replicates BIN1 and CLU and nominates CUGBP2 in interaction with APOE.', *PLoS genetics*, 7(2), p. e1001308.

Van Wilgenburg, B. *et al.* (2013) 'Efficient, Long Term Production of Monocyte-Derived Macrophages from Human Pluripotent Stem Cells under Partly-Defined and Fully-Defined Conditions', *PLoS ONE*, 8(8), p. e71098.

Wilmut, I. *et al.* (1997) 'Viable offspring derived from fetal and adult mammalian cells', *Nature*, 385(6619), pp. 810–813.

Wolf, S. A., Boddeke, H. W. G. M. and Kettenmann, H. (2017) 'Microglia in Physiology and Disease.', *Annual review of physiology*, 79(1), pp. 619–643.

Woodruff, T. M. *et al.* (2010) 'The role of the complement system and the activation fragment C5a in the central nervous system', *Neuromolecular Med*, 12(2), pp. 179–192.

Wright, S. D. *et al.* (1988) 'Complement receptor type three (CD11b/CD18) of human polymorphonuclear leukocytes recognizes fibrinogen.', *Proceedings of the National Academy of Sciences of the United States of America*, 85(20), pp. 7734–8.

Wright, S. D. and Jong, M. T. (1986) 'Adhesion-promoting receptors on human macrophages recognize Escherichia coli by binding to lipopolysaccharide.', *The Journal of experimental medicine*, 164(6), pp. 1876–88.

Wright, S. D. and Silverstein, S. C. (1982) 'Tumor-promoting phorbol esters stimulate C3b and C3b' receptor-mediated phagocytosis in cultured human monocytes.', *The Journal of experimental medicine*, 156(4), pp. 1149–64.

Wu, K. *et al.* (2015) 'TREM-2 promotes macrophage survival and lung disease after respiratory viral infection', *The Journal of Experimental Medicine*, 212(5), pp. 681–697.

Wunderlich, P. *et al.* (2013) 'Sequential proteolytic processing of the triggering receptor expressed on myeloid cells-2 (TREM2) protein by ectodomain shedding and γ-secretase-dependent intramembranous cleavage.', *The Journal of biological chemistry*. in Press, 288(46), pp. 33027–36.

Wyss-Coray, T. *et al.* (2002) 'Prominent neurodegeneration and increased plaque formation in complement-inhibited Alzheimer's mice.', *Proceedings of the National*

Academy of Sciences of the United States of America, 99(16), pp. 10837–42.

Xiang, X. *et al.* (2016) 'TREM2 deficiency reduces the efficacy of immunotherapeutic amyloid clearance.', *EMBO molecular medicine*, 8(9), pp. 992–1004.

Xiang, Z. *et al.* (2006) 'Microglia activation in the brain as inflammatory biomarker of Alzheimer's disease neuropathology and clinical dementia.', *Disease markers*, 22(1–2), pp. 95–102.

Xu, C. *et al.* (2005) 'Basic Fibroblast Growth Factor Supports Undifferentiated Human Embryonic Stem Cell Growth Without Conditioned Medium', *Stem Cells*, 23(3), pp. 315–323.

Xue, F., Janzen, D. M. and Knecht, D. A. (2010) 'Contribution of Filopodia to Cell Migration: A Mechanical Link between Protrusion and Contraction', *International Journal of Cell Biology*, 2010, pp. 1–13.

Yamanaka, S. *et al.* (2012) 'Induced pluripotent stem cells: past, present, and future.', *Cell stem cell*, 10(6), pp. 678–84.

Yamazaki, K. *et al.* (2015) 'A Case of Nasu-Hakola Disease without Fractures or Consanguinity Diagnosed Using Exome Sequencing and Treated with Sodium Valproate.', *Clinical psychopharmacology and neuroscience : the official scientific journal of the Korean College of Neuropsychopharmacology*, 13(3), pp. 324–6.

Yan, W. *et al.* (2002) 'Control of PERK eIF2alpha kinase activity by the endoplasmic reticulum stress-induced molecular chaperone P58IPK.', *Proceedings of the National Academy of Sciences of the United States of America*, 99(25), pp. 15920–5.

Yang, L. B. *et al.* (2000) 'Deficiency of complement defense protein CD59 may contribute to neurodegeneration in Alzheimer's disease.', *The Journal of neuroscience*, 20(20), pp. 7505–9.

Yasojima, K. *et al.* (1999) 'Up-regulated production and activation of the complement system in Alzheimer's disease brain.', *The American journal of pathology*, 154(3), pp. 927–36.

Yeh, F. L. *et al.* (2016) 'TREM2 Binds to Apolipoproteins, Including APOE and CLU/APOJ, and Thereby Facilitates Uptake of Amyloid-Beta by Microglia', *Neuron*, 91(2), pp. 328–340.

Yin, Z. *et al.* (2017) 'Immune hyperreactivity of Aβ plaque-associated microglia in Alzheimer's disease.', *Neurobiology of aging*, 55, pp. 115–122.

Yu, J. *et al.* (2007) 'Induced Pluripotent Stem Cell Lines Derived from Human Somatic

Cells', *Science*, 318(5858), pp. 1917–1920.

Yu, J. *et al.* (2009) 'Human induced pluripotent stem cells free of vector and transgene sequences.', *Science (New York, N.Y.)*. NIH Public Access, 324(5928), pp. 797–801.

Yuan, P. *et al.* (2016) 'TREM2 Haplodeficiency in Mice and Humans Impairs the Microglia Barrier Function Leading to Decreased Amyloid Compaction and Severe Axonal Dystrophy', *Neuron*, 90(4), pp. 724–739.

Zarewych, D. M. *et al.* (1996) 'LPS induces CD14 association with complement receptor type 3, which is reversed by neutrophil adhesion.', *The Journal of Immunology*, 156(2).

Zenaro, E. *et al.* (2015) 'Neutrophils promote Alzheimer's disease-like pathology and cognitive decline via LFA-1 integrin.', *Nature medicine*, 21(8), pp. 880–6.

Zhang, Y. *et al.* (2014) 'An RNA-sequencing transcriptome and splicing database of glia, neurons, and vascular cells of the cerebral cortex.', *The Journal of neuroscience*, 34(36), pp. 11929–47.

Zhang, Y. and Lee, D. H. S. (2011) 'Sink Hypothesis and Therapeutic Strategies for Attenuating Aβ Levels', *The Neuroscientist*, 17(2), pp. 163–173.

Zheng, H. *et al.* (2016) 'Opposing roles of the triggering receptor expressed on myeloid cells 2 and triggering receptor expressed on myeloid cells-like transcript 2 in microglia activation', *Neurobiology of Aging*, 42, pp. 132–141.

Zheng, H. *et al.* (2017) 'TREM2 Promotes Microglial Survival by Activating Wnt/β-Catenin Pathway', *The Journal of Neuroscience*, 37(7), pp. 1772–1784.

Zhong, L. *et al.* (2015) 'DAP12 Stabilizes the C-terminal Fragment of the Triggering Receptor Expressed on Myeloid Cells-2 (TREM2) and Protects against LPS-induced Pro-inflammatory Response.', *The Journal of biological chemistry*, 290(25), pp. 15866–77.

Zhong, L. *et al.* (2017) 'Soluble TREM2 induces inflammatory responses and enhances microglial survival.', *The Journal of experimental medicine*, 214(3), pp. 597–607.

Zhou, M. J. and Brown, E. J. (1994) 'CR3 (Mac-1, alpha M beta 2, CD11b/CD18) and Fc gamma RIII cooperate in generation of a neutrophil respiratory burst: requirement for Fc gamma RIII and tyrosine phosphorylation.', *The Journal of cell biology*, 125(6), pp. 1407–16.

Zhou, W. and Freed, C. R. (2009) 'Adenoviral Gene Delivery Can Reprogram Human Fibroblasts to Induced Pluripotent Stem Cells', *Stem Cells*, 27(11), pp. 2667–2674.